

DRAFT VERSION DECEMBER 20, 2021
 Typeset using L^AT_EX **preprint** style in AASTeX63

Bayesian Time-Resolved Spectroscopy of Multipulse GRBs: Variations of Emission Properties amongst Pulses

LIANG LI,^{1, 2, 3, 4, 5} FELIX RYDE,⁶ ASAFA PE'ER,⁷ HOI-FUNG YU,⁸ AND ZEYNEP ACUNER⁶

¹*ICRANet, Piazza della Repubblica 10, I-65122 Pescara, Italy*

²*INAF – Osservatorio Astronomico d'Abruzzo, Via M. Maggini snc, I-64100, Teramo, Italy*

³*ICRA, Dipartimento di Fisica, Sapienza Università di Roma, P.le Aldo Moro 5, I-00185 Rome, Italy*

⁴*Department of Physics, KTH Royal Institute of Technology, and the Oskar Klein Centre for Cosmoparticle Physics, SE-10691 Stockholm, Sweden*

⁵*Department of Physics, Stockholm University, AlbaNova, SE-10691 Stockholm, Sweden*

⁶*Department of Physics, KTH Royal Institute of Technology, and the Oskar Klein Centre for Cosmoparticle Physics, 10691 Stockholm, Sweden*

⁷*Department of Physics, Bar-Ilan University, Ramat-Gan 52900, Israel*

⁸*Faculty of Science, The University of Hong Kong, Pokfulam, Hong Kong*

(Received 2020 December 4; Revised 2021 February 18; Accepted 2021 February 19;
 Published 2021 June 7)

ABSTRACT

Gamma-ray bursts (GRBs) are highly variable and exhibit strong spectral evolution. In particular, the emission properties vary from pulse to pulse in multipulse bursts. Here we present a time-resolved Bayesian spectral analysis of a compilation of GRB pulses observed by the *Fermi*/Gamma-ray Burst Monitor. The pulses are selected to have at least four timebins with a high statistical significance, which ensures that the spectral fits are well determined and that spectral correlations can be established. The sample consists of 39 bursts, 117 pulses, and 1228 spectra. We confirm the general trend that pulses become softer over time, with mainly the low-energy power-law index α becoming smaller. A few exceptions to this trend exist, with the hardest pulse occurring at late times. The first pulse in a burst is clearly different from the later pulses; three-fourths of them violate the synchrotron line of death, while around half of them significantly prefer photospheric emission. These fractions decrease for subsequent pulses. We also find that in two-thirds of the pulses, the spectral parameters (α and peak energy) track the light-curve variations. This is a larger fraction compared to what is found in previous samples. In conclusion, emission compatible with the GRB photosphere is typically found close to the trigger time, while the chance of detecting synchrotron emission is greatest at late times. This allows for the coexistence of emission mechanisms at late times.

Corresponding author: Liang Li
liang.li@icranet.org

Keywords: Gamma-ray bursts (629); Astronomy data analysis (1858)

1. INTRODUCTION

Gamma-ray burst (GRB) emission exhibits significant variability and spectral evolution. The prompt emission light curves typically have irregular, multipulse temporal profiles, in some cases having a complex structure (e.g., Norris et al. 1996, 2005). The emission spectrum typically changes from having both large spectral peak energies and hard spectral slopes below the peak (so-called hard spectra) to having lower peak energies and softer spectral slopes (soft spectra). Such variations occur both within individual pulse structures and as an overall trend during the burst (Mazets et al. 1982; Ford et al. 1995; Crider et al. 1997).

Within the fireball model of GRBs, there are two main emission sources for the prompt gamma rays. The first is radiation from where the jet becomes transparent, namely, the photosphere region (e.g., Goodman 1986; Rees & Mészáros 2005; Pe'er et al. 2006a). The second is radiation from a region at larger distance from the progenitor, where the kinetic energy of the jet is dissipated and radiated away in the form of synchrotron emission (e.g., Piran et al. 1993; Sari et al. 1998; Lloyd & Petrosian 2000). The time scale for the gamma-ray emission, relative to the launching of the jet, depends on the distances to the different emission sites, r_γ , and the Lorentz factor of the jet, Γ , according to $t_\gamma = r_\gamma/(c\Gamma^2)$, where c is the speed of light. For the typical outflow parameters, the photosphere is expected to occur at $r_\gamma^{\text{ph}} \sim 3 \times 10^{12}$ cm, while the synchrotron emission is expected at larger radii, for instance, $r_\gamma^{\text{IS}} \sim 10^{13}$ cm for internal shocks and $r_\gamma^{\text{ES}} \sim 10^{17}$ cm for external shocks (e.g., Rees & Mészáros 1998). Therefore, a central engine activity will first be observed by its thermal emission and be followed by synchrotron emission, with a delay of a few seconds or even hundreds of seconds (Rees & Meszaros 1994). In such a case, one should expect to observe an initial photospheric emission episode followed by synchrotron emission activity.

Alternatively, variations of the jet property, such as the entropy and magnetization (e.g., Rees & Meszaros 1994; Beloborodov 2013; Uhm & Zhang 2014; Zhang 2018; Li 2019a, 2020; Li & Zhang 2021) can cause the variations in the observed emission. For instance, the interaction between the jet and the surrounding material as the jet passes through the progenitor star will cause a variable mixing and thereby a change in the entropy of the flow (Lazzati et al. 2009; López-Cámara et al. 2014; Ito et al. 2015). This directly affects the properties of the observed emission, since the entropy determines the position of the photosphere, r_{ph} , relative to the saturation radius, r_s (e.g., Mészáros & Rees 2000). If $r_{\text{ph}}/r_s \lesssim 1$, a photosphere will dominate the emission,¹ while in the opposite cases, $r_{\text{ph}}/r_s \gg 1$, the photosphere will be very weak, and only nonthermal emission, such as synchrotron, will be expected. Furthermore, in the case of photospheric emission, the entropy variation will allow for a varying amount of broadening of the spectral shape due to subphotospheric dissipation. The reason is that strong dissipation is not expected below the saturation radius. Therefore, significant spectral broadening of the photospheric spectrum is only expected when $r_{\text{ph}}/r_s \gtrsim 1$. In this alternative scenario, the evolution of the spectral properties of consecutive pulses is interpreted as variations of properties in the jet.

¹ A typical result from an analysis of the photospheric spectra is that the initial radius of the jet is $r_0 \sim \text{few} \times 10^9$ cm (e.g., Pe'er et al. 2007; Ryde & Pe'er 2009; Iyyani et al. 2015). This is also expected theoretically due to interaction between the jet and the progenitor surrounding it, which prevents the jet from accelerating while it is within the star (e.g., Thompson 2006; Gottlieb et al. 2019). A consequence of this fact is that the saturation radius of the jet $r_s = \Gamma r_0 \sim r_{\text{ph}}$.

The two main emission sources can also coexist, giving rise to multicomponent emission spectra (e.g. Ryde 2005; Ryde & Pe'er 2009; Guiriec et al. 2011; Ajello et al. 2020). The observed evolution in spectral shape might then be driven by the relative change in the contribution of the two emission sources in superposition.

In all cases, observed trends and variations among pulses carry important clues to the physics of GRBs. The multipulse nature indicates a continuous ejection from the progenitor, implying that (i) it is not destroyed immediately, (ii) the variation in flux between pulses represents the variation of the available energy, and (iii) the time difference between the pulses represents some characteristic internal time, possibly the fallback time of the material, or accretion into the surface of the newly formed neutron star until it reaches a critical mass and reexplodes. In this paper, we therefore analyze a sample of multipulse bursts in order to investigate whether there is any variation in spectral characteristics depending on the sequel position among pulses within a burst. In particular, we examine the spectral shape, correlations between spectral parameters, and compatibility with photospheric emission. Our sample is obtained from the first 11 yr of the *Fermi* Gamma-ray Burst Monitor (GBM) mission, consisting of 117 well-separated pulses and 1228 spectra from 39 bursts.

The paper is organized as follows. The methods are presented in Section 2. The detailed observational properties are summarized in Section 3. In Section 4, we present an assessment of the compatibility with emission models. The discussion and summary are presented in Sections 5 and Section 6, respectively. Throughout the paper, the standard Λ -CDM cosmology with the parameters $H_0 = 67.4 \text{ kms}^{-1} \text{ Mpc}^{-1}$, $\Omega_M = 0.315$, and $\Omega_\Lambda = 0.685$ are adopted (Planck Collaboration et al. 2018).

2. METHODOLOGY

2.1. Initial Burst Selection

We use data obtained by the *Fermi Gamma-ray Space Telescope*, which was launched in 2008, and carries two instruments: the GBM (Meegan et al. 2009) and the Large Area Telescope (LAT; Atwood et al. 2009). Together, they cover an energy range from a few keV to a few hundred GeV. The GBM harbors 14 detectors, of which 12 are sodium iodide (NaI; 8 keV-1 MeV) and two are bismuth germanate (BGO; 200 keV-40 MeV) scintillators. By 2019 June, *Fermi* had completed 11 yr of operation, and at least 2388 GRBs had been observed.

Among these bursts, we want to identify the ones that have at least two individual emission episodes, which can be assumed to be independent from each other. Since there is no theoretical prediction of the shape and form of individual emission episodes, we choose to make a general definition for our selection, which does not limit the sample to smooth pulses only. Indeed, numerical simulations of jet emission propagating through the progenitor star show that not only smooth pulses are expected but also more complex morphologies (Lazzati et al. 2009; López-Cámarra et al. 2014). This choice also avoids omitting too many bursts. Following Yu et al. (2019), we thus allow subdominant variations on top of the main pulse structures. In addition, we also include emission activities with many smaller spikes but whose heights are limited by an approximate pulse-shaped envelope. The pulse-shaped envelope indicates that such emission could be connected, in spite of its large variability. Examples of the light curves that are selected for the sample are shown in §3.2 and in the Appendix.

We first visually inspected the Time-Tagged Events (TTE) light curves from each of the 2388 GRBs obtained from NASA/HEASARC². We identified more than 120 bursts that had at least two clear emission episodes. The light curves exhibit diverse temporal properties. Some have a precursor-like pulse followed by a main pulse, while others exhibit a main pulse followed by a small pulse, and yet others consist of several pulses with similar strength. Many of the pulses are well separated by quiescent intervals, while others have a slight temporal overlap.

2.2. Detector, Source, and Background Selections

We use the standard selection criteria adopted in GBM catalogs (Goldstein et al. 2012; Gruber et al. 2014; Yu et al. 2016). Following the common practice, we choose the triggered detectors that have a viewing angle of less than 60 degrees (Goldstein et al. 2012). Typically, one to three NaI and one BGO detector are selected. The period of GRB emission that is considered is in most cases somewhat longer than the T_{90} reported in the HEASARC database. This is done so that all relevant features in the light curve can be incorporated. In order to determine the background emission, we select one interval located tens of seconds before the triggered time and one interval located tens of seconds after the emission has ended. We fit the background photon count level with a polynomial function, which typically has an order lower than 4. The optimal order is determined through a likelihood ratio test. The polynomial is applied to fit all the 128 energy channels and then interpolated into the pulse interval to yield the background photon count estimate. In a few bursts, there are several pulses that are separated by long quiescent intervals. In these cases, we select three background intervals to better constrain the background levels (e.g., GRB 140810782). The spectral energy range is set from 10 to 900 keV for the NaI detectors and 300 keV to 30 MeV for the BGO detectors. In order to avoid the K-edge at 33.17 keV, we ignore the range 30 – 40 keV.

2.3. Light-curve Binning

In order to follow and study spectral evolution in individual bursts, detailed time-resolved spectroscopy is needed (see, e.g., Crider et al. 1997; Kaneko et al. 2006; Goldstein et al. 2012). The question is then how to divide the light curve into time bins, since this choice might affect the results. Foremost, it is important to minimize the amount of variation of the emission during a time bin, since such variations will obscure the intrinsic spectral shape. A method to account for this is to identify Bayesian blocks (BBlocks) in the light curve (Scargle et al. 2013). Therefore, we apply the BBlock method with a false-alarm probability $p_0=0.01$ to the TTE light curve of the brightest NaI detector (see Li 2019a; Yu et al. 2019, for further details). This binning is then used for the other detectors as well.

The BBlock method will create time bins that have varied signal-to-noise ratios. Therefore, some time bins will not have enough signal for a fit to be reliable. A suitable measure of the signal-to-noise ratio is the statistical significance S^3 . Dereli-Bégué et al. (2020) demonstrated that to fully determine the spectral shape, a value of $S = 15\text{--}20$ is needed. In particular, this ensures that the model parameters converge properly (see also, e.g., Vianello et al. 2018; Li 2019a,b; Ryde et al. 2019). We therefore follow this recommendation and only select the BBlock time bins that have $S \geq 20$.

² <https://heasarc.gsfc.nasa.gov/W3Browse/fermi/fermigbrst.html>

³ The statistical significance, S , is suitable for data with Poisson sources with Gaussian backgrounds, which is the case for GBM data (Vianello et al. 2018).

This specific selection thus provides time bins during which (i) there is no significant spectral evolution and (ii) there is highly significant data. Such spectra are required in order to make firm inferences on the intrinsic emission spectrum. However, a consequence of this selection is that intervals with rapid variations will be dismissed. This is often the case for the rise phase of pulses, which could carry particular information about the emission process (see further discussion in §5.2). A possibility of incorporating these dismissed intervals would be to perform joint fits of many intervals at the same time by assuming a prescription of the spectral evolution. This would increase the statistical significance while maintaining the temporal resolution. However, since further assumptions need to be made on the spectral evolution (e.g., Ryde & Svensson 1999), such studies are deferred to other publications.

2.4. Sample (Pulse) Definition

The purpose of this study is to relate the emission properties between pulses within a burst. We therefore only consider bursts that have multiple distinguishable pulses. One of the properties that we will relate is the spectral evolution during the individual pulses. Hence, in order to include a pulse in the study, it needs to have at least four time bins with $S \geq 20$ ($N_{(S \geq 20)} \geq 4$). This allows one to determine the spectral evolution and the correlation between spectral parameters. Our final selection criterion is, therefore, that the burst should have at least two such pulses. This criterion strongly reduces the sample size. However, the pulses that pass the criterion will provide well-determined spectra and evolution characteristics. This final selection yields a sample of 39 bursts. From these, we obtain 117 pulses and 1228 time-resolved spectra, of which 103 pulses have $N_{(S \geq 20)} \geq 4$, consisting of 944 spectra.

The properties of our sample are summarized in Table 1, and includes the *Fermi*-GBM ID (column 1), redshift (column 2), and observed duration t_{90} (column 3), together with the used detectors (column 4), and the selected source and background intervals (columns, 5 and 6), the number of total (column 7) and the used ($S \geq 20$, parentheses in column 7) BBlock time bins, and the number of total (column 8) and the used (parentheses in column 8) pulses for each burst. The detector in parentheses is the brightest one, used for the BBlocks and background determinations.

Inevitably, there will be some overlap between many of the pulses. During such periods, emission from both pulses will be present, and the observed spectrum will be a superposition of two spectra. Depending on their mutual strengths, a fit with a single spectral component might give misleading results. We therefore group the pulses in the 39 bursts into three subsamples.

- *Gold*: No overlap, and the pulses are completely independent. There are 13 such pulses, which are listed in Table 2 (column 5).
- *Silver*: Slight overlap. There are 90 such pulses (column 5 in Table 2).
- *Bronze*: Pulses that have less than four time bins $S \geq 20$. There are 14 such pulses (column 5 in Table 2). Note that these pulses are not used in our final statistical analysis.

2.5. Spectral Fitting

The physical model of the GRB spectra is not yet firmly established. Likewise, the possible regimes of the suggested emission models are not either clarified. Therefore, empirical models are typically used in the analysis. This offers the flexibility to explore many different models and, at the same time,

to explore the models without limiting the certain spectral regimes. The typically used functions are the Band function, which is a broken power-law function, and the cutoff power-law (CPL) function (Band et al. 1993; Gruber et al. 2014). Another advantage of these empirical models is that they are used in all catalogs mapping the behavior and characteristics of observed bursts.

However, the empirical models do not necessarily correspond to the underlying physical model (e.g., Lloyd-Ronning & Petrosian 2002; Burgess 2014; Acuner et al. 2019). Therefore, the empirical parameter values that are inferred from the data cannot be directly translated into physical model parameters. However, the way the physical model parameters map onto the Band parameters has been established for a few emission models (e.g., Lloyd & Petrosian 2000; Acuner et al. 2019, see also §4). Moreover, Acuner et al. (2020) showed that the values of, e.g., α can be used to decisively distinguish between various types of emission models, as long as the data have a high signal strength (as is the case in the present study).

We will therefore make use of these empirical functions. The Band function is defined by the low-energy power-law index (α) and the high-energy index (β), which are connected by a smoothly around the break energy (E_0).

The photon number spectrum is defined as

$$f_{\text{BAND}}(E) = A \begin{cases} \left(\frac{E}{E_{\text{piv}}}\right)^{\alpha} \exp\left(-\frac{E}{E_0}\right), & E \leq (\alpha - \beta)E_0 \\ \left[\frac{(\alpha - \beta)E_0}{E_{\text{piv}}}\right]^{(\alpha - \beta)} \exp(\beta - \alpha) \left(\frac{E}{E_{\text{piv}}}\right)^{\beta}, & E \geq (\alpha - \beta)E_0 \end{cases} \quad (1)$$

The energy of the spectral peak of the νF_{ν} spectrum (assuming $\beta < -2$) is in units of keV,

$$E_p = (2 + \alpha)E_0, \quad (2)$$

and A is the normalization factor at 100 keV in units of $\text{ph cm}^{-2}\text{keV}^{-1}\text{s}^{-1}$, E_{piv} is the pivot energy fixed at 100 keV, and α and β are the low- and high-energy power-law photon spectral indices, respectively.

The CPL function is given by

$$f_{\text{CPL}}(E) = A \left(\frac{E}{E_{\text{piv}}}\right)^{\alpha} \exp\left(-\frac{E}{E_c}\right) \quad (3)$$

Note that the CPL model approaches the Band model as β tends to $-\infty$. The peak energy E_p of the νF_{ν} spectrum is related to the E_c through $E_p = (2 + \alpha)E_c$.

The analysis in this work is performed with the Multi-Mission Maximum Likelihood Framework (3ML; Vianello et al. 2015) and we use a Bayesian approach, using the Markov Chain Monte Carlo (MCMC) method (e.g., Foreman-Mackey et al. 2013). We use the typical spectral parameters obtained from the previous *Fermi*-GBM catalog as the prior information of the Bayesian inference.

For the Band model,

$$\begin{cases} A \sim \log \mathcal{N}(\mu = 0, \sigma = 2) \text{ cm}^{-2}\text{keV}^{-1}\text{s}^{-1} \\ \alpha \sim \mathcal{N}(\mu = -1, \sigma = 0.5) \\ \beta \sim \mathcal{N}(\mu = -2, \sigma = 0.5) \\ E_p \sim \log \mathcal{N}(\mu = 2, \sigma = 1) \text{ keV} \end{cases} \quad (4)$$

and for CPL model,

$$\begin{cases} A \sim \log \mathcal{N}(\mu = 0, \sigma = 2) \text{ cm}^{-2}\text{keV}^{-1}\text{s}^{-1} \\ \alpha \sim \mathcal{N}(\mu = -1, \sigma = 0.5) \\ E_c \sim \log \mathcal{N}(\mu = 2, \sigma = 1) \text{ keV} \end{cases} \quad (5)$$

A posterior distribution is obtained from the prior distribution and the likelihood that combines the model and the observed data. The best model parameters are estimated from the posterior probability distribution obtained by MCMC sampling. When using MCMC sampling, in order to obtain the steady-state chains of the parameter distributions, the sampling needs to reach a certain number of times; therefore, the first part of the sample that has not reached the steady-state distribution is discarded. Therefore, for each parameter estimation, we take 10000 MCMC samples and discard the initial 20%. The fitted parameters are estimated by the Maximum A posteriori Probability (MAP) with uncertainties at 1σ (68%) Bayesian credible level and are based the last 80% of the MCMC samples. We also provide all of the analysis results of each time-resolved spectrum, which includes the best parameter value estimates, covariance matrices, and the statistical information criteria. They can be retrieved at doi: <https://zenodo.org/record/4746267>.

2.6. High-energy Power Law, β , and the Preferred Model Selection

For a majority of time-resolved burst spectra, the CPL model is a sufficient model (e.g. Kaneko et al. 2006; Goldstein et al. 2012; Burgess et al. 2019; Yu et al. 2019). However, in some cases, a high-energy power law significantly improves the fit, indicating a significant flux contribution beyond the spectral peak. In the case of synchrotron emission, the high-energy power law provides information about the particle acceleration and the nature of the shocks, while in the case of photospheric emission, it provides information about the energy dissipation in the emitting region.

In order to determine whether a high-energy power law gives significant improvement in our analysis, we compare the information criteria of the Band and the CPL fits. Acuner et al. (2020) showed that the information criteria capture everything important in the fits and that the difference in information criteria can be used in the model comparison. In particular, they showed that a significance of 99% of preferring one model over the other is found for a difference in log evidence greater than 5 (their Eq. 6) and that this corresponds approximately to a difference in information criteria of 10 (further discussion can be found in Acuner 2019⁴). In this work, we therefore adopt the information criterion to compare models, and, following the literature in the field (e.g., Greiner et al. 2016; Yu et al. 2019), we particularly use the deviance information criterion (DIC; Spiegelhalter et al. 2002; Moreno et al. 2013), which is defined as $DIC = -2\log[p(\text{data}|\hat{\theta})] + 2p_{\text{DIC}}$, where $\hat{\theta}$ is the posterior mean of the parameters, and p_{DIC} is a term to penalize the more complex model for overfitting (Gelman et al. 2014). We consequently accept the Band function as the preferred model if the difference between the Band's DIC and the CPL's DIC $\Delta DIC = DIC_{\text{Band}} - DIC_{\text{CPL}} > -10$.

For consistency, one needs to use the same empirical model throughout the whole pulse in order to avoid artificial fluctuation due to change of spectral model (see Yu et al. 2019). Consequently, if one time bin has $\Delta DIC < -10$ then we use the Band function throughout the pulse. Otherwise, we use the simpler CPL model. Therefore, the pulses that are fitted by a Band function have at least one

⁴ Z. Acuner, ‘Statistical Investigations of the Emission Processes in Gamma-ray Bursts’, PhD dissertation, KTH Royal Institute of Technology, Stockholm, 2019.

time bin in which a high-energy power law is significantly detected. The model used for each pulse is listed in column 6 in Table 2.

Among all of the individual time bins, we find that in only 29 % (274/944) is $\Delta\text{DIC} < -10$, i.e., the Band function is preferred. For these time bins, a high-energy power law is required by the data (see also Gruber et al. 2014; Yu et al. 2019). For the sequence of pulses, we find the corresponding fractions to be 36% (122/338) for the first pulse P_1 , 28% (101/361) for P_2 , 22% (34/156) for P_3 , 15% (7/46) for P_4 , 15% (4/26) for P_5 , and 29% (5/17) for P_6 . There is only a weak trend, with the first pulse P_1 having the largest fraction.

Turning over to the pulses, we find that 66% (77/117) of them have at least one time bin with $\Delta\text{DIC} < -10$, therefore the Band function is used for the entire pulse. For the sequence of pulses, we find that the corresponding fractions are 77% (30/39) for P_1 , 69% (27/39) for P_2 , 63% (15/24) for P_3 , 22% (2/9) for P_4 , 50% (2/4) for P_5 , and 50% (1/2) for P_6 . Again, there is only a weak trend, with the first pulse P_1 having a larger fraction.

In addition to the ΔDIC criterion, we also examined the p_{DIC} values following Yu et al. (2019). In some instances, the values were found to be anomalously large (hundreds of thousands), which typically indicates that a local rather than a global minimum of the likelihood function is found. In these cases, we reran the Bayesian fits with new initial values to ensure proper convergence to the global minimum.

3. OBSERVATIONAL PROPERTIES AMONG PULSES

We now investigate how the emission properties vary among the pulses within bursts. We compare the group consisting of the first pulse in every burst (P_1) with the group containing the second pulse in each burst (P_2), and so on. The number of spectra in each pulse group decreases, with the first three groups having above 100 spectra each (338, 361, and 156) and the last three only having a few tens (46, 26, and 17).

The identification and binning of the analyzed pulses, as well as their spectral properties, are listed in Table 2. The table includes the *Fermi*-GBM ID (column 1), the time-series pulse (Column 2), the pulsedwise source intervals (column 3), the total and used ($S \geq 20$) time bins (column 4) by using the BBlocks across the source intervals for each pulse, the identified grade of the pulse (column 5), the best spectral model (column 6), the preferred physical model (column 7), the pulsedwise evolution of the spectral parameters (column 8 for E_p and column 9 for α), and the type of parameter relations with the Spearman's rank coefficient, r , in the parentheses: F - α (column 10), F - E_p (column 11), and α - E_p (column 12). Figure 1 shows the histograms of the number of pulses in each pulse group (left side) and the corresponding number of spectra (right side). In the following section, we only consider the best-fit model for each pulse according to §2.6.

3.1. Parameter Distributions

Figure 2 shows the parameter distributions for every group of pulses, including α , E_p , and the K -corrected energy flux F ($\text{erg cm}^{-2} \text{s}^{-1}$), over the range 1- 10^4 keV, as well as the duration, Δt , of the pulses. In the following figures, the data points are colored orange (P_1), blue-magenta (P_2), violet (P_3), yellow (P_4 or P_{4+5+6})⁵, cyan (P_5), and green (P_6). The best Gaussian fit for each distribution is presented, and the corresponding average values and standard deviations are presented in Table

⁵ Note that, in some cases, we combine the data for the three last pulse groups (P_{4+5+6}), since the parameter distributions are typically similar and an increased sample size improves the fits.

3. The average value of the full sample, including all pulses, $\alpha = -0.84 \pm 0.35$ and $E_p = \log_{10}(214) \pm 0.42$. These values are in agreement with previous catalogs (e.g., [Kaneko et al. 2006](#)).

In order to assess whether the distributions change between the different pulse groups, we use the Kolmogorov-Smirnov (K-S) test. This test determines the chance probability, P , that two distributions are sampled from populations with identical distributions. For our purposes, we use $P < 10^{-2}$ to ensure that the distributions are truly different. In Table 4 we present the P -values for all the α and E_p distributions for the pulse groups.

These results indicate that the groups of pulses could be divided into two categories with two different behaviors. The first category, with P_1 and P_2 , is different from the rest of the pulse groups. In the first group of two pulses (P_1 and P_2), the peak energy E_p does not change, while the spectral slope α exhibits a clear softening. Compared to the second category, with the later pulse groups (P_3 – P_6), there is a change, with both α and E_p decreasing. However, within this second category, the distributions are not significantly different. Based on this analysis alone, it can, therefore, be argued that these two categories represent different types of spectral characteristics and, therefore, possibly different emissions.

The comparison between the fluxes and pulse durations is shown in the bottom panels of Figure 2. The fluxes have a similar pattern as α . There is a steady decrease, except for the last two groups, which have a similar distribution. Finally, the pulse duration distributions are comparable, and the first three groups have increasing average values.

Another way to compare the variation of emission properties in between pulses is to study the maximal value of the parameters of α and E_p in each pulse and how they vary. Note that α_{\max} and $E_{p,\max}$ do not necessarily need to be at the same time bin. In the upper panels in Figure 3, we present $\alpha_{\max} = \alpha_{\max}(t)$ and $E_{p,\max} = E_{p,\max}(t)$ versus time. Here, the trend of softening is again revealed for α_{\max} . Later pulses typically have smaller α_{\max} . There is also a trend that α_{\max} for the first pulse is softer the further it is delayed from the trigger. For $E_{p,\max}$, however, there is no trend, and the distinction between the two categories from the K-S test is not as apparent. This means that, when it comes to $E_{p,\max}$ and α_{\max} , it is mainly the spectral shape that changes and not the location of the peak energy when we compare the six pulse groups.

In the lower panels in Figure 3, the dependency of α_{\max} and $E_{p,\max}$ on pulse duration Δt is shown. The colored star correspond to the average values. For the first three groups, the increase in average pulse duration is correlated with the decrease in the average values of α_{\max} and $E_{p,\max}$ (see Fig. 2). Again, the last group with $P_{(4+5+6)}$ differs from the trend by having a shorter (average) pulse duration. However, instrumental effects might play a role here. The fluxes of later pulses are lower; hence, the full duration of the pulses might not be apparent above the background noise level.

3.2. Spectral Evolution

Early investigations of GRB emission identified a significant correlation between spectral properties, such as a relation between the intensity and the shape of the spectrum ([Wheaton et al. 1973](#)), and a correlation between the intensity and the spectral peak ([Golenetskii et al. 1983](#)). In this section, we classify the evolution of α and E_p relative to the count light curves, as commonly done in the literature (e.g., [Kargatis et al. 1994](#); [Ford et al. 1995](#)). In the §3.3 we will quantify this further by investigating the actual correlations between the parameters.

Examples of the evolution of the spectral parameters E_p , and α , and the νF_ν flux are provided in the upper panels of Figure 4. Here the parameter evolutions are overlaid on the count light curve. In

the Appendix, we further provide the corresponding figures for all bursts (Figure A1, A2, A3) as well as the figures for all bursts for the evolution of the spectral parameter β . Following the traditional classification, we use the notation that the parameter value is denoted as ‘hard’ when referring to large values of both α and E_p , as opposed to soft values (low values of α and E_p). We categorize the evolution in the two main groups: those with a hard-to-soft (*h.-t.-s.*) pattern, that is, the parameters decrease independent of the rise and decay of the pulse, and those with a flux-tracking (*f.-t.*) pattern, that is, the parameters are correlated with the rise and decay of the flux with or without a time lag. In a handful of cases, other patterns are also identified. The classification of the pulses is given in Table 2 (columns 8-9).

For the E_p evolution (see Figure A1 and Column 8 in Table 2), we find that the hard-to-soft and flux-tracking patterns are the two dominant patterns in our multipulse sample. We find that about two-thirds ($63/103 = 61\%$) of the pulses show a flux-tracking pattern and about one-third ($32/103 = 31\%$) of the pulses exhibit a hard-to-soft pattern. Other evolution patterns are rarely observed. For instance, we only identify two cases showing the hard-to-soft-to-hard pattern (e.g., the P_4 in GRB 101014175), one case displaying the soft-to-hard evolution (the P_1 in GRB 170207906), and three cases exhibiting a hard-to-soft followed by a flux-tracking evolution within a pulse (e.g., the P_1 in GRB 091127976). Here we note that previous investigations found that about two-thirds of cases have a hard-to-soft behavior, while a smaller fraction has a flux-tracking behavior (e.g., Ford et al. 1995; Crider et al. 1997; Lu et al. 2012; Yu et al. 2019). This fact is at odds with the observation in our sample. This is further discussed in Section 5.2.

For the α evolution (see Figure A2 and column 9 in Table 2), we find, similarly, that the hard-to-soft and the flux-tracking patterns dominate. The flux-tracking pattern accounts for 65% ($67/103$) of the pulses, while the hard-to-soft pattern accounts for 25% ($26/103$) of the pulses. These two patterns thus account for 90% of the pulses. Among the rest of the pulses, we find that three cases have a soft-to-hard evolution (e.g., the P_1 in GRB 110625881), and one case has a hard-to-soft-to-hard evolution (the P_4 in GRB 101014175). Moreover, we also identify two cases showing a “flat” (or weak rise) behavior throughout the pulse (e.g., the P_1 in GRB 120129580), and two cases have no clear trend at all (e.g., P_1 in GRB 120728434), which is not found in the E_p evolution.

We note that the E_p and α evolutionary patterns during a single pulse are not necessarily the same. In roughly half of the pulses ($51\% = 53/103$), the E_p and α evolution are classified to have the same pattern, while 49% ($50/103$) of the pulses do not have the same pattern.

Finally, the patterns of the spectral evolution for $E_p(t)$ and $\alpha(t)$ can vary from pulse to pulse within a burst. We find that in only about half of the pulses, the patterns of the $E_p(t)$ evolution between two adjacent pulses are the same ($55\% = 35/64$), and the rest 45% ($29/64$) are the inconsistent cases. Similarly, for $\alpha(t)$, we also find that for about half of the pulses, the spectral evolution among different pulses shares a similar pattern, accounting for 58% ($37/64$) of the pulses, while the inconsistent cases account for 42% ($23/64$) of the pulses. However, there is no significant variation in the fraction of pulses that are classified as having a tracking behavior between the six pulse groups, which all have around a two-thirds fraction (Table 5 and Figure 5)

3.3. Parameter Correlations

We now turn to investigating the correlation between the following parameter pairs: $(\log F, \alpha)$, $(\log F, \log E_p)$, and $(\alpha, \log E_p)$. Examples of these relations are provided in the lower panels of Figure 4, where functional fits are made. The leftmost panel shows the fit of $F = F_0 e^{k\alpha}$, where

$k \sim 3.37 \pm 0.49$ (a typical value; Ryde et al. 2019), the middle panel shows the power law between F and E_p with index 1.50 ± 0.15 (a typical value; Borgonovo & Ryde 2001), and finally the rightmost panel shows a fit to $\alpha = k_2 \ln(E_p/E_0) + \alpha_0$, where $k_2 = -2.01 \pm 0.20$. In the Appendix, we further provide the corresponding figures of these correlations for the full sample (Figs. A5, A6, A7).

We visually inspect the correlations and classify them according to the scheme in Yu et al. (2019), who classified them into three behaviors. The first behavior is a monotonic relation, defining Type 1. It can be divided into three categories: type 1p, monotonic positive correlation; type 1n, monotonic negative correlation; and type 1f, flat relation. The second behavior has two piecewise monotonic relations combined at a break point. This behavior is defined as type 2, and is divided into two subcategories, either a concave (type 2p) or a convex (type 2n) function. No clear trend is classified as type 3. The classification is given in Table 2.

The strengths of the correlations are given by the Spearman’s rank r . Strong correlations have $r > 0.7$, and weak correlations have $r < 0.4$. For both the F - α and F - E_p relations, around half of the pulses have strong correlations (47/103 and 54/103), and a quarter have weak correlations (27/103 and 26/103). In contrast, the α - E_p relations have the reverse properties: strong correlations in 21/103 and weak correlations in 57/103.

Among the pulses with strong correlations, we find that for the F - α relation, the vast majority has a positive monotonic relation (1p; 38/47), only a few have a negative relation (1n; 6/47). Similarly, for the F - E_p relation, a vast majority have a positive power law (1p; 45/51). Finally, for the α - E_p -relation, a negative and positive relations are equally common (1n; 9/21) and (1p; 8/21).

The three relations F - α , F - E_p , and E_p - α typically do not have strong correlations at the same time. However, in a few cases, they do: 13 out of the 103 pulses have $r > 0.7$ or $r < -0.7$ for all correlations at the same time. An example of a spectral evolution with simultaneous strong correlations is the single-pulse burst GRB 131231A, where all three relations have monotonic positive correlations (Li et al. 2019). In the following discussions, we summarize the correlations of all of the pulses independent of their r values.

3.3.1. Individual F - α Relation

For each individual burst, the F - α plot is shown in Figure A5, and the identified type, as well as its Spearman’s coefficient r is summarized in column 10 in Table 2. The statistical results are presented in the lower left panel in Figure 5.

We find that the dominant F - α relation is a monotonic correlation in the log-linear plots (type 1) accounting for 87 pulses (84%). Of these, 69 are of type 1p, accounting for 67%, and 16 are of type 1n, accounting for 15%. Among the rest, 13% (13/103) are of type 3.

To identify any change in spectral properties among the pulses, we compare the frequency of the dominating types 1p and 1n in each pulse group. The proportion of the frequencies of these types are all high. For P_1 , the proportion of type 1p versus type 1n is 19/8, and for the following pulses, it is 28/6 (P_2), 14/1 (P_3), 4/1 (P_4), 3/0 (P_5), and 1/0 (P_6). No apparent variation in the relative frequency is identified, apart from the tendency that the negative F - α relations are proportionally more common in P_1 . An example is given by GRB150330, which has three well-separated pulses; the first pulse is a clear type 1n, while the following two pulses have positive relations (type 1p), also studied in detail by Li (2019a). The change in correlation pattern corresponds to a change in the range of α values for the pulses. Li (2019a) therefore suggested that a change in jet properties should account for both of these properties.

We also note that there are only three pulses that are classified as type 2 (relation with a break), and all of these are type 2p and all are identified in the first pulse (GRB 081009, GRB 100719, and GRB 100826). Finally, we find that in 25% (14/57) of cases, the types change between adjacent pulses.

3.3.2. Individual F - E_p Relation

The classification of the F - E_p relation in Figure A6, is shown in column 11 of Table 2, and the lower middle panel of Figure 5. We find that a monotonic correlation in the log-log plots is again the most common type in the F - E_p relation, accounting for 75 (72%) of the pulses, of which 74 (71%) are type 1p (similar to the fraction for the F - α relation), and only one case (P_3 in GRB 090131) is identified as type 1n (a much lower fraction compared to the F - α relation), and no type 1f pulse is found. Among the rest, 18% (19/103) of the pulses have no clear trend (type 3) and 8% (8/103) have a broken power-law behavior (type 2p).

We again compare the frequency of the dominating types, which in this case are type 1p versus type 2p. The proportions are all very high, without any significant variation amongst the groups: 20/6 (P_1), 33/1 (P_2), 14/1 (P_3), 4/0 (P_4), 2/0 (P_5), and 1/0 (P_6). There is a slight tendency, though, for type 2p to be proportionally more prevalent in P_1 . We note that the F - E_p relation does not change between two adjacent pulses for a majority of cases.

3.3.3. Individual α - E_p Relation

For the α - E_p relation (see Figure A7 and column 12 in Table 2), we find that pulses with a monotonic relation (type 1) dominate (72% = 74/103). However, compared to the F - α and F - E_p relations, the number of type 1p and type 1n are more even: 32% = 33/103 and 36% = 37/103, respectively. Type 2 pulses account for 20% (21/103) of cases, of which 15 are type 2p and six are type 2n. Type 3 has 8% (8/103).

The proportion between the frequencies of the two dominating types, type 1p and type 1n, for the six pulse groups are 2/15 (P_1), 18/11 (P_2), 8/7 (P_3), 3/2 (P_4), 2/1 (P_5), and 0/1 (P_6). Apart from P_1 , there is no apparent variation between the pulse groups. However, for P_1 , there is a disparity; only 44% (17/39) are of Type 1, compared 72% for all pulses. Out of these 17, type 1n clearly dominates, in contrast to all other pulses, where type 1p is slightly dominant instead. We note that, in contrast to the other correlations, most of the α - E_p correlations are weak (§3.3). To confirm this tendency, we therefore particularly investigate only the strong correlations (21 pulses with $r > 0.7$). Of these, there are seven P_1 , and they all are of type 1n. Ten cases are P_2 , and of these, three are of type 1n and five of type 1p. We therefore conclude that for the α - E_p relation, the first pulses have (i) a smaller fraction of type 1 and (ii) of these type 1n have a higher fraction compared to the later pulses. Finally, we find that 46% (26/57) of the α - E_p relations change between two adjacent pulses.

4. ASSESSMENT OF THE COMPATIBILITY WITH EMISSION MODELS

In both synchrotron and photosphere models, there are many different types of spectra that can be produced, mainly depending on the location of the emission site and the flow properties. The spectral shape from a synchrotron emitting source depends on the relation between the radiative cooling time and other timescales, related to heating and adiabatic expansion (Lloyd & Petrosian 2000; Tavani et al. 2000). The steepest low-energy power law that is allowed (for isotropically distributed pitch angles) is $\alpha = -2/3$ for slow-cooled emission (SCS), while steeper slopes down to $\alpha = -3/2$ are

expected for (marginally) fast-cooling emission. Similarly, the properties of the emission from the photosphere depend on the emission site and the amount of dissipation that occurs in the vicinity of the photosphere. If there is no energy dissipation, the spectrum is expected to be slightly broader than a Planck function, namely the nondissipative photosphere (NDP; [Beloborodov 2011](#); [Acuner & Ryde 2018](#); [Meng et al. 2019](#)). Typically, though, dissipation is expected around the photosphere, which thus causes the spectral shape to broaden further ([Giannios & Spruit 2005](#); [Rees & Mészáros 2005](#); [Pe'er et al. 2006b](#); [Vurm et al. 2013](#)).

A few attempts have been made to fit particular cases of these models to the data directly (e.g., [Lloyd-Ronning & Petrosian 2002](#); [Ryde 2004, 2005](#); [Ahlgren et al. 2015](#); [Ryde et al. 2017](#); [Oganesyan et al. 2019](#); [Acuner et al. 2020](#); [Burgess et al. 2020](#)). However, such studies are limited by the range of models that are used and by the limited samples that can be studied due to the computationally costly procedures. Alternatively, synthetic data from a certain physical model can be produced by using the detector response. The synthetic data can then be fitted with empirical models, accounting for the limitations of the typically adopted analysis methods. Such a procedure identifies the parameter space of the empirical model that corresponds to that particular physical model.

The relation between α and E_p that such investigations yield for slow-cooled synchrotron (SCS) and the NDP are shown by the green and pink lines in the upper panel of Figure 6. These lines are reproduced from Figure 4 of [Burgess et al. \(2015\)](#) and Figure 3 of [Acuner et al. \(2019\)](#). Using these lines, general assessments of the emission process can be made. For instance, if we assume that the same emission mechanisms operate throughout the pulse, a single data point above the SCS line indicates that the pulse has a higher probability of being of a photospheric origin ([Acuner et al. 2019](#); [Dereli-Bégué et al. 2020](#)).

4.1. Spectral Shape

In the upper panel of Figure 6 we plot the values of α_{\max} and the corresponding value of E_p , with one data point from every pulse. Comparing with the limiting lines for SCS and the NDP, we find that 67% (79/103) of all the pulses have at least one data point above the SCS line and 21% (22/103) of all the pulses have a data point above the NDP line.

The number of pulses that are above the NDP and SCS lines for the sequence of pulses is shown in the lower panel of Figure 6, together with the corresponding fractions. The first two pulses in a burst have a larger fraction above the SCS line. There is a clear decrease in later pulses. There are, however, a couple of bursts in which the hardest spectrum occurs at late times. This fact is reflected in the large fraction for P_5 in Figure 6. Examples of these bursts are GRB 121225 and GRB 140810, where the largest α occurs at around 50s after the trigger.

As mentioned above, the spectra with (E_p, α_{\max}) values lying above the SCS line can be expected to have a higher probability of having a photospheric origin. However, how big this probability is can only be answered by a model comparison of the physical models, for instance, through Bayesian evidence. In any case, for spectra close to the SCS line, a model comparison will be inconclusive, since both models can produce similar spectra (over the observed energy range). [Acuner et al. \(2020\)](#) investigated this point quantitatively and found that a photospheric preference can be claimed, with great confidence, only for spectra with $\alpha \sim > -0.5$, as long as the data have a high significance. To illustrate this point, we perform the Bayesian model comparison for two example time bins in GRB150330 (at 1.4 and 137.0 s). We calculate the Bayesian evidence for the NDP spectrum, Z_{NDP} , and the evidence for the the slow-cooled synchrotron spectrum, Z_{SCS} . As shown in [Acuner](#)

[et al. \(2020\)](#), a log-evidence difference of $\ln Z_{NDP}/\ln Z_{SCS} \gtrsim 2$ indicates that the NDP spectrum is preferred, while if the ratio is less than -2, the SCS spectrum is the preferred model. For the 1.4 s time bin, $\alpha = -0.24$, and we find that $\ln Z_{NDP}/\ln Z_{SCS} = 33.6$, strongly favoring a photospheric origin. Correspondingly, the 137.0 s time bin, which has $\alpha = -0.9$, we find that $\ln Z_{NDP}/\ln Z_{SCS} < -78.9$, strongly favoring an SCS origin (in the comparison between these two specific models). This shows again that the α value can be used to make an approximate model comparison in order to identify the preferred model, which is sufficient for the present study. A full model comparison investigation based on Bayesian evidence is beyond the scope of this paper.

We therefore identify spectra that have $\alpha_{\max} > -0.5$ according to the [Acuner et al. \(2020\)](#) criterion. These spectra are denoted by Ph in the Table 2 and shown by the blue bars in the lower panel of Figure 6. The fraction of these spectra steadily decreases for subsequent pulses. For the first pulse in a burst, nearly half of all pulses (18/39) pass this very stringent criterion. The fraction decreases by approximately a half for every following pulse.

4.2. Spectral Evolution and Correlations

We now examine the spectral evolution and correlations for the pulses that are compatible with photospheric emission (Ph in Table 2). The purpose is to assess whether they have a different characteristics of their spectral properties.

For the photospheric pulses, the majority are classified as flux-tracking or hard-to-soft for both E_p and α . For the E_p -evolution, the tracking pattern is found in about half, or 47% (20/43), which is only somewhat lower than in the full sample. However, for the α evolution flux tracking is still dominant with 63% (27/43), similar to the full sample.

Turning over to the parameter correlations, we find that 47% (20/43), 51% (22/43), and 26% (11/43) have a strong correlation ($r > 0.7$) for the F - α relations, the F - E_p relation, and the α - E_p relation, respectively. These fractions are similar to the ones for the full sample, which indicates that the strength of the correlation does not depend on whether the pulses are photospheric or not.

We again consider the two main types of correlations for each pair of parameters. For the F - α relation, the two main types in the full sample were positive (1p) and negative (1n) monotonic correlations. For the photospheric pulses, these fractions are 60% (26/43) type 1p and 21% (9/43) type 1n. For the F - E_p -relation, the two main patterns are type 1p and convex relation (type 2p) and the photospheric pulses have 60% (26/43) type 1p and 16% (7/43) type 2p. Finally, the α - E_p relation has 21% (9/43) type 1p and 35% (15/43) type 1n. Compared to the full sample (§3) these fractions are not significantly different.

5. DISCUSSION

5.1. Comparison with a Single-pulse Sample

The bursts in our sample were specifically selected, since they have multiple pulses. Here we address the question of whether or not the spectral properties of the pulses in our sample are similar to those of the single-pulse bursts. To do this, we compare the results in [Yu et al. \(2019\)](#), who studied a sample of 37 single-pulse bursts.

In Figure 7 we compare the distributions of duration T_{90} , peak flux, fluence, and the time-integrated spectral shape (E_p , α , and β from the Band function fit). Our sample is shown by magenta lines, and the [Yu et al. \(2019\)](#) sample is shown by the green lines. All of these parameters are collected from the *Fermi*-GBM catalog. Both the peak flux (1024 ms timescale) and the fluence are taken over

the 10-1000 keV range. The average values and standard deviations (1σ error) are presented in Table 6. Both the peak flux and the fluence are approximately double for the multipulse bursts. Also, the α distribution is shifted to softer values for the multipulse bursts. On the other hand, the E_p and β values are similar between the samples. The corresponding probabilities from K-S tests are 0.02, $< 10^{-2}$, $< 10^{-2}$, 0.86, $< 10^{-2}$, and 0.19 for t_{90} , peak flux, fluence, E_p , α , and β , respectively.

In Figure 8 we compare the distributions of the time-resolved spectral parameters. In order to make a consistent comparison, we compare the results from using the CPL function throughout for both samples. This choice is based on the fact that in the Yu et al. (2019) sample, the CPL model is the best model. Likewise, we find that in only 29% of the time-resolved bins is the Band function a better choice (§2.6). We find that the average distribution of α is softer and the flux is larger for the multipulse sample. However, the E_p distributions are similar. These results are similar to the time-integrated spectra comparison. If we instead particularly identify the distribution of P_1 , we find that α distributions have similar peak values. On the other hand, the flux of P_1 is double the corresponding flux for the single-pulse bursts.

We also compare the frequency of the parameter relations between the samples. Most proportions between the patterns are similar. However, for the α - E_p relation, there is a notable difference. In our sample, the proportions are (72%) 74/103 for type 1 and (20%) 21/103 for type 2, while for the single-pulse sample, the proportions are (32%) 12/38 for type 1 and (45%) 17/38 for type 2. There is still a similarity in that the two pattern types are frequent in both samples; there is no strong dominance. However, in the multipulse sample the type 1 pattern is relatively more frequent.

5.2. On the Dominance of the Flux-tracking Pattern

We find that the largest fraction of pulses in our sample follow a tracking pattern, which is at odds with earlier investigations that instead found that the “hard-to-soft” evolution accounts for about two-thirds and the “flux-tracking” evolution only accounts for one-third of the observations (e.g., Ford et al. 1995; Lu et al. 2012; Basak & Rao 2013; Yu et al. 2019).

Lu et al. (2012) argued that if there is a significant overlap between pulses, the classified pattern might be affected. For instance, an apparently flux-tracking pulse might be a consequence of two overlapping hard-to-soft pulses. In our sample, many pulses are slightly overlapping, which means that in the transition period between the pulses, there are contributions from both pulses. Therefore, this might affect our results. To investigate this point, we particularly study the “gold” sample (see column 5 in Table 2). These nine bursts⁶ have 22 pulses that are clearly separated by periods of no emission. Among these, the flux-tracking pattern accounts for 59% (13/22) of the pulses, while the hard-to-soft pattern only accounts for 36% (8/22) of the pulses. These fractions are similar to the ones from the full sample (see §3.2). We conclude, therefore, that our sample is not greatly affected by the overlap between pulses.

Another possible reason for the difference is the binning methods used. We use a combination of BBlocks and significance and only consider the most significant time bins. The advantage of our method is that the substantial variations in the light curve are captured and the spectral fits are reliable. On the other hand, we might miss some of the rising phases of the pulses. Including a larger fraction of the pulse duration by using less significant data ($S < 20$), could change the apparent

⁶ GRB 081009, GRB 101014, GRB 140416, GRB 140508, GRB 150118, GRB 150330, GRB 151231, GRB 160802, and GRB171120.

pattern of evolution. The spectral evolution of the added periods might indeed be different, but more seriously, the spectral fits are less reliable and could therefore give misleading results.

A further uncertainty is the inherent problem in this type of classification. A subjective decision needs to be made on where a pulse starts and ends. This can affect the classification. Another point is the fact that the tracking behavior, in many cases, involves a timelag, both positive and negative. If this lag is large compared to the pulse size, the pulse could be classified as a hard-to-soft (or soft-to-hard) pulse instead. An example is the E_p pattern for GRB120328, where the tracking pattern depends on one data point during the rise phase. The same issue happens for α in other cases⁷. These uncertainties can affect the classification of different samples. However, these cases are not sufficient to explain the whole discrepancy.

Our results thus indicate that the flux-tracking pattern is the prevalent pattern for α and E_p , at least around the peak of the pulse, where the significance is the largest. This is also consistent with the global F - E_p relation in the middle panels in Figure A9.

5.3. Implication for the Radiation Process

Based on the analysis of the change in α and E_p (Section 3.1 and Fig. 2) alone, it was suggested that there are two categories of the pulse groups. The first one, consisting of P_1 and P_2 , has a constant E_p , while α softens. Within the second category, there is not much change, but they are all different from the first two pulses. Moreover, we found that the initial pulses had different spectral properties (frequency of different parameter correlation) as a group (§3.3). These distinctions lead to the possibility that they are due to different emission mechanisms.

In the simplest internal shock model, the late pulses (P_i with $i > 1$) occur above the photosphere and hence must have a synchrotron origin. We do not see such a clear distinction, indicating that at least the most simplest version of the internal shock model does not represent what we see.

For the photospheric scenario, the α value reflects the energy dissipation and photon production below the photosphere (e.g., Pe'er et al. 2006b; Vurm & Beloborodov 2016). The E_p instead is mainly set by properties at high optical depths. Therefore, if the first two pulses are photospheric, the fact that E_p is similar while α varies could be due to similar properties close to the central engine but a varying amount of turbulence in the flow causing the dissipation. The variability and pulse structures of the photospheric emission have been reproduced by numerical simulations of a jet passing through the progenitor surrounding. For instance, López-Cámara et al. (2014) showed that even with a steady central engine, a light curve with a pulse structure and large variability arises. The main cause is the Rayleigh-Taylor instabilities that arise in the contact between the layers of jet and the surrounding progenitor material. This leads to a variable amount of mixing between the layers and thereby a variable baryon load of the jet, which has a direct influence on the radiative efficiency and spectral shape (see, e.g., Rees & Mészáros 2005; Gottlieb et al. 2019).

On the other hand, the pulse groups, P_3-P_6 , all have $\alpha \sim -1$ (Fig. 2). This could be explained by synchrotron emission from electrons that are marginally fast-cooled (Daigne et al. 2011; Yu et al. 2015; Geng et al. 2018). It can thus be argued that the first two pulses are typically photospheric, while the rest are due to synchrotron emission. If this interpretation is correct, one would expect that the two categories would have distinct and different spectral properties. There are several points in the analysis above that, therefore, do not support this interpretation. First, the values of

⁷ GRB 110301, GRB 130606, GRB 131014, GRB 140213, GRB 141222, GRB 160422, and GRB 160802.

$E_{p,\max}$ are similar for all of the pulse groups (Fig. 3); there is no clear distinction between the pulse groups. Second, there is no clear distinction between pulse groups when it comes to the spectral evolution (§3.2) and types of correlations (apart from the initial pulses; §3.3). Third, the average pulse durations are also similar in all pulse groups. All of these points indicate that there is no drastic change in emission pattern between the pulses (apart from α).

On the contrary, the properties of the four last pulse groups can also be interpreted as photospheric emission. Previous studies have shown that pulses that, beyond any doubt, are photospheric do all have significant spectral evolution (e.g., Ryde et al. 2019). In particular, at the end of such pulses, α values down to -1 and below are common, which is interpreted as the result of subphotospheric dissipation with varying jet properties (e.g., Ryde et al. 2010, 2011). Consequently, pulses with $\alpha \sim -1$ could be the result of dissipative photospheres throughout the pulse. Indeed, the observation that the last four pulse groups all peak at around $\alpha \sim -1$ is in line with the theoretical expectations of fully dissipative photospheres, i.e., flows where there is no strong limitation, not on the soft photon production deep in the flow or the amount of dissipation in the parts of the flow where the spectrum is formed (Beloborodov 2010; Vurm et al. 2013).

Even though this line of argument makes the subphotospheric dissipation model appealing for most of the pulses, some admixture of synchrotron pulses is expected. The most prominent example of this is GRB190114C, which, apart from a very hard spectral component, showed a clear afterglow emission component already during the prompt phase (Ajello et al. 2020). This proved that a synchrotron component was present during the prompt phase (see also Axelsson et al. 2012; Iyyani et al. 2013). Further early examples of such a suggestion are given in Ryde (2005); Ryde & Pe'er (2009); Guiriec et al. (2011) and more recently in Wang et al. (2019b); Burgess et al. (2019); Wang et al. (2019a).

Many of these synchrotron components are observed at late times. Combined with the fact that the fraction of (certain) photospheric pulses decreases with pulse number (Fig. 6), emission compatible with synchrotron therefore appears to prevail mainly at the end of the prompt phases. Different possibilities exist for synchrotron emission to arise toward the end of the prompt phase. One example is GRB 150330, for which Li (2019a) suggested that the jet composition changes from a baryon-dominated flow during the first pulse to a Poynting-flux dominated flow during the rest of the burst, producing synchrotron emission (see also Zhang et al. 2018). Alternatively, during the early phases of the afterglow, shocks due to interaction between the jet and slower-moving material ahead of the jet will also produce efficient synchrotron emission (e.g., Duffell & MacFadyen 2015).

However, from the GBM data alone, it is not possible to make a firm conclusion as to whether a soft pulse is due to synchrotron emission or due to photospheric emission subject to dissipation below the photosphere, since they are indistinguishable in many cases (e.g., Acuner et al. 2020). Simultaneous data from other wavelengths can be useful in some cases be useful (e.g., Ravasio et al. 2018; Ahlgren et al. 2019; Ajello et al. 2020) or polarization measurements (e.g., Sharma et al. 2019).

6. SUMMARY

In this paper, we performed time-resolved spectroscopy on a sample of multipulse GRBs observed by *Fermi*-GBM during the first 11 yr of its mission. We investigated the variation in emission properties between the pulses in light of the prediction of emission models. Our sample consists of 39 bursts, from which have 117 distinct pulse structures, entailing 1228 time-resolved spectra. All of the spectra have a very high statistical significance of $S \geq 20$. This ensures that the spectral fits are well determined and that the low-energy power-law index α can be used to discriminate between spectra

that are compatible with the photosphere or with synchrotron emission. The emission properties we studied include the spectral shape and the correlations between spectral shape parameters.

For the sample as a whole, we found that flux-tracking evolution is more common than the hard-to-soft evolution, independent of the E_p or α evolution, differing from previous findings. We also found that a positive correlation is most common for the $F\text{-}\alpha$ and $F\text{-}E_p$ relations. In contrast, for the $\alpha\text{-}E_p$ relation, both the positive and negative correlations are equally common. In addition, we compared our sample to that of the single-pulse sample of [Yu et al. \(2019\)](#). We found that the peak flux is significantly larger and the average α value is softer in our sample, while peak energies are similar. On the other hand, we found that the average α value of the initial pulses of our multi-pulse sample is similar to that of the single-pulse sample.

Specifically, we searched for signatures of any characteristic variation in the emission properties between pulses that might reveal different underlying emission processes. We find that the characteristics of the pulses remain astonishingly similar. It is mainly the low-energy power-law index, α that has a significant softening (gets smaller). In addition, we find that, on average, the first pulse in each burst behaves slightly differently than consecutive pulses when it comes to correlations between spectral shape parameters.

We further assessed the compatibility of the data with emission models for each individual pulse. Assuming that the same emission mechanism operates during a pulse, any single time bin that violates the synchrotron limit indicates that a photospheric origin is more probable (Fig. 6). We also used the criterion that $\alpha_{\max} > -0.5$ which identifies pulses that significantly prefer photospheric emission ([Acuner et al. 2020](#)). The first pulse in a burst is clearly different from the later pulses: three-fourths of them violate the synchrotron emission, and half of them prefer photospheric emission. These fractions decrease rapidly for subsequent pulses.

We argue that in many cases, synchrotron emission in later pulses might contribute to these trends. However, the similarity between pulses, averaging over the whole sample, points to a photospheric origin of most pulses, albeit with greatly varying dissipation properties

We conclude that photospheric emission can be found at any time during the burst duration; however, it is more common in the early phase. In order to make a general statement of the emission mechanism in a GRB, the spectral softening of α between pulses is a property that needs to be considered. In particular, the analysis of individual pulses will be influenced by their occurrence relative to the trigger time. The chance to detect the photosphere is largest among the first few pulses, while synchrotron emission is mainly found at late times. This also allows for the coexistence of emissions at late times.

ACKNOWLEDGMENTS

We would like to thank Drs. Magnus Axelsson, Damien Bégué, Hüsne Dereli-Bégué, and Yu Wang for useful discussions. This research is supported by the Swedish National Space Agency and made use of the High Energy Astrophysics Science Archive Research Center (HEASARC) Online Service at the NASA/Goddard Space Flight Center (GSFC). In particular, we thank the GBM team for providing the tools and data that were used in this research. F.R. is supported by the Göran Gustafsson Foundation for Research in Natural Sciences and Medicine and the Swedish Research Council (Vetenskapsrådet), while A.P. acknowledges support from the EU via the ERC grant O.M.J. Part of this work was performed during Dr. Liang Li's visits with Professors Anzhong Wang, Qiang Wu, and Tao Zhu at the United Center for Gravitational Wave Physics (UCGWP), and Professors Yefei Yuan and Yifu Cai at the University of Science and Technology of China (USTC), China.

Facilities: *Fermi*/GBM

Software: 3ML([Vianello et al. 2015](#))

REFERENCES

- Acuner, Z. 2019, PhD thesis, KTH Royal Institute of Technology, Stockholm, Sweden.
<http://urn.kb.se/resolve?urn=urn:nbn:se:kth:diva-265527>
- Acuner, Z., & Ryde, F. 2018, MNRAS, 475, 1708, doi: [10.1093/mnras/stx3106](https://doi.org/10.1093/mnras/stx3106)
- Acuner, Z., Ryde, F., Pe'er, A., Mortlock, D., & Ahlgren, B. 2020, ApJ, 893, 128, doi: [10.3847/1538-4357/ab80c7](https://doi.org/10.3847/1538-4357/ab80c7)
- Acuner, Z., Ryde, F., & Yu, H.-F. 2019, MNRAS, 487, 5508, doi: [10.1093/mnras/stz1356](https://doi.org/10.1093/mnras/stz1356)
- Ahlgren, B., Larsson, J., Nymark, T., Ryde, F., & Pe'er, A. 2015, MNRAS, 454, L31, doi: [10.1093/mnrasl/slv114](https://doi.org/10.1093/mnrasl/slv114)
- Ahlgren, B., Larsson, J., Valan, V., et al. 2019, ApJ, 880, 76, doi: [10.3847/1538-4357/ab271b](https://doi.org/10.3847/1538-4357/ab271b)
- Ajello, M., Arimoto, M., Axelsson, M., et al. 2020, ApJ, 890, 9, doi: [10.3847/1538-4357/ab5b05](https://doi.org/10.3847/1538-4357/ab5b05)
- Atwood, W. B., Abdo, A. A., Ackermann, M., et al. 2009, ApJ, 697, 1071, doi: [10.1088/0004-637X/697/2/1071](https://doi.org/10.1088/0004-637X/697/2/1071)
- Axelsson, M., Baldini, L., Barbiellini, G., et al. 2012, ApJL, 757, L31, doi: [10.1088/2041-8205/757/2/L31](https://doi.org/10.1088/2041-8205/757/2/L31)
- Band, D., Matteson, J., Ford, L., et al. 1993, ApJ, 413, 281, doi: [10.1086/172995](https://doi.org/10.1086/172995)
- Basak, R., & Rao, A. R. 2013, ApJ, 768, 187, doi: [10.1088/0004-637X/768/2/187](https://doi.org/10.1088/0004-637X/768/2/187)
- Beloborodov, A. M. 2010, MNRAS, 407, 1033, doi: [10.1111/j.1365-2966.2010.16770.x](https://doi.org/10.1111/j.1365-2966.2010.16770.x)
- . 2011, ApJ, 737, 68, doi: [10.1088/0004-637X/737/2/68](https://doi.org/10.1088/0004-637X/737/2/68)
- . 2013, ApJ, 764, 157, doi: [10.1088/0004-637X/764/2/157](https://doi.org/10.1088/0004-637X/764/2/157)
- Borgonovo, L., & Ryde, F. 2001, ApJ, 548, 770, doi: [10.1086/319008](https://doi.org/10.1086/319008)
- Burgess, J. M. 2014, MNRAS, 445, 2589, doi: [10.1093/mnras/stu1925](https://doi.org/10.1093/mnras/stu1925)
- Burgess, J. M., Bégué, D., Greiner, J., et al. 2020, Nature Astronomy, 4, 174, doi: [10.1038/s41550-019-0911-z](https://doi.org/10.1038/s41550-019-0911-z)
- Burgess, J. M., Greiner, J., Bégué, D., & Berlato, F. 2019, MNRAS, 490, 927, doi: [10.1093/mnras/stz2589](https://doi.org/10.1093/mnras/stz2589)
- Burgess, J. M., Ryde, F., & Yu, H.-F. 2015, MNRAS, 451, 1511, doi: [10.1093/mnras/stv775](https://doi.org/10.1093/mnras/stv775)
- Crider, A., Liang, E. P., Smith, I. A., et al. 1997, ApJL, 479, L39, doi: [10.1086/310574](https://doi.org/10.1086/310574)
- Daigne, F., Bošnjak, Ž., & Dubus, G. 2011, A&A, 526, A110, doi: [10.1051/0004-6361/201015457](https://doi.org/10.1051/0004-6361/201015457)
- Dereli-Bégué, H., Pe'er, A., & Ryde, F. 2020, ApJ, 897, 145, doi: [10.3847/1538-4357/ab9a2d](https://doi.org/10.3847/1538-4357/ab9a2d)

- Duffell, P. C., & MacFadyen, A. I. 2015, ApJ, 806, 205, doi: [10.1088/0004-637X/806/2/205](https://doi.org/10.1088/0004-637X/806/2/205)
- Ford, L. A., Band, D. L., Matteson, J. L., et al. 1995, ApJ, 439, 307, doi: [10.1086/175174](https://doi.org/10.1086/175174)
- Foreman-Mackey, D., Hogg, D. W., Lang, D., & Goodman, J. 2013, PASP, 125, 306, doi: [10.1086/670067](https://doi.org/10.1086/670067)
- Gelman, A., Hwang, J., & Vehtari, A. 2014, STATISTICS AND COMPUTING, 24, 997, doi: [10.1007/s11222-013-9416-2](https://doi.org/10.1007/s11222-013-9416-2)
- Geng, J.-J., Huang, Y.-F., Wu, X.-F., Zhang, B., & Zong, H.-S. 2018, ApJS, 234, 3, doi: [10.3847/1538-4365/aa9e84](https://doi.org/10.3847/1538-4365/aa9e84)
- Giannios, D., & Spruit, H. C. 2005, A&A, 430, 1, doi: [10.1051/0004-6361:20047033](https://doi.org/10.1051/0004-6361:20047033)
- Goldstein, A., Burgess, J. M., Preece, R. D., et al. 2012, ApJS, 199, 19, doi: [10.1088/0067-0049/199/1/19](https://doi.org/10.1088/0067-0049/199/1/19)
- Golenetskii, S. V., Mazets, E. P., Aptekar, R. L., & Ilinskii, V. N. 1983, Nature, 306, 451, doi: [10.1038/306451a0](https://doi.org/10.1038/306451a0)
- Goodman, J. 1986, ApJ, 308, L47
- Gottlieb, O., Levinson, A., & Nakar, E. 2019, MNRAS, 488, 1416, doi: [10.1093/mnras/stz1828](https://doi.org/10.1093/mnras/stz1828)
- Greiner, J., Burgess, J. M., Savchenko, V., & Yu, H.-F. 2016, ApJL, 827, L38, doi: [10.3847/2041-8205/827/2/L38](https://doi.org/10.3847/2041-8205/827/2/L38)
- Gruber, D., Goldstein, A., Weller von Ahlefeld, V., et al. 2014, ApJS, 211, 12, doi: [10.1088/0067-0049/211/1/12](https://doi.org/10.1088/0067-0049/211/1/12)
- Guiriec, S., Connaughton, V., Briggs, M. S., et al. 2011, ApJL, 727, L33, doi: [10.1088/2041-8205/727/2/L33](https://doi.org/10.1088/2041-8205/727/2/L33)
- Ito, H., Matsumoto, J., Nagataki, S., Warren, D. C., & Barkov, M. V. 2015, ApJL, 814, L29, doi: [10.1088/2041-8205/814/2/L29](https://doi.org/10.1088/2041-8205/814/2/L29)
- Iyyani, S., Ryde, F., Axelsson, M., et al. 2013, MNRAS, 433, 2739, doi: [10.1093/mnras/stt863](https://doi.org/10.1093/mnras/stt863)
- Iyyani, S., Ryde, F., Ahlgren, B., et al. 2015, MNRAS, 450, 1651, doi: [10.1093/mnras/stv636](https://doi.org/10.1093/mnras/stv636)
- Kaneko, Y., Preece, R. D., Briggs, M. S., et al. 2006, ApJS, 166, 298, doi: [10.1086/505911](https://doi.org/10.1086/505911)
- Kargatis, V. E., Liang, E. P., Hurley, K. C., et al. 1994, ApJ, 422, 260, doi: [10.1086/173724](https://doi.org/10.1086/173724)
- Lazzati, D., Morsony, B. J., & Begelman, M. C. 2009, ApJL, 700, L47, doi: [10.1088/0004-637X/700/1/L47](https://doi.org/10.1088/0004-637X/700/1/L47)
- Li, L. 2019a, ApJS, 242, 16, doi: [10.3847/1538-4365/ab1b78](https://doi.org/10.3847/1538-4365/ab1b78)
- . 2019b, ApJS, 245, 7, doi: [10.3847/1538-4365/ab42de](https://doi.org/10.3847/1538-4365/ab42de)
- . 2020, ApJ, 894, 100, doi: [10.3847/1538-4357/ab8014](https://doi.org/10.3847/1538-4357/ab8014)
- Li, L., & Zhang, B. 2021, ApJS, 253, 43, doi: [10.3847/1538-4365/abded1](https://doi.org/10.3847/1538-4365/abded1)
- Li, L., Geng, J.-J., Meng, Y.-Z., et al. 2019, ApJ, 884, 109, doi: [10.3847/1538-4357/ab40b9](https://doi.org/10.3847/1538-4357/ab40b9)
- Lloyd, N. M., & Petrosian, V. 2000, ApJ
- Lloyd-Ronning, N. M., & Petrosian, V. 2002, ApJ, 565, 182, doi: [10.1086/324484](https://doi.org/10.1086/324484)
- López-Cámara, D., Morsony, B. J., & Lazzati, D. 2014, MNRAS, 442, 2202, doi: [10.1093/mnras/stu1016](https://doi.org/10.1093/mnras/stu1016)
- Lu, R.-J., Wei, J.-J., Liang, E.-W., et al. 2012, ApJ, 756, 112, doi: [10.1088/0004-637X/756/2/112](https://doi.org/10.1088/0004-637X/756/2/112)
- Mazets, E. P., Golenetskii, S. V., Ilinskii, V. N., et al. 1982, Ap&SS, 82, 261, doi: [10.1007/BF00651438](https://doi.org/10.1007/BF00651438)
- Meegan, C., Lichti, G., Bhat, P. N., et al. 2009, ApJ, 702, 791, doi: [10.1088/0004-637X/702/1/791](https://doi.org/10.1088/0004-637X/702/1/791)
- Meng, Y.-Z., Liu, L.-D., Wei, J.-J., Wu, X.-F., & Zhang, B.-B. 2019, ApJ, 882, 26, doi: [10.3847/1538-4357/ab30c7](https://doi.org/10.3847/1538-4357/ab30c7)
- Mészáros, P., & Rees, M. J. 2000, ApJ, 530, 292, doi: [10.1086/308371](https://doi.org/10.1086/308371)
- Moreno, E., Vazquez-Polo, F. J., & Robert, C. P. 2013, arXiv e-prints, arXiv:1310.2905. <https://arxiv.org/abs/1310.2905>
- Norris, J. P., Bonnell, J. T., Kazanas, D., et al. 2005, ApJ, 627, 324, doi: [10.1086/430294](https://doi.org/10.1086/430294)
- Norris, J. P., Nemiroff, R. J., Bonnell, J. T., et al. 1996, ApJ, 459, 393, doi: [10.1086/176902](https://doi.org/10.1086/176902)
- Oganesyan, G., Nava, L., Ghirlanda, G., Melandri, A., & Celotti, A. 2019, A&A, 628, A59, doi: [10.1051/0004-6361/201935766](https://doi.org/10.1051/0004-6361/201935766)
- Pe'er, A., Mészáros, P., & Rees, M. J. 2006a, ApJ, 642, 995, doi: [10.1086/501424](https://doi.org/10.1086/501424)
- . 2006b, ApJ, 652, 482, doi: [10.1086/507595](https://doi.org/10.1086/507595)
- Pe'er, A., Ryde, F., Wijers, R. A. M. J., Mészáros, P., & Rees, M. J. 2007, ApJL, 664, L1, doi: [10.1086/520534](https://doi.org/10.1086/520534)
- Piran, T., Shemi, A., & Narayan, R. 1993, MNRAS, 263, 861, doi: [10.1093/mnras/263.4.861](https://doi.org/10.1093/mnras/263.4.861)
- Planck Collaboration, Aghanim, N., Akrami, Y., et al. 2018, arXiv e-prints, arXiv:1807.06209. <https://arxiv.org/abs/1807.06209>

- Ravasio, M. E., Ghirlanda, G., Nava, L., & Ghisellini, G. 2019, A&A, 625, A60, doi: [10.1051/0004-6361/201834987](https://doi.org/10.1051/0004-6361/201834987)
- Ravasio, M. E., Oganesyan, G., Ghirlanda, G., et al. 2018, A&A, 613, A16, doi: [10.1051/0004-6361/201732245](https://doi.org/10.1051/0004-6361/201732245)
- Rees, M. J., & Meszaros, P. 1994, ApJL, 430, L93, doi: [10.1086/187446](https://doi.org/10.1086/187446)
- Rees, M. J., & Mészáros, P. 1998, ApJL, 496, L1, doi: [10.1086/311244](https://doi.org/10.1086/311244)
- . 2005, ApJ, 628, 847, doi: [10.1086/430818](https://doi.org/10.1086/430818)
- Ryde, F. 2004, ApJ, 614, 827, doi: [10.1086/423782](https://doi.org/10.1086/423782)
- . 2005, ApJL, 625, L95, doi: [10.1086/431239](https://doi.org/10.1086/431239)
- Ryde, F., Lundman, C., & Acuner, Z. 2017, MNRAS, 472, 1897, doi: [10.1093/mnras/stx2019](https://doi.org/10.1093/mnras/stx2019)
- Ryde, F., & Pe'er, A. 2009, ApJ, 702, 1211, doi: [10.1088/0004-637X/702/2/1211](https://doi.org/10.1088/0004-637X/702/2/1211)
- Ryde, F., & Svensson, R. 1999, ApJ, 512, 693, doi: [10.1086/306818](https://doi.org/10.1086/306818)
- Ryde, F., Yu, H.-F., Dereli-Bégué, H., et al. 2019, MNRAS, 484, 1912, doi: [10.1093/mnras/stz083](https://doi.org/10.1093/mnras/stz083)
- Ryde, F., Axelsson, M., Zhang, B. B., et al. 2010, ApJL, 709, L172, doi: [10.1088/2041-8205/709/2/L172](https://doi.org/10.1088/2041-8205/709/2/L172)
- Ryde, F., Pe'er, A., Nymark, T., et al. 2011, MNRAS, 415, 3693, doi: [10.1111/j.1365-2966.2011.18985.x](https://doi.org/10.1111/j.1365-2966.2011.18985.x)
- Sari, R., Piran, T., & Narayan, R. 1998, ApJL, 497, L17, doi: [10.1086/311269](https://doi.org/10.1086/311269)
- Scargle, J. D., Norris, J. P., Jackson, B., & Chiang, J. 2013, ApJ, 764, 167, doi: [10.1088/0004-637X/764/2/167](https://doi.org/10.1088/0004-637X/764/2/167)
- Sharma, V., Iyyani, S., Bhattacharya, D., et al. 2019, ApJL, 882, L10, doi: [10.3847/2041-8213/ab3a48](https://doi.org/10.3847/2041-8213/ab3a48)
- Spiegelhalter, D. J., Best, N. G., Carlin, B. P., & Van Der Linde, A. 2002, Journal of the royal statistical society: Series b (statistical methodology), 64, 583
- Tavani, M., Band, D., & Ghirlanda, G. 2000, in American Institute of Physics Conference Series, Vol. 526, Gamma-ray Bursts, 5th Huntsville Symposium, ed. R. M. Kippen, R. S. Mallozzi, & G. J. Fishman, 185–189, doi: [10.1063/1.1361531](https://doi.org/10.1063/1.1361531)
- Thompson, C. 2006, ApJ, 651, 333, doi: [10.1086/505290](https://doi.org/10.1086/505290)
- Uhm, Z. L., & Zhang, B. 2014, Nature Physics, 10, 351, doi: [10.1038/nphys2932](https://doi.org/10.1038/nphys2932)
- Vianello, G., Gill, R., Granot, J., et al. 2018, ApJ, 864, 163, doi: [10.3847/1538-4357/aad6ea](https://doi.org/10.3847/1538-4357/aad6ea)
- Vianello, G., Lauer, R. J., Younk, P., et al. 2015, arXiv e-prints. <https://arxiv.org/abs/1507.08343>
- Vurm, I., & Beloborodov, A. M. 2016, ApJ, 831, 175, doi: [10.3847/0004-637X/831/2/175](https://doi.org/10.3847/0004-637X/831/2/175)
- Vurm, I., Lyubarsky, Y., & Piran, T. 2013, ApJ, 764, 143, doi: [10.1088/0004-637X/764/2/143](https://doi.org/10.1088/0004-637X/764/2/143)
- Wang, X.-Y., Liu, R.-Y., Zhang, H.-M., Xi, S.-Q., & Zhang, B. 2019a, ApJ, 884, 117, doi: [10.3847/1538-4357/ab426c](https://doi.org/10.3847/1538-4357/ab426c)
- Wang, Y., Li, L., Moradi, R., & Ruffini, R. 2019b, arXiv e-prints. <https://arxiv.org/abs/1901.07505>
- Wheaton, W. A., Ulmer, M. P., Baity, W. A., et al. 1973, ApJL, 185, L57, doi: [10.1086/181320](https://doi.org/10.1086/181320)
- Yu, H.-F., Dereli-Bégué, H., & Ryde, F. 2019, ApJ, 886, 20, doi: [10.3847/1538-4357/ab488a](https://doi.org/10.3847/1538-4357/ab488a)
- Yu, H.-F., Greiner, J., van Eerten, H., et al. 2015, A&A, 573, A81, doi: [10.1051/0004-6361/201424858](https://doi.org/10.1051/0004-6361/201424858)
- Yu, H.-F., Preece, R. D., Greiner, J., et al. 2016, A&A, 588, A135, doi: [10.1051/0004-6361/201527509](https://doi.org/10.1051/0004-6361/201527509)
- Zhang, B. 2018, The Physics of Gamma-Ray Bursts, doi: [10.1017/9781139226530](https://doi.org/10.1017/9781139226530)
- Zhang, B.-B., Zhang, B., Castro-Tirado, A. J., et al. 2018, Nature Astronomy, 2, 69, doi: [10.1038/s41550-017-0309-8](https://doi.org/10.1038/s41550-017-0309-8)

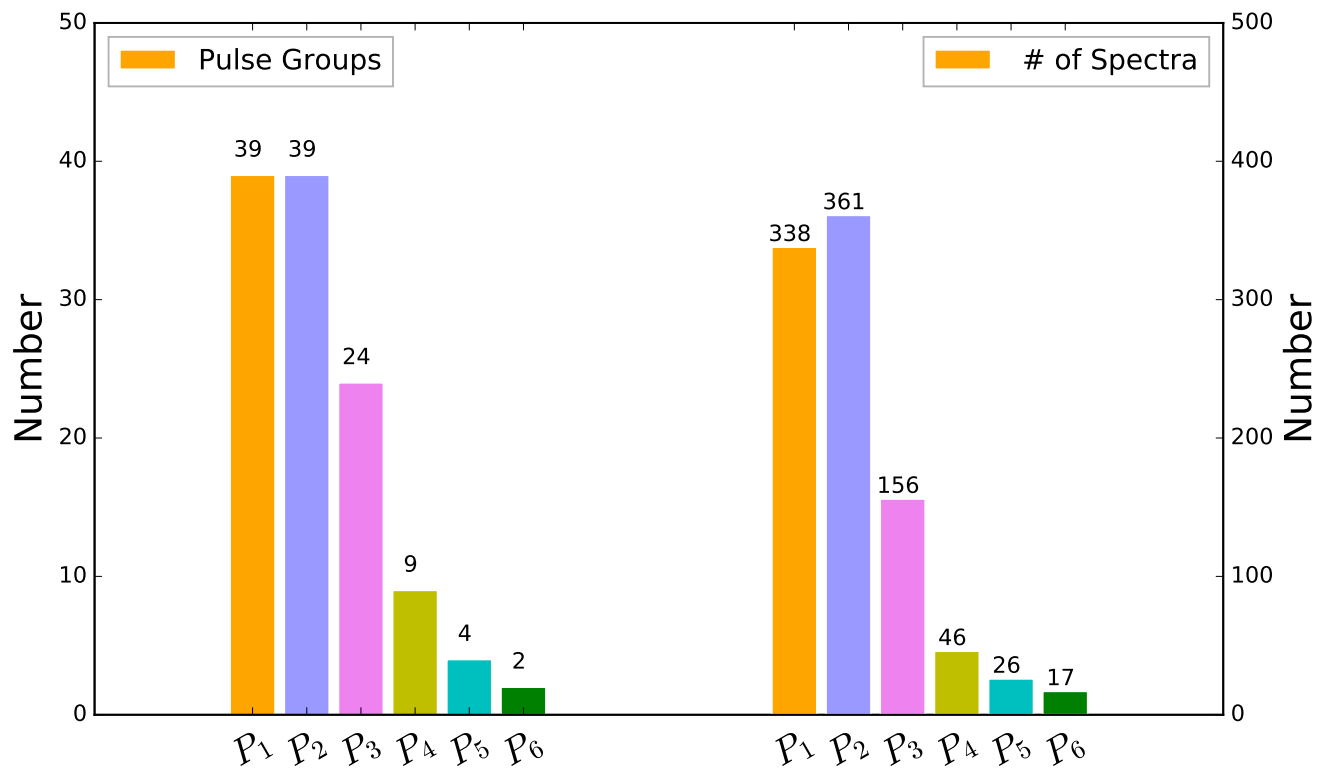


Figure 1. Histograms of the numbers of pulses (left) and spectra (right) in each pulse grouping.

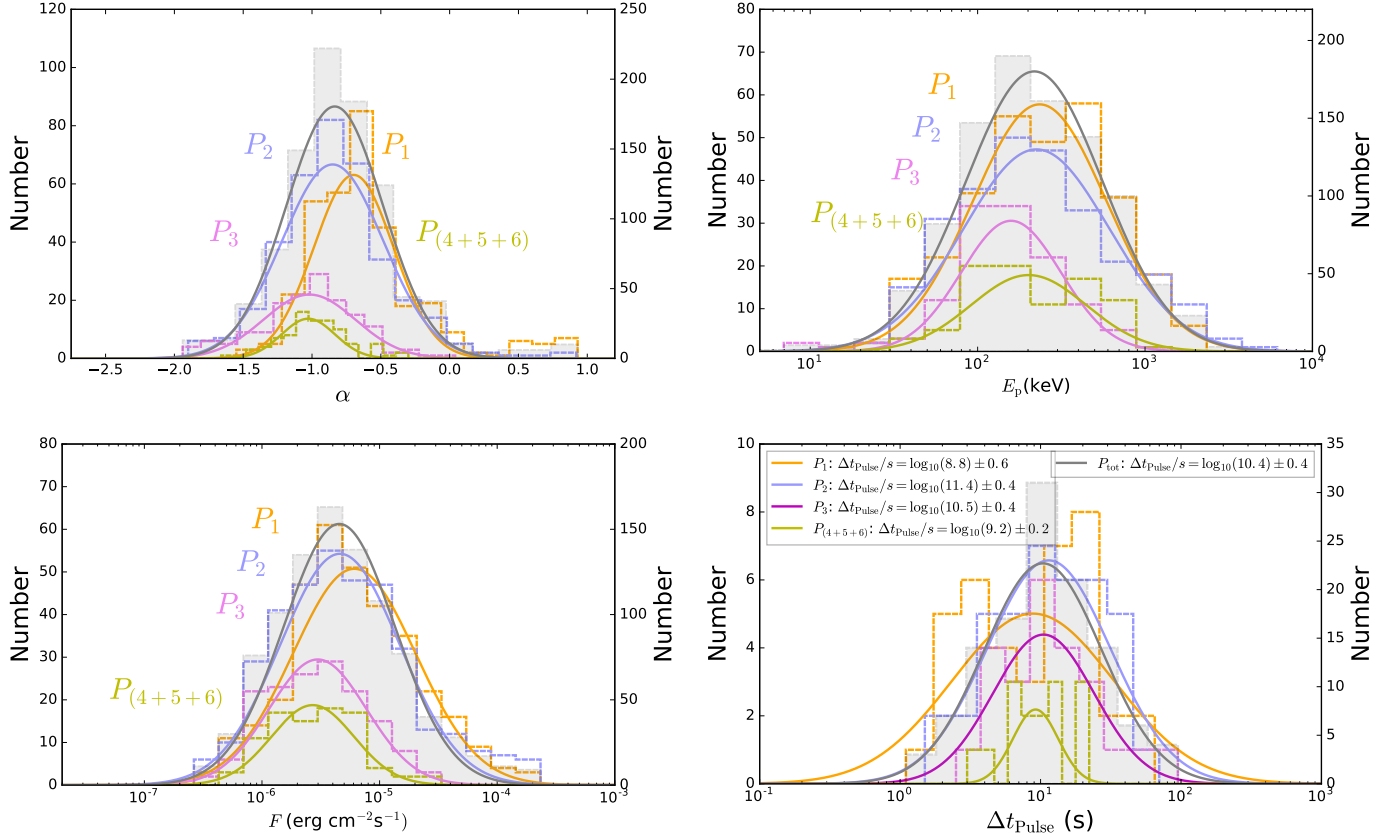


Figure 2. Distributions of α , E_p , and energy flux, as well as the duration (t_{90}) for each pulse group. The distributions correspond to P_1 (orange), P_2 (turquoise), P_3 (violet), P_4 or $P_{(4+5+6)}$ (yellow), P_5 (cyan), and P_6 (pink). The black line is for the full sample. The y-axes on the left are for the pulse groups, while the ones on the right are for the full sample.

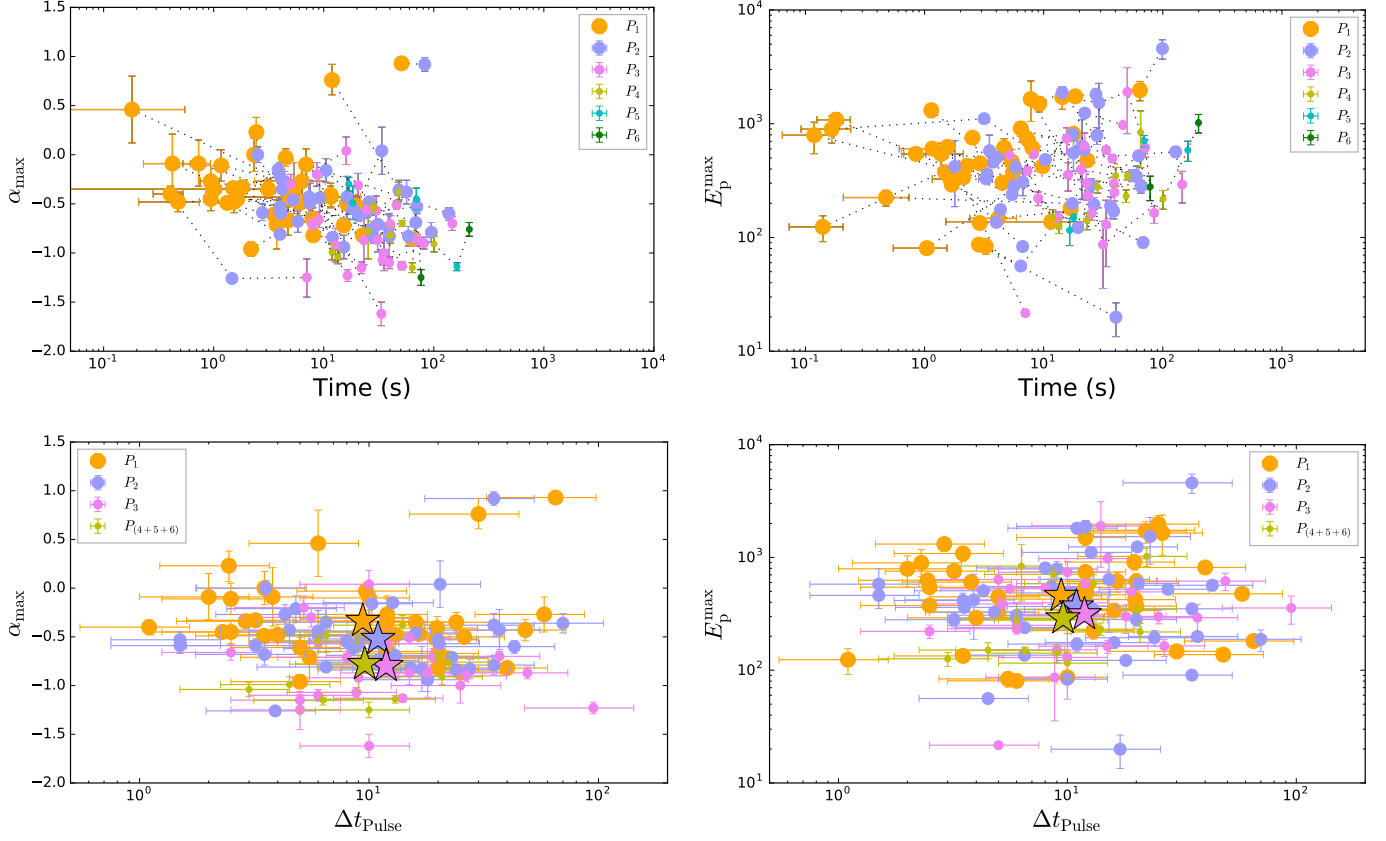


Figure 3. Upper panels: evolution of α_{\max} (left panel) and $E_{p,\max}$ (right panel). Pulses from each individual burst are connected by dashed lines. Color notation is in the same as in Figure 2; lower panels: α_{\max} (left panel) and $E_{p,\max}$ (right panel) vs. pulse duration. The corresponding mean value of each individual pulse group is indicated by colored stars.

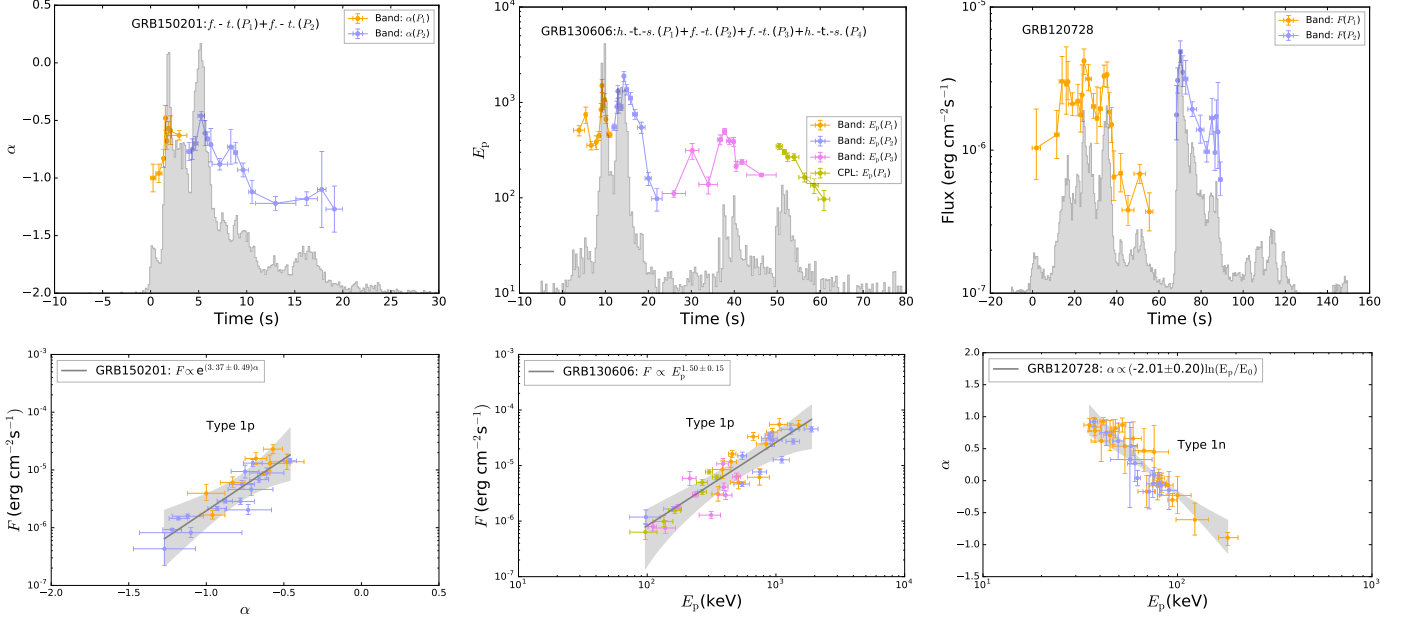


Figure 4. Upper panels: examples of the parameter evolution of the E_p , α , and the νF_ν flux. The count light curves are shown (in arbitrary units) by the gray histograms. Lower panels: examples of the parameter relations of the $F - \alpha$, $F - E_p$, and $\alpha - E_p$, as well as the best-fit relations with the 2σ error region.

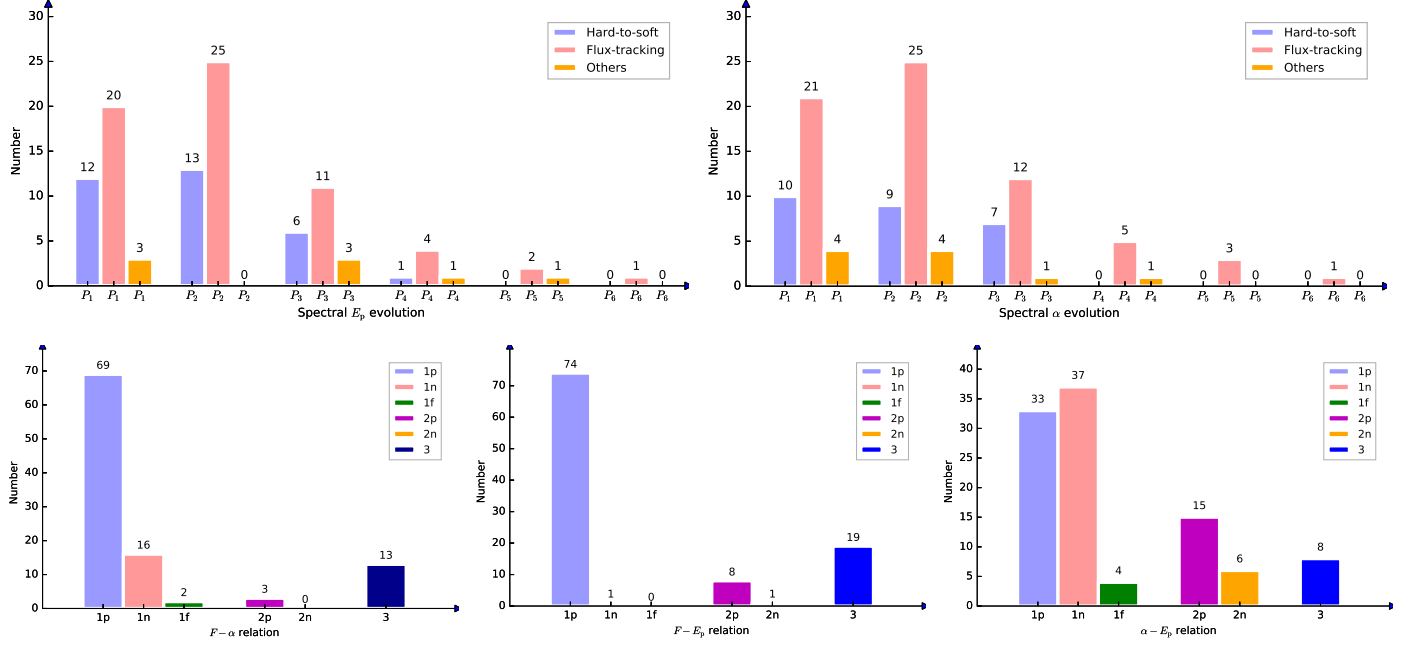


Figure 5. Histograms of the spectral evolution and parameter relations. Upper left panel: E_p evolution. Upper right panel: α evolution. For each pulse, the histograms show the number of hart-to-soft and flux-tracking patterns, as well as some particular cases, denoted as “others”. Lower panels: classification of parameter relations in the entire sample. The histograms display the number pulses in the three main categories, as well as the subcategories for categories 1 and 2, as defined in the text. Lower left panel: $F-\alpha$ relation. Lower middle panel: $F-E_p$ relation. Lower right panel: $\alpha-E_p$ relation.

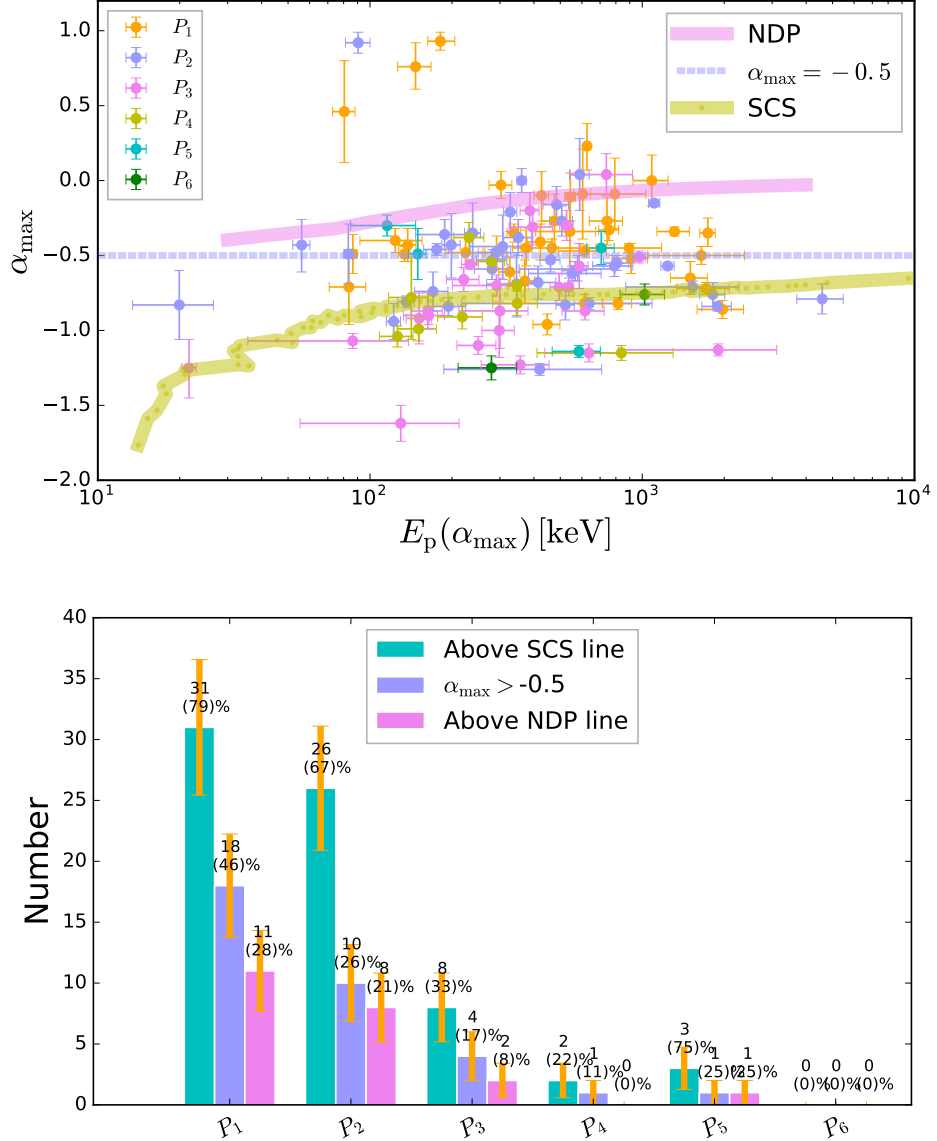


Figure 6. Compatibility with photospheric emission models. Upper panel: α_{\max} vs. the corresponding E_p with the same color notation as in Fig. 2. The pink line is the limiting line for the NDP and the green line is the limiting line for SCS. Lower panel: The number and fraction of α_{\max} bins that lie above the SCS line (green), the number and fraction of bins with $\alpha_{\max} > -0.5$ (blue), and the number and fraction of bins that lie above the NDP line (pink).

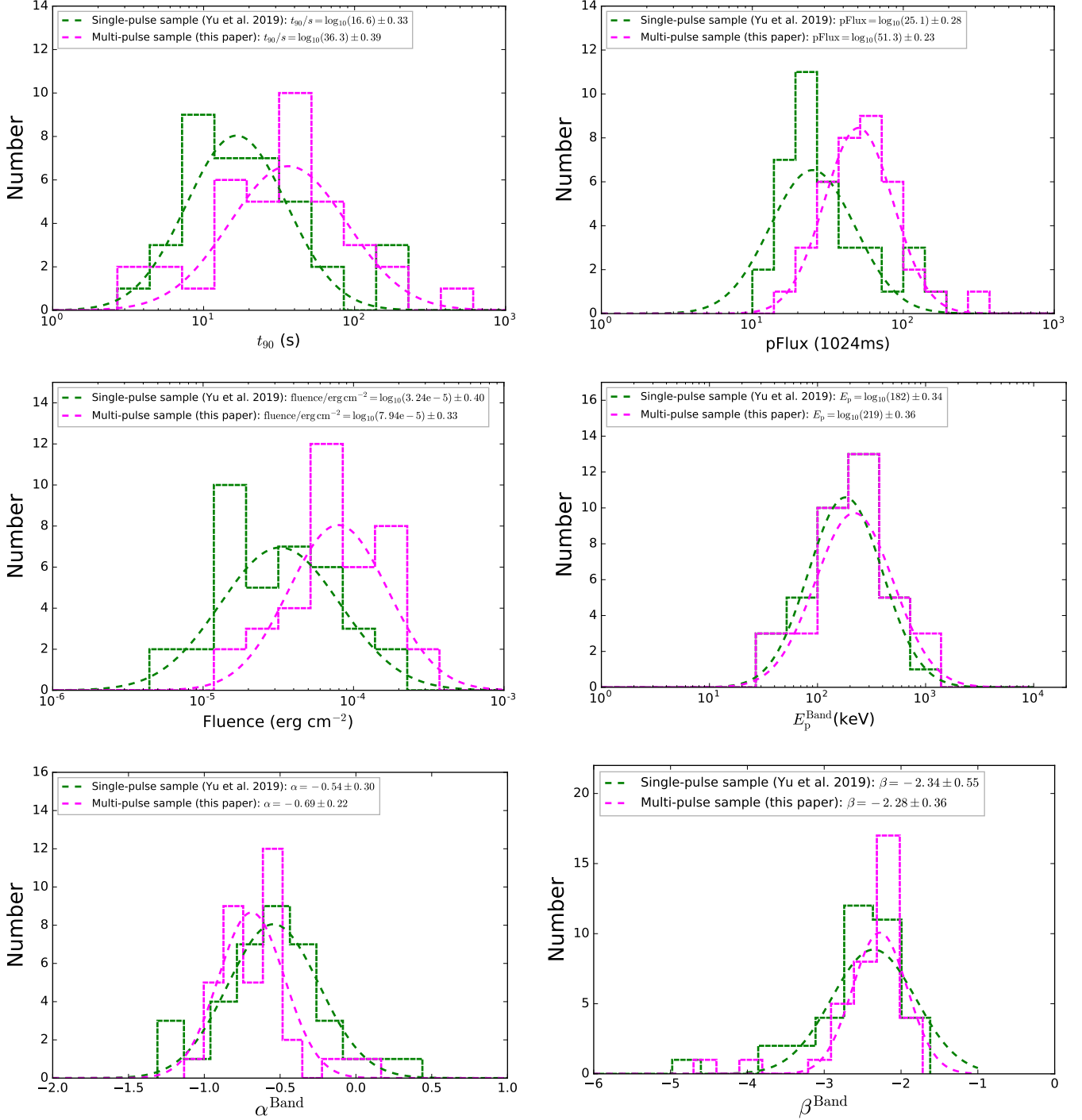


Figure 7. Parameter distributions of the duration T_{90} , peak flux, fluence, E_p , α , and β from time-integrated spectra. The sample in this paper is shown by the magenta curves, while the single-pulse sample in Yu et al. (2019) is shown by the green curves.

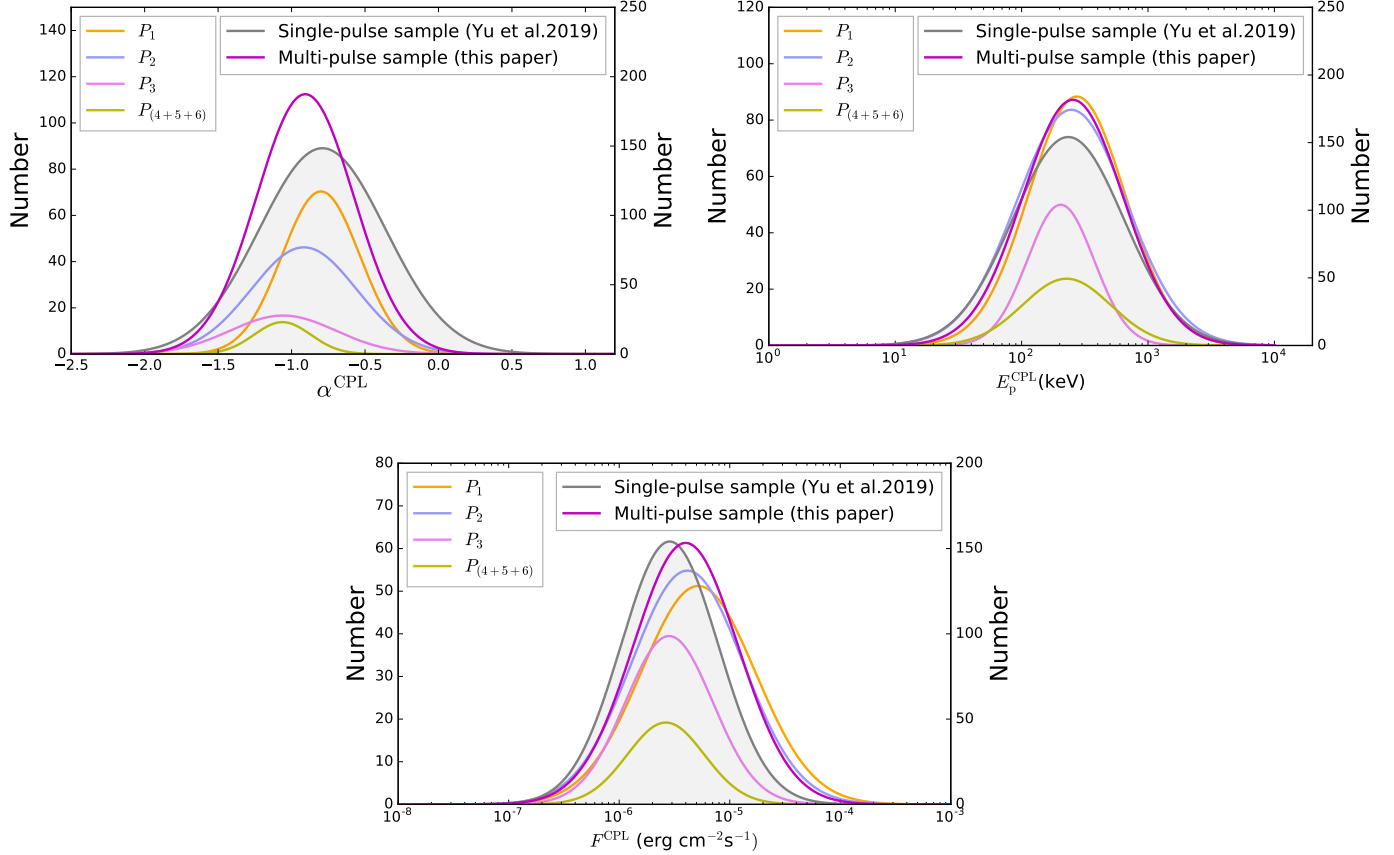


Figure 8. Same as Figure 7, but the analysis is based on the time-resolved spectral results. The y-axes on the left are for the pulse groups, while the ones on the right are for the full samples. The color notation is the same as in Fig. 2 for the pulse group samples. The black line is for the full sample in Yu et al. (2019) while the purple line is for the full sample in this paper.

Table 1. Global Properties of the Sample

GRB	z	T_{90} (s)	Detectors	ΔT_{src} (s)	$[\Delta T_{(\text{bkg},1)}, \Delta T_{(\text{bkg},2)}]$ (s)	Spectra ($N_{S \geq 20}$) (Number)	Pulse ($N_{(S \geq 20)} \geq 4$) (Number)
(1)	(2)	(3)	(4)	(5)	(6)	(7)	(8)
081009140	...	41.345±0.264	(n3)b1	-1 to 52	[-20 to 10, 80 to 100]	23(21)	2(2)
081215784	...	5.568±0.143	n9(na)nbb1	-1 to 10	[-30 to 10, 40 to 60]	27(22)	3(3)
090131090	...	35.073±1.056	(n9)nab1	-1 to 40	[-20 to 10, 60 to 80]	30(16)	3(2)
090618353	0.54	112.386±1.086	(n4)b0	-1 to 150	[-20 to 10, 200 to 220]	28(25)	3(2)
091127976	0.49	8.701±0.571	(n6)n9ab1	-1 to 10	[-20 to 10, 50 to 100]	21(17)	3(3)
100719989	...	21.824±1.305	(n4)n5b0	-1 to 25	[-30 to 20, 60 to 100]	18(12)	3(3)
100826957	...	84.993±0.724	n7n8b1	-1 to 120	[-20 to 10, 200 to 250]	31(26)	3(3)
101014175	...	449.415±1.409	n6(n7)b1	-1 to 230	[-30 to 10, 300 to 320]	110(81)	6(5)
110301214	...	5.693±0.362	n7(n8)nbb1	-1 to 10	[-20 to 10, 40 to 60]	16(14)	2(2)
110625881	...	26.881±0.572	n7n8(nb)b1	-1 to 32	[-20 to 10, 80 to 100]	37(28)	4(3)
120129580	...	3.072±0.362	(n8)b1	-1 to 4	[-20 to 10, 80 to 100]	17(17)	2(2)
120328268	...	29.697±1.056	n7n9(nb)b1	-1 to 40	[-20 to 10, 60 to 80]	23(20)	3(3)
120711115	1.405	44.033±0.724	(n2)nab0	-1 to 120	[-20 to 10, 150 to 160]	30(25)	2(2)
120728434	...	100.481±6.623	n1(n2)b0	-1 to 100	[-20 to 10, 200 to 220]	42(36)	2(2)
121225417	...	58.497±0.820	(n1)n3n5b0	-1 to 75	[-30 to 10, 100 to 120]	26(19)	2(2)
130504978	...	73.217±2.111	n2(n9)nab1	-1 to 84	[-50 to 10, 200 to 220]	51(43)	6(4)
130606497	...	52.225±0.724	n7(n8)b1	-1 to 63	[-40 to 20, 100 to 120]	43(40)	4(4)
131014215	...	3.200±0.091	n9na(nb)b1	-1 to 6	[-50 to 10, 50 to 80]	29(29)	2(2)
131127592	...	18.176±0.724	n1n2(n5)b0	-1 to 22	[-20 to 10, 40 to 60]	30(22)	5(4)
140206275	2.73	146.690±4.419	n0(n1)n3b0	-1 to 50	[-40 to 20, 70 to 90]	23(17)	2(2)
140213807	1.2076	18.624±0.716	n0(n1)n2b0	-1 to 15	[-20 to 10, 40 to 60]	15(11)	2(2)
140416060	...	31.744±1.280	(n2)b0	-1 to 30	[-20 to 10, 60 to 80]	31(26)	4(4)
140508128	1.027	44.288±0.231	(na)b1	-1 to 52	[-20 to 10, 70 to 80]	40(17)	3(2)
140523129	...	19.200±0.362	(n3)n4n5b0	-1 to 25	[-20 to 10, 40 to 60]	41(26)	5(4)
140810782	...	81.665±0.572	n2(n5)b0	-1 to 102	[-110 to 90, 150 to 170, 250 to 270]	33(16)	4(3)
141222691	...	34.049±0.724	n9na(nb)b1	-1 to 40	[-20 to 10, 60 to 80]	18(12)	3(3)
150118409	...	40.193±0.572	n1(n2)n5b0	-1 to 55	[-50 to 30, 80 to 100]	43(29)	3(3)
150201574	...	15.616±0.362	(n3)n4n7b0	-1 to 20	[-20 to 10, 40 to 60]	25(24)	2(2)
150330828	...	153.859±0.810	n1(n2)n5b0	-1 to 180	[-50 to 20, 50 to 60, 220 to 240]	40(34)	3(3)
151231443	...	71.425±0.724	(n8)nbb1	-1 to 80	[-20 to 10, 40 to 50]	23(9)	2(2)
160422499	...	12.288±0.362	n0(n1)n5b0	-1 to 15	[-20 to 10, 40 to 60]	22(22)	3(3)
160802259	...	16.384±0.362	(n2)b0	-1 to 20	[-20 to 10, 60 to 80]	27(22)	3(3)
170207906	...	38.913±0.572	n1(n2)n5b0	-1 to 42	[-20 to 10, 60 to 80]	33(17)	4(4)
171120556	...	44.062±0.383	n0n1(n3)b0	-1 to 48	[-20 to 10, 60 to 80]	21(9)	2(2)
171227000	...	37.633±0.572	(n5)b0	-1 to 60	[-50 to 10, 60 to 100]	43(40)	3(3)
180113418	...	24.576±0.362	n1(n2)n9b0	-1 to 40	[-20 to 10, 60 to 80]	25(22)	2(2)
180120207	...	28.928±0.724	n9na(nb)b1	-1 to 50	[-20 to 10, 60 to 80]	24(20)	2(2)
180722993	...	86.530±1.056	n1(n2)b0	-1 to 110	[-20 to 10, 120 to 140]	18(10)	2(2)
190114873	0.425	116.354±2.563	n3(n4)n7b0	-1 to 110	[-20 to 10, 180 to 200]	51(48)	3(3)

NOTE—*Fermi* burst ID (column 1), redshift (column 2), and T_{90} (column 3), together with the detectors (column 4), source (column 5) and background (column 6) intervals, and total (column 7) and effective ($S \geq 20$, parentheses in column 7) time bins using the BBBlocks across the source intervals, and the number of total (column 8) and the used (parentheses in column 8) pulses for each burst. Note that the detector in parentheses is the brightest one, used for BBBlocks and background fitting.

Table 2. Pulsewise Properties of the Sample

GRB	Pulse	ΔT_{src}	$N_{\text{tot}}(N_{S \geq 20})$	Pulse	Spectral Model	Physical Model	E_p	α	$F - \alpha$	$F - E_p$	$\alpha - E_p$
		(s)	(Number)	(Grade)	(Preferred)	(Preferred)	(Evolution)	(Evolution)	Type(r)	Type(r)	Type(r)
(1)	(2)	(3)	(4)	(5)	(6)	(7)	(8)	(9)	(10)	(11)	(12)
081009140	P_1	0 to 10	18(15)	Gold	Band	Above SCS line	$f.-t.$	$f.-t.$	2p(0.11)	1p(0.41)	3(-0.55)
081009140	P_2	35 to 52	10(6)	Gold	CPL	Above SCS line	$f.-t.$	$h.-t.-s.$	1n(-0.83)	3(0.20)	1p(-0.03)
081215784	P_1	-1 to 2.9	10(8)	Silver	Band	Ph	$h.-t.-s.$	$f.-t.$	1p(0.69)	2p(0.50)	2p(-0.12)
081215784	P_2	2.9 to 4.4	5(5)	Silver	CPL	Above SCS line	$f.-t.$	$f.-t.$	1p(0.70)	1p(0.70)	3(0.20)
081215784	P_3	4.4 to 10	12(9)	Silver	Band	Ph	$f.-t.$	$f.-t.$	1p(0.90)	1p(1.00)	1p(0.90)
090131090	P_1	0 to 5.5	7(2)	Bronze	CPL	Above SCS line
090131090	P_2	5.5 to 10	10(6)	Silver	Band	*	$h.-t.-s.$	$f.-t.$	1p(0.83)	1p(0.77)	1p(0.37)
090131090	P_3	22 to 40	13(8)	Silver	Band	*	$h.-t.-s.$	$f.-t.$	1p(0.75)	1n(-0.14)	1n(-0.29)
090618353	P_1	-1 to 48	5(2)	Bronze	Band	Above SCS line
090618353	P_2	48 to 75.5	11(11)	Silver	Band	*	$f.-t.$	$f.-t.$	3(0.03)	1p(0.79)	1n(-0.17)
090618353	P_3	75.5 to 102	12(12)	Silver	Band	*	$f.-t.$	$f.-t.$	3(-0.21)	1p(0.85)	1n(-0.55)
091127976	P_1	-1 to 1.1	7(6)	Silver	Band	Ph	$h.-t.-s.+f.-t.$	$f.-t.$	1p(0.77)	3(-0.31)	1n(-0.43)
091127976	P_2	1.1 to 5.0	7(7)	Silver	CPL	*	$f.-t.$	$f.-t.$	3(0.28)	1p(0.54)	1n(-0.43)
091127976	P_3	5.0 to 10.0	7(4)	Silver	Band	*	$f.-t.$	$f.-t.$	1p(-0.40)	1p(0.80)	1p(0.20)
100719989	P_1	0 to 3.2	6(4)	Silver	CPL	Ph	$f.-t.$	$h.-t.-s.$	2p(-0.80)	1p(0.80)	1n(-0.40)
100719989	P_2	3.2 to 8	8(7)	Silver	Band	Ph	$f.-t.$	$f.-t.$	1n(0.82)	1p(0.75)	2p(0.54)
100719989	P_3	20 to 25	4(1)	Bronze	CPL	*
100826957	P_1	-1 to 58	20(16)	Silver	Band	Ph	$f.-t.$	$h.-t.-s.$	2p(0.19)	2n(0.77)	1n(-0.31)
100826957	P_2	58 to 71	5(4)	Silver	Band	*	$h.-t.-s.$	$h.-t.-s.$	1p(-0.20)	1p(1.00)	1n(-0.20)
100826957	P_3	71 to 120	6(6)	Silver	CPL	*	$h.-t.-s.$	$h.-t.-s.$	1p(0.29)	1p(0.77)	1n(0.55)
101014175	P_1	0 to 16	35(31)	Silver	Band	Ph	$h.-t.-s.$	$h.-t.-s.$	1p(0.82)	1p(0.48)	1p(0.16)
101014175	P_2	16 to 31.2	25(17)	Silver	CPL	*	$f.-t.$	$f.-t.$	1p(0.64)	1p(0.73)	1p(0.12)
101014175	P_3	31.2 to 40	9(7)	Silver	CPL	*	$f.-t.$	$f.-t.$	1p(0.96)	1p(0.39)	1p(0.43)
101014175	P_4	99.2 to 120	10(8)	Glod	CPL	*	$h.-t.-s.-t.-h.$	$h.-t.-s.-t.-h.$	3(0.18)	3(-0.62)	1p(0.22)
101014175	P_5	155 to 168	9(3)	Bronze	CPL	*
101014175	P_6	197.9 to 220.1	22(15)	Silver	Band	*	$f.-t.$	$f.-t.$	1p(0.82)	1p(0.36)	1n(0.24)
110301214	P_1	-1 to 3.5	7(6)	Silver	Band	Above SCS line	$f.-t.$	$f.-t.$	1p(-0.71)	3(0.49)	1n(-0.26)
110301214	P_2	3.5 to 10	9(8)	Silver	CPL	*	$h.-t.-s.$	$h.-t.-s.$	1n(0.86)	1p(0.95)	1p(0.81)
110625881	P_1	-1 to 9.7	8(3)	Bronze	CPL	Ph
110625881	P_2	9.7 to 20	11(8)	Silver	Band	Ph	$h.-t.-s.$	$f.-t.$	1p(0.95)	2p(0.48)	2p(0.41)
110625881	P_3	20 to 26	8(8)	Silver	Band	Above SCS line	$f.-t.$	$f.-t.$	1p(0.57)	1p(0.81)	1p(0.29)
110625881	P_4	26 to 32	10(9)	Silver	Band	Above SCS line	$f.-t.$	$f.-t.$	1p(0.56)	1p(0.90)	1p(0.24)
120129580	P_1	0 to 2.5	10(10)	Silver	Band	Above SCS line	$f.-t.$	flat	3(0.07)	1p(0.96)	2n(-0.10)
120129580	P_2	2.5 to 4	7(7)	Silver	CPL	Above SCS line	$f.-t.$	$f.-t.$	1p(0.95)	1p(0.04)	1p(-0.09)
120328268	P_1	-1 to 16.5	9(7)	Silver	Band	Above SCS line	$h.-t.-s.$	$f.-t.$	1p(0.56)	3(0.32)	1n(-0.02)
120328268	P_2	16.5 to 25	7(7)	Silver	Band	Above SCS line	$f.-t.$	$f.-t.$	1p(0.89)	3(0)	1n(-0.39)
120328268	P_3	25 to 40	7(6)	Silver	Band	*	$h.-t.-s.$	$f.-t.$	3(-0.03)	3(0.77)	1n(-0.60)
120711115	P_1	60 to 85	9(8)	Silver	CPL	*	$h.-t.-s.+f.-t.$	$h.-t.-s.$	1p(0.86)	3(0.24)	2n(0.17)
120711115	P_2	85 to 120	21(17)	Silver	Band	*	$f.-t.$	$f.-t.$	1p(0.44)	1p(0.81)	2p(0)
120728434	P_1	-1 to 65	26(23)	Silver	Band	Ph	$f.-t.$	chaotic	1n(-0.66)	2p(0.83)	1n(-0.90)
120728434	P_2	65 to 100	16(13)	Silver	Band	Ph	$h.-t.-s.$	chaotic	1n(-0.31)	1p(0.65)	1n(-0.88)
121225417	P_1	-1 to 40	13(6)	Silver	Band	*	$f.-t.$	$h.-t.-s.$	1p(0.26)	1p(0.77)	2p(0.14)

Table 2 continued on next page

Table 2 (*continued*)

GRB	Pulse	ΔT_{src}	$N_{\text{tot}}(N_{S \geq 20})$	Pulse	Spectral Model	Physical Model	E_p	α	$F - \alpha$	$F - E_p$	$\alpha - E_p$
		(s)	(Number)	(Grade)	(Preferred)	(Preferred)	(Evolution)	(Evolution)	Type(r)	Type(r)	Type(r)
(1)	(2)	(3)	(4)	(5)	(6)	(7)	(8)	(9)	(10)	(11)	(12)
121225417	P_2	40 to 75	13(13)	Silver	Band	<i>Ph</i>	<i>h.-t.-s.</i>	<i>h.-t.-s.</i>	1p(0.54)	1p(0.62)	1p(0.01)
130504978	P_1	-1 to 22	11(9)	Silver	Band	*	<i>h.-t.-s.</i>	<i>f.-t.</i>	1p(0.62)	1p(-0.27)	1p(-0.02)
130504978	P_2	22 to 45	15(15)	Silver	Band	*	<i>f.-t.</i>	<i>f.-t.</i>	1p(0.64)	1p(0.60)	1p(0.06)
130504978	P_3	45 to 59	5(3)	Bronze	CPL	*
130504978	P_4	59 to 65.3	5(5)	Silver	CPL	*	<i>f.-t.</i>	<i>f.-t.</i>	1p(0.74)	3(-0.19)	3(-0.74)
130504978	P_5	65.3 to 74	10(9)	Silver	CPL	Above SCS line	<i>f.-t.</i>	<i>f.-t.</i>	1p(0.95)	1p(0.37)	1p(0.25)
130504978	P_6	74 to 84	5(2)	Bronze	CPL	*
130606497	P_1	-1 to 12	13(11)	Silver	Band	Above SCS line	<i>f.-t.</i>	<i>f.-t.</i>	1n(-0.59)	1p(0.80)	1n(-0.84)
130606497	P_2	12 to 24	12(12)	Silver	Band	*	<i>f.-t.</i>	<i>h.-t.-s.</i>	1p(0.64)	1p(0.88)	2n(0.46)
130606497	P_3	24 to 43	10(10)	Silver	Band	Above SCS line	<i>f.-t.</i>	<i>f.-t.</i>	1p(0.43)	1p(0.36)	1n(-0.57)
130606497	P_4	43 to 63	8(7)	Silver	CPL	Above SCS line	<i>h.-t.-s.</i>	<i>f.-t.</i>	1p(0.96)	1p(0.93)	1p(0.82)
131014215	P_1	-1 to 2.45	15(15)	Silver	Band	<i>Ph</i>	<i>f.-t.</i>	<i>f.-t.</i>	1n(-0.30)	1p(0.66)	1f(-0.09)
131014215	P_2	2.45 to 6	14(14)	Silver	Band	<i>Ph</i>	<i>f.-t.</i>	<i>h.-t.-s.</i>	1p(0.74)	1p(0.94)	1p(0.71)
131127592	P_1	0 to 5	5(4)	Silver	CPL	*	<i>f.-t.</i>	<i>f.-t.</i>	3(0.40)	1p(1.00)	1f(0.40)
131127592	P_2	5 to 8.5	7(7)	Silver	Band	*	<i>f.-t.</i>	<i>f.-t.</i>	1p(0.64)	1p(0.93)	1p(0.54)
131127592	P_3	8.5 to 11	4(4)	Silver	CPL	*	<i>h.-t.-s.</i>	<i>h.-t.-s.</i>	1p(1.00)	3(1.00)	2p(1.00)
131127592	P_4	11 to 15.5	5(2)	Bronze	CPL	*
131127592	P_5	15.5 to 22	9(5)	Silver	Band	Above SCS line	<i>f.-t.</i>	<i>f.-t.</i>	1p(0.70)	3(0.60)	1n(-0.10)
140206275	P_1	-1 to 26	15(11)	Silver	Band	<i>Ph</i>	<i>h.-t.-s.</i>	<i>f.-t.</i>	1p(0.62)	2p(0.35)	2p(-0.10)
140206275	P_2	26 to 50	8(6)	Silver	CPL	*	<i>h.-t.-s.</i>	<i>f.-t.</i>	1p(0.89)	1p(0.89)	1p(0.83)
140213807	P_1	-1 to 5	6(4)	Silver	Band	Above SCS line	<i>f.-t.</i>	<i>f.-t.</i>	1p(-0.30)	2p(0.90)	2p(-0.60)
140213807	P_2	5 to 15	9(7)	Silver	Band	Above SCS line	<i>f.-t.</i>	<i>f.-t.</i>	1p(0.90)	1p(0.94)	1p(0.81)
140416060	P_1	-1 to 6	6(4)	Silver	Band	<i>Ph</i>	<i>f.-t.</i>	<i>h.-t.-s.</i>	1p(0.80)	3(0.20)	1n(-0.40)
140416060	P_2	6 to 12	12(11)	Silver	Band	Above SCS line	<i>h.-t.-s.</i>	<i>f.-t.</i>	1p(0.22)	1p(0.38)	2p(-0.71)
140416060	P_3	12 to 21	5(4)	Silver	Band	*	<i>f.-t.</i>	<i>h.-t.-s.</i>	3(0.60)	1p(0.80)	1p(0)
140416060	P_4	21 to 30	10(8)	Gold	Band	*	<i>f.-t.</i>	<i>f.-t.</i>	1n(-0.36)	1p(0.86)	1n(0)
140508128	P_1	-1 to 12	16(10)	Gold	Band	<i>Ph</i>	<i>f.-t.</i>	<i>f.-t.</i>	1p(0.89)	1p(0.42)	2p(0.09)
140508128	P_2	23 to 29	12(4)	Gold	CPL	<i>Ph</i>	<i>h.-t.-s.</i>	<i>f.-t.</i>	1p(1.00)	1p(0.60)	1p(0.60)
140508128	P_3	36 to 42	12(3)	Bronze	CPL	*
140523129	P_1	-1 to 2.5	4(4)	Silver	Band	<i>Ph</i>	<i>f.-t.</i>	<i>f.-t.</i>	3(0.60)	1p(0.80)	2p(0)
140523129	P_2	2.5 to 6.8	11(6)	Silver	Band	<i>Ph</i>	<i>f.-t.</i>	<i>f.-t.</i>	1p(0.71)	3(-0.43)	1n(-0.60)
140523129	P_3	6.8 to 12	10(6)	Silver	Band	<i>Ph</i>	<i>h.-t.-s.</i>	<i>f.-t.</i>	1p(0.49)	1p(0.71)	2n(-0.26)
140523129	P_4	12 to 15	4(1)	Bronze	CPL	*
140523129	P_5	15 to 25	16(10)	Silver	Band	<i>Ph</i>	<i>h.-t.-s.</i>	<i>f.-t.</i>	1p(0.82)	1p(0.53)	1p(0.28)
140810782	P_1	-1 to 20	11(1)	Silver	CPL	*
140810782	P_2	20 to 29	7(4)	Silver	CPL	Above SCS line	<i>f.-t.</i>	<i>h.-t.-s.</i>	3(0.52)	1p(0.94)	1n(0.44)
140810782	P_3	29 to 41	6(6)	Silver	Band	Above SCS line	<i>f.-t.</i>	<i>f.-t.</i>	1p(0.37)	1p(1.00)	1p(0.37)
140810782	P_4	41 to 55	9(5)	Silver	Band	<i>Ph</i>	<i>f.-t.</i>	<i>f.-t.</i>	1p(0.20)	1p(0.70)	1n(-0.50)
141222691	P_1	-1 to 12	7(5)	Silver	Band	<i>Ph</i>	<i>h.-t.-s.</i>	<i>f.-t.</i>	1p(0.30)	2p(0.20)	1n(-0.70)
141222691	P_2	12 to 30	7(6)	Silver	Band	*	<i>f.-t.</i>	<i>h.-t.-s.</i>	1p(0.71)	1p(0.26)	1p(-0.20)
141222691	P_3	30 to 40	4(1)	Bronze	CPL	*
150118409	P_1	-1 to 19.8	19(14)	Silver	Band	<i>Ph</i>	<i>f.-t.</i>	<i>f.-t.</i>	1p(0.62)	1p(0.84)	1n(0.20)
150118409	P_2	19.8 to 40	12(9)	Silver	Band	Above SCS line	<i>f.-t.</i>	<i>f.-t.</i>	1p(0.75)	1p(0.97)	1p(0.65)
150118409	P_3	40 to 55	13(6)	Gold	Band	Above SCS line	<i>f.-t.</i>	<i>h.-t.-s.</i>	1p(0.71)	1p(0.20)	1p(-0.09)

Table 2 continued on next page

Table 2 (*continued*)

GRB	Pulse	ΔT_{src}	$N_{\text{tot}}(N_{S \geq 20})$	Pulse	Spectral Model	Physical Model	E_p	α	$F - \alpha$	$F - E_p$	$\alpha - E_p$	
(1)	(2)	(3)	(4)	(5)	(6)	(Preferred)	(Preferred)	(Evolution)	(Evolution)	Type(r)	Type(r)	Type(r)
		(s)	(Number)	(Grade)			(7)	(8)	(9)	(10)	(11)	(12)
150201574	P_1	-1 to 4	9(8)	Silver	Band	<i>Ph</i>	<i>f.-t.</i>	<i>f.-t.</i>	1p(0.79)	3(0.38)	3(0.02)	
150201574	P_2	4 to 20	16(16)	Silver	Band	<i>Ph</i>	<i>f.-t.</i>	<i>f.-t.</i>	1p(0.89)	1p(0.97)	1p(0.82)	
150330828	P_1	-1 to 10	6(4)	Gold	Band	<i>Ph</i>	<i>h.-t.-s.</i>	<i>s.-t.-h.</i>	1n(-0.40)	3(0.40)	1n(-1.00)	
150330828	P_2	100 to 143	23(22)	Silver	Band	Above SCS line	<i>f.-t.</i>	<i>f.-t.</i>	1p(0.62)	3(0.43)	1n(-0.02)	
150330828	P_3	143 to 180	11(8)	Silver	Band	*	<i>h.-t.-s.</i>	<i>f.-t.</i>	1p(0.71)	3(0.50)	3(0.02)	
151231443	P_1	-1 to 20	12(5)	Gold	Band	Above SCS line	<i>f.-t.</i>	<i>f.-t.</i>	1p(0.50)	1p(1.00)	2p(0.50)	
151231443	P_2	60 to 80	11(4)	Gold	CPL	*	<i>f.-t.</i>	<i>s.-t.-h.</i>	1p(0.74)	1p(0.40)	1n(-0.32)	
160422499	P_1	-1 to 3.8	6(6)	Silver	Band	<i>Ph</i>	<i>f.-t.</i>	<i>h.-t.-s.</i>	1f(-0.78)	1p(0.94)	1n(-0.70)	
160422499	P_2	3.8 to 7	4(4)	Silver	Band	Above SCS line	<i>f.-t.</i>	<i>h.-t.-s.</i>	1n(-0.80)	1p(1.00)	1n(-0.80)	
160422499	P_3	7 to 15	12(12)	Silver	Band	*	<i>f.-t.</i>	<i>h.-t.-s.</i>	1p(0.83)	1p(0.97)	1p(0.81)	
160802259	P_1	-1 to 3.5	9(8)	Gold	Band	<i>Ph</i>	<i>h.-t.-s.</i>	<i>f.-t.</i>	1p(0.48)	2p(0.92)	2p(0.24)	
160802259	P_2	3.5 to 10	8(7)	Silver	Band	<i>Ph</i>	<i>h.-t.-s.</i>	<i>f.-t.</i>	1p(0.71)	1p(0.89)	1p(0.29)	
160802259	P_3	10 to 20	10(7)	Gold	Band	<i>Ph</i>	<i>h.-t.-s.</i>	<i>f.-t.</i>	1p(0.67)	2p(0.93)	2p(0.45)	
170207906	P_1	-1 to 12	13(8)	Silver	Band	<i>Ph</i>	<i>s.-t.-h.</i>	<i>h.-t.-s.</i>	1n(-0.06)	1p(0.95)	2p(0.02)	
170207906	P_2	12 to 20	7(3)	Bronze	CPL	Above SCS line	
170207906	P_3	20 to 30	13(4)	Silver	CPL	<i>Ph</i>	<i>f.-t.</i>	<i>h.-t.-s.</i>	1f(0.40)	3(-0.40)	3(-1.00)	
170207906	P_4	30 to 42	5(2)	Bronze	CPL	*	
171120556	P_1	-1 to 2	14(5)	Gold	Band	<i>Ph</i>	<i>h.-t.-s.</i>	<i>f.-t.</i>	1n(-0.90)	1p(0.90)	1n(-1.00)	
171120556	P_2	37 to 48	7(4)	Gold	Band	Above SCS line	<i>h.-t.-s.</i>	<i>h.-t.-s.</i>	1p(0.80)	1p(0.40)	3(0)	
171227000	P_1	-1 to 24	17(17)	Silver	Band	<i>Ph</i>	<i>f.-t.</i>	<i>h.-t.-s.</i>	1n(0.06)	1p(0.82)	1n(0.09)	
171227000	P_2	24 to 35	15(15)	Silver	CPL	*	<i>f.-t.</i>	<i>f.-t.</i>	1p(0.45)	1p(0.72)	1p(-0.05)	
171227000	P_3	35 to 60	11(8)	Silver	Band	*	<i>f.-t.</i>	<i>h.-t.-s.</i>	1n(0.38)	1p(0.52)	1n(-0.40)	
180113418	P_1	-1 to 19.6	12(10)	Silver	Band	Above SCS line	<i>h.-t.-s.</i>	flat	1n(-0.19)	1p(0.27)	1n(-0.91)	
180113418	P_2	19.6 to 40	13(12)	Silver	Band	<i>Ph</i>	<i>f.-t.</i>	<i>s.-t.-h.</i>	1n(-0.89)	1p(0.90)	1n(-0.95)	
180120207	P_1	-1 to 13	10(9)	Silver	CPL	<i>Ph</i>	<i>h.-t.-s.</i>	<i>h.-t.-s.</i>	1p(0.20)	1p(0.72)	2n(0.53)	
180120207	P_2	13 to 50	14(11)	Silver	Band	<i>Ph</i>	<i>f.-t.</i>	<i>f.-t.</i>	1p(0.32)	1p(0.92)	2n(0.04)	
180722993	P_1	-1 to 30	8(5)	Silver	CPL	<i>Ph</i>	<i>h.-t.-s.</i>	<i>f.-t.</i>	3(-0.50)	1p(0.50)	1f(-0.50)	
180722993	P_2	30 to 100	10(5)	Silver	CPL	<i>Ph</i>	<i>h.-t.-s.</i>	<i>f.-t.</i>	3(0.10)	1p(0.70)	1f(-0.40)	
190114873	P_1	-1 to 2.3	12(11)	Silver	Band	<i>Ph</i>	<i>f.-t.</i>	<i>f.-t.</i>	1p(0.96)	3(0.12)	3(-0.05)	
190114873	P_2	2.3 to 15	24(24)	Silver	Band	<i>Ph</i>	<i>h.-t.-s.</i>	<i>f.-t.</i>	1p(0.93)	1p(-0.04)	1p(-0.22)	
190114873	P_3	15 to 110	15(13)	Silver	Band	*	<i>h.-t.-s.+f.-t.</i>	<i>h.-t.-s.</i>	3(0.76)	1p(-0.36)	1n(-0.21)	

NOTE—*Fermi* burst ID (column 1), the pulse group name (column 2), the source interval of each pulse (column 3), the total and effective ($S \geq 20$) time bins by using the BBlocks across the source intervals (column 4), the identified grade of pulse (column 5), the preferred spectral model indicated by Δ DIC (column 6), and the preferred physical model (column 7), the pulse-wise E_p (column 8) and α (column 9) evolution, and the type of parameter relation with the Spearman’s rank coefficient r in the parentheses for the gold and silver samples: α - E_p relation (column 10), F - E_p relation (column 11), and F - α relation (column 12). In column 7 we make an asterisk for spectra that have α_{max} above the SCS line and *Ph* for the spectra that are classified as being from the photosphere. Note that *Ph* implies that the pulse has at least one time bin that is compatible with the photosphere..

Table 3. Results of the Average and Deviation Values of the Parameter Distribution

Pulse (Group)	Model (Selected)	Spectra (Number)	α (4)	E_p (keV) (5)	F (erg s $^{-1}$ cm $^{-2}$) (6)	β (wellconverged) (7)	β (unconverged) (8)
(1)	(2)	(3)	(4)	(5)	(6)	(7)	(8)
P_1	Best	338	-0.70 ± 0.29	$\log_{10}(234) \pm 0.40$	$\log_{10}(6.17e-6) \pm 0.51$
P_2	Best	361	-0.85 ± 0.37	$\log_{10}(224) \pm 0.44$	$\log_{10}(4.57e-6) \pm 0.51$
P_3	Best	156	-1.02 ± 0.33	$\log_{10}(158) \pm 0.30$	$\log_{10}(2.95e-6) \pm 0.39$
$P_{(4+5+6)}$	Best	89	-1.03 ± 0.19	$\log_{10}(202) \pm 0.34$	$\log_{10}(2.92e-5) \pm 0.39$
Overall	Best	944	-0.84 ± 0.35	$\log_{10}(214) \pm 0.42$	$\log_{10}(4.57e-6) \pm 0.47$

NOTE—Column 1 lists the pulse name, column 2 lists the used model, column 3 lists the number of the spectra for each pulse, columns 4–8 list the average and its deviation (1σ) for the spectral parameters and energy flux.

Table 4. Probability of the Kolmogorov-Smirnov (K-S) Test for the Spectral Parameter Distributions

	$\alpha(P_1)$	$\alpha(P_2)$	$\alpha(P_3)$	$\alpha[P_{(4+5+6)}]$		$E_p(P_1)$	$E_p(P_2)$	$E_p(P_3)$	$E_p[P_{(4+5+6)}]$
$\alpha(P_1)$	1.	$< 10^{-2}$	$< 10^{-2}$	$< 10^{-2}$	$E_p(P_1)$	1.	0.11	$< 10^{-2}$	0.37
$\alpha(P_2)$	$< 10^{-2}$	1.	$< 10^{-2}$	$< 10^{-2}$	$E_p(P_2)$	0.11	1.	$< 10^{-2}$	0.43
$\alpha(P_3)$	$< 10^{-2}$	$< 10^{-2}$	1.	0.12	$E_p(P_3)$	$< 10^{-2}$	$< 10^{-2}$	1.	0.03
$\alpha[P_{(4+5+6)}]$	$< 10^{-2}$	$< 10^{-2}$	0.12	1.	$E_p[P_{(4+5+6)}]$	0.37	0.43	0.03	1.

NOTE—The probability of the K-S Statistic on two samples. The left part is for α distributions, and the right part is for E_p distributions.

Table 5. Statistical Results of the Pulsewise Spectral Evolution

Pulse (Group)	Full Sample		Used Sample		Hard-to-soft		Flux-tracking		Others	
	(Number)	(Number)	(Number)	(Percentage)	(Number)	(Percentage)	(Number)	(Percentage)	(Number)	(Percentage)
(1)	(2)	(3)	(4)	(5)	(6)	(7)	(8)	(9)		
E_p Evolution										
P_1	39	35	12	34%	20	57%	3	9%		
P_2	39	38	13	34%	25	66%	0	0%		
P_3	24	20	7	35%	12	60%	1	5%		
P_4	9	6	1	17%	4	67%	1	16%		
P_5	4	3	1	33%	2	67%	0	0%		
P_6	2	1	0	0%	1	100%	0	0%		
Overall	117	103	34	26%	64	63%	5	3%		
α Evolution										
P_1	39	35	10	29%	21	60%	4	11%		
P_2	39	38	10	26%	25	66%	3	8%		
P_3	24	20	8	40%	12	60%	0	0%		
P_4	9	6	0	0%	5	83%	1	17%		
P_5	4	3	0	0%	3	100%	0	0%		
P_6	2	1	0	0%	1	100%	0	0%		
Overall	117	103	28	27%	67	65%	8	8%		

NOTE—Column 1 lists the pulse groups; column 2 and 3 list the number of the full (gold+silver+bronze) and the used (gold+silver) samples for each pulse group, and columns 4-9 list the number and percentage of the hard-to-soft, Flux-tracking, and the other patterns, respectively.

Table 6. Comparison between the Multipulse Sample in This Paper and the Single-pulse Sample in [Yu et al. \(2019\)](#)

Sample	Sample Source	Sample Size (Number)	$\log_{10}(t_{90})$ (s)	$\log_{10}(\text{Fluence})$ (erg cm $^{-2}$)	$\log_{10}(\text{Peak flux})$	$\log_{10}(E_p)$ (keV)	α	β
(1)	(2)	(3)	(4)	(5)	(6)	(7)	(8)	(9)
Single-pulse sample	Yu et al. (2019)	37 bursts	$\log_{10}(16.6) \pm 0.33$	$\log_{10}(3.24\text{e-}5) \pm 0.40$	$\log_{10}(25.1) \pm 0.28$	$\log_{10}(182) \pm 0.34$	-0.54 ± 0.30	-2.34 ± 0.55
Multi-pulse sample	this paper	39 bursts	$\log_{10}(36.3) \pm 0.39$	$\log_{10}(7.94\text{e-}5) \pm 0.33$	$\log_{10}(51.3) \pm 0.23$	$\log_{10}(219) \pm 0.36$	-0.69 ± 0.22	-2.28 ± 0.36

NOTE—Column 1 lists the samples, column 2 lists the sample source, column 3 list the sample size, columns 4-9 list the average and its deviation (1σ) value of the distributions, including the duration, fluence, peak flux, E_p , α , and β .

APPENDIX

In this appendix, we provide additional figures and tables and present the definition of the fitting models, as well as the discarded sample.

A0.1. *Best Model-based Parameter Evolution in Different pulses*

In Figures A1-A4, we provide the evolution of the spectral parameters E_p , α , νF_ν flux, and β for all the bursts based on the best models defined in Section 2.6.

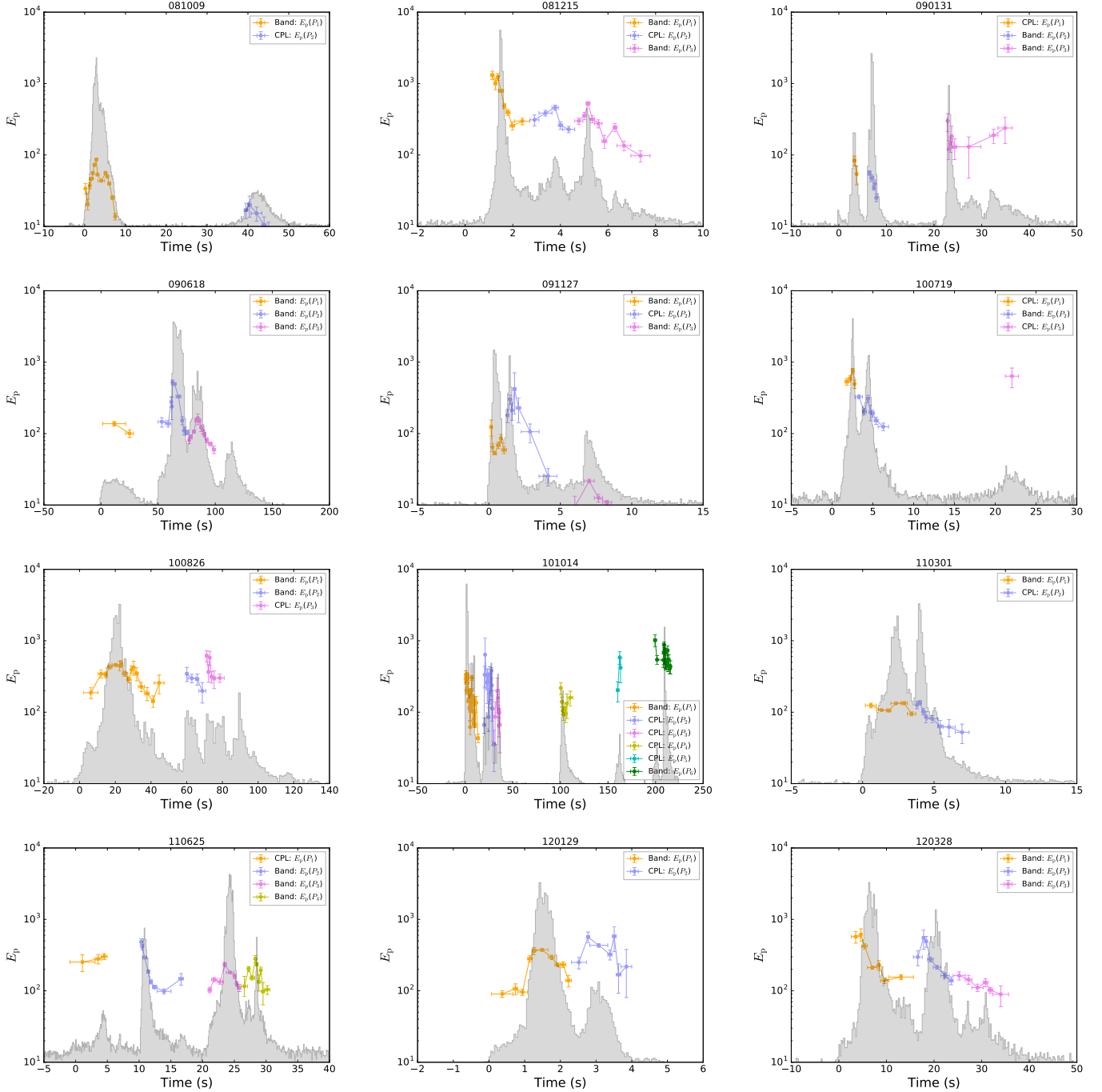


Figure A1. Temporal evolution of the E_p . Data points with solid orange, blue-magenta, violet, yellow, cyan, and green colors indicate time-series pulses of the P_1 , P_2 , P_3 , P_4 , P_5 , and P_6 , respectively. Count rate lightcurves are overlaid in gray. All data points correspond to a statistical significance $S \geq 20$.

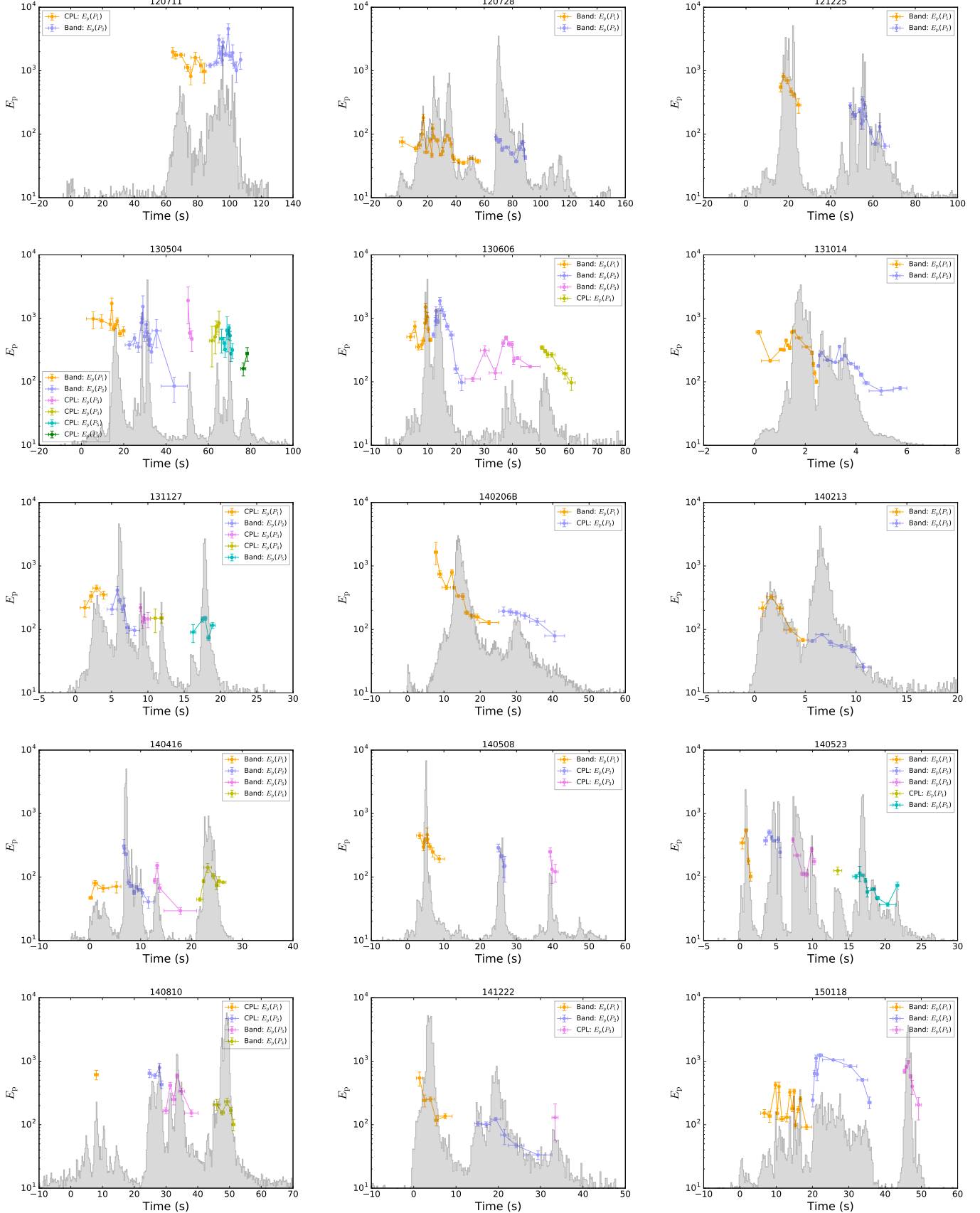


Fig. A1—Continued

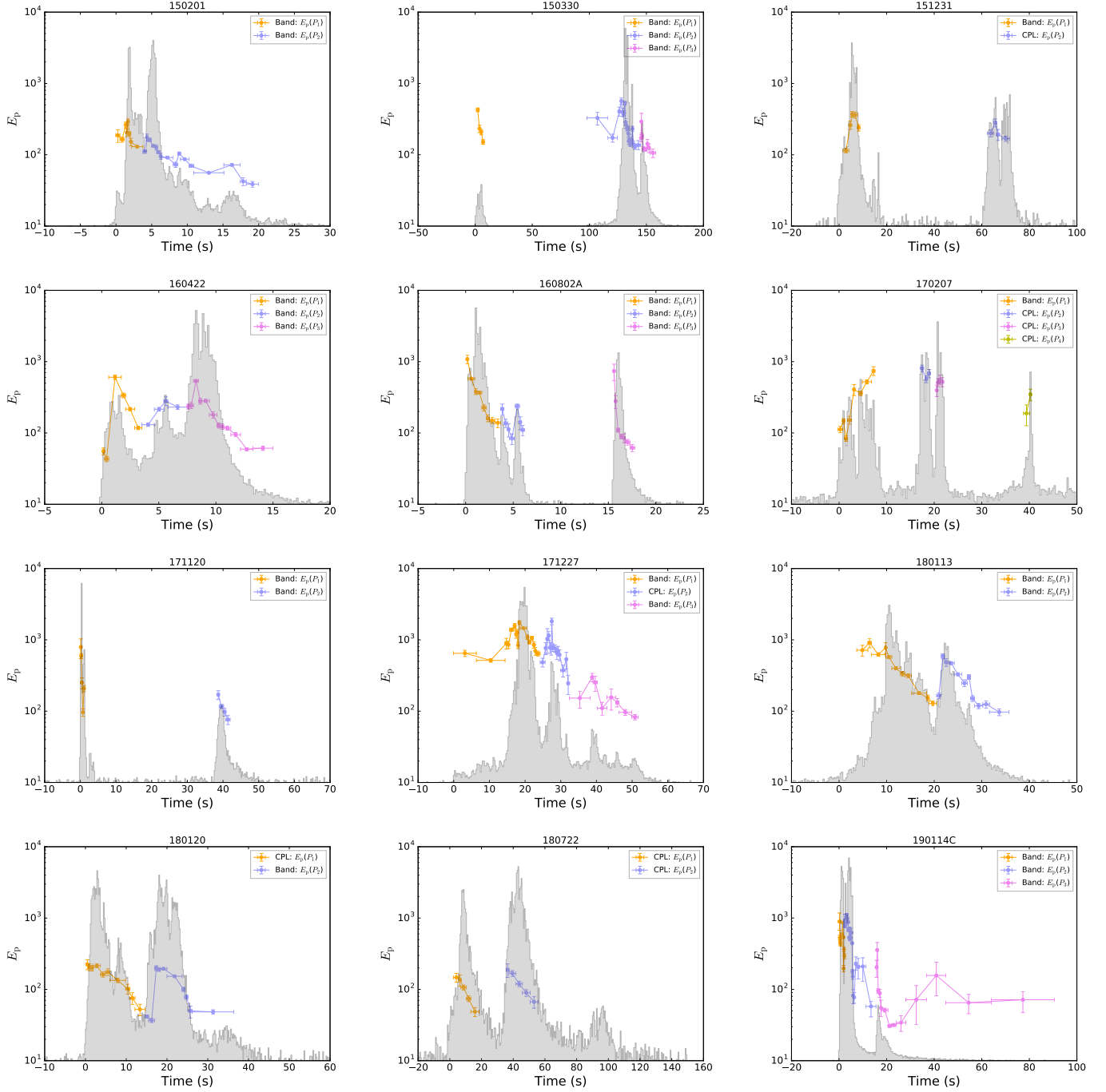


Fig. A1—Continued

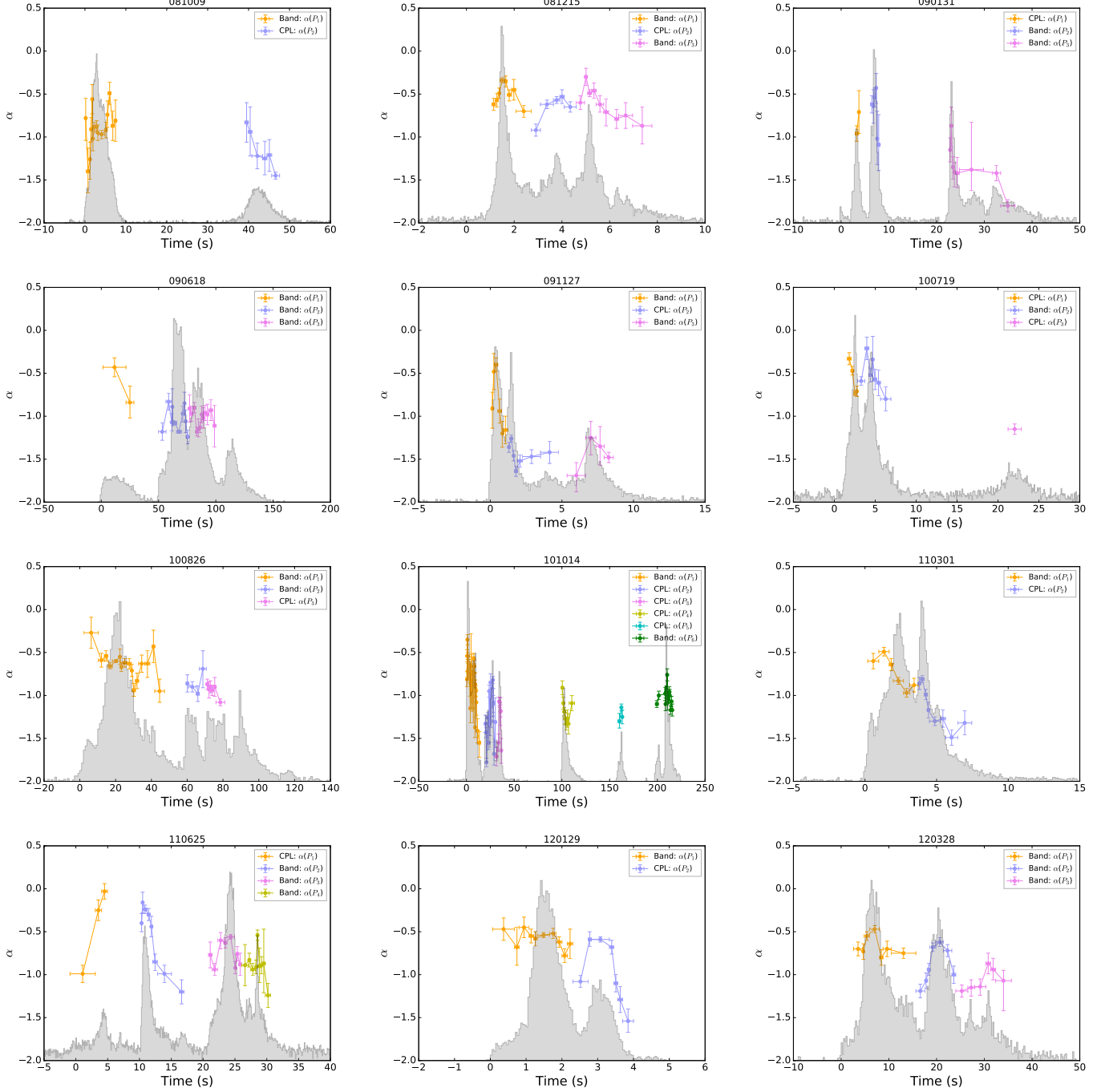


Figure A2. Temporal evolution of the α index. The symbols and colors are the same as in Figure A1.

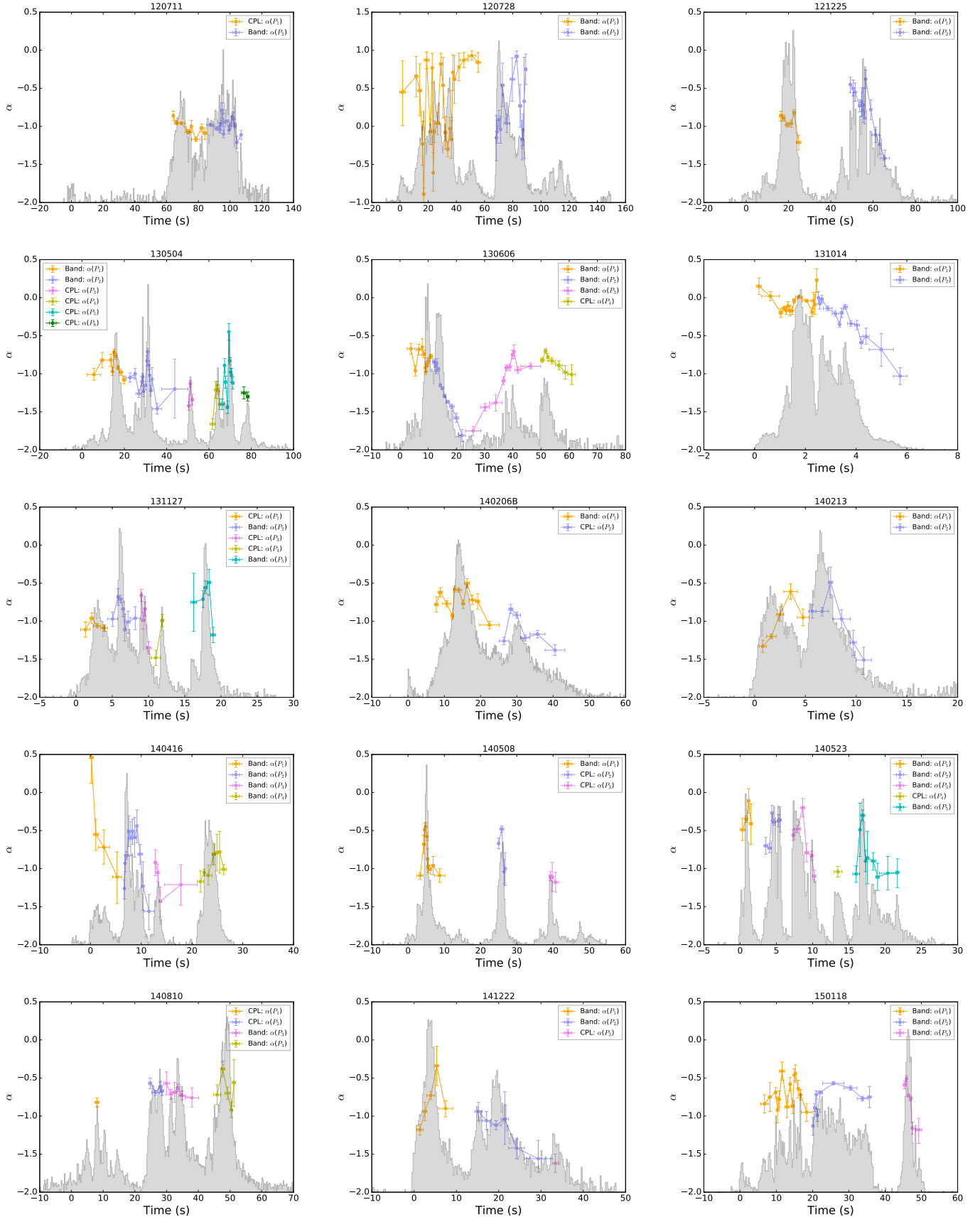


Fig. A2— Continued

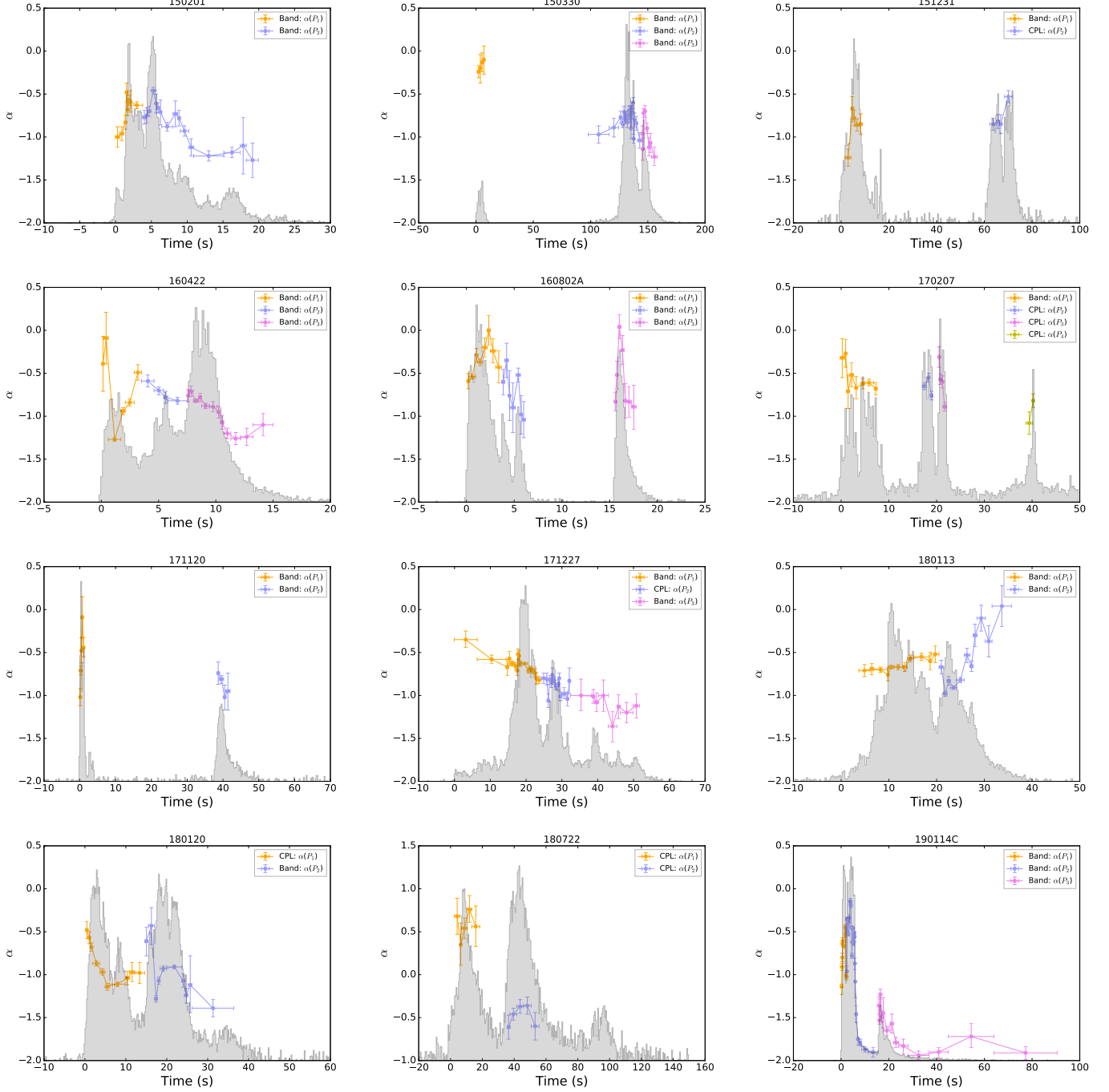


Fig. A2—Continued

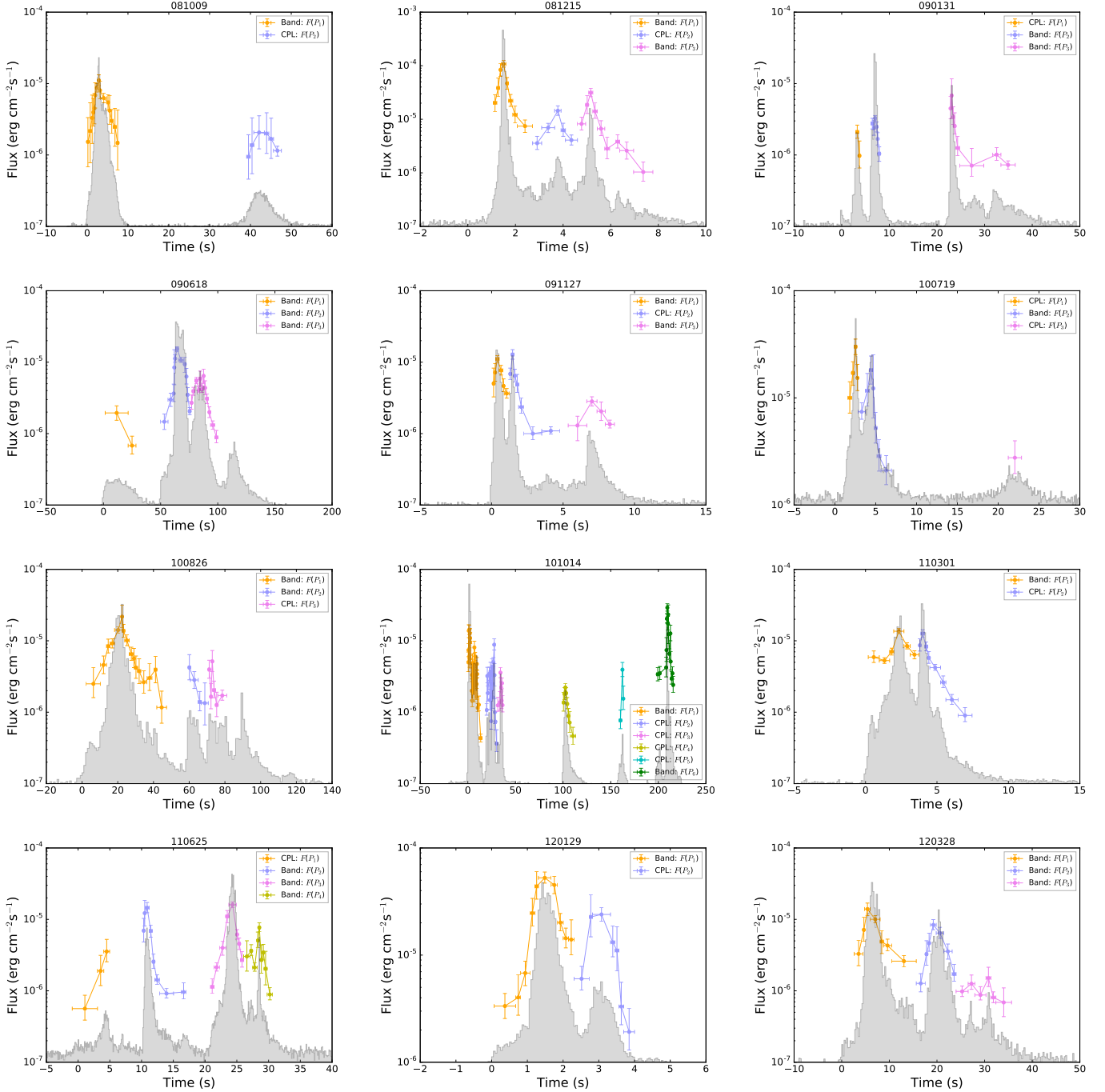


Figure A3. Temporal evolution of energy flux F . The symbols and colors are the same as in Figure A1.

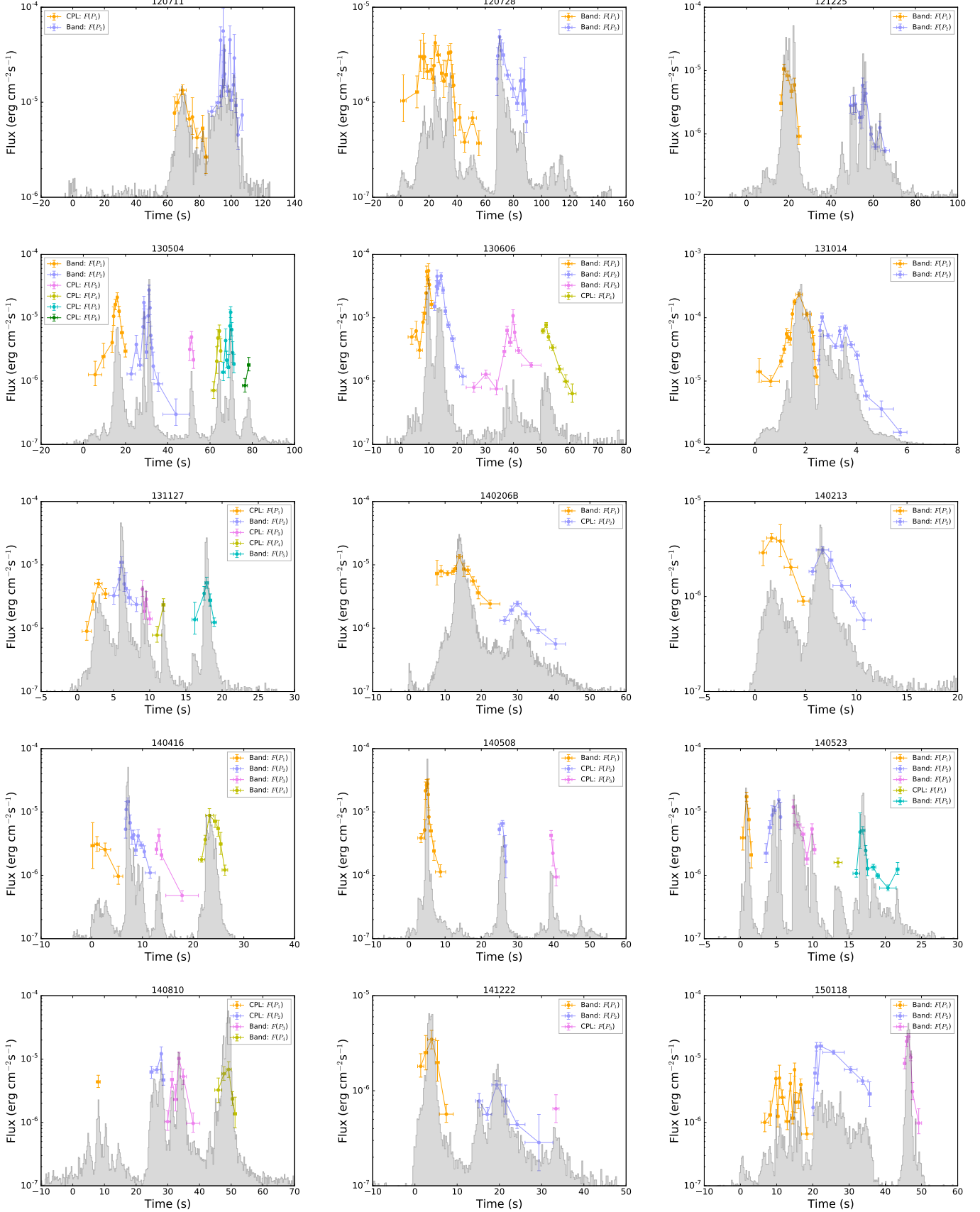


Fig. A3— Continued

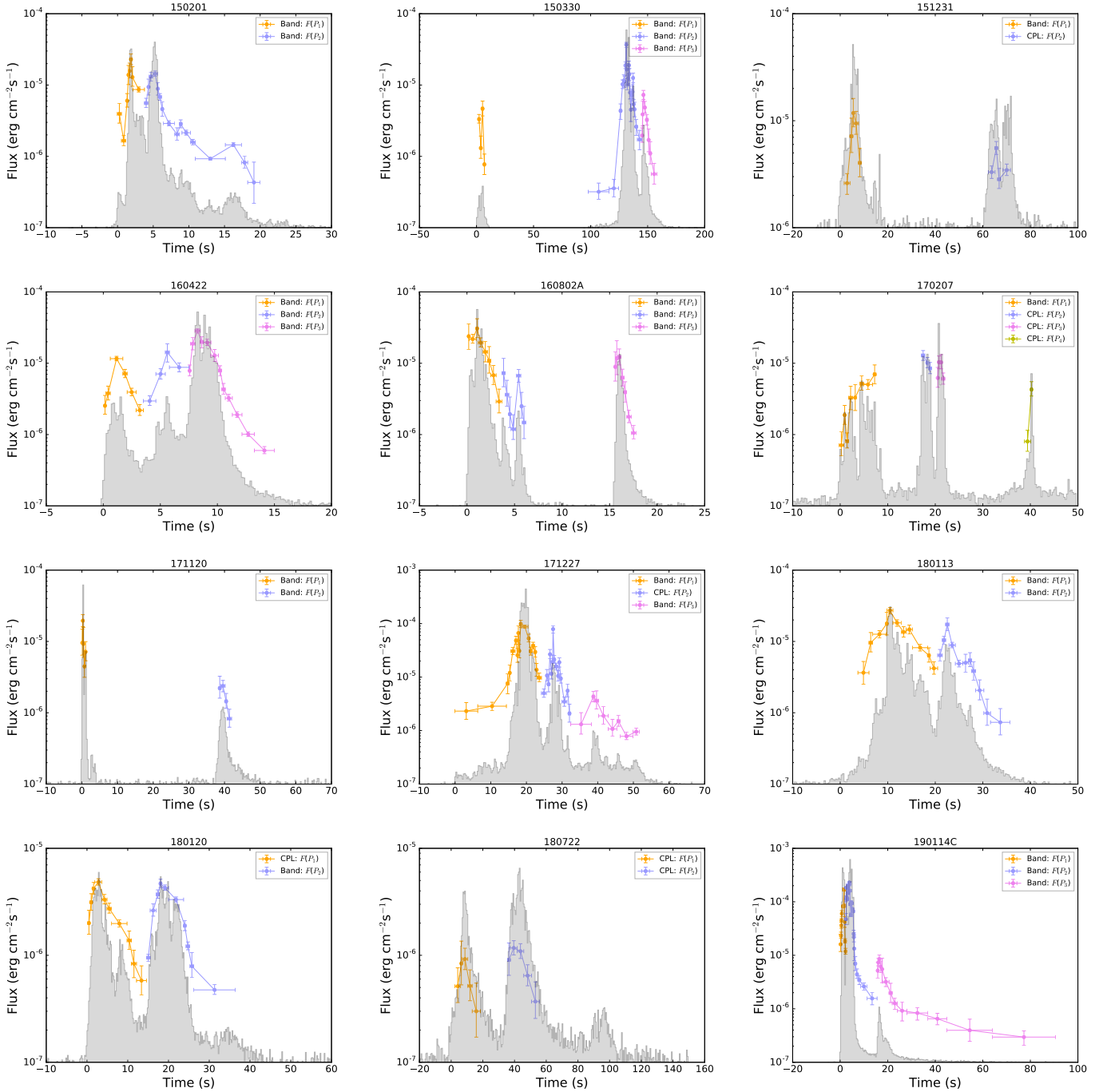


Fig. A3—Continued

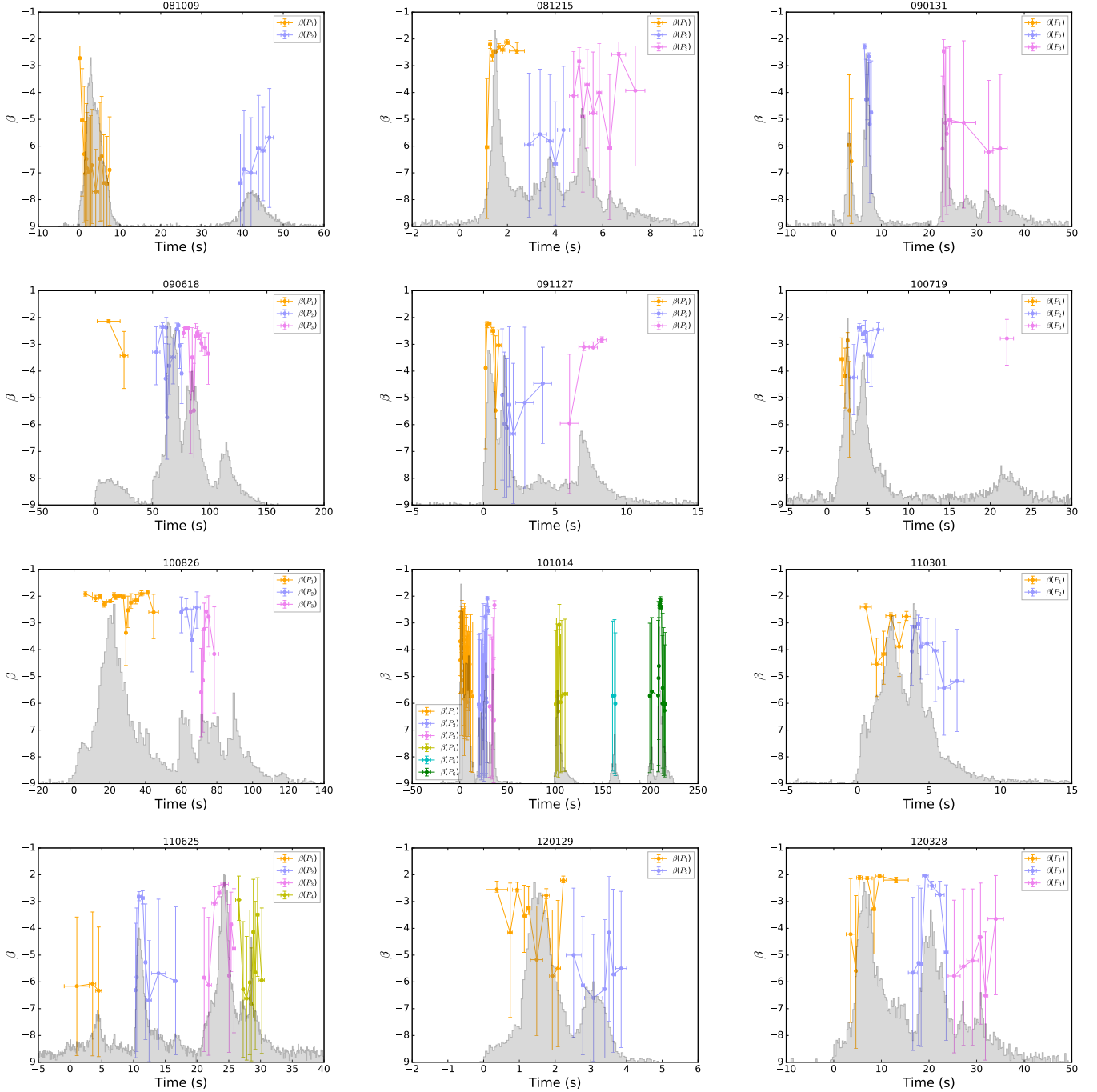


Figure A4. Temporal evolution of the β index of the Band model. The symbols and colors are the same as in Figure A2.

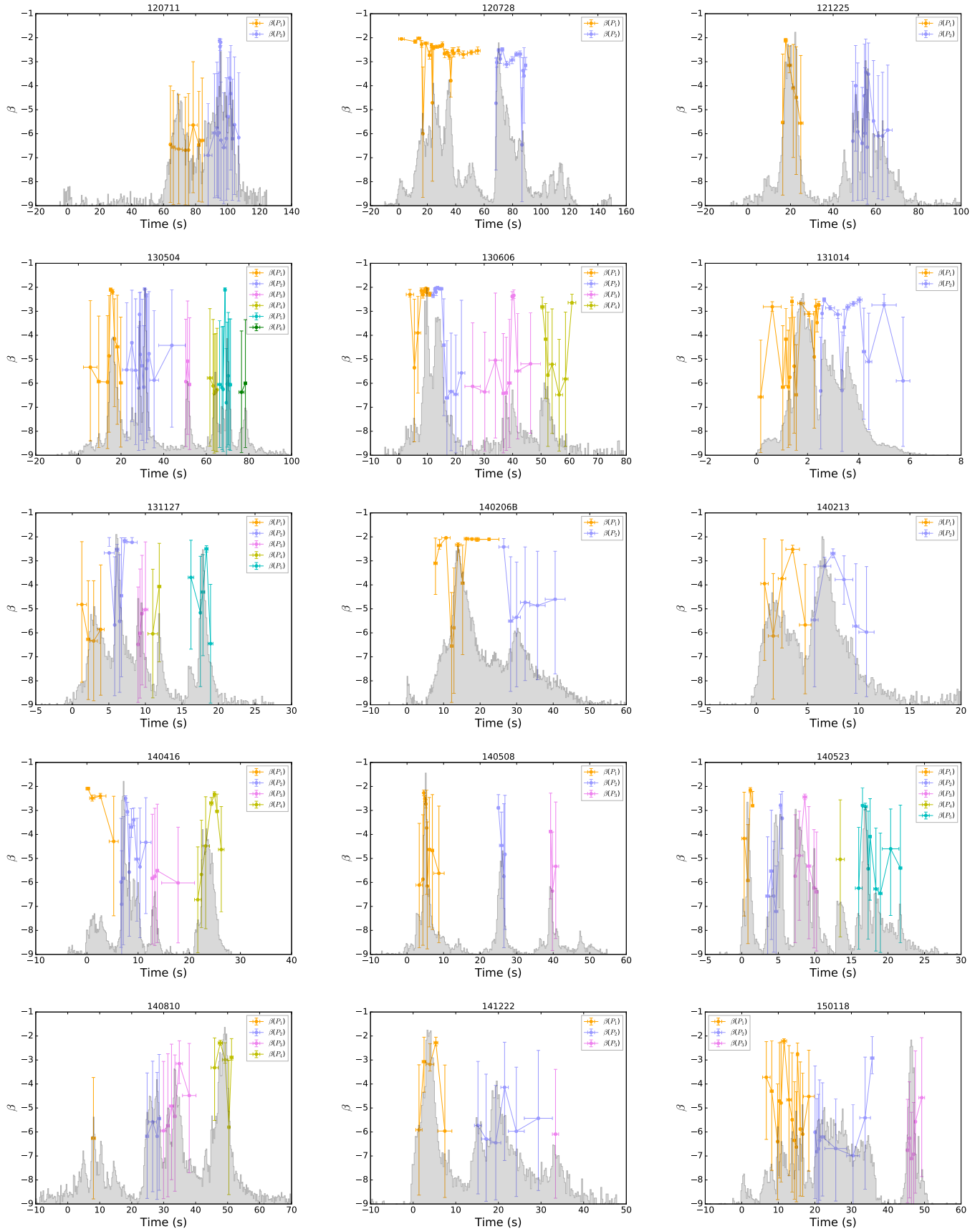


Fig. A4— Continued

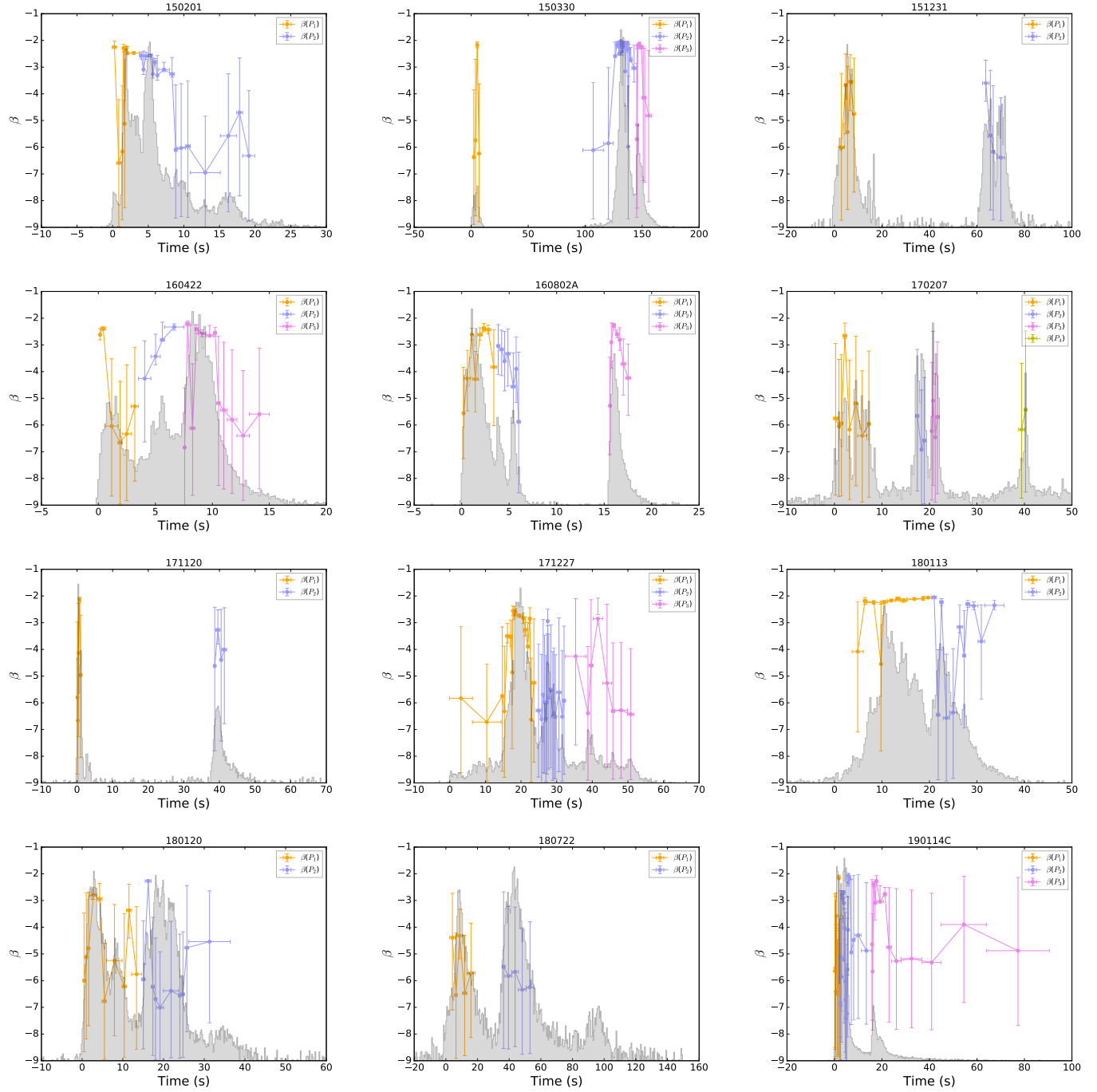


Fig. A4—Continued

A0.2. *Best Model-based Parameter Relations in Different pulses*

In Figures A5-A7, we provide the F - α , F - E_p , and α - E_p relations for all the bursts based on the best models defined in Section 2.6.

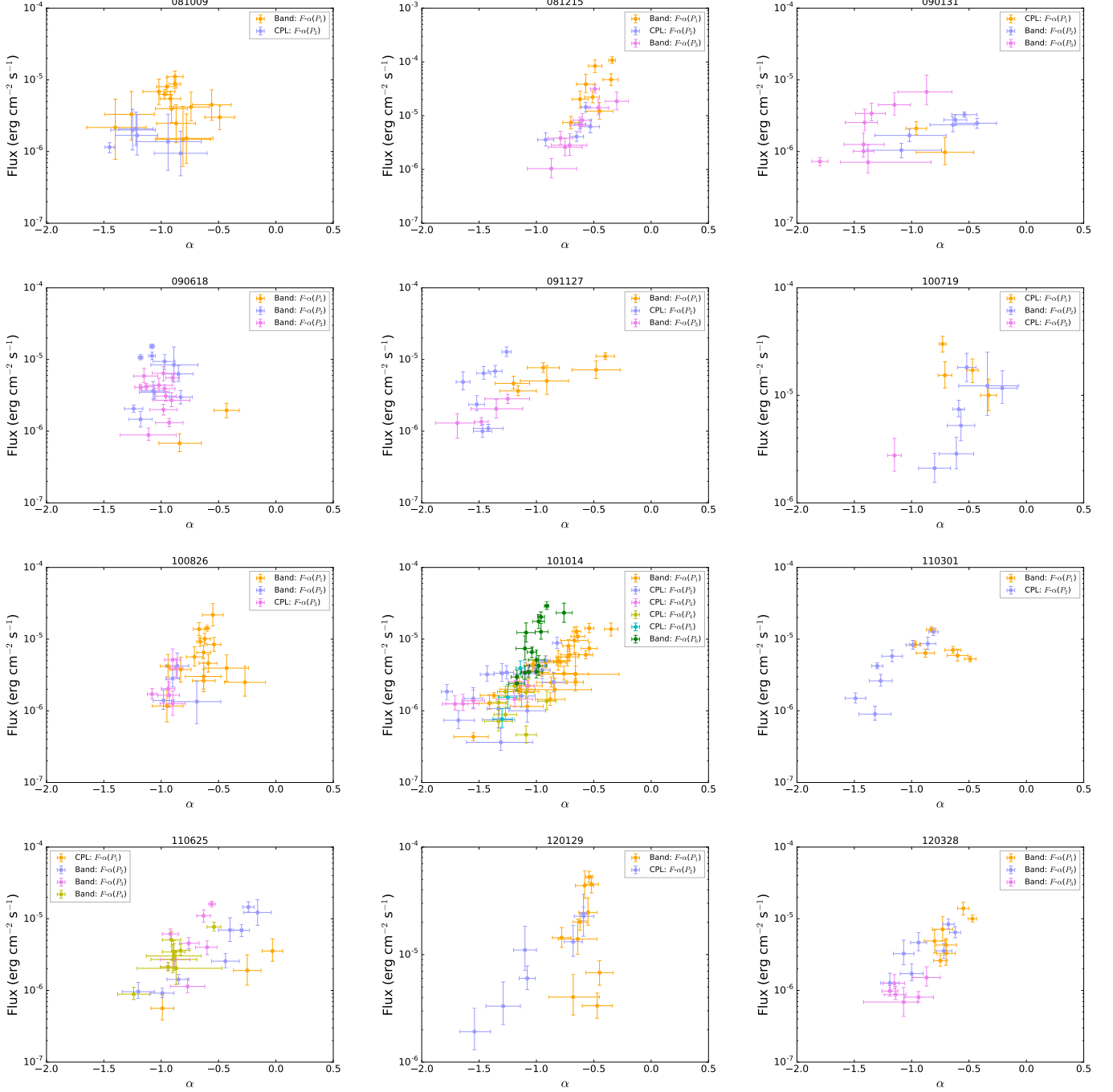


Figure A5. The $F\text{-}\alpha$ relation. Data points with solid orange, blue-magenta, violet, yellow, cyan, and green colors indicate time-series pulses of the P_1 , P_2 , P_3 , P_4 , P_5 , and P_6 , respectively. All data points correspond to a statistical significance $S \geq 20$.

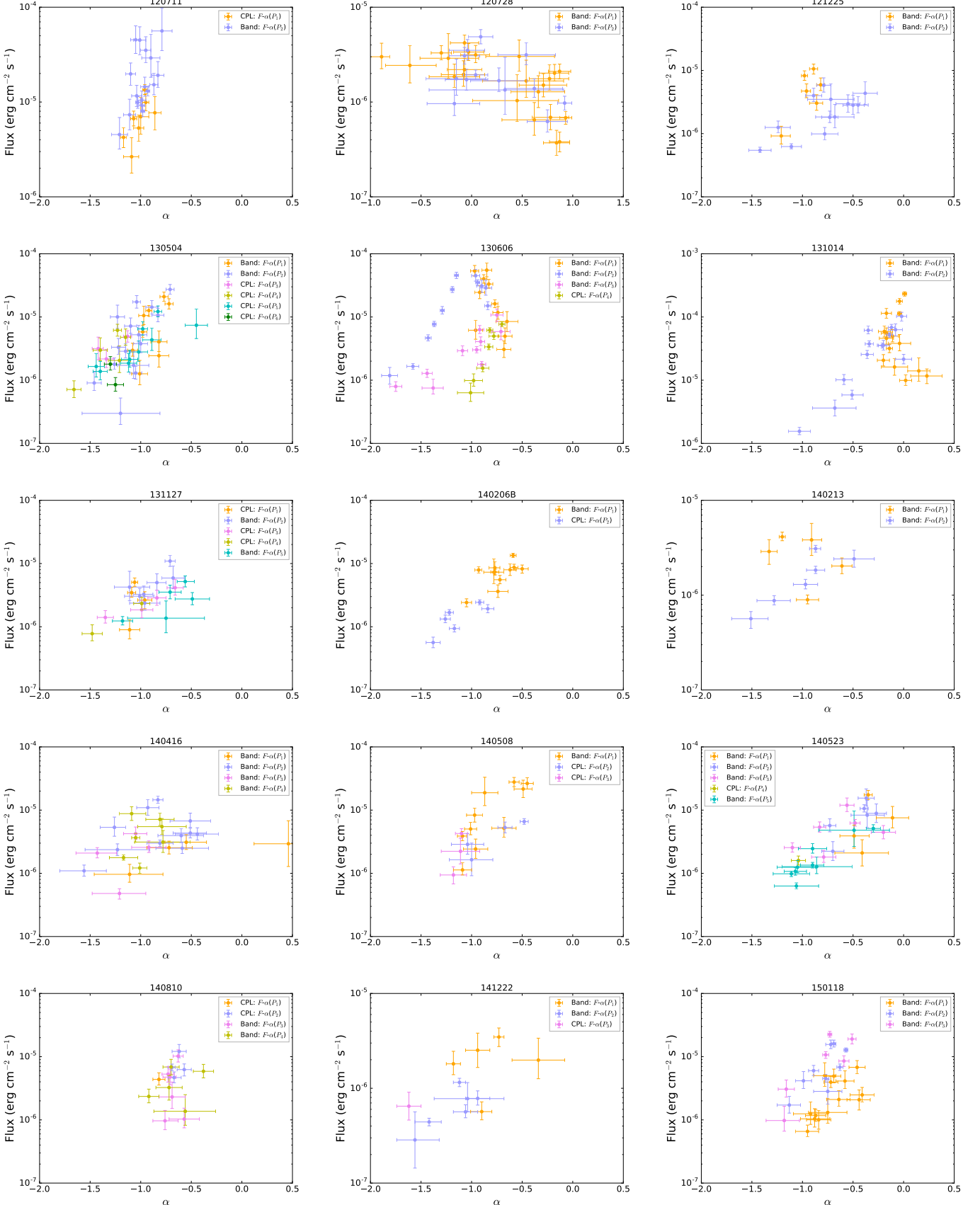


Fig. A5— Continued

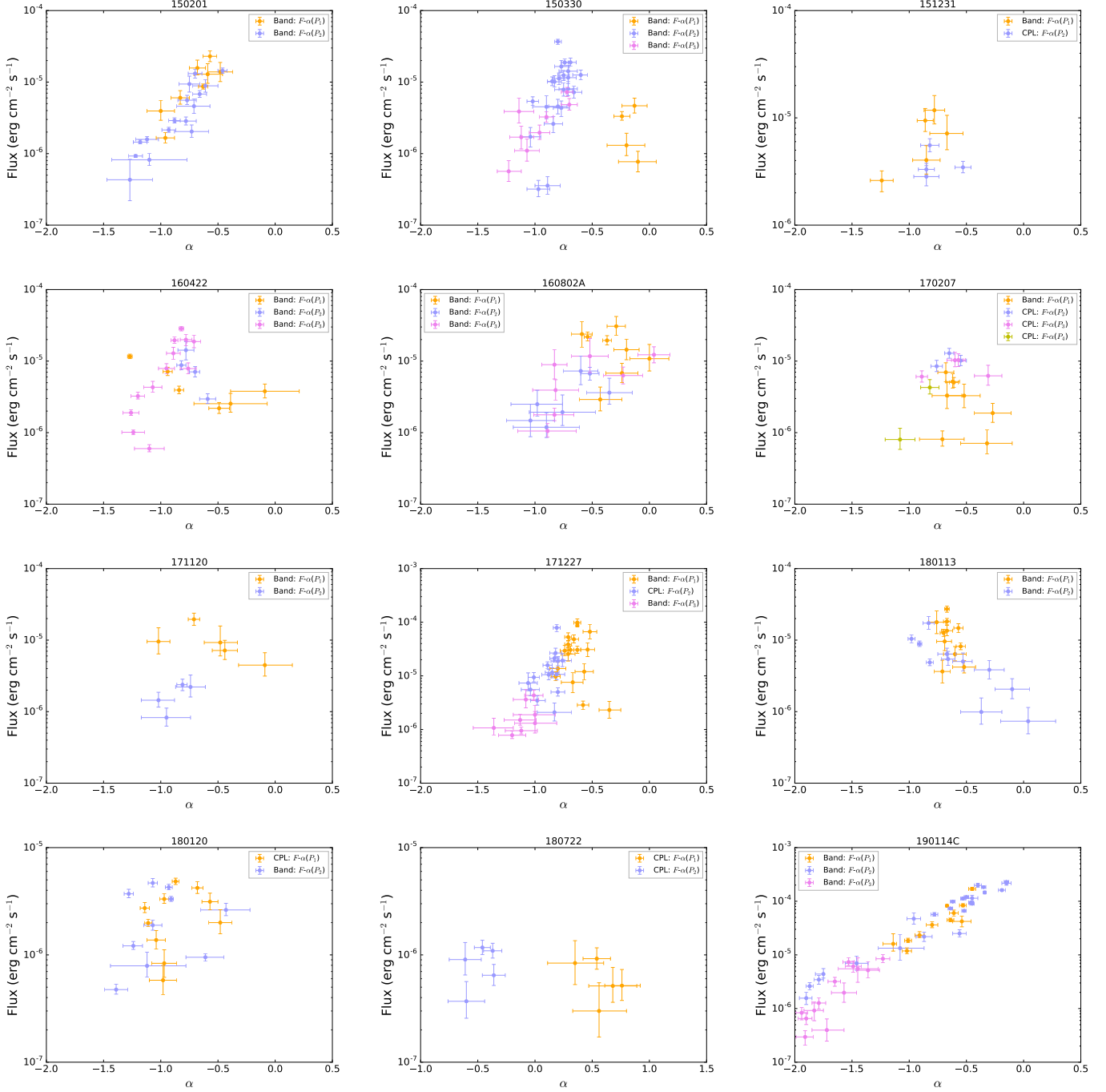


Fig. A5—Continued

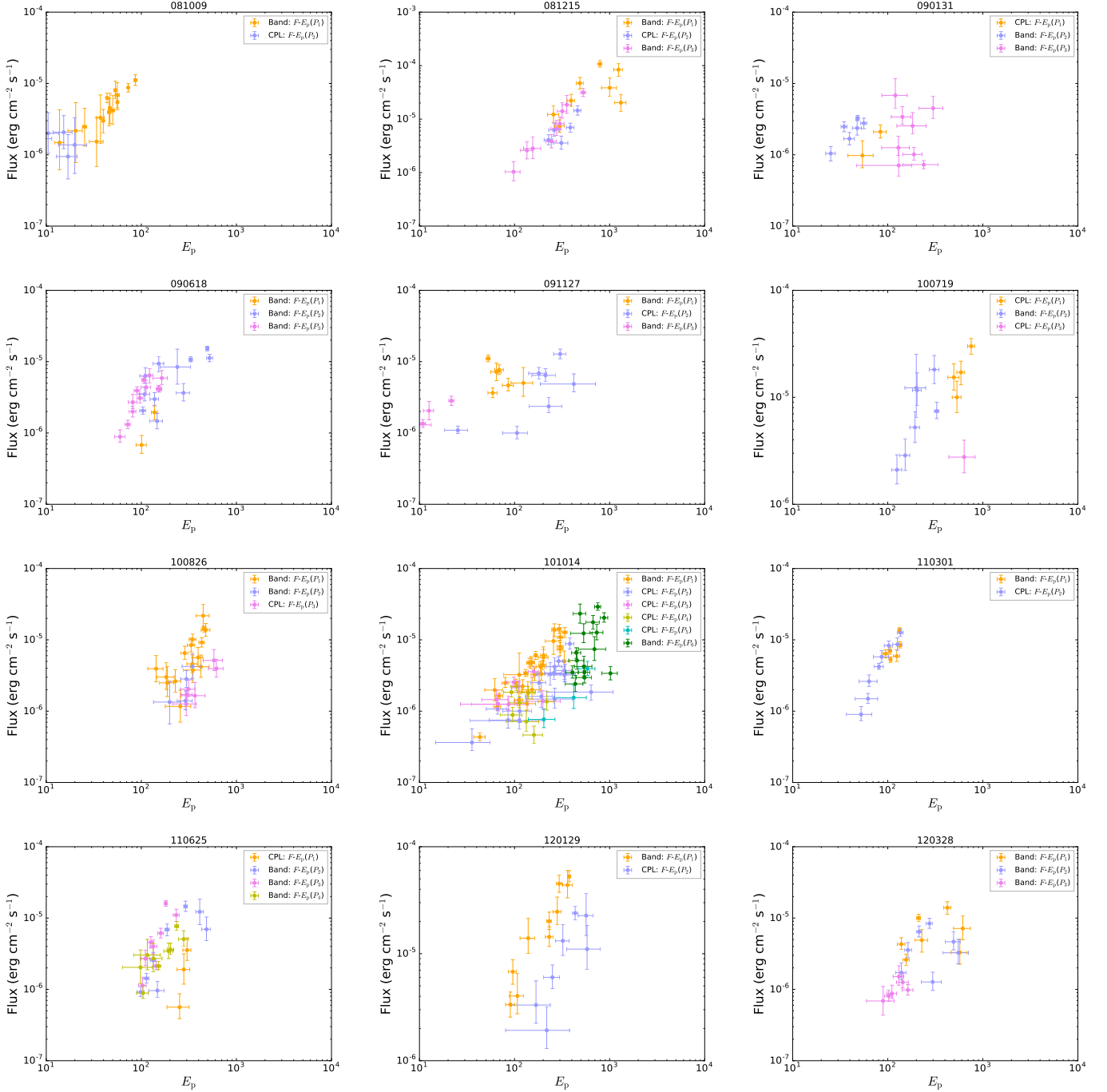


Figure A6. The $F \cdot E_p$ relation. The symbols and colors are the same as in Figure A5.

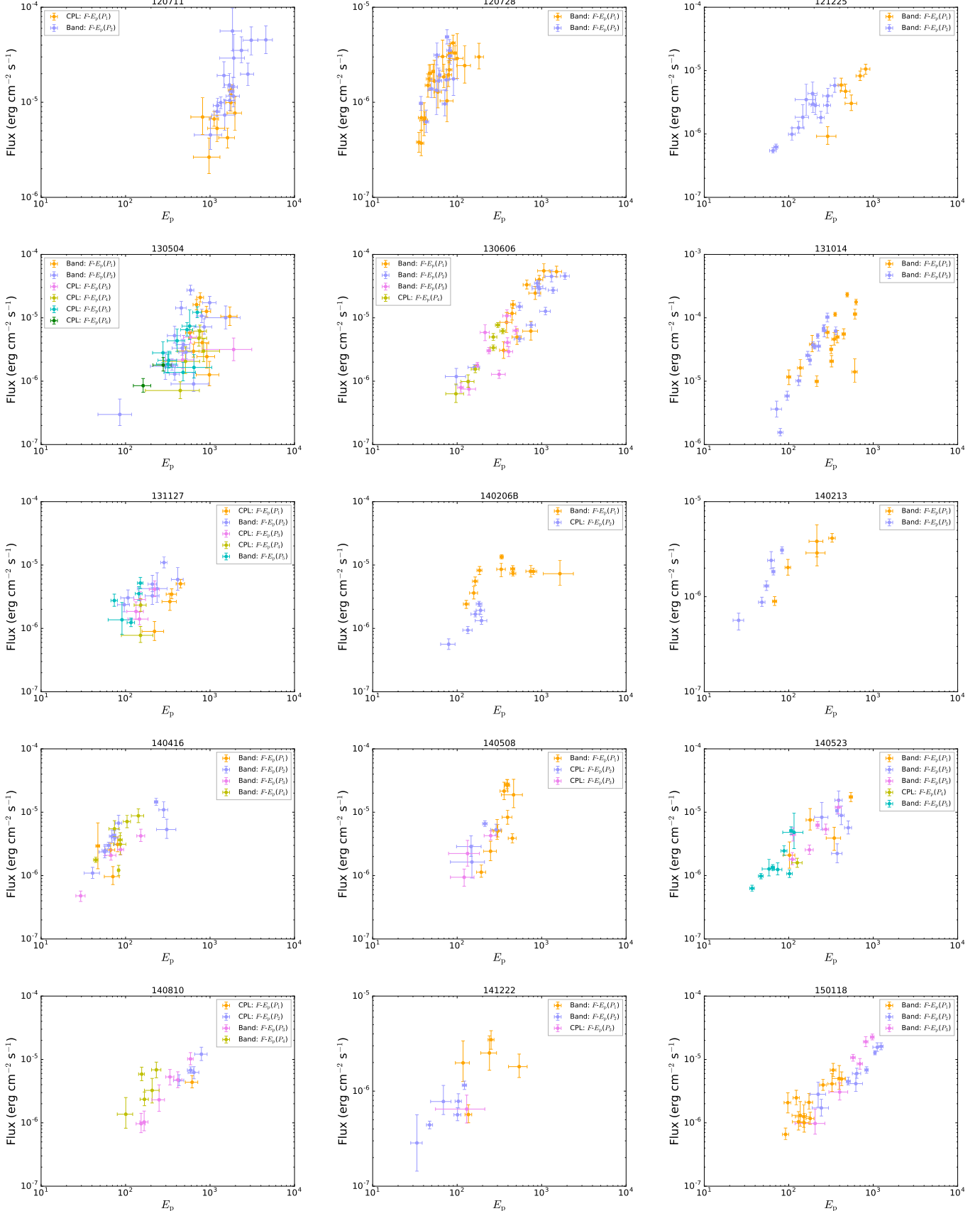


Fig. A6—Continued

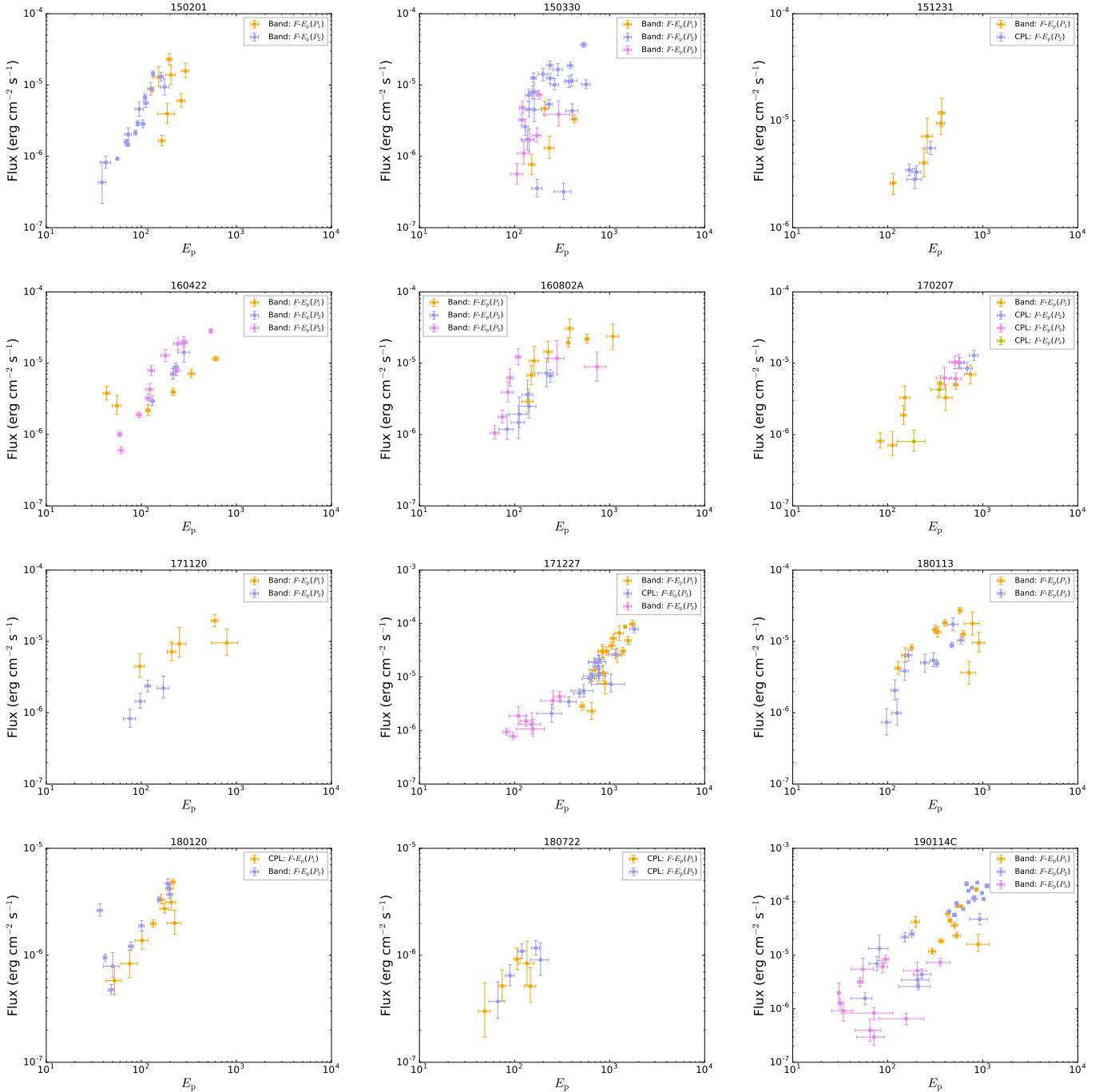


Fig. A6—Continued

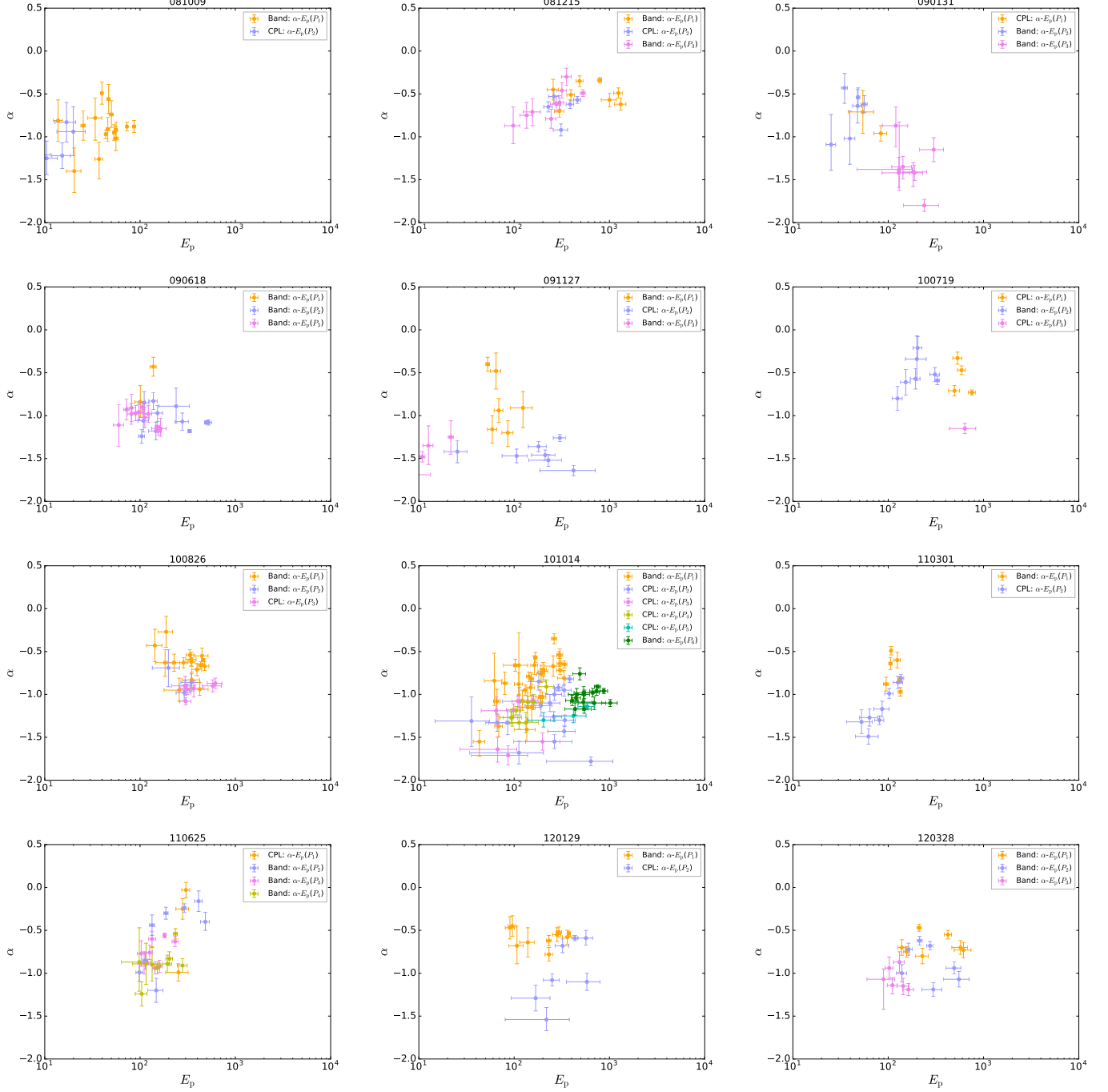


Figure A7. The α - E_p relation. The symbols and colors are the same as in Figure A5.

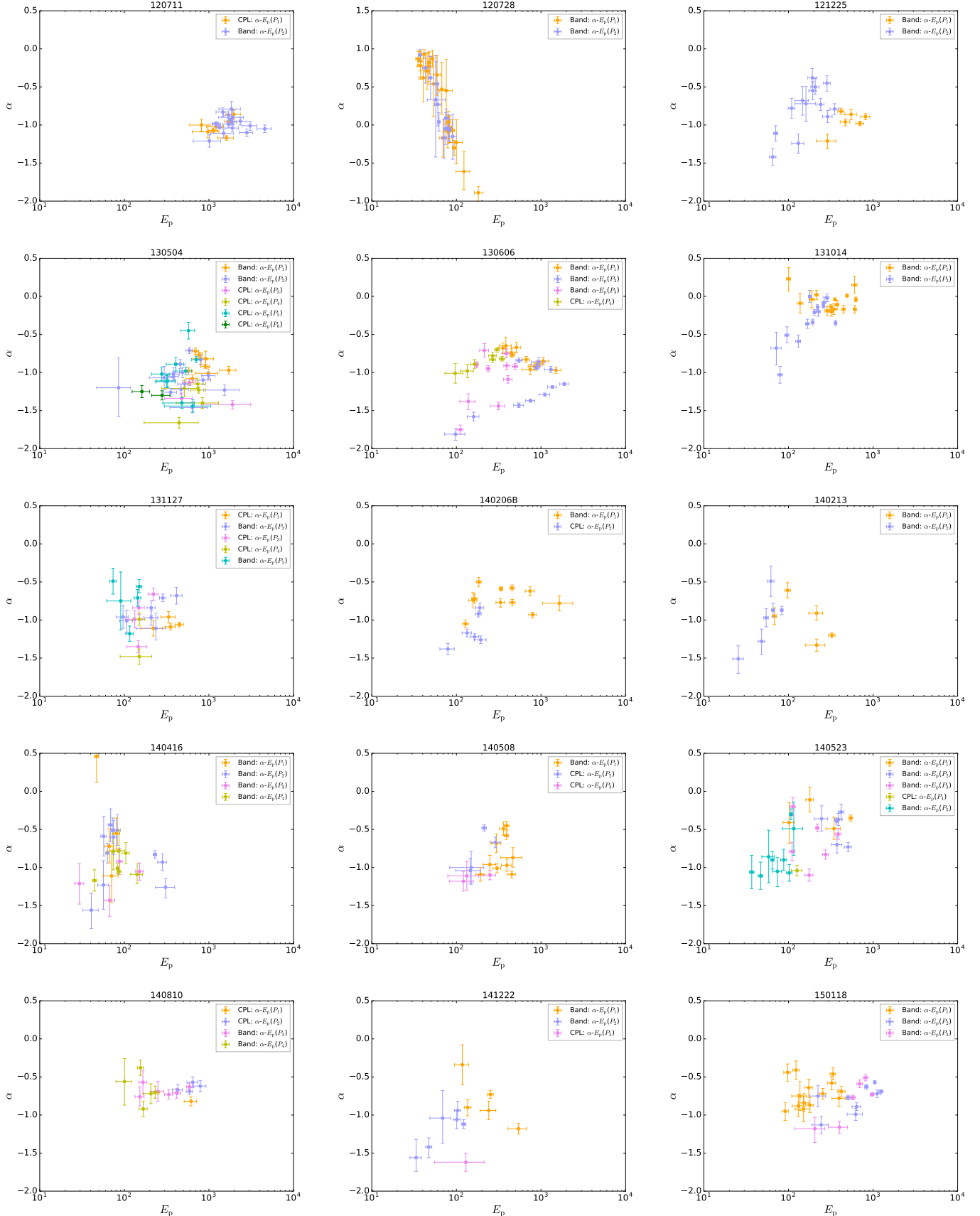


Fig. A7— Continued

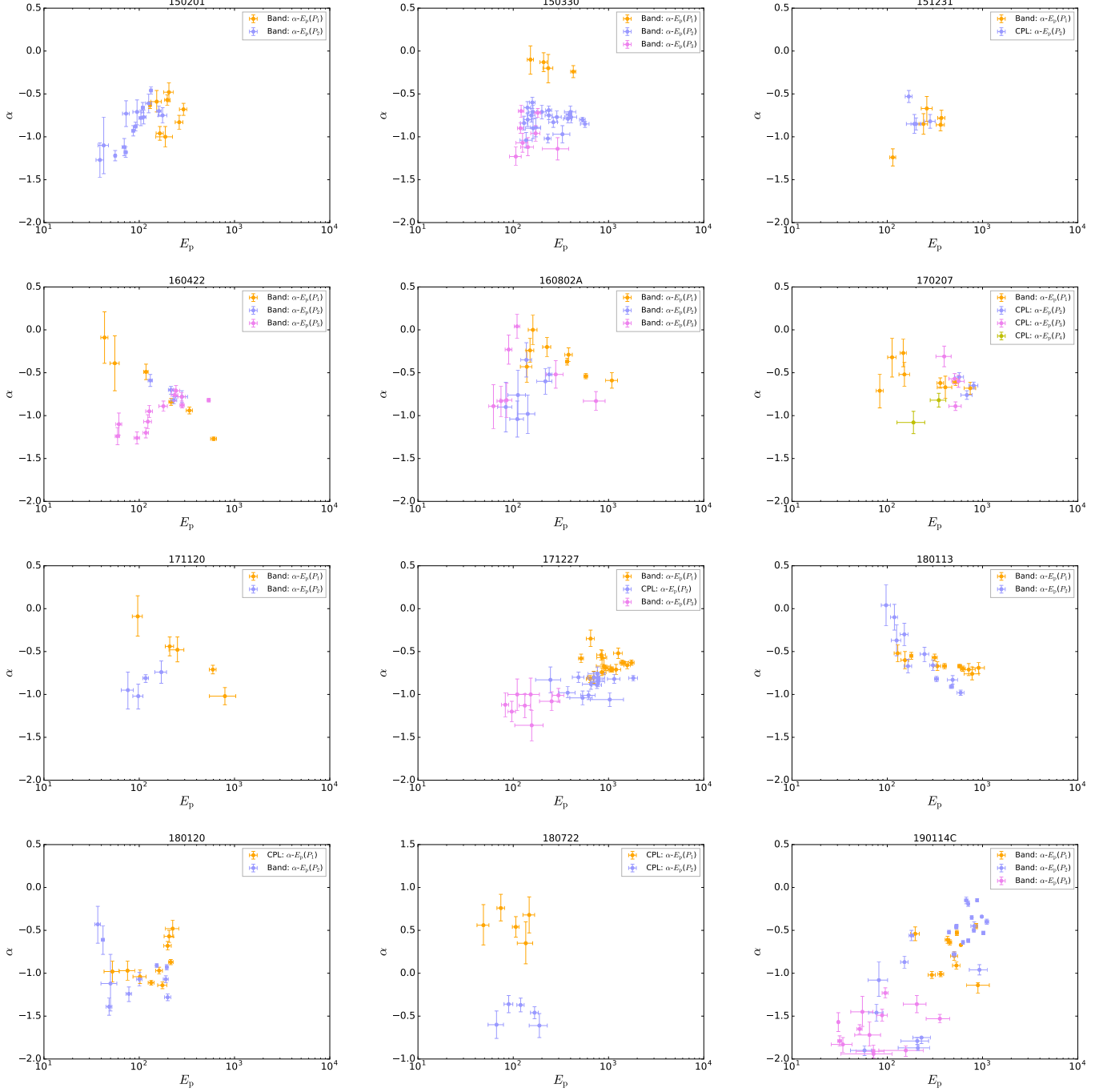


Fig. A7—Continued

A0.3. Single Model-based Parameter Distributions in Different Pulses

In Figure A8, we provide the results of the parameter distributions, separated by two empirical photon models (Band and CPL). The overall parameter distributions we studied include four parameters (α , β , E_p , and F) in the Band model and three parameters (α , E_p , and F) in the CPL model. The corresponding average values and standard deviations from the best Gaussian fit for each distribution is presented in Table A1.

The main results of parameter distributions (α , E_p and F) among pulses obtained from a single model (Fig.A8), either the Band model or the CPL model, are consistent with the finding in the best model (Fig.2), as we discussed in the main text. For the β distribution, we find a bimodal distribution for each time-series pulse sample, as well as the global sample, where the harder peak is at ~ -2.3 and the softer peak is at ~ -6.1 . The two peaks are basically the same for all different time-series pulses. We also find that the β indices are typically softer (about half of the Band spectra; the obtained β indices cannot be well converged) than some previous catalogs, whose analysis is based on the frequency analysis method, but consistent with the results found in Yu et al. (2019), who also adopted a fully Bayesian method but for a single-pulse sample.

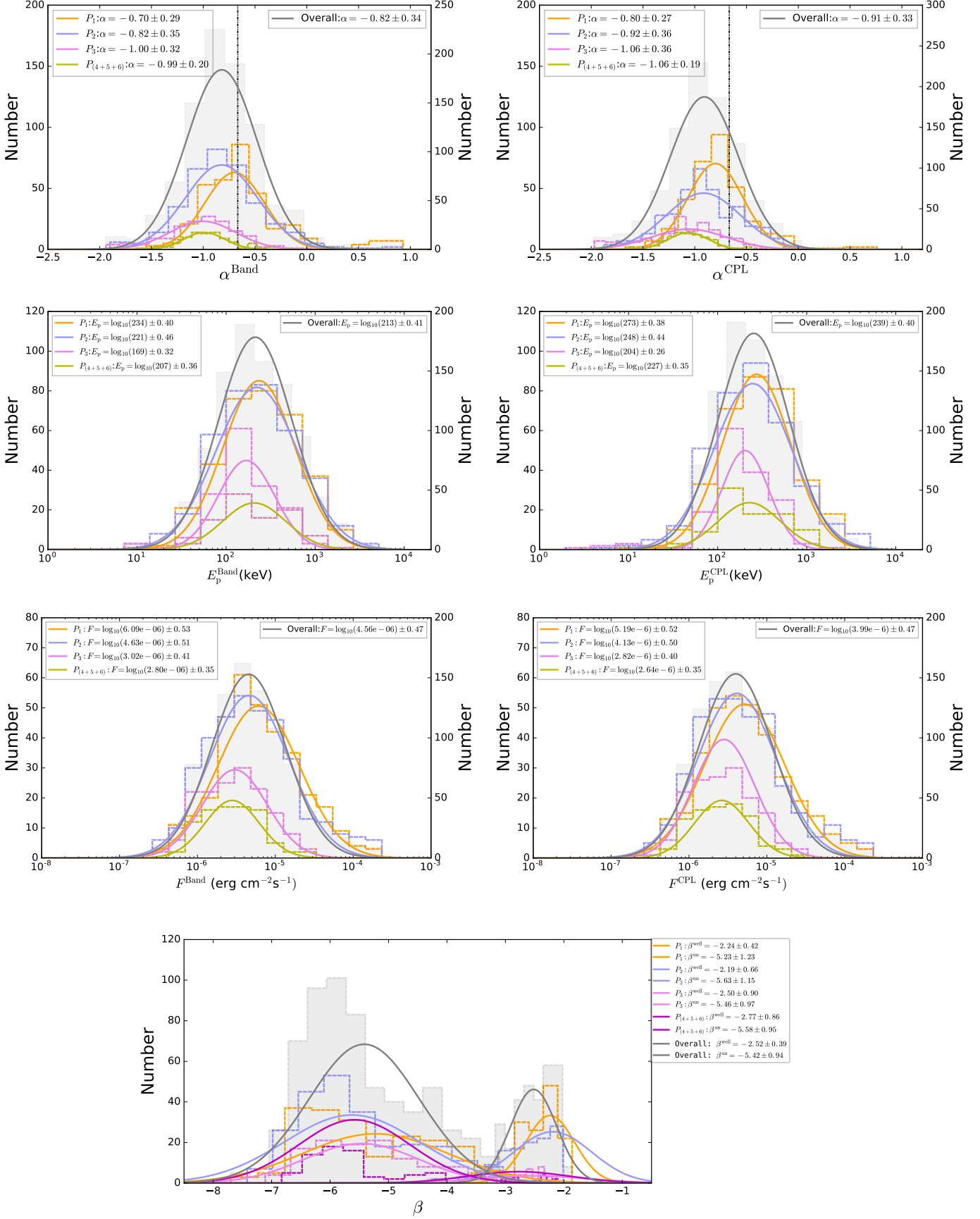


Figure A8. Same as Figure 2, but the analysis is based on the spectral parameters derived from single model (Band or CPL). Colors are the same as in Fig. 2. Left panels are for the Band model, and right panels are for the CPL model. The lower panel shows the distribution of β for the Band model.

Table A1. Results of the Average and Deviation Values of the Parameter Distribution

Pulse (Group)	Model (Selected)	Spectra (Number)	α (4)	E_p (keV) (5)	F (erg s $^{-1}$ cm $^{-2}$) (6)	β (well-converged) (7)	β (un-converged) (8)
(1)	(2)	(3)	(4)	(5)	(6)	(7)	(8)
P_1	CPL	338	-0.80±0.27	$\log_{10}(273)±0.38$	$\log_{10}(5.19e-6)±0.52$
P_2	CPL	361	-0.92±0.36	$\log_{10}(248)±0.44$	$\log_{10}(4.13e-6)±0.50$
P_3	CPL	156	-1.06±0.36	$\log_{10}(204)±0.26$	$\log_{10}(2.82e-6)±0.40$
$P_{(4+5+6)}$	CPL	89	-1.06±0.19	$\log_{10}(218)±0.31$	$\log_{10}(2.98e-6)±0.38$
Overall	CPL	944	-0.91±0.33	$\log_{10}(239)±0.40$	$\log_{10}(3.99e-6)±0.47$
P_1	Band	338	-0.70±0.29	$\log_{10}(234)±0.40$	$\log_{10}(6.09e-6)±0.53$	-2.24±0.42	-5.23±1.23
P_2	Band	361	-0.82±0.35	$\log_{10}(221)±0.46$	$\log_{10}(4.63e-6)±0.51$	-2.19±0.66	-5.63±1.15
P_3	Band	156	-1.00±0.32	$\log_{10}(169)±0.32$	$\log_{10}(3.02e-6)±0.41$	-2.50±0.90	-5.46±0.97
$P_{(4+5+6)}$	Band	89	-0.99±0.20	$\log_{10}(207)±0.36$	$\log_{10}(2.98e-6)±0.39$	-2.77±0.86	-5.58±0.95
Overall	Band	944	-0.82±0.34	$\log_{10}(213)±0.41$	$\log_{10}(4.56e-6)±0.47$	-2.52±0.39	-5.42±0.94

NOTE—Same as Table 3 but the results are based on single empirical photon model.

A0.4. Single Model-based Parameter Relations in Different Pulses

We show global pulsedwise parameter relations for our full sample in Figure A9. We present each parameter relation based on the two different photon models (the Band and CPL): F - α relation based on the Band model (first left panel), F - α relation based on the CPL model (first right panel), F - E_p relation based on the Band model (second left panel), F - E_p relation based on the CPL model (second right panel), α - E_p relation based on the Band model (third left panel), α - E_p relation based on the CPL model (third right panel), and α - β relation based on the Band model (bottom panel).

We find that there is no significant difference in the global parameter relations between the Band and CPL models. In addition, the F - E_p Golenetskii relation based on the Band model shows a stronger monotonic positive correlation than the CPL model. For the F - α relation, a cluster of data points that significantly deviate from the peak of the distribution (probably mainly contributed by the Type 2 in the individual parameter relations) mainly come from the early (P_1) pulse. In short, the global F - α relation shows a monotone positive correlation following a break behavior. Such a break may be originated from thermal emission. The global F - E_p relation displays the type 1p behavior, while the global α - E_p shows an anticorrelation type 1n behavior. Finally, we do not find a clear trend in the global $\alpha - \beta$ relation.

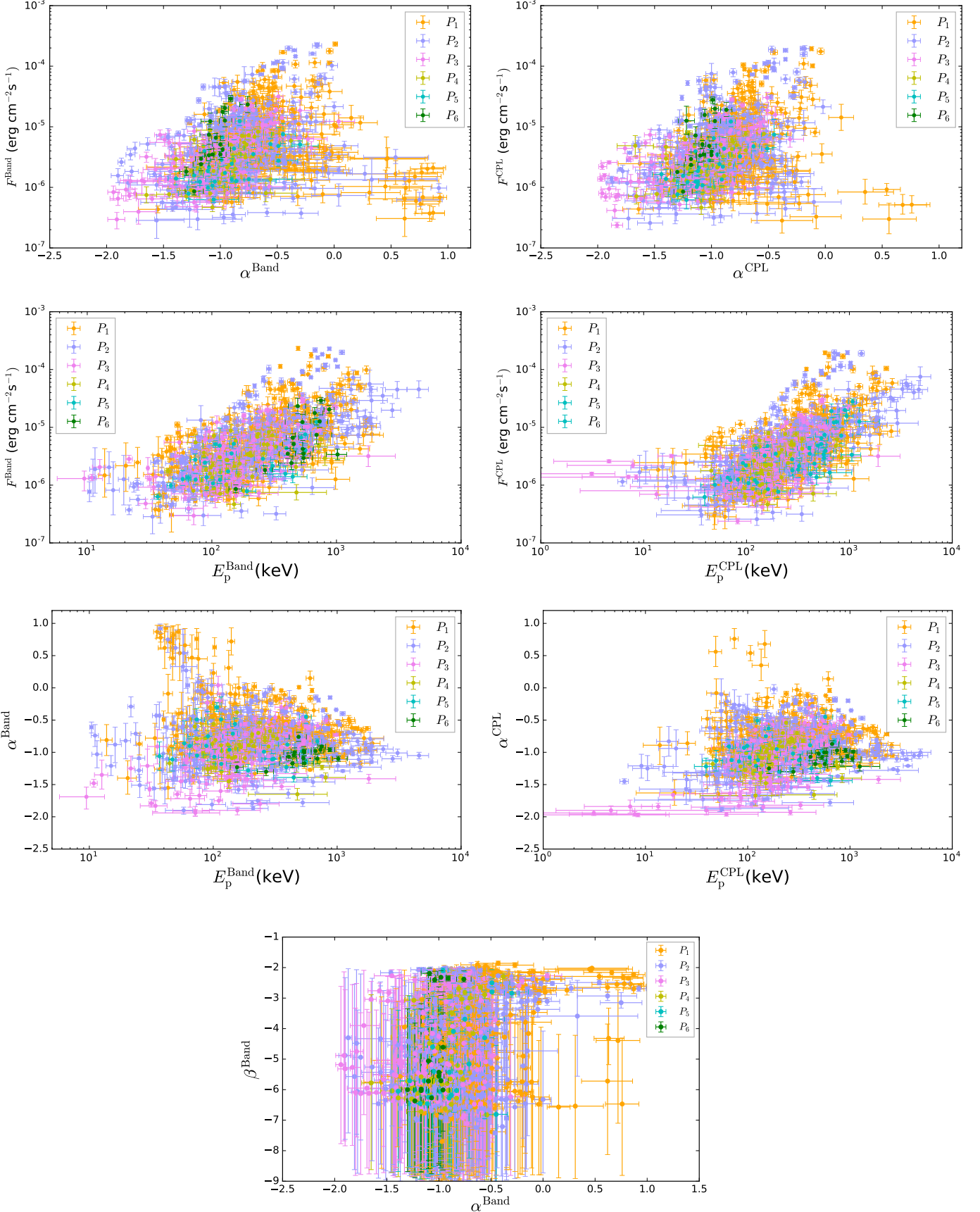


Figure A9. Pulsewise global relations of the fitted parameters of the Band and CPL models with statistical significance $S \geq 20$. The colors are the same as in Figure 2. Left panels are for the Band model, right panels are for the CPL model, and the bottom panel is only for the Band model.

A1. ADDITIONAL TABLES

The spectral parameters for each time bin are obtained by applying both the Band and CPL models to fit all 944 spectra. The results of the time-resolved spectral fits for each burst in our global sample, which include the start and stop times of the BBlocks (column 1), the statistical significance S (column 2); the best-fitted parameters of the CPL model (columns 3-7), including the normalization K , the low-energy power-law photon spectral index α , the break energy E_c , peak energy⁸ E_p , and the νF_ν flux F ; and the best-fit parameters of the Band model (columns 8-12), containing the normalization, the low-energy power-law photon spectral index α , the high-energy power-law photon spectral index β , the peak energy E_p , and the νF_ν flux F ; the ΔDIC (column 13), the $p_{\text{DIC}}^{\text{CPL}}$ based on the CPL model fitting (column 14), and the $p_{\text{DIC}}^{\text{Band}}$ based on the Band model fitting (column 15), are listed in Tables A2-A40 in Appendix. For the definition of ΔDIC , as well as the discussion for p_{DIC} , please see §2.6 for details.

⁸ We note that in a few cases, the value of E_p is close to the lower limit of the detector range. Since the effective area decreases rapidly at the edges of the detector energy range and the determination of α suffers from the lack of dynamical range below the peak, the time bins with $E_p < 20$ keV should be largely ignored (see, e.g., [Ravasio et al. 2019](#)).

Table A2. Time-resolved Spectral Fit Results of GRB 081009140

$t_{\text{start}} \sim t_{\text{stop}}$	S	Cutoff Power-Law Fitting				Band Fitting				Difference				
		K	α	E_c	E_p	F	K	α	β	E_p	F	ΔDIC	$p_{\text{DIC}}^{\text{CPL}}$	$p_{\text{DIC}}^{\text{Band}}$
(1)	(2)	(3)	(4)	(5)	(6)	(7)	(8)	(9)	(10)	(11)	(12)	(13)	(14)	(15)
Pulse 1														
0.000~0.368	21.46	$0.08^{+0.03}_{-0.02}$	$-1.36^{+0.17}_{-0.15}$	75^{+17}_{-18}	48^{+17}_{-16}	$1.31^{+0.71 \times 10^{-6}}_{-0.41 \times 10^{-6}}$	$0.38^{+0.19}_{-0.21}$	$-0.78^{+0.23}_{-0.26}$	$-2.72^{+0.46}_{-0.02}$	34^{+6}_{-6}	$1.53^{+1.81 \times 10^{-6}}_{-0.85 \times 10^{-6}}$	-13.5	0.8	-5.4
0.368~1.114	47.31	$0.12^{+0.05}_{-0.05}$	$-1.63^{+0.20}_{-0.19}$	52^{+14}_{-14}	19^{+12}_{-11}	$2.46^{+1.87 \times 10^{-6}}_{-1.04 \times 10^{-6}}$	$0.23^{+0.14}_{-0.12}$	$-1.40^{+0.27}_{-0.25}$	$-5.04^{+1.93}_{-1.93}$	20^{+4}_{-4}	$2.17^{+3.21 \times 10^{-6}}_{-1.39 \times 10^{-6}}$	-11.9	-16.9	-28.5
1.114~1.358	39.81	$0.24^{+0.09}_{-0.09}$	$-1.36^{+0.20}_{-0.20}$	62^{+16}_{-16}	40^{+16}_{-16}	$3.45^{+2.55}_{-2.55}$	$0.32^{+0.10}_{-0.15}$	$-1.26^{+0.20}_{-0.23}$	$-6.30^{+2.53}_{-2.55}$	37^{+4}_{-4}	$3.31^{+3.59 \times 10^{-6}}_{-1.86 \times 10^{-6}}$	-7.4	-7.0	-15.0
1.358~1.662	57.46	$0.66^{+0.17}_{-0.18}$	$-0.94^{+0.14}_{-0.14}$	44^{+6}_{-6}	47^{+9}_{-9}	$4.06^{+1.59 \times 10^{-6}}_{-1.21 \times 10^{-6}}$	$0.70^{+0.19}_{-0.20}$	$-0.91^{+0.14}_{-0.14}$	$-7.03^{+1.96}_{-1.99}$	46^{+2}_{-2}	$3.95^{+2.24 \times 10^{-6}}_{-1.41 \times 10^{-6}}$	1.8	-0.5	0.9
1.662~1.895	58.56	$1.53^{+0.46}_{-0.46}$	$-0.62^{+0.16}_{-0.16}$	35^{+4}_{-4}	48^{+8}_{-8}	$4.71^{+2.35 \times 10^{-6}}_{-1.65 \times 10^{-6}}$	$1.71^{+0.56}_{-0.59}$	$-0.56^{+0.17}_{-0.17}$	$-6.48^{+2.07}_{-2.29}$	47^{+2}_{-2}	$4.49^{+2.77 \times 10^{-6}}_{-2.29 \times 10^{-6}}$	3.7	-6.1	-2.4
1.895~2.042	58.16	$0.74^{+0.20}_{-0.20}$	$-1.04^{+0.14}_{-0.14}$	60^{+9}_{-10}	57^{+12}_{-12}	$6.84^{+3.00 \times 10^{-6}}_{-1.98 \times 10^{-6}}$	$0.77^{+0.20}_{-0.20}$	$-1.02^{+0.14}_{-0.14}$	$-6.84^{+2.10}_{-2.14}$	56^{+3}_{-3}	$6.85^{+3.40 \times 10^{-6}}_{-2.31 \times 10^{-6}}$	2.0	-0.3	1.6
2.042~2.724	139.74	$0.95^{+0.09}_{-0.09}$	$-0.88^{+0.05}_{-0.05}$	65^{+4}_{-4}	73^{+5}_{-5}	$8.68^{+1.08 \times 10^{-6}}_{-1.08 \times 10^{-6}}$	$0.95^{+0.09}_{-0.09}$	$-0.88^{+0.05}_{-0.05}$	$-6.96^{+2.02}_{-2.08}$	73^{+2}_{-2}	$8.74^{+1.22 \times 10^{-6}}_{-1.14 \times 10^{-6}}$	-0.1	2.7	2.8
2.724~3.004	102.13	$0.98^{+0.12}_{-0.12}$	$-0.89^{+0.07}_{-0.07}$	78^{+7}_{-7}	87^{+9}_{-9}	$11.29^{+1.92 \times 10^{-6}}_{-1.78 \times 10^{-6}}$	$0.99^{+0.12}_{-0.12}$	$-0.88^{+0.07}_{-0.07}$	$-6.91^{+2.05}_{-2.08}$	87^{+3}_{-3}	$11.11^{+2.14 \times 10^{-6}}_{-1.74 \times 10^{-6}}$	0.7	2.6	3.0
3.004~3.291	91.74	$1.04^{+0.19}_{-0.19}$	$-0.96^{+0.09}_{-0.09}$	52^{+5}_{-5}	54^{+7}_{-7}	$8.09^{+2.16 \times 10^{-6}}_{-1.61 \times 10^{-6}}$	$1.07^{+0.19}_{-0.20}$	$-0.95^{+0.09}_{-0.09}$	$-6.72^{+2.09}_{-2.17}$	53^{+2}_{-2}	$8.03^{+2.81 \times 10^{-6}}_{-2.94 \times 10^{-6}}$	0.8	1.6	2.4
3.291~4.845	178.12	$0.98^{+0.10}_{-0.10}$	$-0.98^{+0.05}_{-0.05}$	43^{+2}_{-2}	44^{+3}_{-3}	$6.28^{+0.79 \times 10^{-6}}_{-0.78 \times 10^{-6}}$	$0.98^{+0.10}_{-0.10}$	$-0.97^{+0.05}_{-0.05}$	$-7.70^{+1.59}_{-1.60}$	44^{+1}_{-1}	$6.26^{+1.03 \times 10^{-6}}_{-0.89 \times 10^{-6}}$	0.8	2.5	3.0
4.845~5.379	92.71	$0.73^{+0.12}_{-0.12}$	$-0.93^{+0.09}_{-0.09}$	53^{+5}_{-5}	57^{+7}_{-7}	$5.54^{+1.30 \times 10^{-6}}_{-1.09 \times 10^{-6}}$	$0.75^{+0.13}_{-0.13}$	$-0.92^{+0.09}_{-0.09}$	$-6.47^{+2.10}_{-2.33}$	56^{+2}_{-2}	$5.46^{+1.54 \times 10^{-6}}_{-1.21 \times 10^{-6}}$	0.4	1.6	2.2
5.379~5.654	58.38	$0.90^{+0.27}_{-0.27}$	$-0.78^{+0.16}_{-0.15}$	42^{+6}_{-6}	51^{+10}_{-10}	$4.59^{+2.18 \times 10^{-6}}_{-1.48 \times 10^{-6}}$	$1.00^{+0.30}_{-0.30}$	$-0.74^{+0.16}_{-0.16}$	$-6.38^{+2.23}_{-2.23}$	50^{+2}_{-2}	$4.18^{+2.65 \times 10^{-6}}_{-2.65 \times 10^{-6}}$	2.1	-2.2	-0.1
5.654~6.403	77.43	$1.63^{+0.43}_{-0.43}$	$-0.48^{+0.13}_{-0.13}$	26^{+2}_{-2}	40^{+5}_{-5}	$3.02^{+0.26 \times 10^{-6}}_{-0.18 \times 10^{-6}}$	$1.62^{+0.44}_{-0.43}$	$-0.49^{+0.13}_{-0.13}$	$-7.38^{+1.80}_{-1.82}$	40^{+1}_{-1}	$3.01^{+1.32 \times 10^{-6}}_{-1.00 \times 10^{-6}}$	2.3	-1.8	0.4
6.403~7.223	66.04	$0.99^{+0.40}_{-0.38}$	$-0.86^{+0.18}_{-0.18}$	23^{+3}_{-3}	26^{+5}_{-5}	$2.40^{+0.69 \times 10^{-6}}_{-0.69 \times 10^{-6}}$	$0.95^{+0.35}_{-0.34}$	$-0.87^{+0.17}_{-0.17}$	$-7.40^{+1.76}_{-1.78}$	25^{+1}_{-1}	$2.47^{+2.03 \times 10^{-6}}_{-1.15 \times 10^{-6}}$	11.4	-15.5	-4.1
7.223~7.710	31.68	$1.44^{+0.96}_{-0.89}$	$-0.89^{+0.28}_{-0.30}$	12^{+2}_{-2}	14^{+4}_{-4}	$1.84^{+0.49 \times 10^{-6}}_{-1.17 \times 10^{-6}}$	$1.68^{+0.95}_{-0.92}$	$-0.81^{+0.24}_{-0.24}$	$-6.89^{+1.98}_{-2.06}$	14^{+1}_{-1}	$1.48^{+0.86 \times 10^{-6}}_{-0.86 \times 10^{-6}}$	21.7	-32.1	-10.5
Pulse 2														
39.073~39.961	26.55	$0.70^{+0.41}_{-0.35}$	$-0.83^{+0.23}_{-0.23}$	14^{+2}_{-2}	17^{+4}_{-4}	$0.95^{+0.98 \times 10^{-6}}_{-0.49 \times 10^{-6}}$	$0.65^{+0.41}_{-0.38}$	$-0.88^{+0.27}_{-0.28}$	$-7.38^{+1.83}_{-1.80}$	16^{+2}_{-2}	$0.82^{+1.71 \times 10^{-6}}_{-0.51 \times 10^{-6}}$	-1.5	-11.0	-12.7
39.961~40.823	37.34	$0.65^{+0.41}_{-0.38}$	$-0.94^{+0.29}_{-0.28}$	19^{+4}_{-4}	20^{+7}_{-7}	$1.37^{+1.94 \times 10^{-6}}_{-0.83 \times 10^{-6}}$	$0.90^{+0.45}_{-0.54}$	$-0.82^{+0.27}_{-0.28}$	$-6.87^{+2.19}_{-2.14}$	20^{+2}_{-2}	$1.27^{+2.00 \times 10^{-6}}_{-0.81 \times 10^{-6}}$	17.1	-57.0	-40.3
40.823~43.426	81.42	$0.45^{+0.16}_{-0.16}$	$-1.22^{+0.15}_{-0.15}$	20^{+2}_{-2}	15^{+3}_{-3}	$2.07^{+1.48 \times 10^{-6}}_{-0.85 \times 10^{-6}}$	$0.47^{+0.17}_{-0.16}$	$-1.21^{+0.16}_{-0.15}$	$-7.00^{+2.06}_{-2.08}$	15^{+1}_{-1}	$2.04^{+1.73 \times 10^{-6}}_{-0.97 \times 10^{-6}}$	10.4	-20.1	-9.7
43.426~44.500	46.19	$0.60^{+0.28}_{-0.27}$	$-1.25^{+0.19}_{-0.19}$	14^{+2}_{-2}	10^{+3}_{-3}	$2.00^{+0.90 \times 10^{-6}}_{-0.95 \times 10^{-6}}$	$1.10^{+0.54}_{-0.52}$	$-1.03^{+0.21}_{-0.21}$	$-6.09^{+2.30}_{-1.98}$	12^{+1}_{-1}	$1.89^{+2.54 \times 10^{-6}}_{-1.16 \times 10^{-6}}$	2.0	-25.4	-24.9
44.500~45.653	37.00	$0.62^{+0.27}_{-0.27}$	$-1.21^{+0.18}_{-0.19}$	12^{+1}_{-1}	9^{+2}_{-2}	$1.68^{+1.60 \times 10^{-6}}_{-0.79 \times 10^{-6}}$	$2.28^{+0.18}_{-0.08}$	$-0.74^{+0.17}_{-0.17}$	$-6.17^{+1.62}_{-1.87}$	11^{+1}_{-1}	$1.33^{+1.48 \times 10^{-6}}_{-0.70 \times 10^{-6}}$	1.3	-7.7	-7.7
45.653~47.578	28.55	$0.21^{+0.02}_{-0.02}$	$-1.45^{+0.04}_{-0.04}$	11^{+1}_{-1}	6^{+1}_{-1}	$1.15^{+0.18 \times 10^{-6}}_{-0.19 \times 10^{-6}}$	$2.14^{+0.60}_{-0.64}$	$-0.61^{+0.08}_{-0.09}$	$-5.68^{+1.83}_{-2.61}$	$10.4^{+0.3}_{-0.3}$	$0.77^{+0.37 \times 10^{-6}}_{-0.26 \times 10^{-6}}$	1.4	1.6	-0.7

Note—Column (1) list the start and stop times of the BBlocks time bins; Column (2) lists the significance S of the time bin; Column (3)–(6) list the best-fit parameters for the CPL model: normalisation K , the low-energy power-law index α , and the cut-off energy E_c ; and the peak energy E_p ; Column (7) lists the derived CPL (νF_ν) energy flux F ; Column (8)–(11) lists the best-fit parameters for the Band model: normalisation K , the low-energy power-law index α , the high-energy power-law index β , and the peak energy E_p ; Column (12) lists the Band (νF_ν) energy flux F ; Column (13) lists the Deviance Information Criterion (DIC) for the CPL and the Band model, respectively. Columns (14) and (15) list the effective number of parameters (p_{DIC}) for the CPL and Band model, respectively.

Table A3. Time-resolved Spectral Fit Results of GRB 081215784

$t_{\text{start}} \sim t_{\text{stop}}$	S	Cutoff Power-Law Fitting						Band Fitting						Difference	
		K	α	E_c	E_p	F	K	α	β	E_p	F	ΔDIC	$p_{\text{DIC}}^{\text{CPL}}$	$p_{\text{DIC}}^{\text{Band}}$	
(1)	(2)	(3)	(4)	(5)	(6)	(7)	(8)	(9)	(10)	(11)	(12)	(13)	(14)	(15)	
Pulse 1															
1.064~1.217	25.29	0.27 ^{+0.04} _{-0.04}	-0.63 ^{+0.07} _{-0.07}	984 ⁺¹⁶⁸ ₋₁₆₅	1348 ⁺²⁴⁰ ₋₂₃₆	19.77 ^{+10.03} _{-6.27}	10.05×10^{-6}	0.26 ^{+0.04} _{-0.04}	-0.62 ^{+0.07} _{-0.07}	-6.04 ^{+2.56} _{-2.66}	1313 ⁺¹⁷⁶ ₋₁₈₁	20.28 ^{+8.23} _{-6.25}	10^{-6}	-0.4	2.3
1.217~1.333	35.25	0.62 ^{+0.07} _{-0.07}	-0.77 ^{+0.04} _{-0.04}	1507 ⁺²²⁶ ₋₂₂₇	1854 ⁺²⁸⁵ ₋₂₈₆	42.89 ^{+14.68} _{-11.40}	$\times 10^{-6}$	0.45 ^{+0.07} _{-0.07}	-0.57 ^{+0.08} _{-0.08}	-2.21 ^{+0.15} _{-0.14}	1002 ⁺¹⁸¹ ₋₁₈₁	38.44 ^{+20.81} _{-11.97}	$\times 10^{-6}$	-20.8	2.7
1.333~1.409	41.78	0.77 ^{+0.08} _{-0.08}	-0.61 ^{+0.04} _{-0.04}	1208 ⁺¹³⁰ ₋₁₃₀	1679 ⁺¹⁸⁷ ₋₁₈₇	85.70 ^{+28.88} _{-19.46}	$\times 10^{-6}$	0.64 ^{+0.08} _{-0.08}	-0.49 ^{+0.06} _{-0.06}	-2.62 ^{+0.22} _{-0.20}	1241 ⁺¹³⁶ ₋₁₃₅	83.91 ^{+26.67} _{-21.10}	$\times 10^{-6}$	-16.4	2.8
1.409~1.597	100.52	1.15 ^{+0.06} _{-0.06}	-0.50 ^{+0.02} _{-0.02}	723 ⁺⁴⁰ ₋₄₁	1085 ⁺⁶² ₋₆₅	101.40 ^{+15.07} _{-14.34}	$\times 10^{-6}$	0.90 ^{+0.06} _{-0.06}	-0.34 ^{+0.03} _{-0.03}	-2.48 ^{+0.08} _{-0.08}	792 ⁺³⁸ ₋₃₈	107.50 ^{+17.71} _{-13.71}	$\times 10^{-6}$	-124.8	2.9
1.597~1.699	53.58	0.89 ^{+0.09} _{-0.09}	-0.47 ^{+0.05} _{-0.05}	397 ⁺³⁸ ₋₃₈	607 ⁺⁶¹ ₋₆₂	34.62 ^{+11.37} _{-7.64}	$\times 10^{-6}$	0.77 ^{+0.08} _{-0.08}	-0.35 ^{+0.06} _{-0.06}	-2.30 ^{+0.12} _{-0.12}	487 ⁺⁴¹ ₋₄₀	46.90 ^{+13.27} _{-10.59}	$\times 10^{-6}$	-35.0	2.6
1.699~1.888	55.12	0.90 ^{+0.07} _{-0.07}	-0.61 ^{+0.05} _{-0.05}	343 ⁺³¹ ₋₃₁	477 ⁺⁴⁷ ₋₄₇	17.22 ^{+4.39} _{-3.39}	$\times 10^{-6}$	0.82 ^{+0.07} _{-0.07}	-0.51 ^{+0.06} _{-0.07}	-2.41 ^{+0.17} _{-0.15}	394 ⁺³⁷ ₋₃₇	22.15 ^{+6.87} _{-4.74}	$\times 10^{-6}$	-15.8	2.8
1.888~2.082	38.27	0.69 ^{+0.07} _{-0.07}	-0.69 ^{+0.07} _{-0.07}	295 ⁺³⁹ ₋₅₆	386 ⁺⁵⁵ ₋₅₆	8.07 ^{+3.02} _{-1.90}	$\times 10^{-6}$	0.57 ^{+0.07} _{-0.07}	-0.45 ^{+0.12} _{-0.12}	-2.12 ^{+0.10} _{-0.09}	257 ⁺³⁴ ₋₃₄	12.19 ^{+5.67} _{-3.67}	$\times 10^{-6}$	-19.3	2.5
2.082~2.720	53.70	0.63 ^{+0.04} _{-0.04}	-0.81 ^{+0.05} _{-0.04}	317 ⁺³² ₋₃₃	377 ⁺⁴² ₋₄₁	5.65 ^{+1.24} _{-1.04}	$\times 10^{-6}$	0.58 ^{+0.04} _{-0.04}	-0.70 ^{+0.07} _{-0.07}	-2.45 ^{+0.30} _{-0.08}	298 ⁺³⁴ ₋₃₄	7.45 ^{+2.24} _{-1.76}	$\times 10^{-6}$	-11.6	2.7
2.720~3.100	32.67	0.63 ^{+0.06} _{-0.06}	-0.92 ^{+0.07} _{-0.07}	288 ⁺⁴⁶ ₋₄₆	311 ⁺⁵³ ₋₅₄	3.58 ^{+1.22} _{-0.84}	$\times 10^{-6}$	0.63 ^{+0.06} _{-0.06}	-0.91 ^{+0.07} _{-0.07}	-5.95 ^{+2.67} _{-2.71}	302 ⁺³² ₋₃₂	3.69 ^{+0.93} _{-0.73}	$\times 10^{-6}$	0.2	2.5
Pulse 2															
3.100~3.646	55.02	0.50 ^{+0.04} _{-0.04}	-0.62 ^{+0.05} _{-0.05}	280 ⁺²⁴ ₋₂₃	386 ⁺³⁶ ₋₃₅	6.97 ^{+1.43} _{-1.30}	$\times 10^{-6}$	0.49 ^{+0.04} _{-0.04}	-0.61 ^{+0.05} _{-0.05}	-5.56 ^{+2.43} _{-2.76}	378 ⁺²⁴ ₋₂₃	7.11 ^{+1.35} _{-1.09}	$\times 10^{-6}$	-0.8	2.8
3.646~3.915	56.78	0.70 ^{+0.05} _{-0.05}	-0.57 ^{+0.04} _{-0.04}	322 ⁺²⁵ ₋₂₆	460 ⁺³⁹ ₋₃₉	14.46 ^{+3.34} _{-2.60}	$\times 10^{-6}$	0.69 ^{+0.05} _{-0.05}	-0.55 ^{+0.05} _{-0.05}	-5.81 ^{+2.48} _{-2.77}	452 ⁺²⁷ ₋₂₇	14.55 ^{+2.94} _{-2.20}	$\times 10^{-6}$	-0.6	2.6
3.915~4.097	37.82	0.67 ^{+0.07} _{-0.07}	-0.53 ^{+0.08} _{-0.08}	178 ⁺¹⁹ ₋₂₀	261 ⁺³¹ ₋₃₂	6.25 ^{+2.19} _{-1.44}	$\times 10^{-6}$	0.66 ^{+0.07} _{-0.07}	-0.52 ^{+0.08} _{-0.08}	-6.66 ^{+2.31} _{-2.20}	257 ⁺¹⁹ ₋₁₈	6.42 ^{+1.68} _{-1.30}	$\times 10^{-6}$	0.7	2.6
4.097~4.603	45.86	0.64 ^{+0.05} _{-0.05}	-0.65 ^{+0.06} _{-0.06}	169 ⁺¹⁵ ₋₁₆	228 ⁺²³ ₋₂₃	4.08 ^{+1.01} _{-0.77}	$\times 10^{-6}$	0.64 ^{+0.05} _{-0.05}	-0.64 ^{+0.07} _{-0.07}	-5.40 ^{+2.38} _{-2.87}	222 ⁺¹⁴ ₋₁₄	4.28 ^{+0.93} _{-0.69}	$\times 10^{-6}$	-1.3	2.3
4.603~4.947	48.18	0.71 ^{+0.05} _{-0.05}	-0.66 ^{+0.05} _{-0.05}	244 ⁺²² ₋₂₃	327 ⁺³² ₋₃₃	7.31 ^{+1.94} _{-1.41}	$\times 10^{-6}$	0.68 ^{+0.06} _{-0.06}	-0.60 ^{+0.08} _{-0.08}	-4.12 ^{+2.87} _{-2.87}	300 ⁺³² ₋₃₂	8.21 ^{+2.67} _{-1.92}	$\times 10^{-6}$	-6.8	2.8
Pulse 3															
4.947~5.076	44.08	0.63 ^{+0.07} _{-0.07}	-0.44 ^{+0.07} _{-0.07}	273 ⁺²⁹ ₋₂₉	425 ⁺⁴⁸ ₋₄₉	15.81 ^{+5.91} _{-4.37}	$\times 10^{-6}$	0.54 ^{+0.07} _{-0.07}	-0.30 ^{+0.10} _{-0.10}	-2.84 ^{+0.51} _{-0.51}	355 ⁺⁴² ₋₄₁	18.57 ^{+8.99} _{-5.72}	$\times 10^{-6}$	-8.9	2.5
5.076~5.248	68.99	0.99 ^{+0.07} _{-0.07}	-0.51 ^{+0.04} _{-0.04}	365 ⁺²⁶ ₋₂₆	544 ⁺⁴² ₋₄₁	30.30 ^{+6.31} _{-5.31}	$\times 10^{-6}$	0.97 ^{+0.07} _{-0.07}	-0.49 ^{+0.04} _{-0.04}	-4.90 ^{+1.81} _{-2.82}	527 ⁺³⁰ ₋₃₀	31.46 ^{+6.49} _{-5.03}	$\times 10^{-6}$	-3.8	2.9
5.248~5.439	49.94	0.82 ^{+0.07} _{-0.07}	-0.54 ^{+0.05} _{-0.05}	248 ⁺²² ₋₂₂	362 ⁺³⁴ ₋₃₄	12.37 ^{+3.13} _{-2.65}	$\times 10^{-6}$	0.76 ^{+0.08} _{-0.08}	-0.46 ^{+0.09} _{-0.09}	-3.71 ^{+1.31} _{-2.36}	318 ⁺³⁷ ₋₃₆	14.07 ^{+6.04} _{-3.62}	$\times 10^{-6}$	-10.1	2.7
5.439~5.750	44.87	0.71 ^{+0.06} _{-0.06}	-0.68 ^{+0.06} _{-0.06}	228 ⁺²⁴ ₋₂₄	300 ⁺³⁴ ₋₃₄	6.28 ^{+1.65} _{-1.33}	$\times 10^{-6}$	0.68 ^{+0.07} _{-0.07}	-0.62 ^{+0.10} _{-0.09}	-4.77 ^{+2.28} _{-3.17}	277 ⁺³³ ₋₃₇	6.66 ^{+2.74} _{-1.72}	$\times 10^{-6}$	-3.2	2.7
5.750~5.952	23.60	0.63 ^{+0.09} _{-0.09}	-0.83 ^{+0.13} _{-0.13}	163 ⁺³⁷ ₋₃₈	191 ⁺⁴⁸ ₋₄₉	2.29 ^{+1.31} _{-0.73}	$\times 10^{-6}$	0.60 ^{+0.07} _{-0.07}	-0.71 ^{+0.15} _{-0.16}	-4.01 ^{+1.83} _{-3.19}	156 ⁺³³ ₋₃₁	2.82 ^{+1.84} _{-1.00}	$\times 10^{-6}$	-7.3	1.4
6.202~6.380	26.12	0.68 ^{+0.08} _{-0.08}	-0.80 ^{+0.10} _{-0.10}	210 ⁺⁴⁰ ₋₄₀	252 ⁺⁵³ ₋₅₂	3.73 ^{+1.85} _{-1.14}	$\times 10^{-6}$	0.67 ^{+0.09} _{-0.09}	-0.79 ^{+0.11} _{-0.11}	-6.07 ^{+2.74} _{-2.68}	244 ⁺³⁰ ₋₃₀	3.83 ^{+1.29} _{-0.92}	$\times 10^{-6}$	0.6	2.8
6.380~6.961	32.45	0.61 ^{+0.05} _{-0.05}	-0.99 ^{+0.08} _{-0.08}	191 ⁺³⁴ ₋₃₈	193 ⁺³⁷ ₋₃₈	1.82 ^{+0.68} _{-0.45}	$\times 10^{-6}$	0.55 ^{+0.06} _{-0.06}	-0.75 ^{+0.15} _{-0.15}	-2.58 ^{+0.47} _{-0.47}	135 ⁺²¹ ₋₂₁	2.60 ^{+0.80} _{-0.80}	$\times 10^{-6}$	-11.2	2.3
6.961~7.771	23.23	0.51 ^{+0.05} _{-0.05}	-1.03 ^{+0.13} _{-0.13}	119 ⁺²⁷ ₋₂₇	116 ⁺³⁰ ₋₃₀	0.87 ^{+0.36} _{-0.21}	$\times 10^{-6}$	0.48 ^{+0.05} _{-0.05}	-0.87 ^{+0.22} _{-0.21}	-3.93 ^{+1.66} _{-2.82}	98 ⁺¹⁷ ₋₁₈	1.04 ^{+0.56} _{-0.34}	$\times 10^{-6}$	-5.1	1.7

Note—All columns are the same as Table A2 but for GRB 081215784.

Table A4. Time-resolved Spectral Fit Results of GRB 090131090

$t_{\text{start}} \sim t_{\text{stop}}$	S	Cutoff Power-Law Fitting						Band Fitting						Difference		
		K	α	E_c	E_p	F	K	α	β	E_p	F	ΔDIC	$p_{\text{DIC}}^{\text{CPL}}$	$p_{\text{DIC}}^{\text{Band}}$	(14)	(15)
(1)	(2)	(3)	(4)	(5)	(6)	(7)	(8)	(9)	(10)	(11)	(12)	(13)	(14)	(15)		
Pulse 1																
2.963~3.560	48.79	1.56 ^{+0.10} _{-0.09}	-0.96 ^{+0.09} _{-0.05}	80 ⁺¹⁰ ₋₁₀	84 ⁺¹³ ₋₁₃	2.10 ^{+0.52} _{-0.39} × 10 ⁻⁶	1.54 ^{+0.10} _{-0.11}	-0.92 ^{+0.11} _{-0.11}	-5.96 ^{+2.62} _{-2.65}	81 ⁺⁵ ₋₅	2.11 ^{+0.30} _{-0.24} × 10 ⁻⁶	-0.1	2.6	2.7		
3.560~3.900	24.03	1.15 ^{+0.13} _{-0.13}	-0.71 ^{+0.25} _{-0.25}	42 ⁺⁹ ₋₉	54 ⁺¹⁶ ₋₁₆	0.98 ^{+0.59} _{-0.32} × 10 ⁻⁶	1.12 ^{+0.13} _{-0.13}	-0.65 ^{+0.26} _{-0.26}	-6.57 ^{+2.33} _{-2.32}	52 ⁺⁴ ₋₄	0.98 ^{+0.19} _{-0.16} × 10 ⁻⁶	1.8	1.3	3.1		
Pulse 2																
6.140~6.715	46.22	1.61 ^{+0.10} _{-0.11}	-1.22 ^{+0.10} _{-0.10}	123 ⁺²⁴ ₋₂₅	96 ⁺²³ ₋₂₃	2.03 ^{+0.64} _{-0.37} × 10 ⁻⁶	1.51 ^{+0.10} _{-0.10}	-0.62 ^{+0.10} _{-0.10}	-2.28 ^{+0.09} _{-0.08}	56 ⁺⁴ ₋₄	2.77 ^{+0.50} _{-0.45} × 10 ⁻⁶	-34.1	2.0	3.1		
6.715~6.809	25.06	2.62 ^{+0.33} _{-0.33}	-0.67 ^{+0.33} _{-0.33}	42 ⁺¹² ₋₁₂	55 ⁺²¹ ₋₂₁	2.20 ^{+2.31} _{-0.88} × 10 ⁻⁶	2.74 ^{+0.31} _{-0.32}	-0.64 ^{+0.19} _{-0.20}	-4.26 ^{+1.50} _{-2.50}	48 ⁺⁵ ₋₅	2.37 ^{+0.66} _{-0.48} × 10 ⁻⁶	-2.5	-1.9	-0.0		
6.809~7.232	70.73	3.80 ^{+0.18} _{-0.18}	-0.64 ^{+0.11} _{-0.11}	37 ⁺³ ₋₃	50 ⁺⁶ ₋₆	3.19 ^{+0.71} _{-0.53} × 10 ⁻⁶	3.82 ^{+0.16} _{-0.16}	-0.54 ^{+0.11} _{-0.11}	-4.25 ^{+0.77} _{-0.77}	48 ⁺² ₋₂	3.27 ^{+0.30} _{-0.26} × 10 ⁻⁶	-7.9	2.7	0.7		
7.232~7.495	41.35	3.39 ^{+0.23} _{-0.23}	-1.29 ^{+0.17} _{-0.17}	66 ⁺¹⁵ ₋₁₆	47 ⁺¹⁶ ₋₁₆	2.49 ^{+0.75} _{-0.51} × 10 ⁻⁶	3.58 ^{+0.32} _{-0.32}	-0.43 ^{+0.17} _{-0.17}	-2.66 ^{+0.14} _{-0.13}	35 ⁺² ₋₂	2.48 ^{+0.42} _{-0.38} × 10 ⁻⁶	-20.2	1.1	3.3		
7.495~7.628	20.99	2.59 ^{+0.30} _{-0.30}	-1.32 ^{+0.31} _{-0.31}	72 ⁺²⁹ ₋₃₀	49 ⁺³⁰ ₋₃₀	1.75 ^{+1.18} _{-0.45} × 10 ⁻⁶	2.52 ^{+0.29} _{-0.29}	-1.02 ^{+0.30} _{-0.30}	-5.18 ^{+2.29} _{-2.29}	40 ⁺⁵ ₋₅	1.68 ^{+0.38} _{-0.30} × 10 ⁻⁶	3.0	-3.7	1.2		
7.628~8.119	27.24	2.20 ^{+0.16} _{-0.16}	-1.57 ^{+0.23} _{-0.24}	58 ⁺¹⁹ ₋₁₉	25 ⁺¹⁶ ₋₁₆	1.22 ^{+0.34} _{-0.20} × 10 ⁻⁶	2.32 ^{+0.28} _{-0.28}	-1.09 ^{+0.35} _{-0.30}	-4.75 ^{+1.93} _{-3.01}	25 ⁺³ ₋₃	1.04 ^{+0.26} _{-0.23} × 10 ⁻⁶	-3.1	-0.6	-1.9		
Pulse 3																
22.793~22.899	22.42	1.31 ^{+0.18} _{-0.18}	-1.18 ^{+0.13} _{-0.12}	405 ⁺¹⁵³ ₋₁₅₈	332 ⁺¹³⁶ ₋₁₃₈	4.39 ^{+3.26} _{-1.67} × 10 ⁻⁶	1.29 ^{+0.19} _{-0.19}	-1.15 ^{+0.14} _{-0.14}	-6.10 ^{+2.71} _{-2.71}	300 ⁺⁸¹ ₋₈₈	4.49 ^{+2.17} _{-1.30} × 10 ⁻⁶	1.3	0.5	1.7		
22.899~23.265	54.61	2.05 ^{+0.12} _{-0.13}	-1.20 ^{+0.06} _{-0.06}	252 ⁺⁴³ ₋₄₃	201 ⁺³⁸ ₋₃₈	4.91 ^{+1.22} _{-0.96} × 10 ⁻⁶	1.84 ^{+0.16} _{-0.16}	-0.87 ^{+0.45} _{-0.25}	-2.47 ^{+1.50} _{-0.70}	120 ⁺⁴⁰ ₋₃₃	6.80 ^{+4.83} _{-2.28} × 10 ⁻⁶	-24.9	2.5	-12.6		
23.265~23.554	39.82	2.12 ^{+0.16} _{-0.16}	-1.43 ^{+0.09} _{-0.09}	291 ⁺⁸⁰ ₋₈₆	166 ⁺⁵³ ₋₅₆	3.28 ^{+1.02} _{-0.71} × 10 ⁻⁶	2.08 ^{+0.16} _{-0.16}	-1.35 ^{+0.12} _{-0.12}	-5.13 ^{+2.82} _{-2.82}	143 ⁺³³ ₋₃₄	3.40 ^{+1.34} _{-0.71} × 10 ⁻⁶	-1.8	1.5	0.4		
23.554~23.898	31.50	1.51 ^{+0.13} _{-0.13}	-1.53 ^{+0.09} _{-0.10}	528 ⁺²⁵⁰ ₋₂₄₀	248 ⁺¹²⁷ ₋₁₂₄	2.64 ^{+1.05} _{-0.67} × 10 ⁻⁶	1.45 ^{+0.14} _{-0.16}	-1.41 ^{+0.11} _{-0.17}	-5.54 ^{+3.20} _{-3.01}	183 ⁺⁷⁰ ₋₅₈	2.54 ^{+1.35} _{-0.59} × 10 ⁻⁶	-3.9	0.2	-3.0		
23.898~24.762	29.43	0.88 ^{+0.07} _{-0.07}	-1.51 ^{+0.12} _{-0.12}	341 ⁺¹⁵⁶ ₋₁₅₆	167 ⁺⁸⁷ ₋₈₇	1.20 ^{+0.52} _{-0.52} × 10 ⁻⁶	0.86 ^{+0.08} _{-0.08}	-1.42 ^{+0.18} _{-0.18}	-5.03 ^{+2.74} _{-2.74}	129 ⁺³⁹ ₋₃₉	1.26 ^{+0.57} _{-0.27} × 10 ⁻⁶	-0.9	-1.0	-0.7		
24.762~29.825	37.63	0.49 ^{+0.03} _{-0.03}	-1.58 ^{+0.07} _{-0.07}	420 ⁺¹⁴⁴ ₋₁₅₂	176 ⁺⁶⁷ ₋₇₀	0.69 ^{+0.17} _{-0.13} × 10 ⁻⁶	0.48 ^{+0.03} _{-0.03}	-1.38 ^{+0.55} _{-0.24}	-5.13 ^{+3.07} _{-3.18}	136 ⁺⁴⁸ ₋₈₃	0.71 ^{+0.53} _{-0.20} × 10 ⁻⁶	-43.5	1.0	-42.0		
31.639~33.425	32.92	0.57 ^{+0.04} _{-0.04}	-1.44 ^{+0.09} _{-0.09}	375 ⁺¹³⁴ ₋₁₃₈	210 ⁺⁸² ₋₈₄	0.98 ^{+0.37} _{-0.22} × 10 ⁻⁶	0.57 ^{+0.04} _{-0.04}	-1.42 ^{+0.09} _{-0.09}	-6.22 ^{+2.67} _{-2.65}	189 ⁺⁴⁵ ₋₄₅	1.01 ^{+0.26} _{-0.17} × 10 ⁻⁶	1.6	0.7	2.4		
33.425~36.437	26.44	0.52 ^{+0.03} _{-0.03}	-1.82 ^{+0.05} _{-0.06}	1825 ⁺¹¹⁴³ ₋₁₀₆₆	329 ⁺²²⁵ ₋₂₂₁	0.75 ^{+0.17} _{-0.14} × 10 ⁻⁶	0.51 ^{+0.04} _{-0.03}	-1.80 ^{+0.07} _{-0.07}	-6.09 ^{+2.76} _{-2.72}	239 ⁺¹⁰¹ ₋₉₅	0.73 ^{+0.10} _{-0.10} × 10 ⁻⁶	0.1	1.6	2.0		

Note—All columns are the same as Table A2 but for GRB 090131090.

Table A5. Time-resolved Spectral Fit Results of GRB 090618353

$t_{\text{start}} \sim t_{\text{stop}}$	S	Cutoff Power-Law Fitting						Band Fitting						Difference	
		K	α	E_c	E_p	F	K	α	β	E_p	F	ΔDIC	$p_{\text{DIC}}^{\text{CPL}}$	$p_{\text{DIC}}^{\text{Band}}$	
(1)	(2)	(3)	(4)	(5)	(6)	(7)	(8)	(9)	(10)	(11)	(12)	(13)	(14)	(15)	
Pulse 1															
1.511~21.588	54.02	$0.28^{+0.02}_{-0.02}$	$-0.89^{+0.05}_{-0.02}$	208^{+20}_{-20}	231^{+25}_{-25}	$1.23^{+0.29}_{-0.21} \times 10^{-6}$	$0.21^{+0.02}_{-0.11}$	$-0.43^{+0.11}_{-0.11}$	$-2.14^{+0.06}_{-0.06}$	1.38^{+10}_{-10}	$1.95^{+0.50}_{-0.41} \times 10^{-6}$	-23.1	2.7	3.3	
21.588~28.423	30.65	$0.35^{+0.13}_{-0.04}$	$-0.98^{+0.13}_{-0.13}$	112^{+20}_{-21}	114^{+25}_{-23}	$0.61^{+0.26}_{-0.17} \times 10^{-6}$	$0.33^{+0.04}_{-0.04}$	$0.84^{+0.19}_{-0.18}$	$-3.42^{+0.90}_{-1.23}$	101^{+12}_{-13}	$0.68^{+0.24}_{-0.16} \times 10^{-6}$	-1.5	1.8	1.9	
Pulse 2															
49.994~56.456	52.09	$0.68^{+0.04}_{-0.04}$	$-1.25^{+0.06}_{-0.06}$	220^{+34}_{-34}	165^{+29}_{-29}	$1.31^{+0.29}_{-0.22} \times 10^{-6}$	$0.65^{+0.04}_{-0.04}$	$-1.18^{+0.10}_{-0.10}$	$-3.29^{+0.94}_{-1.22}$	1.47^{+21}_{-24}	$1.47^{+0.41}_{-0.32} \times 10^{-6}$	-2.2	2.5	1.5	
56.456~61.167	68.70	$0.79^{+0.04}_{-0.04}$	$-1.07^{+0.05}_{-0.05}$	210^{+21}_{-22}	195^{+22}_{-23}	$2.19^{+0.39}_{-0.39} \times 10^{-6}$	$0.70^{+0.05}_{-0.05}$	$-0.83^{+0.10}_{-0.10}$	$-2.34^{+0.07}_{-0.07}$	1.38^{+14}_{-14}	$2.98^{+0.69}_{-0.58} \times 10^{-6}$	-11.7	2.7	3.3	
61.167~61.714	33.28	$0.94^{+0.11}_{-0.11}$	$-1.10^{+0.09}_{-0.09}$	330^{+81}_{-82}	297^{+78}_{-80}	$3.55^{+1.87}_{-1.05} \times 10^{-6}$	$0.92^{+0.11}_{-0.11}$	$-1.07^{+0.10}_{-0.10}$	$-4.28^{+1.31}_{-1.32}$	2.78^{+47}_{-47}	$3.64^{+1.28}_{-0.83} \times 10^{-6}$	0.8	1.9	2.6	
61.714~62.186	43.95	$1.37^{+0.13}_{-0.13}$	$-1.13^{+0.07}_{-0.07}$	441^{+95}_{-91}	384^{+88}_{-88}	$6.43^{+2.57}_{-1.72} \times 10^{-6}$	$1.18^{+0.18}_{-0.18}$	$-0.89^{+0.20}_{-0.20}$	$-2.37^{+0.39}_{-0.35}$	239^{+89}_{-81}	$8.42^{+6.54}_{-3.59} \times 10^{-6}$	-15.3	2.1	-6.5	
62.186~63.088	77.72	$1.61^{+0.09}_{-0.09}$	$-1.08^{+0.03}_{-0.03}$	568^{+59}_{-59}	523^{+57}_{-57}	$11.06^{+1.99}_{-1.53} \times 10^{-6}$	$1.61^{+0.09}_{-0.09}$	$-1.08^{+0.03}_{-0.03}$	$-5.73^{+1.55}_{-1.56}$	522^{+41}_{-40}	$11.24^{+1.13}_{-1.27} \times 10^{-6}$	0.5	2.9	3.2	
63.088~65.675	154.67	$2.21^{+0.06}_{-0.06}$	$-1.08^{+0.02}_{-0.02}$	544^{+28}_{-28}	501^{+28}_{-28}	$14.60^{+2.27}_{-1.93} \times 10^{-6}$	$2.20^{+0.06}_{-0.06}$	$-1.08^{+0.02}_{-0.02}$	$-3.80^{+0.81}_{-0.81}$	494^{+20}_{-20}	$15.26^{+1.13}_{-1.10} \times 10^{-6}$	-2.7	3.0	2.7	
65.675~69.986	182.25	$2.68^{+0.06}_{-0.06}$	$-1.19^{+0.02}_{-0.02}$	423^{+20}_{-20}	343^{+19}_{-18}	$10.17^{+0.65}_{-0.62} \times 10^{-6}$	$2.66^{+0.06}_{-0.06}$	$-1.18^{+0.02}_{-0.02}$	$-3.48^{+0.71}_{-0.70}$	330^{+15}_{-15}	$10.71^{+0.97}_{-0.78} \times 10^{-6}$	-3.7	3.0	2.3	
69.986~72.196	126.64	$2.68^{+0.08}_{-0.08}$	$-1.18^{+0.03}_{-0.03}$	267^{+18}_{-18}	219^{+17}_{-17}	$7.14^{+0.64}_{-0.57} \times 10^{-6}$	$2.40^{+0.14}_{-0.13}$	$-0.97^{+0.09}_{-0.09}$	$-2.43^{+0.22}_{-0.22}$	152^{+20}_{-20}	$9.38^{+2.27}_{-2.15} \times 10^{-6}$	-16.1	3.0	-4.0	
72.196~72.989	63.05	$2.16^{+0.14}_{-0.14}$	$-1.21^{+0.06}_{-0.06}$	227^{+35}_{-35}	179^{+31}_{-31}	$4.63^{+1.33}_{-0.81} \times 10^{-6}$	$1.86^{+0.15}_{-0.15}$	$-0.85^{+0.13}_{-0.13}$	$-2.28^{+0.12}_{-0.12}$	110^{+13}_{-13}	$6.30^{+1.39}_{-1.35} \times 10^{-6}$	-15.6	2.6	3.6	
72.989~74.292	62.80	$1.88^{+0.11}_{-0.11}$	$-1.20^{+0.07}_{-0.07}$	158^{+21}_{-22}	127^{+20}_{-20}	$3.11^{+0.68}_{-0.51} \times 10^{-6}$	$1.78^{+0.13}_{-0.13}$	$-1.06^{+0.13}_{-0.13}$	$-3.05^{+0.58}_{-0.58}$	108^{+13}_{-13}	$3.50^{+0.68}_{-0.68} \times 10^{-6}$	-5.2	2.6	1.0	
74.292~76.569	57.72	$1.46^{+0.08}_{-0.08}$	$-1.27^{+0.07}_{-0.07}$	148^{+18}_{-18}	108^{+18}_{-18}	$2.00^{+0.39}_{-0.30} \times 10^{-6}$	$1.44^{+0.09}_{-0.09}$	$-1.24^{+0.08}_{-0.08}$	$-4.09^{+1.12}_{-1.12}$	104^{+8}_{-8}	$2.05^{+0.26}_{-0.22} \times 10^{-6}$	0.6	2.6	3.1	
Pulse 3															
76.569~77.566	46.94	$1.65^{+0.13}_{-0.12}$	$-1.20^{+0.10}_{-0.10}$	134^{+26}_{-26}	108^{+25}_{-25}	$2.32^{+0.74}_{-0.49} \times 10^{-6}$	$1.50^{+0.13}_{-0.13}$	$-0.91^{+0.16}_{-0.16}$	$-2.58^{+0.20}_{-0.17}$	81^{+8}_{-9}	$2.70^{+0.77}_{-0.50} \times 10^{-6}$	-8.7	2.0	4.0	
77.566~79.852	81.18	$2.00^{+0.09}_{-0.09}$	$-1.28^{+0.05}_{-0.05}$	179^{+20}_{-21}	129^{+17}_{-17}	$3.14^{+0.46}_{-0.37} \times 10^{-6}$	$1.78^{+0.09}_{-0.09}$	$-0.97^{+0.09}_{-0.09}$	$-2.38^{+0.07}_{-0.07}$	90^{+6}_{-6}	$3.92^{+0.52}_{-0.48} \times 10^{-6}$	-25.5	2.8	4.0	
79.852~82.690	115.07	$2.30^{+0.08}_{-0.08}$	$-1.17^{+0.04}_{-0.04}$	176^{+18}_{-13}	146^{+13}_{-13}	$4.45^{+0.51}_{-0.41} \times 10^{-6}$	$2.06^{+0.08}_{-0.08}$	$-0.90^{+0.06}_{-0.06}$	$-2.41^{+0.06}_{-0.06}$	106^{+5}_{-5}	$5.55^{+0.57}_{-0.55} \times 10^{-6}$	-33.4	2.9	3.9	
82.690~83.810	68.39	$2.04^{+0.11}_{-0.11}$	$-1.18^{+0.05}_{-0.05}$	191^{+22}_{-20}	157^{+22}_{-21}	$4.08^{+0.73}_{-0.57} \times 10^{-6}$	$2.03^{+0.11}_{-0.11}$	$-1.18^{+0.05}_{-0.05}$	$-5.52^{+1.49}_{-1.56}$	154^{+10}_{-9}	$4.09^{+0.42}_{-0.36} \times 10^{-6}$	0.6	2.8	3.2	
83.810~85.511	99.71	$2.51^{+0.10}_{-0.10}$	$-1.23^{+0.04}_{-0.04}$	240^{+22}_{-22}	185^{+19}_{-19}	$5.51^{+0.71}_{-0.60} \times 10^{-6}$	$2.41^{+0.15}_{-0.16}$	$-1.15^{+0.12}_{-0.12}$	$-3.49^{+1.11}_{-1.27}$	164^{+23}_{-32}	$5.89^{+1.63}_{-1.10} \times 10^{-6}$	-5.5	2.8	-2.0	
85.511~86.800	74.18	$1.99^{+0.10}_{-0.10}$	$-1.14^{+0.05}_{-0.05}$	180^{+19}_{-19}	155^{+19}_{-19}	$4.14^{+0.58}_{-0.58} \times 10^{-6}$	$1.97^{+0.11}_{-0.11}$	$-1.13^{+0.06}_{-0.06}$	$-5.47^{+1.77}_{-1.77}$	151^{+9}_{-9}	$4.16^{+0.47}_{-0.39} \times 10^{-6}$	0.4	2.8	3.1	
86.800~88.398	90.05	$2.36^{+0.10}_{-0.10}$	$-1.24^{+0.04}_{-0.04}$	237^{+25}_{-25}	180^{+21}_{-21}	$4.95^{+0.78}_{-0.58} \times 10^{-6}$	$2.10^{+0.13}_{-0.12}$	$-0.98^{+0.10}_{-0.10}$	$-2.71^{+0.10}_{-0.10}$	122^{+10}_{-15}	$6.41^{+1.59}_{-1.37} \times 10^{-6}$	-36.2	2.9	-18.0	
88.398~89.456	62.74	$1.97^{+0.12}_{-0.12}$	$-1.21^{+0.07}_{-0.07}$	181^{+26}_{-26}	143^{+24}_{-24}	$3.60^{+0.73}_{-0.67} \times 10^{-6}$	$1.82^{+0.13}_{-0.13}$	$-1.02^{+0.12}_{-0.12}$	$-2.57^{+0.24}_{-0.24}$	112^{+13}_{-13}	$4.37^{+1.12}_{-1.12} \times 10^{-6}$	-7.6	2.6	3.4	
89.456~91.658	72.41	$1.62^{+0.09}_{-0.08}$	$-1.14^{+0.06}_{-0.06}$	134^{+15}_{-15}	116^{+15}_{-15}	$2.58^{+0.49}_{-0.36} \times 10^{-6}$	$1.52^{+0.08}_{-0.08}$	$-0.96^{+0.09}_{-0.09}$	$-2.66^{+0.18}_{-0.16}$	97^{+7}_{-7}	$3.08^{+0.48}_{-0.45} \times 10^{-6}$	-10.9	2.8	3.9	
91.658~93.656	54.31	$1.34^{+0.08}_{-0.08}$	$-1.11^{+0.09}_{-0.09}$	103^{+14}_{-14}	91^{+15}_{-15}	$1.80^{+0.41}_{-0.32} \times 10^{-6}$	$1.30^{+0.09}_{-0.09}$	$-0.98^{+0.12}_{-0.12}$	$-2.96^{+0.39}_{-0.30}$	81^{+7}_{-6}	$2.00^{+0.38}_{-0.32} \times 10^{-6}$	-5.5	2.6	3.3	
93.656~97.633	56.07	$1.02^{+0.06}_{-0.06}$	$-1.06^{+0.09}_{-0.09}$	84^{+10}_{-10}	79^{+12}_{-12}	$1.22^{+0.24}_{-0.19} \times 10^{-6}$	$0.98^{+0.06}_{-0.06}$	$-0.93^{+0.12}_{-0.12}$	$-3.12^{+0.39}_{-0.31}$	72^{+5}_{-4}	$1.32^{+0.19}_{-0.17} \times 10^{-6}$	-5.1	2.6	3.6	
97.633~100.000	31.23	$0.89^{+0.08}_{-0.08}$	$-1.32^{+0.16}_{-0.16}$	104^{+26}_{-26}	71^{+24}_{-26}	$0.84^{+0.35}_{-0.20} \times 10^{-6}$	$0.86^{+0.08}_{-0.08}$	$-1.11^{+0.24}_{-0.25}$	$-3.35^{+0.78}_{-0.77}$	60^{+7}_{-7}	$0.88^{+0.22}_{-0.14} \times 10^{-6}$	-0.6	0.8	2.5	

Note—All columns are the same as Table A2 but for GRB 090618353.

Table A6. Time-resolved Spectral Fit Results of GRB 0911127976

$t_{\text{start}} \sim t_{\text{stop}}$	S	Cutoff Power-Law Fitting				Band Fitting				Difference				
		K	α	E_c	E_p	F	K	α	β	E_p	F	ΔDIC	$p_{\text{DIC}}^{\text{CPL}}$	$p_{\text{DIC}}^{\text{Band}}$
(1)	(2)	(3)	(4)	(5)	(6)	(7)	(8)	(9)	(10)	(11)	(12)	(13)	(14)	(15)
Pulse 1														
0.073~0.207	32.13	1.98 $^{+0.16}_{-0.16}$	-1.10 $^{+0.09}_{-0.09}$	174 $^{+34}_{-35}$	157 $^{+35}_{-35}$	4.20 $^{+1.49}_{-1.01} \times 10^{-6}$	1.88 $^{+0.19}_{-0.19}$	-0.91 $^{+0.19}_{-0.23}$	-3.88 $^{+1.71}_{-3.02}$	124 $^{+31}_{-32}$	5.03 $^{+3.23}_{-1.76} \times 10^{-6}$	-11.6	2.2	-6.2
0.207~0.282	32.79	3.30 $^{+0.28}_{-0.28}$	-1.17 $^{+0.11}_{-0.11}$	146 $^{+32}_{-32}$	121 $^{+31}_{-32}$	5.26 $^{+2.12}_{-1.25} \times 10^{-6}$	2.94 $^{+0.26}_{-0.27}$	-0.48 $^{+0.21}_{-0.21}$	-2.28 $^{+0.13}_{-0.10}$	65 $^{+8}_{-8}$	7.17 $^{+2.40}_{-1.76} \times 10^{-6}$	-15.4	2.0	2.7
0.282~0.526	82.83	6.15 $^{+0.20}_{-0.20}$	-1.29 $^{+0.04}_{-0.04}$	156 $^{+16}_{-16}$	111 $^{+13}_{-13}$	8.59 $^{+0.99}_{-0.86} \times 10^{-6}$	5.54 $^{+0.21}_{-0.21}$	-0.40 $^{+0.08}_{-0.08}$	-2.22 $^{+0.04}_{-0.04}$	53 $^{+2}_{-2}$	11.08 $^{+1.31}_{-1.10} \times 10^{-6}$	-86.8	2.8	3.1
0.526~0.782	72.41	5.17 $^{+0.19}_{-0.19}$	-1.24 $^{+0.05}_{-0.05}$	122 $^{+12}_{-12}$	93 $^{+11}_{-11}$	6.44 $^{+0.88}_{-0.69} \times 10^{-6}$	4.91 $^{+0.20}_{-0.20}$	-0.94 $^{+0.14}_{-0.14}$	-2.50 $^{+0.13}_{-0.13}$	69 $^{+7}_{-7}$	7.68 $^{+1.33}_{-1.07} \times 10^{-6}$	-17.3	2.8	3.3
0.782~0.886	36.25	3.75 $^{+0.26}_{-0.26}$	-1.30 $^{+0.10}_{-0.10}$	134 $^{+26}_{-23}$	94 $^{+23}_{-23}$	4.50 $^{+1.29}_{-0.80} \times 10^{-6}$	3.66 $^{+0.27}_{-0.28}$	-1.20 $^{+0.14}_{-0.14}$	-5.47 $^{+2.79}_{-2.94}$	86 $^{+12}_{-12}$	4.65 $^{+1.19}_{-1.75} \times 10^{-6}$	-1.2	2.4	1.6
0.886~1.223	50.75	3.39 $^{+0.14}_{-0.15}$	-1.37 $^{+0.08}_{-0.08}$	111 $^{+17}_{-17}$	70 $^{+14}_{-14}$	3.30 $^{+0.53}_{-0.40} \times 10^{-6}$	3.31 $^{+0.15}_{-0.15}$	-1.16 $^{+0.16}_{-0.16}$	-3.04 $^{+0.58}_{-0.03}$	59 $^{+7}_{-6}$	3.65 $^{+0.63}_{-0.51} \times 10^{-6}$	-12.9	2.5	-1.4
Pulse 2														
1.223~1.377	49.49	3.81 $^{+0.20}_{-0.20}$	-1.36 $^{+0.06}_{-0.06}$	282 $^{+54}_{-56}$	180 $^{+38}_{-40}$	6.86 $^{+1.40}_{-1.11} \times 10^{-6}$	3.75 $^{+0.21}_{-0.21}$	-1.32 $^{+0.07}_{-0.08}$	-4.89 $^{+2.47}_{-3.18}$	162 $^{+24}_{-24}$	7.13 $^{+1.98}_{-1.13} \times 10^{-6}$	-2.1	2.4	1.6
1.377~1.555	67.49	4.25 $^{+0.18}_{-0.18}$	-1.26 $^{+0.04}_{-0.04}$	408 $^{+54}_{-55}$	302 $^{+43}_{-44}$	12.79 $^{+2.19}_{-1.75} \times 10^{-6}$	4.24 $^{+0.17}_{-0.17}$	-1.26 $^{+0.04}_{-0.04}$	-5.97 $^{+2.68}_{-2.68}$	292 $^{+28}_{-28}$	12.85 $^{+1.48}_{-1.26} \times 10^{-6}$	-0.2	2.8	2.8
1.555~1.692	41.56	3.65 $^{+0.21}_{-0.21}$	-1.46 $^{+0.06}_{-0.06}$	392 $^{+95}_{-101}$	212 $^{+57}_{-59}$	6.43 $^{+1.56}_{-1.11} \times 10^{-6}$	3.63 $^{+0.22}_{-0.22}$	-1.46 $^{+0.06}_{-0.06}$	-6.13 $^{+2.59}_{-2.60}$	205 $^{+33}_{-34}$	6.60 $^{+1.10}_{-0.85} \times 10^{-6}$	0.8	2.2	2.9
1.692~1.889	34.65	2.64 $^{+0.16}_{-0.16}$	-1.64 $^{+0.06}_{-0.06}$	1167 $^{+781}_{-618}$	420 $^{+290}_{-233}$	4.86 $^{+1.88}_{-1.09} \times 10^{-6}$	2.65 $^{+0.16}_{-0.16}$	-1.64 $^{+0.07}_{-0.07}$	-5.26 $^{+0.07}_{-0.07}$	403 $^{+245}_{-184}$	5.20 $^{+1.38}_{-1.08} \times 10^{-6}$	-0.9	0.1	-0.2
1.889~2.258	27.75	1.43 $^{+0.09}_{-0.09}$	-1.52 $^{+0.07}_{-0.07}$	477 $^{+162}_{-162}$	229 $^{+84}_{-84}$	2.36 $^{+0.78}_{-0.78} \times 10^{-6}$	1.42 $^{+0.09}_{-0.09}$	-1.51 $^{+0.07}_{-0.07}$	-6.34 $^{+2.63}_{-2.61}$	210 $^{+45}_{-45}$	2.40 $^{+0.48}_{-0.48} \times 10^{-6}$	1.1	1.4	2.6
2.258~3.506	31.02	0.84 $^{+0.05}_{-0.05}$	-1.47 $^{+0.08}_{-0.08}$	200 $^{+49}_{-51}$	106 $^{+30}_{-31}$	1.00 $^{+0.24}_{-0.17} \times 10^{-6}$	0.83 $^{+0.05}_{-0.05}$	-1.38 $^{+0.14}_{-0.13}$	-5.18 $^{+2.82}_{-3.19}$	92 $^{+17}_{-19}$	1.04 $^{+0.30}_{-0.18} \times 10^{-6}$	-1.9	1.9	0.9
3.506~4.777	42.25	2.17 $^{+0.08}_{-0.08}$	-1.42 $^{+0.13}_{-0.13}$	44 $^{+7}_{-7}$	25 $^{+7}_{-7}$	1.09 $^{+0.15}_{-0.10} \times 10^{-6}$	2.21 $^{+0.09}_{-0.09}$	-1.28 $^{+0.17}_{-0.17}$	-4.46 $^{+1.35}_{-2.24}$	25 $^{+2}_{-2}$	1.07 $^{+0.14}_{-0.14} \times 10^{-6}$	-6.0	2.1	-0.5
Pulse 3														
5.358~6.660	38.69	2.80 $^{+0.11}_{-0.11}$	-1.84 $^{+0.10}_{-0.10}$	44 $^{+7}_{-7}$	7 $^{+5}_{-5}$	1.39 $^{+0.09}_{-0.11} \times 10^{-6}$	2.92 $^{+0.11}_{-0.21}$	-1.69 $^{+0.15}_{-0.19}$	-5.95 $^{+2.58}_{-2.62}$	9 $^{+4}_{-4}$	1.30 $^{+0.45}_{-0.50} \times 10^{-6}$	-18.1	2.0	-16.9
6.660~7.376	72.62	5.96 $^{+0.15}_{-0.15}$	-1.66 $^{+0.08}_{-0.08}$	55 $^{+7}_{-7}$	19 $^{+5}_{-5}$	3.19 $^{+0.19}_{-0.19} \times 10^{-6}$	6.40 $^{+0.21}_{-0.34}$	-1.25 $^{+0.19}_{-0.20}$	-3.10 $^{+0.19}_{-0.19}$	22 $^{+1}_{-1}$	2.83 $^{+0.45}_{-0.39} \times 10^{-6}$	-11.5	2.6	2.2
7.376~7.954	42.90	5.12 $^{+0.20}_{-0.20}$	-1.90 $^{+0.07}_{-0.07}$	46 $^{+6}_{-6}$	5 $^{+3}_{-3}$	2.58 $^{+0.16}_{-0.15} \times 10^{-6}$	6.52 $^{+0.16}_{-0.16}$	-1.35 $^{+0.23}_{-0.22}$	-3.11 $^{+0.10}_{-0.10}$	13 $^{+1}_{-2}$	2.05 $^{+0.71}_{-0.52} \times 10^{-6}$	-2.8	2.0	1.3
7.954~8.591	29.43	2.96 $^{+0.16}_{-0.16}$	-1.94 $^{+0.04}_{-0.04}$	52 $^{+6}_{-6}$	3 $^{+2}_{-2}$	1.57 $^{+0.11}_{-0.11} \times 10^{-6}$	3.89 $^{+0.36}_{-0.36}$	-1.48 $^{+0.17}_{-0.06}$	-2.83 $^{+0.11}_{-0.11}$	11 $^{+1}_{-1}$	1.35 $^{+0.19}_{-0.15} \times 10^{-6}$	-9.4	1.9	2.4

Note—All columns are the same as Table A2 but for GRB 0911127976.

Table A7. Time-resolved Spectral Fit Results of GRB 100719989

$t_{\text{start}} \sim t_{\text{stop}}$	S	Cutoff Power-Law Fitting						Band Fitting						Difference				
		K			E_p			K			α			F	ΔDIC	$p_{\text{DIC}}^{\text{CPD}}$	$p_{\text{DIC}}^{\text{Band}}$	
		(1)	(2)	(3)	(4)	(5)	(6)	(7)	(8)	(9)	(10)	(11)	(12)	(13)	(14)	(15)		
Pulse 1																		
1.596~2.044	33.85	0.22 ^{+0.03}	-0.33 ^{+0.07}	320 ⁺³²	534 ⁺⁵⁷	10.01 ^{+4.13}	$\times 10^{-6}$	0.22 ^{+0.03}	-0.31 ^{+0.07}	-3.55 ^{+0.79}	517 ⁺³⁷	11.03 ^{+3.89}	$\times 10^{-6}$	-2.4	2.4	2.8		
2.044~2.366	44.23	0.45 ^{+0.05}	-0.47 ^{+0.05}	385 ⁺³⁴	589 ⁺⁵⁶	17.11 ^{+4.60}	$\times 10^{-6}$	0.44 ^{+0.05}	-0.45 ^{+0.06}	-4.18 ^{+1.04}	573 ⁺³⁷	17.53 ^{+3.32}	$\times 10^{-6}$	-0.8	2.7	2.8		
2.366~2.681	62.78	1.18 ^{+0.08}	-0.73 ^{+0.03}	594 ⁺⁴⁹	755 ⁺⁶⁴	30.05 ^{+5.35}	$\times 10^{-6}$	1.14 ^{+0.08}	-0.7 ^{+0.04}	-2.86 ^{+0.30}	693 ⁺⁵³	33.79 ^{+7.00}	$\times 10^{-6}$	-8.9	2.9	3.8		
2.681~2.841	36.98	1.00 ^{+0.11}	-0.71 ^{+0.06}	384 ⁺⁴⁸	495 ⁺⁶⁶	15.37 ^{+5.17}	$\times 10^{-6}$	0.99 ^{+0.11}	-0.70 ^{+0.06}	-5.47 ^{+1.83}	483 ⁺⁴³	15.62 ^{+4.27}	$\times 10^{-6}$	0.3	2.7	2.9		
Pulse 2																		
2.841~3.725	55.65	0.59 ^{+0.04}	-0.61 ^{+0.04}	242 ⁺¹⁷	336 ⁺²⁶	7.10 ^{+1.43}	$\times 10^{-6}$	0.59 ^{+0.04}	-0.59 ^{+0.05}	-4.24 ^{+1.23}	327 ⁺¹⁹	7.43 ^{+1.56}	$\times 10^{-6}$	-0.2	2.9	3.1		
3.725~4.216	54.30	0.77 ^{+0.06}	-0.52 ^{+0.05}	190 ⁺¹⁴	281 ⁺²³	8.50 ^{+1.87}	$\times 10^{-6}$	0.60 ^{+0.07}	-0.2 ^{+0.13}	-2.37 ^{+0.15}	203 ⁺²¹	11.66 ^{+5.25}	$\times 10^{-6}$	-14.7	2.8	2.3		
4.216~4.594	63.82	1.15 ^{+0.08}	-0.65 ^{+0.04}	277 ⁺²⁰	374 ⁺²⁹	14.54 ^{+2.90}	$\times 10^{-6}$	1.03 ^{+0.09}	-0.52 ^{+0.08}	-2.62 ^{+0.21}	309 ⁺³⁵	18.17 ^{+6.42}	$\times 10^{-6}$	-8.7	2.9	2.5		
4.594~4.800	37.94	1.08 ^{+0.11}	-0.65 ^{+0.07}	205 ⁺²³	277 ⁺³⁵	8.95 ^{+3.01}	$\times 10^{-6}$	0.88 ^{+0.18}	-0.34 ^{+0.27}	-2.54 ^{+0.43}	200 ⁺⁵¹	12.26 ^{+13.05}	$\times 10^{-6}$	-15.0	2.6	-6.2		
4.800~5.158	34.28	0.82 ^{+0.08}	-0.65 ^{+0.08}	158 ⁺²⁰	213 ⁺²⁹	4.69 ^{+1.74}	$\times 10^{-6}$	0.77 ^{+0.09}	-0.57 ^{+0.12}	-3.37 ^{+0.85}	194 ⁺²²	5.24 ^{+2.10}	$\times 10^{-6}$	-2.6	2.5	2.2		
5.158~5.645	27.79	0.66 ^{+0.08}	-0.70 ^{+0.10}	130 ⁺¹⁹	168 ⁺²⁸	2.54 ^{+1.11}	$\times 10^{-6}$	0.63 ^{+0.08}	-0.61 ^{+0.15}	-3.44 ^{+0.94}	153 ⁺¹⁸	2.86 ^{+1.20}	$\times 10^{-6}$	-0.9	2.3	2.6		
5.645~6.923	29.76	0.62 ^{+0.06}	-0.99 ^{+0.10}	157 ⁺²⁹	159 ⁺³³	1.52 ^{+0.58}	$\times 10^{-6}$	0.56 ^{+0.06}	-0.80 ^{+0.14}	-2.45 ^{+0.25}	125 ⁺¹⁵	2.10 ^{+0.79}	$\times 10^{-6}$	-8.6	1.9	3.5		
Pulse 3																		
21.232~22.852	30.06	0.43 ^{+0.04}	-1.15 ^{+0.06}	749 ⁺²²⁰	637 ⁺¹⁹²	2.76 ^{+1.21}	$\times 10^{-6}$	0.40 ^{+0.04}	-1.08 ^{+0.09}	-2.78 ^{+0.71}	476 ⁺¹⁴⁴	3.16 ^{+1.54}	$\times 10^{-6}$	-5.1	1.3	-0.7		

Note—All columns are the same as Table A2 but for GRB 100719989.

Table A8. Time-resolved Spectral Fit Results of GRB 100826957

$t_{\text{start}} \sim t_{\text{stop}}$	S	Cutoff Power-Law Fitting						Band Fitting						Difference		
		K	α	E_c	E_p	F	K	α	β	E_p	F	ΔDIC	$p_{\text{DIC}}^{\text{GL}}$	$p_{\text{DIC}}^{\text{Band}}$		
(1)	(2)	(3)	(4)	(5)	(6)	(7)	(8)	(9)	(10)	(11)	(12)	(13)	(14)	(15)		
Pulse 1																
2.350~10.360	33.80	$0.14^{+0.01}_{-0.01}$	$-0.72^{+0.06}_{-0.06}$	275^{+34}_{-34}	352^{+47}_{-47}	$1.32^{+0.43}_{-0.28} \times 10^{-6}$	$0.10^{+0.01}_{-0.01}$	$-0.27^{+0.18}_{-0.18}$	$-1.92^{+0.08}_{-0.08}$	188^{+32}_{-32}	$2.50^{+1.74}_{-0.90} \times 10^{-6}$	-39.7	2.5	-3.9		
10.360~13.706	41.03	$0.22^{+0.02}_{-0.02}$	$-0.76^{+0.04}_{-0.04}$	412^{+48}_{-49}	511^{+61}_{-63}	$3.08^{+0.76}_{-0.57} \times 10^{-6}$	$0.19^{+0.02}_{-0.02}$	$-0.59^{+0.08}_{-0.08}$	$-2.08^{+0.11}_{-0.11}$	345^{+43}_{-43}	$4.60^{+1.52}_{-1.13} \times 10^{-6}$	-20.5	2.7	3.1		
13.706~15.608	54.28	$0.33^{+0.02}_{-0.02}$	$-0.68^{+0.04}_{-0.04}$	346^{+29}_{-29}	456^{+41}_{-41}	$5.08^{+1.03}_{-0.84} \times 10^{-6}$	$0.29^{+0.02}_{-0.02}$	$-0.54^{+0.06}_{-0.06}$	$-2.02^{+0.07}_{-0.07}$	334^{+30}_{-30}	$8.40^{+2.15}_{-1.65} \times 10^{-6}$	-35.4	2.9	3.6		
15.608~18.208	75.38	$0.41^{+0.02}_{-0.02}$	$-0.70^{+0.03}_{-0.03}$	379^{+24}_{-24}	493^{+33}_{-33}	$6.55^{+0.95}_{-0.78} \times 10^{-6}$	$0.39^{+0.02}_{-0.02}$	$-0.66^{+0.04}_{-0.03}$	$-2.30^{+0.11}_{-0.11}$	432^{+28}_{-29}	$9.20^{+1.47}_{-1.27} \times 10^{-6}$	-23.2	3.0	3.9		
18.208~22.288	112.66	$0.50^{+0.01}_{-0.01}$	$-0.69^{+0.02}_{-0.02}$	440^{+18}_{-18}	576^{+26}_{-26}	$10.11^{+0.95}_{-0.90} \times 10^{-6}$	$0.45^{+0.02}_{-0.02}$	$-0.60^{+0.02}_{-0.02}$	$-2.19^{+0.05}_{-0.05}$	459^{+20}_{-20}	$14.15^{+1.43}_{-1.29} \times 10^{-6}$	-107.6	2.9	4.0		
22.288~22.536	38.51	$0.61^{+0.07}_{-0.06}$	$-0.72^{+0.07}_{-0.07}$	547^{+100}_{-103}	700^{+133}_{-137}	$14.13^{+4.32}_{-4.32} \times 10^{-6}$	$0.51^{+0.06}_{-0.06}$	$-0.55^{+0.09}_{-0.09}$	$-1.96^{+0.09}_{-0.09}$	447^{+70}_{-70}	$21.76^{+9.52}_{-6.41} \times 10^{-6}$	-34.8	2.1	3.0		
22.536~23.880	64.13	$0.49^{+0.03}_{-0.03}$	$-0.77^{+0.03}_{-0.03}$	528^{+48}_{-48}	649^{+61}_{-62}	$9.36^{+1.78}_{-1.51} \times 10^{-6}$	$0.44^{+0.03}_{-0.03}$	$-0.67^{+0.05}_{-0.05}$	$-2.04^{+0.08}_{-0.08}$	476^{+51}_{-50}	$13.79^{+3.15}_{-2.60} \times 10^{-6}$	-47.3	2.9	3.6		
23.880~26.405	71.64	$0.45^{+0.02}_{-0.02}$	$-0.79^{+0.03}_{-0.03}$	442^{+33}_{-34}	534^{+43}_{-43}	$6.38^{+0.98}_{-0.82} \times 10^{-6}$	$0.39^{+0.02}_{-0.02}$	$-0.62^{+0.05}_{-0.05}$	$-1.98^{+0.05}_{-0.05}$	346^{+28}_{-28}	$10.11^{+1.95}_{-1.56} \times 10^{-6}$	-65.7	2.9	3.7		
26.405~28.845	56.39	$0.39^{+0.02}_{-0.02}$	$-0.79^{+0.04}_{-0.04}$	343^{+32}_{-32}	415^{+41}_{-41}	$4.06^{+0.74}_{-0.66} \times 10^{-6}$	$0.34^{+0.02}_{-0.02}$	$-0.63^{+0.06}_{-0.06}$	$-2.03^{+0.07}_{-0.07}$	286^{+26}_{-26}	$6.52^{+2.61}_{-2.19} \times 10^{-6}$	-39.2	2.8	3.7		
28.845~29.285	32.27	$0.42^{+0.04}_{-0.04}$	$-0.72^{+0.07}_{-0.07}$	323^{+50}_{-49}	413^{+67}_{-67}	$5.07^{+1.82}_{-1.37} \times 10^{-6}$	$0.42^{+0.05}_{-0.05}$	$-0.71^{+0.07}_{-0.07}$	$-3.37^{+1.00}_{-1.00}$	396^{+48}_{-48}	$5.65^{+2.17}_{-1.44} \times 10^{-6}$	-0.9	2.5	2.6		
29.285~31.086	42.56	$0.41^{+0.03}_{-0.03}$	$-0.10^{+0.05}_{-0.05}$	549^{+96}_{-96}	544^{+99}_{-100}	$3.47^{+0.94}_{-0.72} \times 10^{-6}$	$0.39^{+0.03}_{-0.03}$	$-0.94^{+0.08}_{-0.07}$	$-2.53^{+0.05}_{-0.05}$	423^{+94}_{-95}	$4.19^{+1.93}_{-1.21} \times 10^{-6}$	-6.6	2.5	0.8		
31.086~32.868	33.85	$0.29^{+0.02}_{-0.02}$	$-0.91^{+0.06}_{-0.06}$	409^{+67}_{-68}	446^{+77}_{-78}	$2.48^{+0.86}_{-0.59} \times 10^{-6}$	$0.27^{+0.03}_{-0.03}$	$-0.83^{+0.09}_{-0.09}$	$-2.24^{+0.33}_{-0.33}$	349^{+76}_{-76}	$3.77^{+1.83}_{-1.26} \times 10^{-6}$	-7.4	2.5	1.9		
32.883~36.275	35.35	$0.22^{+0.02}_{-0.02}$	$-0.79^{+0.06}_{-0.06}$	251^{+33}_{-33}	304^{+42}_{-42}	$1.54^{+0.44}_{-0.32} \times 10^{-6}$	$0.19^{+0.02}_{-0.02}$	$-0.63^{+0.10}_{-0.10}$	$-2.16^{+0.22}_{-0.22}$	228^{+34}_{-34}	$2.63^{+1.16}_{-1.02} \times 10^{-6}$	-8.7	2.6	2.8		
36.444~39.116	34.14	$0.28^{+0.02}_{-0.02}$	$-0.93^{+0.06}_{-0.06}$	308^{+51}_{-52}	329^{+58}_{-58}	$1.57^{+0.55}_{-0.39} \times 10^{-6}$	$0.23^{+0.03}_{-0.03}$	$-0.63^{+0.15}_{-0.15}$	$-1.91^{+0.11}_{-0.08}$	183^{+38}_{-38}	$3.01^{+1.75}_{-1.00} \times 10^{-6}$	-18.5	2.5	-0.7		
40.421~41.847	32.35	$0.35^{+0.03}_{-0.03}$	$-0.92^{+0.08}_{-0.08}$	295^{+60}_{-62}	319^{+69}_{-71}	$1.96^{+0.83}_{-0.54} \times 10^{-6}$	$0.27^{+0.03}_{-0.03}$	$-0.43^{+0.16}_{-0.16}$	$-1.86^{+0.07}_{-0.07}$	143^{+26}_{-26}	$3.94^{+2.08}_{-1.36} \times 10^{-6}$	-26.1	1.9	0.2		
41.847~47.316	26.62	$0.19^{+0.02}_{-0.02}$	$-0.10^{+0.07}_{-0.07}$	368^{+82}_{-87}	342^{+81}_{-81}	$0.87^{+0.36}_{-0.23} \times 10^{-6}$	$0.18^{+0.02}_{-0.02}$	$-0.95^{+0.14}_{-0.13}$	$-2.60^{+0.67}_{-1.00}$	257^{+74}_{-78}	$1.17^{+0.81}_{-0.47} \times 10^{-6}$	-6.9	1.9	-1.7		
Pulse 2																
59.502~60.693	38.31	$0.43^{+0.03}_{-0.03}$	$-0.95^{+0.06}_{-0.05}$	419^{+73}_{-73}	440^{+81}_{-80}	$3.34^{+1.03}_{-0.81} \times 10^{-6}$	$0.40^{+0.04}_{-0.04}$	$-0.86^{+0.10}_{-0.10}$	$-2.60^{+0.57}_{-0.77}$	345^{+79}_{-77}	$4.23^{+2.16}_{-1.39} \times 10^{-6}$	-5.7	2.5	0.6		
60.693~65.048	51.64	$0.35^{+0.02}_{-0.02}$	$-0.96^{+0.04}_{-0.04}$	342^{+38}_{-38}	355^{+42}_{-42}	$2.12^{+0.40}_{-0.34} \times 10^{-6}$	$0.34^{+0.02}_{-0.02}$	$-0.90^{+0.06}_{-0.06}$	$-2.48^{+0.38}_{-0.29}$	298^{+41}_{-39}	$2.83^{+0.88}_{-0.67} \times 10^{-6}$	-6.2	2.8	2.5		
65.048~66.813	25.69	$0.28^{+0.03}_{-0.03}$	$-1.00^{+0.08}_{-0.08}$	312^{+71}_{-72}	312^{+75}_{-76}	$1.29^{+0.59}_{-0.34} \times 10^{-6}$	$0.27^{+0.03}_{-0.03}$	$-0.98^{+0.09}_{-0.09}$	$-3.63^{+1.15}_{-1.20}$	291^{+52}_{-52}	$1.39^{+0.56}_{-0.34} \times 10^{-6}$	0.2	2.1	2.5		
66.813~70.685	23.37	$0.16^{+0.02}_{-0.02}$	$-0.91^{+0.09}_{-0.09}$	258^{+56}_{-57}	281^{+66}_{-66}	$0.82^{+0.40}_{-0.24} \times 10^{-6}$	$0.15^{+0.02}_{-0.02}$	$-0.69^{+0.21}_{-0.22}$	$-2.42^{+0.58}_{-0.58}$	198^{+61}_{-64}	$1.34^{+1.23}_{-0.68} \times 10^{-6}$	-15.7	1.9	-9.7		
Pulse 3																
70.685~71.717	30.99	$0.30^{+0.03}_{-0.03}$	$-0.87^{+0.06}_{-0.06}$	546^{+91}_{-93}	617^{+108}_{-110}	$3.96^{+1.38}_{-0.97} \times 10^{-6}$	$0.30^{+0.03}_{-0.03}$	$-0.87^{+0.06}_{-0.05}$	$-5.59^{+1.64}_{-1.66}$	604^{+75}_{-76}	$3.92^{+1.10}_{-0.71} \times 10^{-6}$	0.5	2.6	3.0		
71.717~72.677	20.24	$0.26^{+0.03}_{-0.03}$	$-0.93^{+0.09}_{-0.10}$	342^{+91}_{-91}	366^{+102}_{-103}	$1.65^{+0.87}_{-0.53} \times 10^{-6}$	$0.25^{+0.03}_{-0.03}$	$-0.92^{+0.10}_{-0.10}$	$-5.15^{+1.87}_{-1.93}$	356^{+73}_{-74}	$1.73^{+0.79}_{-0.51} \times 10^{-6}$	0.7	1.8	2.3		
72.677~73.166	29.65	$0.45^{+0.05}_{-0.05}$	$-0.90^{+0.07}_{-0.07}$	527^{+115}_{-115}	580^{+132}_{-132}	$5.15^{+2.16}_{-1.45} \times 10^{-6}$	$0.43^{+0.05}_{-0.05}$	$-0.87^{+0.08}_{-0.08}$	$-3.23^{+0.97}_{-1.19}$	537^{+102}_{-105}	$5.84^{+2.77}_{-2.17} \times 10^{-6}$	-0.8	2.2	2.4		
73.166~74.718	34.01	$0.38^{+0.03}_{-0.03}$	$-0.94^{+0.06}_{-0.06}$	296^{+49}_{-51}	314^{+55}_{-57}	$2.04^{+0.69}_{-0.44} \times 10^{-6}$	$0.36^{+0.03}_{-0.03}$	$-0.85^{+0.10}_{-0.10}$	$-2.57^{+0.54}_{-0.60}$	256^{+51}_{-50}	$2.79^{+1.52}_{-0.90} \times 10^{-6}$	-4.6	2.5	1.7		
74.718~76.054	21.94	$0.23^{+0.03}_{-0.03}$	$-0.90^{+0.11}_{-0.11}$	270^{+69}_{-70}	297^{+82}_{-83}	$1.26^{+0.64}_{-0.40} \times 10^{-6}$	$0.22^{+0.03}_{-0.03}$	$-0.81^{+0.14}_{-0.14}$	$-2.77^{+0.78}_{-1.13}$	249^{+55}_{-55}	$1.74^{+1.31}_{-0.71} \times 10^{-6}$	-2.4	1.4	1.4		
76.054~81.000	53.90	$0.42^{+0.02}_{-0.02}$	$-0.88^{+0.04}_{-0.04}$	328^{+41}_{-41}	302^{+40}_{-40}	$1.71^{+0.32}_{-0.24} \times 10^{-6}$	$0.42^{+0.02}_{-0.02}$	$-0.66^{+0.05}_{-0.05}$	$-4.16^{+1.76}_{-2.20}$	280^{+32}_{-33}	$1.84^{+0.53}_{-0.32} \times 10^{-6}$	-2.1	2.7	1.8		

Note—All columns are the same as Table A2 but for GRB 100826957.

Table A9. Time-resolved Spectral Fit Results of GRB 101014175

$t_{\text{start}} \sim t_{\text{stop}}$	S	Cutoff Power-Law Fitting						Band Fitting						Difference	
		K	α	E_c	E_p	F	K	α	β	E_p	F	ΔDIC	$p_{\text{DIC}}^{\text{CPL}}$	$p_{\text{DIC}}^{\text{Band}}$	
Pulse 1															
0.322~0.565	31.24	0.59 $^{+0.07}_{-0.07}$	-0.83 $^{+0.08}_{-0.08}$	301 $^{+57}_{-58}$	352 $^{+72}_{-72}$	$4.51^{+2.13}_{-1.31} \times 10^{-6}$	0.58 $^{+0.07}_{-0.07}$	-0.81 $^{+0.09}_{-0.09}$	3.69 $^{+1.11}_{-1.27}$	334 $^{+47}_{-47}$	5.01 $^{+1.95}_{-1.31} \times 10^{-6}$	-0.1	2.3	2.8	
0.565~0.842	45.15	0.61 $^{+0.06}_{-0.06}$	-0.55 $^{+0.06}_{-0.06}$	213 $^{+21}_{-22}$	309 $^{+33}_{-34}$	7.09 $^{+2.14}_{-2.14} \times 10^{-6}$	0.60 $^{+0.06}_{-0.06}$	-0.54 $^{+0.07}_{-0.07}$	4.39 $^{+1.19}_{-1.23}$	301 $^{+22}_{-21}$	7.42 $^{+1.67}_{-1.43} \times 10^{-6}$	0.2	2.7	2.9	
0.842~1.171	70.30	0.80 $^{+0.05}_{-0.05}$	-0.43 $^{+0.05}_{-0.05}$	186 $^{+12}_{-12}$	293 $^{+21}_{-21}$	11.34 $^{+2.26}_{-1.95} \times 10^{-6}$	0.75 $^{+0.06}_{-0.06}$	-0.35 $^{+0.06}_{-0.06}$	-2.78 $^{+0.24}_{-0.22}$	263 $^{+16}_{-16}$	13.80 $^{+2.97}_{-2.71} \times 10^{-6}$	-11.9	2.9	3.8	
1.171~1.596	91.61	1.17 $^{+0.06}_{-0.06}$	-0.56 $^{+0.03}_{-0.03}$	214 $^{+12}_{-12}$	308 $^{+18}_{-18}$	13.37 $^{+2.11}_{-1.60} \times 10^{-6}$	1.14 $^{+0.06}_{-0.06}$	-0.54 $^{+0.04}_{-0.04}$	3.87 $^{+0.86}_{-1.11}$	296 $^{+14}_{-14}$	14.20 $^{+2.28}_{-1.92} \times 10^{-6}$	-2.3	2.9	2.5	
1.596~1.756	41.54	1.21 $^{+0.11}_{-0.11}$	-0.72 $^{+0.08}_{-0.08}$	159 $^{+21}_{-21}$	204 $^{+30}_{-30}$	5.89 $^{+2.00}_{-1.39} \times 10^{-6}$	1.20 $^{+0.11}_{-0.12}$	0.71 $^{+0.08}_{-0.08}$	5.60 $^{+1.63}_{-1.60}$	202 $^{+16}_{-16}$	6.06 $^{+1.28}_{-1.06} \times 10^{-6}$	0.6	2.7	3.0	
1.756~1.957	36.67	0.99 $^{+0.10}_{-0.10}$	-0.79 $^{+0.09}_{-0.09}$	183 $^{+28}_{-28}$	221 $^{+38}_{-38}$	4.80 $^{+1.89}_{-1.21} \times 10^{-6}$	0.96 $^{+0.10}_{-0.10}$	-0.73 $^{+0.10}_{-0.10}$	3.13 $^{+0.75}_{-0.97}$	202 $^{+24}_{-24}$	5.65 $^{+2.31}_{-1.39} \times 10^{-6}$	-2.8	2.5	2.8	
1.957~2.269	69.06	1.08 $^{+0.07}_{-0.07}$	-0.66 $^{+0.04}_{-0.04}$	259 $^{+20}_{-20}$	347 $^{+29}_{-29}$	11.97 $^{+2.43}_{-1.95} \times 10^{-6}$	1.07 $^{+0.07}_{-0.07}$	-0.65 $^{+0.04}_{-0.04}$	-3.96 $^{+1.02}_{-1.21}$	338 $^{+20}_{-20}$	12.75 $^{+2.15}_{-1.95} \times 10^{-6}$	-1.0	2.9	2.9	
2.269~2.441	39.30	0.99 $^{+0.10}_{-0.10}$	-0.79 $^{+0.08}_{-0.08}$	262 $^{+41}_{-41}$	317 $^{+54}_{-53}$	7.46 $^{+2.77}_{-1.84} \times 10^{-6}$	0.91 $^{+0.11}_{-0.11}$	-0.67 $^{+0.12}_{-0.12}$	-2.69 $^{+0.54}_{-0.60}$	257 $^{+46}_{-46}$	9.60 $^{+5.08}_{-3.34} \times 10^{-6}$	-4.9	2.5	2.2	
2.441~2.658	55.94	1.08 $^{+0.08}_{-0.08}$	-0.65 $^{+0.05}_{-0.05}$	230 $^{+21}_{-21}$	311 $^{+30}_{-30}$	10.55 $^{+2.47}_{-2.05} \times 10^{-6}$	1.06 $^{+0.08}_{-0.08}$	-0.64 $^{+0.06}_{-0.06}$	-4.29 $^{+1.19}_{-1.28}$	303 $^{+21}_{-20}$	10.89 $^{+2.13}_{-1.78} \times 10^{-6}$	0.1	2.8	3.0	
2.658~3.879	92.65	1.31 $^{+0.05}_{-0.05}$	-0.90 $^{+0.04}_{-0.04}$	152 $^{+10}_{-10}$	167 $^{+13}_{-13}$	3.93 $^{+0.53}_{-0.45} \times 10^{-6}$	1.24 $^{+0.05}_{-0.05}$	-0.79 $^{+0.05}_{-0.05}$	-2.62 $^{+0.15}_{-0.15}$	143 $^{+8}_{-8}$	4.78 $^{+0.75}_{-0.63} \times 10^{-6}$	-14.9	3.0	3.8	
3.879~4.183	27.26	0.97 $^{+0.09}_{-0.09}$	-1.24 $^{+0.11}_{-0.11}$	238 $^{+72}_{-72}$	181 $^{+60}_{-60}$	1.92 $^{+0.89}_{-0.56} \times 10^{-6}$	0.94 $^{+0.10}_{-0.10}$	-1.15 $^{+0.14}_{-0.14}$	-3.63 $^{+1.18}_{-1.19}$	153 $^{+35}_{-35}$	2.00 $^{+0.93}_{-0.93} \times 10^{-6}$	-0.4	1.6	1.2	
4.183~4.426	33.25	0.78 $^{+0.08}_{-0.08}$	-0.77 $^{+0.09}_{-0.09}$	159 $^{+25}_{-25}$	195 $^{+34}_{-34}$	3.36 $^{+1.46}_{-1.30} \times 10^{-6}$	0.77 $^{+0.08}_{-0.08}$	-0.76 $^{+0.10}_{-0.10}$	5.49 $^{+1.71}_{-1.71}$	192 $^{+19}_{-19}$	3.22 $^{+0.87}_{-0.63} \times 10^{-6}$	0.7	2.5	3.0	
4.426~4.792	25.57	0.75 $^{+0.08}_{-0.08}$	-0.90 $^{+0.14}_{-0.14}$	106 $^{+22}_{-22}$	117 $^{+28}_{-28}$	1.47 $^{+0.63}_{-0.42} \times 10^{-6}$	0.73 $^{+0.08}_{-0.07}$	-0.88 $^{+0.13}_{-0.13}$	-5.13 $^{+1.64}_{-1.68}$	112 $^{+11}_{-11}$	1.44 $^{+0.34}_{-0.25} \times 10^{-6}$	0.7	2.1	3.0	
4.792~4.865	20.81	1.26 $^{+0.20}_{-0.20}$	-0.86 $^{+0.19}_{-0.19}$	120 $^{+33}_{-33}$	137 $^{+44}_{-48}$	2.95 $^{+2.64}_{-2.20} \times 10^{-6}$	1.21 $^{+0.21}_{-0.21}$	-0.66 $^{+0.38}_{-0.38}$	-4.78 $^{+2.51}_{-2.51}$	112 $^{+26}_{-35}$	3.24 $^{+3.27}_{-3.27} \times 10^{-6}$	-2.8	0.3	-1.1	
4.865~5.141	54.66	1.62 $^{+0.11}_{-0.11}$	-0.83 $^{+0.07}_{-0.07}$	131 $^{+13}_{-13}$	154 $^{+18}_{-18}$	4.71 $^{+1.12}_{-0.76} \times 10^{-6}$	1.61 $^{+0.11}_{-0.11}$	-0.82 $^{+0.07}_{-0.07}$	-5.84 $^{+1.47}_{-1.47}$	152 $^{+8}_{-8}$	4.85 $^{+0.67}_{-0.51} \times 10^{-6}$	0.6	2.8	3.2	
5.141~5.348	28.44	1.64 $^{+0.15}_{-0.15}$	-1.12 $^{+0.16}_{-0.16}$	88 $^{+22}_{-22}$	78 $^{+24}_{-24}$	1.79 $^{+0.75}_{-0.44} \times 10^{-6}$	1.62 $^{+0.15}_{-0.15}$	-0.84 $^{+0.32}_{-0.29}$	-4.17 $^{+1.79}_{-1.71}$	62 $^{+13}_{-13}$	1.98 $^{+0.87}_{-0.59} \times 10^{-6}$	-7.4	1.5	-2.7	
5.766~5.973	39.44	1.45 $^{+0.12}_{-0.12}$	-1.03 $^{+0.08}_{-0.08}$	197 $^{+32}_{-33}$	191 $^{+35}_{-36}$	4.15 $^{+1.29}_{-0.92} \times 10^{-6}$	1.44 $^{+0.12}_{-0.12}$	-1.03 $^{+0.08}_{-0.08}$	-5.57 $^{+1.68}_{-1.67}$	187 $^{+19}_{-19}$	4.20 $^{+0.77}_{-0.66} \times 10^{-6}$	0.8	2.6	3.1	
5.973~6.233	31.12	1.21 $^{+0.12}_{-0.12}$	-1.11 $^{+0.12}_{-0.12}$	147 $^{+34}_{-35}$	131 $^{+35}_{-36}$	2.17 $^{+0.83}_{-0.59} \times 10^{-6}$	1.19 $^{+0.11}_{-0.11}$	-1.07 $^{+0.12}_{-0.12}$	-4.29 $^{+1.21}_{-1.29}$	122 $^{+15}_{-15}$	2.24 $^{+0.52}_{-0.52} \times 10^{-6}$	0.8	1.9	3.0	
6.233~6.579	49.36	1.47 $^{+0.09}_{-0.09}$	-1.04 $^{+0.06}_{-0.06}$	211 $^{+29}_{-29}$	203 $^{+30}_{-30}$	4.36 $^{+1.02}_{-0.80} \times 10^{-6}$	1.46 $^{+0.10}_{-0.10}$	-1.03 $^{+0.06}_{-0.06}$	-4.76 $^{+1.48}_{-1.51}$	198 $^{+18}_{-17}$	4.48 $^{+0.73}_{-0.66} \times 10^{-6}$	0.6	2.8	3.1	
6.678~7.090	61.73	0.92 $^{+0.06}_{-0.06}$	-0.74 $^{+0.04}_{-0.04}$	249 $^{+22}_{-22}$	314 $^{+29}_{-29}$	7.72 $^{+1.56}_{-1.26} \times 10^{-6}$	0.91 $^{+0.06}_{-0.06}$	-0.72 $^{+0.05}_{-0.05}$	-3.86 $^{+1.07}_{-1.06}$	303 $^{+22}_{-22}$	8.06 $^{+1.78}_{-1.32} \times 10^{-6}$	-0.7	2.8	2.6	
7.090~7.302	21.28	0.97 $^{+0.12}_{-0.12}$	-1.21 $^{+0.16}_{-0.16}$	207 $^{+71}_{-71}$	163 $^{+65}_{-65}$	1.74 $^{+1.14}_{-0.58} \times 10^{-6}$	0.94 $^{+0.12}_{-0.12}$	-1.15 $^{+0.17}_{-0.17}$	-3.89 $^{+1.19}_{-1.22}$	138 $^{+28}_{-30}$	1.86 $^{+0.73}_{-0.70} \times 10^{-6}$	2.1	0.1	2.5	
7.302~7.513	33.20	0.81 $^{+0.09}_{-0.09}$	-0.68 $^{+0.10}_{-0.10}$	127 $^{+18}_{-19}$	168 $^{+27}_{-28}$	3.24 $^{+1.41}_{-0.95} \times 10^{-6}$	0.80 $^{+0.09}_{-0.09}$	-0.66 $^{+0.11}_{-0.11}$	-4.80 $^{+1.31}_{-1.36}$	163 $^{+14}_{-14}$	3.26 $^{+0.92}_{-0.58} \times 10^{-6}$	0.5	2.5	3.0	
7.513~7.846	63.11	1.25 $^{+0.08}_{-0.08}$	-0.57 $^{+0.06}_{-0.06}$	117 $^{+9}_{-9}$	168 $^{+14}_{-14}$	5.97 $^{+1.38}_{-0.98} \times 10^{-6}$	1.25 $^{+0.08}_{-0.08}$	-0.57 $^{+0.06}_{-0.06}$	-5.96 $^{+1.40}_{-1.41}$	167 $^{+7}_{-7}$	6.05 $^{+0.80}_{-0.72} \times 10^{-6}$	0.8	2.9	3.3	
7.846~8.669	63.66	1.11 $^{+0.06}_{-0.06}$	-0.68 $^{+0.06}_{-0.06}$	80 $^{+6}_{-6}$	105 $^{+9}_{-9}$	2.44 $^{+0.45}_{-0.38} \times 10^{-6}$	1.10 $^{+0.06}_{-0.06}$	-1.10 $^{+0.06}_{-0.06}$	-6.66 $^{+0.07}_{-0.07}$	103 $^{+4}_{-4}$	2.51 $^{+0.31}_{-0.25} \times 10^{-6}$	-1.2	2.9	3.0	
8.669~9.062	34.70	1.68 $^{+0.12}_{-0.12}$	-1.39 $^{+0.12}_{-0.12}$	118 $^{+26}_{-26}$	72 $^{+21}_{-22}$	1.62 $^{+0.47}_{-0.29} \times 10^{-6}$	1.67 $^{+0.12}_{-0.12}$	-1.37 $^{+0.12}_{-0.12}$	-5.57 $^{+1.66}_{-1.67}$	69 $^{+6}_{-6}$	1.64 $^{+0.17}_{-0.15} \times 10^{-6}$	1.1	2.2	3.2	
9.062~9.337	42.66	1.80 $^{+0.14}_{-0.14}$	-0.92 $^{+0.11}_{-0.11}$	78 $^{+11}_{-12}$	84 $^{+15}_{-15}$	2.45 $^{+0.70}_{-0.51} \times 10^{-6}$	1.77 $^{+0.13}_{-0.13}$	-0.87 $^{+0.13}_{-0.13}$	-4.22 $^{+1.10}_{-1.22}$	80 $^{+6}_{-6}$	2.48 $^{+0.49}_{-0.32} \times 10^{-6}$	0.0	2.5	3.0	
9.337~9.473	39.70	1.80 $^{+0.17}_{-0.17}$	-0.92 $^{+0.10}_{-0.10}$	142 $^{+23}_{-23}$	153 $^{+28}_{-29}$	4.60 $^{+1.74}_{-1.07} \times 10^{-6}$	1.80 $^{+0.17}_{-0.17}$	-0.92 $^{+0.10}_{-0.10}$	-4.81 $^{+1.39}_{-1.46}$	149 $^{+13}_{-13}$	4.74 $^{+1.10}_{-0.78} \times 10^{-6}$	0.7	2.5	3.1	

Table A9 continued on next page

Table A9 (*continued*)

$t_{\text{start}} \sim t_{\text{stop}}$	S	Cutoff Power-Law Fitting						Band Fitting						Difference	
		K	α	E_c	E_p	F	K	α	β	E_p	F	ΔDIC	$p_{\text{DIC}}^{\text{CPL}}$	$p_{\text{DIC}}^{\text{Band}}$	
(1)	(2)	(3)	(4)	(5)	(6)	(7)	(8)	(9)	(10)	(11)	(12)	(13)	(14)	(15)	
9.473~10.066	63.64	1.53 $^{+0.08}_{-0.06}$	-0.97 $^{+0.06}_{-0.06}$	129 $^{+12}_{-13}$	133 $^{+15}_{-15}$	3.33 $^{+0.67}_{-0.46} \times 10^{-6}$	1.52 $^{+0.08}_{-0.08}$	-0.95 $^{+0.06}_{-0.06}$	-4.54 $^{+1.22}_{-1.26}$	131 $^{+7}_{-7}$	3.42 $^{+0.42}_{-0.36} \times 10^{-6}$	0.1	2.9	3.0	
10.066~10.629	32.77	1.13 $^{+0.08}_{-0.08}$	-1.13 $^{+0.13}_{-0.13}$	80 $^{+15}_{-16}$	69 $^{+17}_{-17}$	1.13 $^{+0.39}_{-0.23} \times 10^{-6}$	1.11 $^{+0.09}_{-0.08}$	-1.08 $^{+0.14}_{-0.14}$	-4.54 $^{+1.22}_{-1.22}$	66 $^{+5}_{-5}$	1.15 $^{+0.16}_{-0.12} \times 10^{-6}$	1.1	2.2	3.1	
11.289~11.861	28.49	0.89 $^{+0.08}_{-0.08}$	-1.44 $^{+0.13}_{-0.13}$	283 $^{+131}_{-126}$	159 $^{+82}_{-80}$	1.24 $^{+0.72}_{-0.32} \times 10^{-6}$	0.88 $^{+0.08}_{-0.08}$	-1.41 $^{+0.14}_{-0.14}$	-5.56 $^{+2.87}_{-2.99}$	136 $^{+31}_{-36}$	1.27 $^{+0.41}_{-0.22} \times 10^{-6}$	2.0	-1.2	1.4	
11.861~15.168	29.91	0.56 $^{+0.03}_{-0.03}$	-1.64 $^{+0.13}_{-0.14}$	142 $^{+49}_{-52}$	51 $^{+26}_{-27}$	0.44 $^{+0.13}_{-0.07} \times 10^{-6}$	0.55 $^{+0.03}_{-0.03}$	-1.55 $^{+0.13}_{-0.17}$	5.75 $^{+2.79}_{-2.83}$	43 $^{+6}_{-6}$	0.43 $^{+0.06}_{-0.05} \times 10^{-6}$	2.6	-0.1	2.8	
Pulse 2															
19.219~20.281	42.12	1.16 $^{+0.06}_{-0.06}$	-1.33 $^{+0.10}_{-0.10}$	99 $^{+19}_{-19}$	66 $^{+16}_{-16}$	1.07 $^{+0.24}_{-0.16} \times 10^{-6}$	1.15 $^{+0.06}_{-0.06}$	-1.30 $^{+0.10}_{-0.11}$	-6.04 $^{+2.61}_{-2.67}$	64 $^{+5}_{-5}$	1.09 $^{+0.10}_{-0.09} \times 10^{-6}$	0.2	2.3	2.8	
20.281~20.678	40.24	1.38 $^{+0.09}_{-0.09}$	-1.43 $^{+0.06}_{-0.06}$	588 $^{+172}_{-183}$	335 $^{+104}_{-110}$	3.22 $^{+1.03}_{-0.65} \times 10^{-6}$	1.38 $^{+0.09}_{-0.09}$	-1.42 $^{+0.06}_{-0.06}$	-6.15 $^{+2.53}_{-2.63}$	320 $^{+68}_{-74}$	3.31 $^{+0.74}_{-0.55} \times 10^{-6}$	0.6	2.1	2.6	
20.678~21.236	27.07	1.06 $^{+0.07}_{-0.07}$	-1.78 $^{+0.05}_{-0.05}$	2904 $^{+1922}_{-1800}$	639 $^{+447}_{-422}$	1.85 $^{+0.48}_{-0.42} \times 10^{-6}$	1.06 $^{+0.07}_{-0.07}$	-1.78 $^{+0.06}_{-0.06}$	-6.06 $^{+2.67}_{-2.68}$	527 $^{+333}_{-291}$	1.83 $^{+0.40}_{-0.32} \times 10^{-6}$	0.2	1.8	2.0	
22.319~22.775	45.88	1.30 $^{+0.08}_{-0.08}$	-1.26 $^{+0.06}_{-0.06}$	352 $^{+68}_{-68}$	260 $^{+54}_{-54}$	3.44 $^{+0.84}_{-0.63} \times 10^{-6}$	1.29 $^{+0.08}_{-0.08}$	-1.25 $^{+0.06}_{-0.06}$	-6.24 $^{+2.60}_{-2.62}$	253 $^{+32}_{-32}$	3.49 $^{+0.66}_{-0.46} \times 10^{-6}$	0.2	2.6	2.9	
22.775~23.612	32.79	0.89 $^{+0.06}_{-0.06}$	-1.55 $^{+0.08}_{-0.08}$	588 $^{+296}_{-276}$	265 $^{+141}_{-133}$	1.48 $^{+0.62}_{-0.38} \times 10^{-6}$	0.88 $^{+0.06}_{-0.06}$	-1.53 $^{+0.09}_{-0.09}$	-5.69 $^{+2.94}_{-2.92}$	225 $^{+77}_{-79}$	1.51 $^{+0.46}_{-0.28} \times 10^{-6}$	0.7	0.2	1.3	
23.612~23.992	34.71	0.65 $^{+0.06}_{-0.06}$	-0.95 $^{+0.07}_{-0.07}$	319 $^{+56}_{-57}$	335 $^{+63}_{-64}$	3.72 $^{+1.27}_{-1.04} \times 10^{-6}$	0.65 $^{+0.06}_{-0.06}$	-0.95 $^{+0.07}_{-0.07}$	-6.05 $^{+2.49}_{-2.60}$	329 $^{+40}_{-41}$	3.78 $^{+0.91}_{-0.73} \times 10^{-6}$	0.3	2.6	2.9	
23.992~25.076	29.17	0.70 $^{+0.05}_{-0.05}$	-1.33 $^{+0.14}_{-0.14}$	128 $^{+36}_{-36}$	86 $^{+30}_{-30}$	0.75 $^{+0.31}_{-0.31} \times 10^{-6}$	0.69 $^{+0.05}_{-0.05}$	-1.04 $^{+0.39}_{-0.34}$	-4.20 $^{+1.93}_{-1.93}$	65 $^{+15}_{-15}$	0.83 $^{+0.43}_{-0.23} \times 10^{-6}$	-9.2	0.8	-5.8	
25.076~25.385	31.38	0.73 $^{+0.07}_{-0.07}$	-0.85 $^{+0.10}_{-0.10}$	158 $^{+26}_{-26}$	181 $^{+34}_{-34}$	2.51 $^{+0.93}_{-0.66} \times 10^{-6}$	0.73 $^{+0.07}_{-0.07}$	-0.84 $^{+0.09}_{-0.10}$	-6.55 $^{+2.36}_{-2.36}$	177 $^{+16}_{-17}$	2.52 $^{+0.58}_{-0.42} \times 10^{-6}$	0.4	2.6	3.0	
25.385~25.625	37.53	1.03 $^{+0.09}_{-0.09}$	-1.00 $^{+0.07}_{-0.07}$	264 $^{+47}_{-47}$	264 $^{+50}_{-51}$	4.20 $^{+1.37}_{-0.99} \times 10^{-6}$	1.02 $^{+0.09}_{-0.09}$	-0.99 $^{+0.08}_{-0.08}$	-6.31 $^{+2.45}_{-2.48}$	256 $^{+32}_{-31}$	4.24 $^{+0.99}_{-0.75} \times 10^{-6}$	0.5	2.6	3.0	
25.625~26.015	35.97	1.12 $^{+0.08}_{-0.08}$	-1.30 $^{+0.06}_{-0.06}$	487 $^{+130}_{-136}$	341 $^{+96}_{-101}$	3.34 $^{+1.20}_{-0.77} \times 10^{-6}$	1.12 $^{+0.08}_{-0.08}$	-1.29 $^{+0.07}_{-0.07}$	-5.98 $^{+2.67}_{-2.71}$	321 $^{+63}_{-64}$	3.34 $^{+0.80}_{-0.55} \times 10^{-6}$	0.4	2.1	2.6	
26.015~26.342	24.61	0.68 $^{+0.07}_{-0.07}$	-1.13 $^{+0.12}_{-0.12}$	220 $^{+61}_{-61}$	191 $^{+59}_{-61}$	1.61 $^{+0.88}_{-0.48} \times 10^{-6}$	0.68 $^{+0.08}_{-0.08}$	-1.12 $^{+0.12}_{-0.12}$	-6.25 $^{+2.44}_{-2.50}$	182 $^{+31}_{-33}$	1.65 $^{+0.52}_{-0.34} \times 10^{-6}$	1.2	1.8	2.8	
26.342~27.372	76.31	0.92 $^{+0.04}_{-0.04}$	-0.92 $^{+0.04}_{-0.04}$	270 $^{+23}_{-23}$	291 $^{+27}_{-27}$	5.03 $^{+0.79}_{-0.67} \times 10^{-6}$	0.88 $^{+0.04}_{-0.04}$	-0.85 $^{+0.05}_{-0.05}$	-2.77 $^{+0.43}_{-0.49}$	253 $^{+23}_{-22}$	6.06 $^{+1.30}_{-1.08} \times 10^{-6}$	-9.1	2.9	2.2	
27.513~27.927	63.80	0.98 $^{+0.06}_{-0.06}$	-0.82 $^{+0.04}_{-0.04}$	324 $^{+30}_{-30}$	382 $^{+38}_{-38}$	8.81 $^{+1.90}_{-1.39} \times 10^{-6}$	0.98 $^{+0.06}_{-0.06}$	-0.81 $^{+0.04}_{-0.04}$	-5.81 $^{+2.58}_{-2.81}$	376 $^{+25}_{-25}$	9.00 $^{+1.62}_{-1.15} \times 10^{-6}$	-0.8	2.9	2.6	
27.927~28.130	29.55	1.08 $^{+0.11}_{-0.10}$	-1.10 $^{+0.10}_{-0.10}$	264 $^{+67}_{-70}$	237 $^{+66}_{-68}$	3.31 $^{+1.47}_{-1.00} \times 10^{-6}$	1.04 $^{+0.11}_{-0.11}$	-1.03 $^{+0.12}_{-0.13}$	-5.01 $^{+2.72}_{-3.21}$	204 $^{+42}_{-42}$	3.49 $^{+1.81}_{-0.95} \times 10^{-6}$	-1.9	1.2	1.2	
28.130~28.553	22.53	0.64 $^{+0.07}_{-0.07}$	-1.08 $^{+0.16}_{-0.16}$	123 $^{+34}_{-36}$	114 $^{+37}_{-39}$	1.00 $^{+0.55}_{-0.31} \times 10^{-6}$	0.63 $^{+0.07}_{-0.07}$	-1.03 $^{+0.17}_{-0.17}$	-5.96 $^{+2.75}_{-2.82}$	104 $^{+15}_{-15}$	1.02 $^{+0.33}_{-0.21} \times 10^{-6}$	1.2	1.2	2.7	
28.553~29.339	20.98	0.70 $^{+0.06}_{-0.06}$	-1.68 $^{+0.14}_{-0.14}$	351 $^{+139}_{-198}$	112 $^{+91}_{-78}$	0.74 $^{+0.27}_{-0.17} \times 10^{-6}$	1.11 $^{+0.08}_{-0.09}$	-0.71 $^{+0.17}_{-0.18}$	-2.08 $^{+0.06}_{-0.06}$	24 $^{+2}_{-2}$	0.93 $^{+0.17}_{-0.18} \times 10^{-6}$	-0.4	0.3	1.4	
29.339~31.161	22.28	0.66 $^{+0.05}_{-0.05}$	-1.31 $^{+0.28}_{-0.30}$	52 $^{+20}_{-20}$	36 $^{+20}_{-21}$	0.36 $^{+0.20}_{-0.08} \times 10^{-6}$	1.09 $^{+0.07}_{-0.07}$	-0.29 $^{+0.15}_{-0.16}$	-2.54 $^{+0.15}_{-0.15}$	22 $^{+1}_{-1}$	0.37 $^{+0.08}_{-0.07} \times 10^{-6}$	5.5	-6.8	2.2	
Pulse 3															
31.161~31.775	30.99	1.28 $^{+0.09}_{-0.09}$	-1.71 $^{+0.11}_{-0.11}$	298 $^{+140}_{-134}$	86 $^{+52}_{-51}$	1.25 $^{+0.39}_{-0.22} \times 10^{-6}$	1.26 $^{+0.09}_{-0.09}$	-1.67 $^{+0.13}_{-0.13}$	-6.12 $^{+2.66}_{-2.64}$	77 $^{+11}_{-18}$	1.25 $^{+0.18}_{-0.13} \times 10^{-6}$	2.6	0.1	2.6	
33.347~33.952	28.54	0.94 $^{+0.07}_{-0.07}$	-1.55 $^{+0.10}_{-0.10}$	441 $^{+211}_{-200}$	199 $^{+105}_{-100}$	1.38 $^{+0.56}_{-0.32} \times 10^{-6}$	0.93 $^{+0.07}_{-0.07}$	-1.53 $^{+0.11}_{-0.11}$	-6.11 $^{+2.59}_{-2.61}$	177 $^{+45}_{-54}$	1.38 $^{+0.34}_{-0.22} \times 10^{-6}$	1.4	0.5	1.9	
33.952~34.526	63.20	1.56 $^{+0.08}_{-0.08}$	-1.07 $^{+0.05}_{-0.05}$	170 $^{+19}_{-19}$	159 $^{+19}_{-19}$	3.58 $^{+0.66}_{-0.54} \times 10^{-6}$	1.55 $^{+0.08}_{-0.08}$	-1.06 $^{+0.05}_{-0.06}$	-6.25 $^{+2.64}_{-2.58}$	156 $^{+10}_{-10}$	3.67 $^{+0.45}_{-0.39} \times 10^{-6}$	0.1	2.9	3.0	
34.526~35.351	60.31	1.35 $^{+0.07}_{-0.07}$	-1.08 $^{+0.06}_{-0.06}$	119 $^{+14}_{-14}$	110 $^{+15}_{-15}$	2.22 $^{+0.42}_{-0.35} \times 10^{-6}$	1.34 $^{+0.07}_{-0.07}$	-1.04 $^{+0.08}_{-0.07}$	-4.74 $^{+1.94}_{-2.98}$	105 $^{+7}_{-7}$	2.30 $^{+0.37}_{-0.26} \times 10^{-6}$	-3.4	2.8	1.4	
35.351~35.620	27.90	1.58 $^{+0.14}_{-0.14}$	-1.19 $^{+0.16}_{-0.16}$	80 $^{+18}_{-18}$	65 $^{+19}_{-20}$	1.45 $^{+0.52}_{-0.33} \times 10^{-6}$	1.57 $^{+0.14}_{-0.14}$	-1.16 $^{+0.16}_{-0.16}$	-6.67 $^{+2.31}_{-2.30}$	61 $^{+5}_{-5}$	1.45 $^{+0.20}_{-0.16} \times 10^{-6}$	1.3	2.0	3.2	
35.620~36.126	52.56	1.85 $^{+0.10}_{-0.10}$	-1.18 $^{+0.07}_{-0.07}$	120 $^{+16}_{-16}$	98 $^{+16}_{-16}$	2.55 $^{+0.47}_{-0.42} \times 10^{-6}$	1.84 $^{+0.10}_{-0.10}$	-1.17 $^{+0.08}_{-0.08}$	-6.62 $^{+2.33}_{-2.33}$	97 $^{+6}_{-6}$	2.53 $^{+0.26}_{-0.23} \times 10^{-6}$	0.4	2.7	3.1	
36.126~36.700	32.36	1.44 $^{+0.10}_{-0.10}$	-1.64 $^{+0.14}_{-0.15}$	186 $^{+82}_{-80}$	67 $^{+39}_{-40}$	1.26 $^{+0.44}_{-0.25} \times 10^{-6}$	1.53 $^{+0.18}_{-0.18}$	-0.91 $^{+0.27}_{-0.27}$	-2.34 $^{+0.17}_{-0.11}$	35 $^{+6}_{-6}$	1.41 $^{+0.43}_{-0.32} \times 10^{-6}$	-3.9	-1.4	2.1	

Table A9 continued on next page

Table A9 (*continued*)

$t_{\text{start}} \sim t_{\text{stop}}$	S	Cutoff Power-Law Fitting						Band Fitting						Difference	
		K	α	E_c	E_p	F	K	α	β	E_p	F	ΔDIC	$p_{\text{DIC}}^{\text{CPL}}$	$p_{\text{DIC}}^{\text{Band}}$	
(1)	(2)	(3)	(4)	(5)	(6)	(7)	(8)	(9)	(10)	(11)	(12)	(13)	(14)	(15)	
Pulse 4															
99.917~100.943	30.62	0.36 $^{+0.03}_{-0.03}$	-0.91 $^{+0.08}_{-0.08}$	200 $^{+34}_{-35}$	218 $^{+40}_{-40}$	1.37 $^{+0.52}_{-0.33} \times 10^{-6}$	0.35 $^{+0.03}_{-0.03}$	-0.90 $^{+0.09}_{-0.09}$	6.03 $^{+2.75}_{-2.69}$	211 $^{+24}_{-24}$	1.41 $^{+0.41}_{-0.25} \times 10^{-6}$	0.3	2.5	2.9	
100.943~101.869	45.61	0.90 $^{+0.05}_{-0.05}$	-1.09 $^{+0.07}_{-0.07}$	154 $^{+21}_{-22}$	140 $^{+22}_{-22}$	1.81 $^{+0.41}_{-0.31} \times 10^{-6}$	0.89 $^{+0.05}_{-0.05}$	-1.06 $^{+0.08}_{-0.08}$	5.75 $^{+2.93}_{-2.90}$	133 $^{+13}_{-12}$	1.86 $^{+0.43}_{-0.29} \times 10^{-6}$	-0.5	2.8	2.6	
101.869~102.915	66.01	1.56 $^{+0.06}_{-0.06}$	-1.19 $^{+0.05}_{-0.05}$	129 $^{+14}_{-14}$	105 $^{+13}_{-13}$	2.22 $^{+0.31}_{-0.26} \times 10^{-6}$	1.55 $^{+0.06}_{-0.06}$	-1.17 $^{+0.06}_{-0.06}$	5.58 $^{+2.54}_{-2.95}$	102 $^{+6}_{-6}$	2.26 $^{+0.26}_{-0.17} \times 10^{-6}$	-1.3	2.8	2.3	
102.915~103.668	49.29	1.51 $^{+0.07}_{-0.07}$	-1.27 $^{+0.07}_{-0.07}$	127 $^{+19}_{-19}$	93 $^{+16}_{-17}$	1.84 $^{+0.36}_{-0.27} \times 10^{-6}$	1.51 $^{+0.07}_{-0.07}$	-1.26 $^{+0.07}_{-0.07}$	6.30 $^{+2.44}_{-2.47}$	90 $^{+6}_{-6}$	1.86 $^{+0.14}_{-0.14} \times 10^{-6}$	0.4	2.7	3.1	
103.668~105.122	46.33	0.97 $^{+0.05}_{-0.05}$	-1.33 $^{+0.07}_{-0.07}$	168 $^{+30}_{-31}$	113 $^{+23}_{-24}$	1.31 $^{+0.30}_{-0.19} \times 10^{-6}$	0.95 $^{+0.05}_{-0.05}$	-1.24 $^{+0.09}_{-0.09}$	3.07 $^{+0.76}_{-1.18}$	97 $^{+11}_{-11}$	1.58 $^{+0.34}_{-0.28} \times 10^{-6}$	-8.4	2.4	0.3	
105.122~106.270	32.46	0.72 $^{+0.05}_{-0.05}$	-1.27 $^{+0.10}_{-0.10}$	131 $^{+28}_{-29}$	95 $^{+25}_{-25}$	0.89 $^{+0.25}_{-0.18} \times 10^{-6}$	0.72 $^{+0.05}_{-0.05}$	-1.26 $^{+0.11}_{-0.10}$	5.96 $^{+2.55}_{-2.63}$	91 $^{+9}_{-9}$	0.90 $^{+0.13}_{-0.13} \times 10^{-6}$	0.7	2.1	3.0	
106.270~107.533	27.18	0.50 $^{+0.04}_{-0.04}$	-1.33 $^{+0.12}_{-0.12}$	198 $^{+61}_{-68}$	133 $^{+47}_{-51}$	0.72 $^{+0.30}_{-0.19} \times 10^{-6}$	0.49 $^{+0.04}_{-0.04}$	-1.30 $^{+0.12}_{-0.12}$	5.72 $^{+2.81}_{-2.83}$	117 $^{+18}_{-20}$	0.71 $^{+0.18}_{-0.18} \times 10^{-6}$	1.5	0.4	2.5	
107.593~113.181	26.43	0.21 $^{+0.01}_{-0.01}$	-1.09 $^{+0.09}_{-0.09}$	176 $^{+37}_{-37}$	160 $^{+37}_{-37}$	0.46 $^{+0.15}_{-0.11} \times 10^{-6}$	0.21 $^{+0.01}_{-0.01}$	-1.07 $^{+0.09}_{-0.09}$	5.65 $^{+2.79}_{-2.89}$	151 $^{+19}_{-19}$	0.47 $^{+0.12}_{-0.07} \times 10^{-6}$	0.1	2.1	2.6	
Pulse 5															
159.039~161.453	23.36	0.38 $^{+0.03}_{-0.03}$	-1.30 $^{+0.09}_{-0.08}$	291 $^{+82}_{-85}$	203 $^{+63}_{-64}$	0.77 $^{+0.30}_{-0.18} \times 10^{-6}$	0.37 $^{+0.03}_{-0.03}$	-1.28 $^{+0.09}_{-0.09}$	5.71 $^{+2.78}_{-2.82}$	191 $^{+34}_{-37}$	0.79 $^{+0.22}_{-0.13} \times 10^{-6}$	0.4	1.8	2.5	
161.836~162.767	39.07	0.61 $^{+0.04}_{-0.04}$	-1.14 $^{+0.04}_{-0.04}$	681 $^{+132}_{-134}$	585 $^{+116}_{-118}$	3.93 $^{+0.94}_{-0.78} \times 10^{-6}$	0.61 $^{+0.04}_{-0.04}$	-1.14 $^{+0.04}_{-0.04}$	5.71 $^{+2.83}_{-2.90}$	563 $^{+85}_{-87}$	3.98 $^{+0.96}_{-0.67} \times 10^{-6}$	-0.6	2.6	2.5	
162.767~163.660	20.51	0.43 $^{+0.04}_{-0.04}$	-1.25 $^{+0.08}_{-0.08}$	559 $^{+149}_{-205}$	419 $^{+149}_{-160}$	1.55 $^{+0.77}_{-0.46} \times 10^{-6}$	0.42 $^{+0.04}_{-0.04}$	-1.23 $^{+0.08}_{-0.08}$	6.01 $^{+2.64}_{-2.69}$	389 $^{+98}_{-109}$	1.57 $^{+0.57}_{-0.39} \times 10^{-6}$	0.7	1.3	2.1	
Pulse 6															
197.910~200.965	24.96	0.28 $^{+0.02}_{-0.02}$	-1.10 $^{+0.04}_{-0.04}$	1174 $^{+247}_{-244}$	1056 $^{+227}_{-225}$	3.35 $^{+0.95}_{-0.95} \times 10^{-6}$	0.27 $^{+0.02}_{-0.02}$	-1.10 $^{+0.04}_{-0.04}$	5.72 $^{+2.71}_{-2.87}$	1020 $^{+186}_{-191}$	3.39 $^{+0.80}_{-0.65} \times 10^{-6}$	-0.5	2.7	2.5	
200.965~202.147	29.13	0.39 $^{+0.03}_{-0.03}$	-1.00 $^{+0.05}_{-0.05}$	560 $^{+94}_{-96}$	560 $^{+98}_{-96}$	3.42 $^{+1.01}_{-0.77} \times 10^{-6}$	0.39 $^{+0.03}_{-0.03}$	-1.00 $^{+0.05}_{-0.05}$	5.56 $^{+2.76}_{-2.92}$	543 $^{+74}_{-74}$	3.50 $^{+0.86}_{-0.64} \times 10^{-6}$	-0.4	2.7	2.6	
202.147~202.860	15.52	0.27 $^{+0.03}_{-0.03}$	-1.10 $^{+0.08}_{-0.08}$	805 $^{+278}_{-293}$	724 $^{+259}_{-271}$	2.19 $^{+1.40}_{-0.78} \times 10^{-6}$	0.27 $^{+0.03}_{-0.03}$	-1.09 $^{+0.08}_{-0.08}$	6.05 $^{+2.69}_{-2.66}$	692 $^{+205}_{-212}$	2.29 $^{+1.06}_{-0.69} \times 10^{-6}$	0.4	1.9	2.4	
207.989~208.434	23.26	0.46 $^{+0.05}_{-0.05}$	-1.00 $^{+0.07}_{-0.07}$	584 $^{+154}_{-159}$	584 $^{+160}_{-164}$	3.90 $^{+1.96}_{-1.07} \times 10^{-6}$	0.45 $^{+0.05}_{-0.05}$	-0.98 $^{+0.07}_{-0.08}$	5.71 $^{+2.80}_{-2.85}$	537 $^{+115}_{-112}$	4.23 $^{+1.68}_{-1.11} \times 10^{-6}$	-0.2	2.1	2.2	
208.434~208.717	26.62	0.86 $^{+0.07}_{-0.07}$	-1.14 $^{+0.05}_{-0.05}$	967 $^{+282}_{-279}$	832 $^{+247}_{-247}$	7.19 $^{+2.47}_{-2.42} \times 10^{-6}$	0.83 $^{+0.08}_{-0.08}$	-1.10 $^{+0.07}_{-0.08}$	5.06 $^{+2.88}_{-2.86}$	740 $^{+224}_{-227}$	4.00 $^{+3.66}_{-2.27} \times 10^{-6}$	-3.3	2.3	0.5	
208.717~209.100	53.48	1.25 $^{+0.06}_{-0.06}$	-0.97 $^{+0.03}_{-0.03}$	879 $^{+94}_{-95}$	905 $^{+101}_{-101}$	19.89 $^{+3.69}_{-2.86} \times 10^{-6}$	1.24 $^{+0.07}_{-0.06}$	-0.96 $^{+0.03}_{-0.03}$	4.61 $^{+1.81}_{-2.75}$	875 $^{+82}_{-80}$	20.40 $^{+3.58}_{-2.69} \times 10^{-6}$	-3.5	2.9	1.7	
209.100~209.773	78.55	1.55 $^{+0.05}_{-0.05}$	-0.99 $^{+0.02}_{-0.02}$	1064 $^{+91}_{-91}$	1075 $^{+94}_{-95}$	27.81 $^{+3.23}_{-3.23} \times 10^{-6}$	1.41 $^{+0.05}_{-0.05}$	-0.91 $^{+0.02}_{-0.02}$	2.35 $^{+0.09}_{-0.09}$	751 $^{+55}_{-54}$	29.09 $^{+3.83}_{-3.06} \times 10^{-6}$	-42.5	3.0	3.9	
209.773~210.245	51.50	1.25 $^{+0.06}_{-0.06}$	-1.06 $^{+0.03}_{-0.03}$	1002 $^{+151}_{-151}$	941 $^{+145}_{-145}$	15.70 $^{+3.73}_{-2.73} \times 10^{-6}$	1.17 $^{+0.07}_{-0.07}$	-0.98 $^{+0.05}_{-0.05}$	2.32 $^{+0.22}_{-0.14}$	669 $^{+109}_{-110}$	17.65 $^{+4.35}_{-3.57} \times 10^{-6}$	-15.4	2.8	3.4	
210.245~210.395	38.34	1.28 $^{+0.11}_{-0.11}$	-0.87 $^{+0.05}_{-0.05}$	592 $^{+94}_{-95}$	669 $^{+110}_{-111}$	19.10 $^{+6.20}_{-4.40} \times 10^{-6}$	1.15 $^{+0.11}_{-0.11}$	-0.76 $^{+0.07}_{-0.07}$	2.38 $^{+0.17}_{-0.09}$	488 $^{+76}_{-78}$	23.32 $^{+8.43}_{-6.19} \times 10^{-6}$	-14.5	2.6	2.8	
210.395~210.583	28.99	1.43 $^{+0.13}_{-0.13}$	-1.22 $^{+0.07}_{-0.07}$	1599 $^{+903}_{-815}$	1247 $^{+713}_{-646}$	12.58 $^{+9.25}_{-5.02} \times 10^{-6}$	1.26 $^{+0.11}_{-0.12}$	-1.09 $^{+0.08}_{-0.08}$	2.19 $^{+0.17}_{-0.17}$	534 $^{+126}_{-146}$	12.33 $^{+4.47}_{-3.20} \times 10^{-6}$	-12.8	-0.2	1.4	
210.583~212.582	50.48	0.73 $^{+0.03}_{-0.03}$	-1.08 $^{+0.03}_{-0.03}$	578 $^{+62}_{-60}$	531 $^{+60}_{-60}$	5.13 $^{+0.81}_{-0.60} \times 10^{-6}$	0.71 $^{+0.03}_{-0.03}$	-1.04 $^{+0.04}_{-0.04}$	2.40 $^{+0.28}_{-0.28}$	446 $^{+51}_{-51}$	6.59 $^{+1.15}_{-1.09} \times 10^{-6}$	-12.6	2.9	2.7	
212.582~212.762	30.63	0.99 $^{+0.09}_{-0.09}$	-0.97 $^{+0.05}_{-0.05}$	726 $^{+145}_{-146}$	748 $^{+154}_{-154}$	12.43 $^{+4.25}_{-3.08} \times 10^{-6}$	0.98 $^{+0.09}_{-0.09}$	-0.96 $^{+0.06}_{-0.05}$	6.01 $^{+2.53}_{-2.62}$	733 $^{+118}_{-116}$	12.66 $^{+3.81}_{-2.66} \times 10^{-6}$	-0.2	2.6	2.7	
212.762~213.150	28.13	0.69 $^{+0.06}_{-0.06}$	-1.02 $^{+0.06}_{-0.06}$	504 $^{+110}_{-112}$	494 $^{+112}_{-114}$	4.84 $^{+1.93}_{-1.13} \times 10^{-6}$	0.68 $^{+0.06}_{-0.06}$	-1.00 $^{+0.07}_{-0.07}$	5.43 $^{+2.80}_{-2.99}$	453 $^{+82}_{-83}$	5.12 $^{+1.88}_{-1.25} \times 10^{-6}$	-0.5	2.5	2.4	
213.150~214.550	27.34	0.51 $^{+0.03}_{-0.03}$	-1.18 $^{+0.05}_{-0.05}$	691 $^{+154}_{-161}$	566 $^{+131}_{-136}$	2.94 $^{+0.89}_{-0.66} \times 10^{-6}$	0.51 $^{+0.03}_{-0.03}$	-1.17 $^{+0.05}_{-0.05}$	5.98 $^{+2.80}_{-2.72}$	545 $^{+97}_{-99}$	5.96 $^{+0.76}_{-0.49} \times 10^{-6}$	0.1	2.5	2.7	
214.550~215.095	27.12	0.63 $^{+0.05}_{-0.05}$	-1.07 $^{+0.06}_{-0.06}$	442 $^{+88}_{-86}$	411 $^{+86}_{-86}$	3.49 $^{+1.24}_{-0.79} \times 10^{-6}$	0.63 $^{+0.05}_{-0.05}$	-1.07 $^{+0.06}_{-0.06}$	6.27 $^{+2.45}_{-2.48}$	407 $^{+61}_{-61}$	3.49 $^{+0.85}_{-0.59} \times 10^{-6}$	0.4	2.7	3.0	
215.095~215.998	22.29	0.51 $^{+0.04}_{-0.04}$	-1.18 $^{+0.06}_{-0.06}$	558 $^{+146}_{-152}$	458 $^{+124}_{-129}$	2.35 $^{+0.97}_{-0.58} \times 10^{-6}$	0.51 $^{+0.04}_{-0.04}$	-1.17 $^{+0.07}_{-0.07}$	6.03 $^{+2.67}_{-2.66}$	435 $^{+89}_{-94}$	2.41 $^{+0.77}_{-0.53} \times 10^{-6}$	0.4	2.2	2.6	

Table A9 continued on next page

Table A9 (*continued*)

$t_{\text{start}} \sim t_{\text{stop}}$	S	Cutoff Power-Law Fitting						Band Fitting			Difference			
		K	α	E_c	E_p	F	K	α	β	E_p	F	ΔDIC	$p_{\text{DIC}}^{\text{CPL}}$	
													$p_{\text{DIC}}^{\text{Band}}$	
(1)	(2)	(3)	(4)	(5)	(6)	(7)	(8)	(9)	(10)	(11)	(12)	(13)	(14)	(15)

Note—All columns are the same as Table A2 but for GRB 101014175.

Table A10. Time-resolved Spectral Fit Results of GRB 110301214

$t_{\text{start}} \sim t_{\text{stop}}$	S	Cutoff Power-Law Fitting						Band Fitting						Difference		
		K	α	E_c	E_p	F	K	α	β	E_p	F	Δ_{DIC}	$p_{\text{DIC}}^{\text{CPL}}$	$p_{\text{DIC}}^{\text{Band}}$		
(1)	(2)	(3)	(4)	(5)	(6)	(7)	(8)	(9)	(10)	(11)	(12)	(13)	(14)	(15)		
Pulse 1																
0.190~0.963	78.55	1.38 $^{+0.06}$ -0.82 $^{+0.05}$	1.35 $^{+11}$ -0.56 $^{+14}$	4.36 $^{+0.76}$ -0.56 $^{+10}$	1.26 $^{+0.07}$ -0.60 $^{+0.09}$	-2.41 $^{+0.12}$ -0.49 $^{+0.11}$	124 $^{+9}$ -10 $^{+6}$	5.90 $^{+1.31}$ -0.93 $^{+10}$	-27.2	2.8	3.9					
0.963~1.686	102.59	1.89 $^{+0.08}$ -0.52 $^{+0.05}$	0.52 $^{+0.05}$ -0.08	74 $^{+3}$ -3	109 $^{+6}$ -6	5.15 $^{+0.68}$ -0.57	1.87 $^{+0.08}$ -0.08	-0.49 $^{+0.05}$ -0.05	-4.54 $^{+0.97}$ -0.05	107 $^{+3}$ -3	5.28 $^{+0.54}$ -0.46	-1.5	3.0	2.8		
1.686~1.974	81.20	2.97 $^{+0.15}$ -0.68 $^{+0.06}$	0.68 $^{+0.15}$ -0.15	83 $^{+6}$ -6	109 $^{+9}$ -9	6.79 $^{+1.14}$ -0.94	10 $^{+6}$ -10	2.92 $^{+0.15}$ -0.64	-4.16 $^{+0.85}$ -0.07	106 $^{+4}$ -4	7.04 $^{+0.84}$ -0.72	-1.9	2.9	2.8		
1.974~2.688	159.10	4.50 $^{+0.12}$ -0.94 $^{+0.03}$	1.46 $^{+6}$ -6	155 $^{+8}$ -6	11.84 $^{+0.96}$ -0.87	10 $^{+6}$ -6	4.27 $^{+0.12}$ -0.12	-0.83 $^{+0.04}$ -0.04	-2.73 $^{+0.11}$ -0.10	133 $^{+5}$ -5	13.60 $^{+1.20}$ -1.02	-26.9	3.0	4.0		
2.688~3.128	103.34	3.69 $^{+0.14}$ -1.00 $^{+0.04}$	1.00 $^{+0.04}$ -0.11	139 $^{+10}$ -10	139 $^{+11}$ -11	8.14 $^{+0.97}$ -0.87	10 $^{+6}$ -6	3.64 $^{+0.14}$ -0.14	-0.97 $^{+0.05}$ -0.05	134 $^{+6}$ -6	8.43 $^{+0.94}$ -0.73	-1.7	2.9	2.7		
3.128~3.725	97.15	3.26 $^{+0.12}$ -0.04	1.04 $^{+0.04}$ -0.04	116 $^{+8}$ -8	112 $^{+9}$ -9	5.56 $^{+0.72}$ -0.59	10 $^{+6}$ -6	3.10 $^{+0.13}$ -0.13	-0.88 $^{+0.08}$ -0.08	2.76 $^{+0.19}$ -0.15	95 $^{+6}$ -6	6.40 $^{+0.84}$ -0.81	-10.8	2.9	3.8	
Pulse 2																
3.725~3.876	65.77	3.82 $^{+0.23}$ -0.86 $^{+0.07}$	0.86 $^{+0.07}$ -0.07	111 $^{+11}$ -11	126 $^{+15}$ -15	8.63 $^{+2.04}$ -1.46	10 $^{-6}$ -6	3.75 $^{+0.24}$ -0.24	-0.82 $^{+0.08}$ -0.08	4.06 $^{+0.97}$ -0.08	121 $^{+7}$ -7	9.07 $^{+1.43}$ -1.18	-1.4	2.9	2.7	
3.876~4.126	107.60	4.69 $^{+0.19}$ -0.81 $^{+0.04}$	0.81 $^{+0.04}$ -0.04	114 $^{+7}$ -7	136 $^{+10}$ -9	12.62 $^{+1.67}$ -1.44	10 $^{-6}$ -6	4.53 $^{+0.20}$ -0.20	-0.73 $^{+0.06}$ -0.06	-3.14 $^{+0.31}$ -0.27	126 $^{+6}$ -6	13.71 $^{+1.82}$ -1.46	-9.1	3.0	3.7	
4.126~4.359	85.64	5.08 $^{+0.23}$ -0.99 $^{+0.06}$	0.99 $^{+0.06}$ -0.06	101 $^{+8}$ -8	102 $^{+10}$ -8	8.31 $^{+1.30}$ -1.07	10 $^{-6}$ -6	4.84 $^{+0.24}$ -0.24	-0.83 $^{+0.10}$ -0.10	-3.03 $^{+0.32}$ -0.32	90 $^{+6}$ -6	9.18 $^{+1.32}$ -1.06	-7.1	2.9	3.1	
4.359~4.502	54.81	4.72 $^{+0.30}$ -1.17 $^{+0.09}$	1.17 $^{+0.09}$ -0.09	104 $^{+15}$ -15	86 $^{+16}$ -16	5.78 $^{+1.27}$ -0.94	10 $^{-6}$ -6	4.60 $^{+0.33}$ -0.33	-1.06 $^{+0.15}$ -0.15	-3.88 $^{+0.09}$ -0.09	79 $^{+8}$ -8	5.93 $^{+1.36}$ -0.91	-0.7	2.6	1.9	
4.502~5.251	94.07	3.83 $^{+0.12}$ -1.30 $^{+0.05}$	1.30 $^{+0.05}$ -0.05	115 $^{+10}$ -10	81 $^{+9}$ -9	4.22 $^{+0.45}$ -0.36	10 $^{-6}$ -6	3.79 $^{+0.12}$ -0.12	-1.26 $^{+0.07}$ -0.06	-3.76 $^{+0.92}$ -0.92	77 $^{+4}$ -4	4.41 $^{+0.49}$ -0.33	-2.4	2.9	2.0	
5.251~5.625	51.77	2.84 $^{+0.16}$ -1.27 $^{+0.10}$	1.27 $^{+0.10}$ -0.10	87 $^{+14}$ -15	64 $^{+14}$ -14	2.62 $^{+0.60}$ -0.41	10 $^{-6}$ -6	2.79 $^{+0.16}$ -0.17	-1.16 $^{+0.14}$ -0.14	-4.04 $^{+1.23}$ -1.90	59 $^{+5}$ -5	2.70 $^{+0.35}$ -0.29	-3.0	2.4	1.6	
5.625~6.472	44.93	1.69 $^{+0.09}$ -1.49 $^{+0.09}$	1.22 $^{+24}$ -25	62 $^{+16}$ -17	1.49 $^{+0.28}$ -0.20	10 $^{-6}$ -6	1.68 $^{+0.09}$ -0.09	-1.45 $^{+0.11}$ -0.11	-5.43 $^{+1.74}$ -1.76	60 $^{+5}$ -5	1.50 $^{+0.12}$ -0.12	-1.2	2.4	3.3		
6.472~7.454	34.35	1.16 $^{+0.08}$ -1.32 $^{+0.14}$	1.32 $^{+17}$ -17	52 $^{+16}$ -16	0.90 $^{+0.26}$ -0.16	0.90 $^{+0.16}$ -0.16	10 $^{-6}$ -6	1.14 $^{+0.08}$ -0.08	-1.23 $^{+0.16}$ -0.17	-5.17 $^{+1.93}$ -1.89	49 $^{+4}$ -4	0.90 $^{+0.11}$ -0.09	-1.1	1.8	2.9	

Note—All columns are the same as Table A2 but for GRB 110301214.

Table A11. Time-resolved Spectral Fit Results of GRB 110625881

$t_{\text{start}} \sim t_{\text{stop}}$	S	Cutoff Power-Law Fitting						Band Fitting						Difference	
		K	α	E_c	E_p	F	K	α	β	E_p	F	ΔDIC	$p_{\text{DIC}}^{\text{CPL}}$	$p_{\text{DIC}}^{\text{Band}}$	
(1)	(2)	(3)	(4)	(5)	(6)	(7)	(8)	(9)	(10)	(11)	(12)	(13)	(14)	(15)	
Pulse 1															
-0.917~3.056	20.65	0.15+0.02 -0.99+0.10 250+61 253+67 0.56+0.30 × 10 ⁻⁶	0.14+0.02 -0.97+0.11 6.16+2.58 237+37 0.59+0.20 × 10 ⁻⁶	0.21+0.04 -0.40+0.11 6.31+2.50 484+52 6.96+3.37 × 10 ⁻⁶	0.8	1.2	1.4	2.4							
3.056~4.045	26.24	0.11+0.02 -0.25+0.12 160+22 280+43 1.90+1.24 × 10 ⁻⁶	0.10+0.02 -0.22+0.13 6.07+2.68 272+21 1.97+0.99 × 10 ⁻⁶	0.26+0.05 -0.16+0.12 5.82+2.55 412+37 12.23+6.16 × 10 ⁻⁶	-0.2	1.6	1.6	1.8							
4.045~4.967	36.11	0.11+0.02 -0.03+0.09 154+13 303+29 3.55+1.70 × 10 ⁻⁶	0.11+0.02 -0.02+0.09 6.33+2.38 298+14 3.75+1.17 × 10 ⁻⁶	0.22+0.05 -0.11+0.02 6.33+2.46 298+14 3.75+0.90 × 10 ⁻⁶	0.8	1.9	2.6								
Pulse 2															
10.229~10.436	23.41	0.21+0.04 -0.40+0.11 308+52 493+90 6.88+5.01 × 10 ⁻⁶	0.21+0.04 -0.40+0.11 6.31+2.50 484+52 6.96+3.37 × 10 ⁻⁶	0.21+0.04 -0.40+0.11 6.31+2.50 484+52 6.96+3.37 × 10 ⁻⁶	0.8	1.2	2.1								
10.436~10.553	28.72	0.27+0.05 -0.19+0.10 235+50 426+59 11.65+7.04 × 10 ⁻⁶	0.26+0.05 -0.16+0.12 5.82+2.55 412+37 12.23+6.16 × 10 ⁻⁶	0.26+0.05 -0.16+0.12 5.82+2.55 412+37 12.23+6.16 × 10 ⁻⁶	-0.2	1.6	1.6	1.8							
10.553~11.203	88.13	0.60+0.03 -0.33+0.04 195+9 325+16 12.33+1.64 × 10 ⁻⁶	0.55+0.04 -0.24+0.05 6.28+2.32 292+12 14.56+2.17 × 10 ⁻⁶	0.55+0.04 -0.24+0.05 6.28+2.32 292+12 14.56+2.17 × 10 ⁻⁶	-13.9	2.9	3.9								
11.203~11.671	55.71	0.67+0.05 -0.40+0.06 130+9 208+17 5.70+1.33 × 10 ⁻⁶	0.63+0.05 -0.30+0.07 2.87+2.27 187+10 6.90+1.28 × 10 ⁻⁶	0.63+0.05 -0.30+0.07 2.87+2.27 187+10 6.90+1.28 × 10 ⁻⁶	-11.7	2.8	3.8								
11.671~12.075	33.76	0.62+0.06 -0.48+0.10 91+10 138+18 2.47+0.96 × 10 ⁻⁶	0.61+0.07 -0.44+0.12 5.27+2.18 134+9 2.56+0.51 × 10 ⁻⁶	0.61+0.07 -0.44+0.12 5.27+2.18 134+9 2.56+0.51 × 10 ⁻⁶	-1.5	2.5	2.0								
12.075~12.817	32.99	0.69+0.06 -0.86+0.09 101+13 115+18 1.41+0.42 × 10 ⁻⁶	0.69+0.06 -0.85+0.09 6.69+2.23 113+7 1.43+0.26 × 10 ⁻⁶	0.69+0.06 -0.85+0.09 6.69+2.23 113+7 1.43+0.26 × 10 ⁻⁶	0.6	2.6	3.1								
12.817~15.034	38.80	0.57+0.03 -1.03+0.08 107+13 103+16 0.90+0.19 × 10 ⁻⁶	0.56+0.04 -0.99+0.10 5.63+2.77 108+8 0.92+0.17 × 10 ⁻⁶	0.56+0.04 -0.99+0.10 5.63+2.77 108+8 0.92+0.17 × 10 ⁻⁶	-0.4	2.6	2.5								
16.261~16.980	20.04	0.53+0.06 -1.23+0.13 213+55 213+67 164+60 0.95+0.54 × 10 ⁻⁶	0.51+0.06 -1.20+0.14 5.97+2.77 148+28 0.96+0.33 × 10 ⁻⁶	0.51+0.06 -1.20+0.14 5.97+2.77 148+28 0.96+0.33 × 10 ⁻⁶	1.6	0.6	2.4								
Pulse 3															
20.848~21.396	22.54	0.58+0.06 -0.81+0.14 91+17 108+24 1.17+0.54 × 10 ⁻⁶	0.57+0.07 -0.77+0.15 5.84+2.60 103+9 1.14+0.33 × 10 ⁻⁶	0.57+0.07 -0.77+0.15 5.84+2.60 103+9 1.14+0.33 × 10 ⁻⁶	0.5	1.9	2.7								
21.396~22.262	45.82	0.86+0.05 -0.95+0.07 139+15 146+19 2.13+0.50 × 10 ⁻⁶	0.86+0.05 -0.94+0.07 6.12+2.54 144+9 2.13+0.33 × 10 ⁻⁶	0.86+0.05 -0.94+0.07 6.12+2.54 144+9 2.13+0.33 × 10 ⁻⁶	0.4	2.7	3.0								
22.262~23.251	65.14	0.97+0.05 -0.73+0.05 122+8 155+12 3.28+0.42 × 10 ⁻⁶	0.91+0.05 -0.60+0.09 1.03+0.61 134+11 4.00+0.91 × 10 ⁻⁶	0.91+0.05 -0.60+0.09 1.03+0.61 134+11 4.00+0.91 × 10 ⁻⁶	-12.6	2.9	2.0								
23.251~23.744	76.45	1.25+0.06 -0.71+0.04 210+14 271+20 8.94+1.45 × 10 ⁻⁶	1.17+0.07 -0.63+0.06 2.68+0.28 233+17 11.01+2.28 × 10 ⁻⁶	1.17+0.07 -0.63+0.06 2.68+0.28 233+17 11.01+2.28 × 10 ⁻⁶	-12.0	2.9	3.2								
23.744~24.916	154.00	2.09+0.05 -0.76+0.02 196+7 243+9 12.06+0.94 × 10 ⁻⁶	1.83+0.05 -0.56+0.03 2.36+0.05 181+6 16.04+1.47 × 10 ⁻⁶	1.83+0.05 -0.56+0.03 2.36+0.05 181+6 16.04+1.47 × 10 ⁻⁶	-109.4	3.0	4.0								
24.916~25.171	54.73	2.13+0.13 -0.94+0.06 155+17 165+20 6.00+1.19 × 10 ⁻⁶	2.12+0.13 -0.92+0.07 5.77+2.67 160+11 6.14+0.16 × 10 ⁻⁶	2.12+0.13 -0.92+0.07 5.77+2.67 160+11 6.14+0.16 × 10 ⁻⁶	-0.6	2.8	2.5								
25.171~25.565	55.30	1.59+0.09 -0.83+0.06 116+10 135+14 4.08+0.81 × 10 ⁻⁶	1.55+0.10 -0.76+0.09 3.86+1.21 126+9 4.55+0.93 × 10 ⁻⁶	1.55+0.10 -0.76+0.09 3.86+1.21 126+9 4.55+0.93 × 10 ⁻⁶	-6.7	2.8	3.3								
25.565~26.069	44.24	1.28+0.08 -0.97+0.08 117+14 121+18 2.50+0.64 × 10 ⁻⁶	1.25+0.09 -0.88+0.13 4.76+2.24 110+12 2.70+0.55 × 10 ⁻⁶	1.25+0.09 -0.88+0.13 4.76+2.24 110+12 2.70+0.55 × 10 ⁻⁶	-4.1	2.7	2.2								
Pulse 4															
26.069~27.101	49.89	1.04+0.05 -1.18+0.06 210+29 172+27 2.25+0.46 × 10 ⁻⁶	0.95+0.08 -0.89+0.24 2.94+1.08 116+43 3.03+1.99 × 10 ⁻⁶	0.95+0.08 -0.89+0.24 2.94+1.08 116+43 3.03+1.99 × 10 ⁻⁶	-32.8	2.7	-23.0								
27.101~27.422	38.07	0.88+0.08 -0.84+0.08 179+25 207+32 3.61+1.16 × 10 ⁻⁶	0.87+0.08 -0.83+0.08 6.28+2.53 203+16 3.63+0.54 × 10 ⁻⁶	0.87+0.08 -0.83+0.08 6.28+2.53 203+16 3.63+0.54 × 10 ⁻⁶	0.2	2.6	2.9								
27.422~28.201	41.61	0.83+0.06 -0.95+0.07 147+17 155+21 2.14+0.50 × 10 ⁻⁶	0.82+0.06 -0.94+0.07 6.62+2.32 152+10 2.12+0.33 × 10 ⁻⁶	0.82+0.06 -0.94+0.07 6.62+2.32 152+10 2.12+0.33 × 10 ⁻⁶	0.7	2.7	3.2								
28.201~28.406	32.02	0.97+0.10 -0.92+0.08 267+47 288+55 5.05+1.95 × 10 ⁻⁶	0.96+0.10 -0.91+0.08 6.02+2.70 279+33 5.06+1.58 × 10 ⁻⁶	0.96+0.10 -0.91+0.08 6.02+2.70 279+33 5.06+1.58 × 10 ⁻⁶	0.3	2.3	2.8								
28.406~28.678	51.00	0.94+0.07 -0.54+0.06 163+13 238+21 7.68+1.79 × 10 ⁻⁶	0.94+0.07 -0.54+0.06 6.83+2.10 235+11 7.69+1.24 × 10 ⁻⁶	0.94+0.07 -0.54+0.06 6.83+2.10 235+11 7.69+1.24 × 10 ⁻⁶	0.5	2.8	3.1								
28.678~29.059	28.48	0.98+0.08 -1.05+0.09 171+32 162+34 2.29+0.73 × 10 ⁻⁶	0.93+0.10 -0.90+0.21 4.14+1.97 134+32 2.71+1.68 × 10 ⁻⁶	0.93+0.10 -0.90+0.21 4.14+1.97 134+32 2.71+1.68 × 10 ⁻⁶	-7.9	2.3	-2.9								
29.059~29.289	30.30	0.92+0.10 -0.90+0.10 182+32 201+40 3.24+1.30 × 10 ⁻⁶	0.91+0.10 -0.89+0.10 5.65+2.67 194+21 3.43+0.73 × 10 ⁻⁶	0.91+0.10 -0.89+0.10 5.65+2.67 194+21 3.43+0.73 × 10 ⁻⁶	0.3	2.3	2.8								
29.289~29.771	27.08	0.95+0.09 -1.20+0.11 171+41 137+38 1.66+0.41 × 10 ⁻⁶	0.89+0.10 -0.87+0.34 3.49+1.38 183+21 2.04+0.83 × 10 ⁻⁶	0.89+0.10 -0.87+0.34 3.49+1.38 183+21 2.04+0.83 × 10 ⁻⁶	-18.7	1.6	-12.5								
29.771~30.629	21.68	0.65+0.06 -1.29+0.13 163+49 115+40 0.86+0.40 × 10 ⁻⁶	0.63+0.06 -1.24+0.14 5.94+2.70 104+14 0.89+0.23 × 10 ⁻⁶	0.63+0.06 -1.24+0.14 5.94+2.70 104+14 0.89+0.23 × 10 ⁻⁶	1.6	0.9	2.8								

Note—All columns are the same as Table A2 but for GRB 110625881.

Table A12. Time-resolved Spectral Fit Results of GRB 120129580

$t_{\text{start}} \sim t_{\text{stop}}$	S	Cutoff Power-Law Fitting				Band Fitting				Difference				
		K	α	E_c	E_p	F	K	α	β	E_p	F	ΔDIC	$p^{\text{CPL}}_{\text{DIC}}$	$p^{\text{Band}}_{\text{DIC}}$
(1)	(2)	(3)	(4)	(5)	(6)	(7)	(8)	(9)	(10)	(11)	(12)	(13)	(14)	(15)
Pulse 1														
0.066~0.676	46.41	$1.02^{+0.09}_{-0.11}$	$-0.75^{+0.11}_{-0.11}$	96^{+14}_{-14}	120^{+20}_{-20}	$2.44^{+0.90}_{-0.59} \times 10^{-6}$	$0.97^{+0.08}_{-0.08}$	$-0.47^{+0.13}_{-0.13}$	$-2.55^{+0.31}_{-0.31}$	90^{+10}_{-10}	$3.35^{+1.04}_{-0.79} \times 10^{-6}$	-12.2	2.5	2.0
0.676~0.812	30.71	$1.60^{+0.24}_{-0.24}$	$-0.84^{+0.19}_{-0.19}$	113^{+30}_{-32}	131^{+41}_{-43}	$3.56^{+3.15}_{-1.36} \times 10^{-6}$	$1.52^{+0.21}_{-0.21}$	$-0.68^{+0.23}_{-0.23}$	$-4.16^{+1.85}_{-1.85}$	107^{+18}_{-19}	$4.03^{+2.49}_{-2.28} \times 10^{-6}$	-3.5	0.3	0.3
0.812~1.070	51.73	$1.89^{+0.17}_{-0.17}$	$-0.74^{+0.10}_{-0.10}$	103^{+14}_{-14}	130^{+20}_{-20}	$5.04^{+1.80}_{-1.25} \times 10^{-6}$	$1.77^{+0.14}_{-0.15}$	$-0.45^{+0.12}_{-0.12}$	$-2.56^{+0.28}_{-0.28}$	96^{+9}_{-10}	$6.80^{+1.97}_{-1.61} \times 10^{-6}$	-11.2	2.6	2.1
1.070~1.209	68.40	$1.98^{+0.18}_{-0.18}$	$-0.60^{+0.06}_{-0.06}$	222^{+23}_{-23}	311^{+35}_{-35}	$21.04^{+5.93}_{-4.94} \times 10^{-6}$	$1.89^{+0.19}_{-0.19}$	$-0.55^{+0.08}_{-0.08}$	$-3.54^{+1.15}_{-1.15}$	281^{+28}_{-29}	$24.66^{+9.16}_{-5.90} \times 10^{-6}$	-7.3	2.7	0.1
1.209~1.310	76.56	$2.72^{+0.23}_{-0.24}$	$-0.66^{+0.05}_{-0.05}$	315^{+33}_{-33}	422^{+47}_{-47}	$38.49^{+11.21}_{-7.94} \times 10^{-6}$	$2.51^{+0.26}_{-0.26}$	$-0.58^{+0.08}_{-0.08}$	$-3.23^{+0.25}_{-0.25}$	361^{+43}_{-40}	$43.84^{+16.15}_{-10.55} \times 10^{-6}$	-9.8	2.7	-0.2
1.310~1.665	170.07	$3.16^{+0.12}_{-0.13}$	$-0.56^{+0.02}_{-0.02}$	267^{+10}_{-10}	384^{+16}_{-16}	$51.08^{+5.86}_{-5.10} \times 10^{-6}$	$3.12^{+0.14}_{-0.14}$	$-0.54^{+0.03}_{-0.03}$	$-5.17^{+2.00}_{-2.00}$	375^{+15}_{-16}	$52.65^{+6.96}_{-5.67} \times 10^{-6}$	-3.4	2.9	0.9
1.665~1.843	109.53	$3.23^{+0.20}_{-0.20}$	$-0.63^{+0.04}_{-0.04}$	252^{+17}_{-17}	345^{+26}_{-26}	$38.41^{+7.11}_{-5.50} \times 10^{-6}$	$2.96^{+0.21}_{-0.21}$	$-0.52^{+0.06}_{-0.06}$	$-2.77^{+0.25}_{-0.25}$	295^{+20}_{-20}	$45.13^{+9.28}_{-7.66} \times 10^{-6}$	-12.9	2.9	3.5
1.843~2.002	81.93	$2.82^{+0.21}_{-0.21}$	$-0.64^{+0.06}_{-0.06}$	174^{+15}_{-15}	237^{+23}_{-23}	$19.82^{+4.76}_{-3.86} \times 10^{-6}$	$2.79^{+0.21}_{-0.21}$	$-0.62^{+0.06}_{-0.06}$	$-5.78^{+2.47}_{-2.47}$	232^{+14}_{-14}	$20.13^{+4.34}_{-3.24} \times 10^{-6}$	-0.4	2.8	2.7
2.002~2.151	63.39	$2.65^{+0.23}_{-0.22}$	$-0.80^{+0.07}_{-0.07}$	201^{+26}_{-26}	241^{+34}_{-34}	$13.79^{+4.35}_{-2.92} \times 10^{-6}$	$2.60^{+0.23}_{-0.23}$	$-0.78^{+0.08}_{-0.08}$	$-5.50^{+2.54}_{-2.54}$	232^{+21}_{-21}	$14.36^{+3.50}_{-2.68} \times 10^{-6}$	-0.6	2.7	2.6
2.151~2.306	52.74	$2.63^{+0.25}_{-0.25}$	$-1.00^{+0.09}_{-0.09}$	241^{+57}_{-52}	241^{+57}_{-57}	$9.56^{+4.19}_{-2.60} \times 10^{-6}$	$2.21^{+0.25}_{-0.25}$	$-0.64^{+0.17}_{-0.17}$	$-2.21^{+0.16}_{-0.16}$	$13.99^{+7.38}_{-3.93} \times 10^{-6}$	-15.9	1.9	2.3	
Pulse 2														
2.306~2.729	58.68	$1.75^{+0.13}_{-0.13}$	$-1.08^{+0.07}_{-0.07}$	272^{+47}_{-48}	250^{+47}_{-48}	$6.01^{+1.83}_{-1.28} \times 10^{-6}$	$1.72^{+0.13}_{-0.13}$	$-1.05^{+0.07}_{-0.08}$	$-5.00^{+0.25}_{-0.25}$	236^{+32}_{-31}	$6.43^{+1.90}_{-1.26} \times 10^{-6}$	-1.4	2.5	2.1
2.729~2.822	38.80	$0.90^{+0.14}_{-0.14}$	$-0.59^{+0.09}_{-0.08}$	402^{+66}_{-66}	567^{+100}_{-99}	$22.71^{+13.67}_{-7.90} \times 10^{-6}$	$0.89^{+0.14}_{-0.14}$	$-0.58^{+0.09}_{-0.09}$	$-6.13^{+2.57}_{-2.57}$	553^{+67}_{-67}	$22.43^{+9.31}_{-6.05} \times 10^{-6}$	0.2	2.2	2.6
2.822~3.327	110.53	$1.35^{+0.07}_{-0.07}$	$-0.59^{+0.03}_{-0.03}$	308^{+18}_{-18}	434^{+27}_{-27}	$23.96^{+3.69}_{-3.32} \times 10^{-6}$	$1.35^{+0.07}_{-0.07}$	$-0.58^{+0.03}_{-0.03}$	$-6.60^{+2.37}_{-2.37}$	430^{+17}_{-17}	$24.14^{+3.01}_{-2.54} \times 10^{-6}$	0.2	2.9	3.0
3.327~3.455	46.67	$1.38^{+0.16}_{-0.16}$	$-0.68^{+0.08}_{-0.08}$	244^{+36}_{-36}	322^{+52}_{-52}	$13.18^{+5.56}_{-3.54} \times 10^{-6}$	$1.37^{+0.16}_{-0.16}$	$-0.67^{+0.09}_{-0.09}$	$-6.27^{+2.59}_{-2.59}$	315^{+30}_{-30}	$13.53^{+3.89}_{-3.02} \times 10^{-6}$	0.3	2.5	2.9
3.455~3.561	33.47	$1.76^{+0.23}_{-0.23}$	$-1.10^{+0.10}_{-0.10}$	644^{+227}_{-241}	579^{+214}_{-227}	$11.04^{+7.30}_{-3.93} \times 10^{-6}$	$1.62^{+0.24}_{-0.24}$	$-1.00^{+0.13}_{-0.14}$	$-4.16^{+2.09}_{-2.09}$	423^{+140}_{-142}	$12.34^{+8.55}_{-4.99} \times 10^{-6}$	-5.8	0.8	-1.7
3.561~3.697	26.67	$1.99^{+0.27}_{-0.26}$	$-1.29^{+0.15}_{-0.15}$	237^{+85}_{-94}	168^{+70}_{-75}	$3.31^{+2.26}_{-1.08} \times 10^{-6}$	$1.92^{+0.26}_{-0.26}$	$-1.06^{+0.12}_{-0.12}$	$-5.72^{+2.53}_{-2.53}$	132^{+39}_{-32}	$3.42^{+2.53}_{-0.95} \times 10^{-6}$	-8.9	0.7	-7.6
3.697~4.000	21.85	$1.27^{+0.15}_{-0.15}$	$-1.54^{+0.14}_{-0.14}$	474^{+319}_{-268}	218^{+161}_{-138}	$1.92^{+1.24}_{-0.62} \times 10^{-6}$	$1.22^{+0.16}_{-0.16}$	$-1.44^{+0.19}_{-0.19}$	$-5.50^{+2.88}_{-2.95}$	151^{+65}_{-55}	$1.84^{+0.79}_{-0.44} \times 10^{-6}$	0.3	0.2	1.0

Note—All columns are the same as Table A2 but for GRB 120129580.

Table A13. Time-resolved Spectral Fit Results of GRB 120328268

$t_{\text{start}} \sim t_{\text{stop}}$	S	Cutoff Power-Law Fitting						Band Fitting						Difference		
		K	α	E_c	E_p	F	K	α	β	E_p	F	ΔDIC	$p_{\text{DIC}}^{\text{CPL}}$	$p_{\text{DIC}}^{\text{Band}}$		
(1)	(2)	(3)	(4)	(5)	(6)	(7)	(8)	(9)	(10)	(11)	(12)	(13)	(14)	(15)		
Pulse 1																
2.602~4.487	29.97	0.15 $^{+0.01}_{-0.01}$	-0.74 $^{+0.06}_{-0.06}$	51.1 $^{+96}_{-97}$	6.44 $^{+125}_{-126}$	2.97 $^{+1.36}_{-0.86}$	10^{-6}	0.14 $^{+0.02}_{-0.02}$	-0.70 $^{+0.08}_{-0.08}$	-4.22 $^{+2.06}_{-2.06}$	573 $^{+103}_{-108}$	3.29 $^{+1.76}_{-1.04}$	$\times 10^{-6}$	-5.4	2.2	-0.3
4.487~4.817	28.87	0.36 $^{+0.04}_{-0.04}$	-0.76 $^{+0.08}_{-0.07}$	54.1 $^{+124}_{-130}$	6.71 $^{+1.60}_{-1.65}$	6.95 $^{+3.83}_{-2.31}$	$\times 10^{-6}$	0.34 $^{+0.04}_{-0.04}$	-0.73 $^{+0.09}_{-0.09}$	-5.59 $^{+2.81}_{-2.81}$	6.16 $^{+1.23}_{-1.24}$	7.14 $^{+3.53}_{-2.17}$	$\times 10^{-6}$	-0.5	1.8	1.8
4.817~5.993	69.84	0.46 $^{+0.02}_{-0.02}$	-0.69 $^{+0.03}_{-0.03}$	45.3 $^{+38}_{-38}$	59.3 $^{+52}_{-52}$	9.78 $^{+1.79}_{-1.50}$	$\times 10^{-6}$	0.40 $^{+0.02}_{-0.02}$	-0.55 $^{+0.05}_{-0.05}$	-2.11 $^{+0.08}_{-0.08}$	424 $^{+38}_{-37}$	13.96 $^{+2.97}_{-2.64}$	$\times 10^{-6}$	-30.0	2.8	3.2
5.993~8.058	106.36	0.71 $^{+0.02}_{-0.02}$	-0.65 $^{+0.03}_{-0.03}$	21.2 $^{+10}_{-10}$	286 $^{+15}_{-15}$	6.19 $^{+0.69}_{-0.62}$	$\times 10^{-6}$	0.63 $^{+0.02}_{-0.02}$	-0.47 $^{+0.04}_{-0.04}$	-2.13 $^{+0.06}_{-0.06}$	211 $^{+1.06}_{-1.06}$	10.02 $^{+1.32}_{-1.11}$	$\times 10^{-6}$	-75.0	2.9	3.9
8.058~8.770	47.75	0.71 $^{+0.04}_{-0.04}$	-0.88 $^{+0.05}_{-0.05}$	289 $^{+31}_{-31}$	268 $^{+37}_{-37}$	3.74 $^{+0.99}_{-0.72}$	$\times 10^{-6}$	0.68 $^{+0.05}_{-0.05}$	-0.80 $^{+0.09}_{-0.09}$	-3.28 $^{+1.17}_{-1.67}$	228 $^{+36}_{-36}$	4.89 $^{+2.08}_{-1.56}$	$\times 10^{-6}$	-9.3	2.6	-1.8
8.770~10.470	61.39	0.69 $^{+0.03}_{-0.03}$	-0.95 $^{+0.05}_{-0.05}$	20.2 $^{+21}_{-21}$	21.2 $^{+24}_{-24}$	2.48 $^{+0.46}_{-0.34}$	$\times 10^{-6}$	0.62 $^{+0.03}_{-0.03}$	-0.70 $^{+0.09}_{-0.09}$	-2.05 $^{+0.04}_{-0.04}$	139 $^{+13}_{-13}$	4.30 $^{+6.98}_{-6.98}$	$\times 10^{-6}$	-30.5	2.8	2.7
10.470~15.658	70.99	0.45 $^{+0.02}_{-0.02}$	-0.89 $^{+0.04}_{-0.03}$	17.8 $^{+13}_{-13}$	19.7 $^{+16}_{-16}$	1.65 $^{+0.23}_{-0.19}$	$\times 10^{-6}$	0.42 $^{+0.02}_{-0.02}$	-0.75 $^{+0.06}_{-0.06}$	-2.20 $^{+0.11}_{-0.10}$	156 $^{+12}_{-12}$	2.60 $^{+0.52}_{-0.45}$	$\times 10^{-6}$	-15.8	2.9	3.8
Pulse 2																
15.658~17.519	29.19	0.37 $^{+0.03}_{-0.03}$	-1.21 $^{+0.08}_{-0.08}$	40.4 $^{+124}_{-129}$	31.9 $^{+103}_{-107}$	1.25 $^{+0.56}_{-0.34}$	$\times 10^{-6}$	0.37 $^{+0.03}_{-0.03}$	-1.19 $^{+0.08}_{-0.08}$	-5.66 $^{+2.83}_{-2.90}$	297 $^{+68}_{-72}$	1.27 $^{+0.47}_{-0.30}$	$\times 10^{-6}$	0.4	1.0	1.7
17.519~18.082	23.89	0.44 $^{+0.04}_{-0.04}$	-1.09 $^{+0.08}_{-0.08}$	66.8 $^{+234}_{-246}$	60.8 $^{+219}_{-230}$	3.09 $^{+1.99}_{-1.97}$	$\times 10^{-6}$	0.43 $^{+0.05}_{-0.05}$	-1.07 $^{+0.09}_{-0.09}$	-5.30 $^{+2.89}_{-2.89}$	552 $^{+154}_{-170}$	3.26 $^{+1.77}_{-0.98}$	$\times 10^{-6}$	-0.5	0.8	1.0
18.082~18.618	33.01	0.50 $^{+0.04}_{-0.04}$	-0.95 $^{+0.06}_{-0.06}$	49.1 $^{+102}_{-102}$	51.6 $^{+112}_{-113}$	4.40 $^{+1.84}_{-1.12}$	$\times 10^{-6}$	0.49 $^{+0.04}_{-0.04}$	-0.94 $^{+0.07}_{-0.07}$	-5.33 $^{+2.83}_{-3.08}$	493 $^{+85}_{-88}$	4.66 $^{+1.78}_{-1.08}$	$\times 10^{-6}$	-0.9	2.4	2.1
18.618~19.841	61.88	0.57 $^{+0.03}_{-0.03}$	-0.82 $^{+0.04}_{-0.04}$	32.8 $^{+34}_{-34}$	38.7 $^{+42}_{-42}$	5.09 $^{+1.07}_{-1.07}$	$\times 10^{-6}$	0.51 $^{+0.03}_{-0.03}$	-0.68 $^{+0.05}_{-0.05}$	-2.03 $^{+0.03}_{-0.03}$	275 $^{+22}_{-22}$	8.38 $^{+1.56}_{-1.20}$	$\times 10^{-6}$	-45.0	2.8	2.8
19.841~21.408	83.44	0.71 $^{+0.03}_{-0.03}$	-0.71 $^{+0.03}_{-0.03}$	19.4 $^{+12}_{-12}$	25.0 $^{+17}_{-17}$	4.68 $^{+0.62}_{-0.57}$	$\times 10^{-6}$	0.67 $^{+0.03}_{-0.03}$	-0.62 $^{+0.05}_{-0.05}$	-2.41 $^{+0.17}_{-0.17}$	213 $^{+14}_{-14}$	6.44 $^{+1.31}_{-1.00}$	$\times 10^{-6}$	-15.1	2.9	3.8
21.408~23.190	65.60	0.67 $^{+0.03}_{-0.03}$	-0.82 $^{+0.04}_{-0.04}$	16.1 $^{+13}_{-13}$	18.9 $^{+16}_{-16}$	2.58 $^{+0.41}_{-0.36}$	$\times 10^{-6}$	0.64 $^{+0.03}_{-0.03}$	-0.72 $^{+0.07}_{-0.07}$	-2.75 $^{+0.07}_{-0.07}$	163 $^{+15}_{-15}$	3.57 $^{+0.95}_{-0.79}$	$\times 10^{-6}$	-13.0	2.9	-0.6
23.190~24.011	36.58	0.72 $^{+0.03}_{-0.05}$	-1.05 $^{+0.05}_{-0.08}$	15.8 $^{+28}_{-28}$	15.0 $^{+29}_{-30}$	1.61 $^{+0.53}_{-0.36}$	$\times 10^{-6}$	0.71 $^{+0.05}_{-0.05}$	-1.00 $^{+0.10}_{-0.10}$	-4.90 $^{+2.52}_{-3.29}$	139 $^{+17}_{-18}$	1.72 $^{+0.63}_{-0.36}$	$\times 10^{-6}$	-2.1	2.3	1.6
Pulse 3																
24.011~26.546	36.85	0.46 $^{+0.03}_{-0.03}$	-1.20 $^{+0.07}_{-0.07}$	21.4 $^{+44}_{-43}$	17.1 $^{+38}_{-37}$	0.95 $^{+0.26}_{-0.18}$	$\times 10^{-6}$	0.46 $^{+0.03}_{-0.03}$	-1.19 $^{+0.07}_{-0.07}$	-5.78 $^{+2.83}_{-2.87}$	163 $^{+21}_{-21}$	0.98 $^{+0.19}_{-0.15}$	$\times 10^{-6}$	0.1	2.2	2.6
26.546~27.946	36.93	0.63 $^{+0.04}_{-0.04}$	-1.19 $^{+0.07}_{-0.08}$	19.1 $^{+38}_{-38}$	15.5 $^{+33}_{-34}$	1.22 $^{+0.34}_{-0.25}$	$\times 10^{-6}$	0.62 $^{+0.04}_{-0.04}$	-1.15 $^{+0.09}_{-0.10}$	-5.42 $^{+2.89}_{-2.95}$	143 $^{+21}_{-20}$	1.26 $^{+0.41}_{-0.21}$	$\times 10^{-6}$	-0.5	2.3	2.2
27.946~30.301	36.44	0.53 $^{+0.03}_{-0.03}$	-1.17 $^{+0.08}_{-0.08}$	14.2 $^{+24}_{-24}$	11.8 $^{+23}_{-23}$	0.83 $^{+0.22}_{-0.15}$	$\times 10^{-6}$	0.53 $^{+0.03}_{-0.03}$	-1.14 $^{+0.09}_{-0.10}$	-5.21 $^{+2.68}_{-2.68}$	111 $^{+13}_{-13}$	0.87 $^{+0.27}_{-0.13}$	$\times 10^{-6}$	-1.3	2.5	2.0
30.301~31.317	33.54	0.54 $^{+0.04}_{-0.04}$	-0.94 $^{+0.09}_{-0.09}$	13.6 $^{+22}_{-23}$	14.4 $^{+27}_{-27}$	1.29 $^{+0.43}_{-0.28}$	$\times 10^{-6}$	0.53 $^{+0.04}_{-0.04}$	-0.87 $^{+0.12}_{-0.12}$	-4.33 $^{+2.02}_{-2.02}$	131 $^{+16}_{-17}$	1.51 $^{+0.63}_{-0.36}$	$\times 10^{-6}$	-4.2	2.3	0.6
31.317~32.368	24.21	0.47 $^{-0.04}_{-0.04}$	-0.96 $^{+0.12}_{-0.12}$	10.2 $^{+19}_{-19}$	10.6 $^{+23}_{-23}$	0.79 $^{+0.33}_{-0.28}$	$\times 10^{-6}$	0.47 $^{+0.04}_{-0.04}$	-0.94 $^{+0.13}_{-0.12}$	-6.51 $^{+2.38}_{-2.38}$	102 $^{+10}_{-10}$	0.81 $^{+0.12}_{-0.16}$	$\times 10^{-6}$	1.0	2.2	3.1
32.368~35.661	27.56	0.40 $^{+0.03}_{-0.03}$	-1.47 $^{+0.10}_{-0.10}$	31.5 $^{+134}_{-135}$	16.7 $^{+78}_{-78}$	0.57 $^{+0.24}_{-0.24}$	$\times 10^{-6}$	0.40 $^{+0.03}_{-0.04}$	-1.07 $^{+0.12}_{-0.12}$	-3.65 $^{+1.62}_{-2.83}$	89 $^{+28}_{-29}$	0.69 $^{+0.41}_{-0.25}$	$\times 10^{-6}$	-59.9	-1.0	-57.8
35.661~40.000	15.91	0.25 $^{+0.02}_{-0.02}$	-1.63 $^{+0.11}_{-0.10}$	52.7 $^{+299}_{-299}$	195 $^{+140}_{-123}$	0.34 $^{+0.13}_{-0.09}$	$\times 10^{-6}$	0.25 $^{+0.02}_{-0.02}$	-1.50 $^{+0.14}_{-0.17}$	-5.40 $^{+2.98}_{-3.06}$	118 $^{+33}_{-37}$	0.33 $^{+0.12}_{-0.07}$	$\times 10^{-6}$	-0.9	0.4	0.1

Note—All columns are the same as Table A2 but for GRB 120328268.

Table A14. Time-resolved Spectral Fit Results of GRB 12071115

$t_{\text{start}} \sim t_{\text{stop}}$	S	Cutoff Power-Law Fitting						Band Fitting						Difference	
		K	α	E_c	E_p	F	K	α	β	E_p	F	ΔDIC	$p_{\text{DIC}}^{\text{CPL}}$	$p_{\text{DIC}}^{\text{Band}}$	
(1)	(2)	(3)	(4)	(5)	(6)	(7)	(8)	(9)	(10)	(11)	(12)	(13)	(14)	(15)	
Pulse 1															
63.488~64.961	20.65	0.15 $^{+0.02}_{-0.02}$	-0.86 $^{+0.06}_{-0.06}$	1729 $^{+324}_{-321}$	1971 $^{+383}_{-381}$	7.71 $^{+3.67}_{-2.51} \times 10^{-6}$	0.15 $^{+0.02}_{-0.02}$	-0.86 $^{+0.06}_{-0.06}$	-6.45 $^{+2.44}_{-2.42}$	1924 $^{+297}_{-183}$	7.63 $^{+2.98}_{-2.36} \times 10^{-6}$	-0.3	2.5	2.5	
64.961~67.130	37.39	0.30 $^{+0.02}_{-0.02}$	-0.95 $^{+0.03}_{-0.03}$	1679 $^{+324}_{-213}$	1763 $^{+65}_{-228}$	9.92 $^{+2.29}_{-1.86} \times 10^{-6}$	0.30 $^{+0.02}_{-0.02}$	-0.95 $^{+0.03}_{-0.03}$	-6.56 $^{+2.36}_{-2.31} \times 10^{-6}$	10.01 $^{+2.03}_{-1.62}$	0.2	2.9	3.0		
67.130~71.711	67.94	0.42 $^{+0.02}_{-0.02}$	-0.96 $^{+0.02}_{-0.02}$	1702 $^{+115}_{-117}$	1770 $^{+124}_{-126}$	13.40 $^{+1.82}_{-1.41} \times 10^{-6}$	0.42 $^{+0.02}_{-0.02}$	-0.96 $^{+0.02}_{-0.02}$	-6.64 $^{+2.27}_{-2.28}$	1757 $^{+99}_{-100}$	13.36 $^{+1.36}_{-1.32} \times 10^{-6}$	-0.0	3.0	3.0	
71.711~75.400	50.21	0.47 $^{+0.03}_{-0.03}$	-1.07 $^{+0.03}_{-0.03}$	1204 $^{+147}_{-142}$	1119 $^{+134}_{-140}$	6.68 $^{+1.34}_{-1.08} \times 10^{-6}$	0.47 $^{+0.03}_{-0.03}$	-1.07 $^{+0.03}_{-0.03}$	-6.69 $^{+2.21}_{-2.28}$	1111 $^{+109}_{-109}$	6.69 $^{+1.04}_{-0.83} \times 10^{-6}$	0.4	2.9	3.1	
75.400~75.693	21.66	0.57 $^{+0.09}_{-0.09}$	-1.00 $^{+0.08}_{-0.08}$	816 $^{+214}_{-224}$	7.00 $^{+4.15}_{-2.43} \times 10^{-6}$	0.57 $^{+0.09}_{-0.09}$	-0.99 $^{+0.08}_{-0.08}$	-6.68 $^{+2.35}_{-2.31} \times 10^{-6}$	7.86 $^{+152}_{-154}$	7.25 $^{+3.13}_{-2.13} \times 10^{-6}$	0.6	2.1	2.7		
75.693~81.191	35.69	0.31 $^{+0.02}_{-0.02}$	-1.17 $^{+0.03}_{-0.03}$	1941 $^{+411}_{-409}$	1611 $^{+346}_{-345}$	4.24 $^{+1.13}_{-0.93} \times 10^{-6}$	0.31 $^{+0.02}_{-0.02}$	-1.17 $^{+0.04}_{-0.04}$	-5.64 $^{+2.64}_{-2.82}$	1545 $^{+297}_{-289}$	4.23 $^{+1.01}_{-0.79} \times 10^{-6}$	-0.7	2.7	2.5	
81.191~82.871	27.91	0.31 $^{+0.03}_{-0.03}$	-1.02 $^{+0.05}_{-0.05}$	1236 $^{+174}_{-172}$	5.32 $^{+1.99}_{-1.77} \times 10^{-6}$	0.30 $^{+0.03}_{-0.03}$	-1.02 $^{+0.05}_{-0.05}$	-6.47 $^{+2.24}_{-2.25}$	1168 $^{+200}_{-202}$	5.23 $^{+1.67}_{-1.44} \times 10^{-6}$	0.5	2.5	2.9		
82.871~85.341	21.23	0.24 $^{+0.03}_{-0.03}$	-1.09 $^{+0.07}_{-0.07}$	1070 $^{+361}_{-359}$	2.65 $^{+1.56}_{-0.87} \times 10^{-6}$	0.24 $^{+0.03}_{-0.03}$	-1.08 $^{+0.07}_{-0.07}$	-6.28 $^{+2.60}_{-2.57}$	911 $^{+230}_{-238}$	2.65 $^{+1.22}_{-0.75} \times 10^{-6}$	0.7	1.0	1.8		
Pulse 2															
85.341~90.264	58.68	0.39 $^{+0.02}_{-0.02}$	-0.99 $^{+0.02}_{-0.02}$	1198 $^{+116}_{-115}$	1210 $^{+119}_{-119}$	8.05 $^{+1.20}_{-1.18} \times 10^{-6}$	0.39 $^{+0.02}_{-0.02}$	-0.98 $^{+0.02}_{-0.02}$	-6.90 $^{+2.15}_{-2.13}$	1210 $^{+97}_{-98}$	8.00 $^{+1.04}_{-0.94} \times 10^{-6}$	0.4	2.8	3.0	
90.264~93.305	56.59	0.51 $^{+0.03}_{-0.03}$	-1.03 $^{+0.02}_{-0.02}$	1396 $^{+157}_{-158}$	1354 $^{+155}_{-156}$	9.82 $^{+1.78}_{-1.44} \times 10^{-6}$	0.51 $^{+0.03}_{-0.03}$	-1.03 $^{+0.03}_{-0.02}$	-5.97 $^{+2.47}_{-2.70}$	1340 $^{+125}_{-127}$	9.93 $^{+1.48}_{-1.34} \times 10^{-6}$	-0.8	2.9	2.5	
93.305~93.390	20.72	1.01 $^{+0.15}_{-0.15}$	-1.01 $^{+0.05}_{-0.05}$	3309 $^{+706}_{-713}$	3276 $^{+718}_{-725}$	45.91 $^{+13.37}_{-13.37} \times 10^{-6}$	0.99 $^{+0.15}_{-0.15}$	-1.01 $^{+0.06}_{-0.06}$	-5.76 $^{+2.74}_{-2.84}$	3074 $^{+594}_{-603}$	44.97 $^{+17.14}_{-13.43} \times 10^{-6}$	-0.1	2.8	2.8	
93.390~94.046	24.78	0.46 $^{+0.05}_{-0.05}$	-1.05 $^{+0.05}_{-0.05}$	2018 $^{+433}_{-433}$	1917 $^{+424}_{-423}$	11.29 $^{+3.30}_{-3.19} \times 10^{-6}$	0.45 $^{+0.05}_{-0.05}$	-1.04 $^{+0.05}_{-0.05}$	-6.05 $^{+2.56}_{-2.61}$	1894 $^{+346}_{-343}$	11.61 $^{+3.41}_{-2.64} \times 10^{-6}$	-0.1	2.7	2.7	
94.128~94.940	31.95	0.42 $^{+0.04}_{-0.04}$	-0.96 $^{+0.04}_{-0.04}$	1839 $^{+287}_{-286}$	1913 $^{+307}_{-308}$	14.19 $^{+4.46}_{-3.05} \times 10^{-6}$	0.41 $^{+0.04}_{-0.04}$	-0.96 $^{+0.04}_{-0.04}$	-5.96 $^{+2.54}_{-2.73}$	1866 $^{+242}_{-242}$	14.47 $^{+3.82}_{-3.82} \times 10^{-6}$	-0.7	2.8	2.5	
94.940~94.989	22.35	1.20 $^{+0.18}_{-0.18}$	-1.00 $^{+0.05}_{-0.05}$	4891 $^{+1274}_{-1300}$	4891 $^{+1298}_{-1323}$	75.11 $^{+36.05}_{-22.47} \times 10^{-6}$	0.80 $^{+0.17}_{-0.18}$	-0.79 $^{+0.10}_{-0.10}$	-2.12 $^{+0.10}_{-0.09}$	1844 $^{+534}_{-530}$	56.17 $^{+21.97}_{-21.29} \times 10^{-6}$	-21.7	2.5	0.8	
94.990~95.532	29.78	0.43 $^{+0.05}_{-0.05}$	-0.89 $^{+0.05}_{-0.05}$	1723 $^{+72}_{-72}$	19.01 $^{+7.72}_{-7.72} \times 10^{-6}$	0.39 $^{+0.05}_{-0.05}$	-0.83 $^{+0.06}_{-0.06}$	-2.37 $^{+0.22}_{-0.22}$	1461 $^{+251}_{-248}$	19.14 $^{+7.54}_{-4.94} \times 10^{-6}$	-16.2	2.5	3.4		
95.532~95.742	28.10	0.84 $^{+0.09}_{-0.09}$	-1.05 $^{+0.04}_{-0.04}$	4455 $^{+912}_{-909}$	4232 $^{+85}_{-85}$	40.29 $^{+13.66}_{-9.63} \times 10^{-6}$	0.69 $^{+0.09}_{-0.09}$	-0.95 $^{+0.05}_{-0.05}$	-2.19 $^{+0.14}_{-0.13}$	2352 $^{+479}_{-488}$	35.14 $^{+13.62}_{-12.87} \times 10^{-6}$	-18.2	2.8	3.0	
95.742~95.986	22.29	0.69 $^{+0.09}_{-0.09}$	-1.10 $^{+0.05}_{-0.05}$	3193 $^{+703}_{-717}$	2874 $^{+652}_{-665}$	19.56 $^{+8.43}_{-5.51} \times 10^{-6}$	0.68 $^{+0.09}_{-0.09}$	-1.10 $^{+0.05}_{-0.05}$	-6.27 $^{+2.43}_{-2.50}$	2806 $^{+491}_{-511}$	19.79 $^{+6.02}_{-4.84} \times 10^{-6}$	0.2	2.8	3.0	
95.986~99.201	53.71	0.34 $^{+0.02}_{-0.02}$	-0.93 $^{+0.02}_{-0.02}$	1686 $^{+135}_{-135}$	1804 $^{+148}_{-148}$	13.09 $^{+1.89}_{-1.83} \times 10^{-6}$	0.34 $^{+0.02}_{-0.02}$	-0.93 $^{+0.02}_{-0.02}$	-6.58 $^{+2.28}_{-2.35}$	1806 $^{+119}_{-119}$	13.04 $^{+1.61}_{-1.50} \times 10^{-6}$	0.0	2.9	3.0	
99.201~99.292	20.82	0.90 $^{+0.14}_{-0.14}$	-1.05 $^{+0.05}_{-0.05}$	4977 $^{+1046}_{-1038}$	45.02 $^{+19.13}_{-13.62} \times 10^{-6}$	0.89 $^{+0.14}_{-0.14} \times 10^{-6}$	0.10 $^{+0.05}_{-0.05}$	-1.05 $^{+0.05}_{-0.05}$	-6.20 $^{+2.57}_{-2.57}$	45.82 $^{+892}_{-887}$	45.36 $^{+18.28}_{-18.28} \times 10^{-6}$	0.5	2.8	3.1	
99.292~100.983	35.41	0.37 $^{+0.03}_{-0.03}$	-1.00 $^{+0.04}_{-0.04}$	1803 $^{+282}_{-284}$	1803 $^{+291}_{-293}$	10.37 $^{+2.93}_{-2.18} \times 10^{-6}$	0.37 $^{+0.03}_{-0.03}$	-0.99 $^{+0.04}_{-0.04}$	-5.29 $^{+2.45}_{-2.45}$	1712 $^{+259}_{-262}$	10.46 $^{+2.61}_{-2.22} \times 10^{-6}$	-1.9	2.8	1.9	
100.983~101.935	35.02	0.35 $^{+0.04}_{-0.04}$	-0.89 $^{+0.04}_{-0.04}$	1654 $^{+236}_{-237}$	1836 $^{+270}_{-271}$	14.98 $^{+4.75}_{-3.55} \times 10^{-6}$	0.34 $^{+0.04}_{-0.04}$	-0.87 $^{+0.04}_{-0.04}$	-3.68 $^{+1.08}_{-1.08}$	1039 $^{+204}_{-209}$	15.22 $^{+3.80}_{-3.30} \times 10^{-6}$	-6.5	2.8	1.3	
101.935~102.055	22.25	0.79 $^{+0.12}_{-0.12}$	-0.97 $^{+0.06}_{-0.06}$	2443 $^{+579}_{-579}$	2517 $^{+614}_{-622}$	32.83 $^{+17.76}_{-10.79} \times 10^{-6}$	0.70 $^{+0.14}_{-0.14}$	-0.90 $^{+0.09}_{-0.09}$	-4.33 $^{+2.00}_{-2.00}$	1910 $^{+651}_{-619}$	29.17 $^{+22.39}_{-17.17} \times 10^{-6}$	-6.6	2.6	-1.2	
102.055~103.840	43.49	0.45 $^{+0.03}_{-0.03}$	-0.99 $^{+0.04}_{-0.03}$	1236 $^{+172}_{-172}$	1248 $^{+172}_{-178}$	9.11 $^{+2.27}_{-1.72} \times 10^{-6}$	0.45 $^{+0.03}_{-0.03}$	-0.99 $^{+0.03}_{-0.03}$	-6.21 $^{+2.49}_{-2.57}$	1230 $^{+137}_{-139}$	9.25 $^{+1.82}_{-1.41} \times 10^{-6}$	-0.2	2.7	2.7	
103.840~104.759	24.45	0.57 $^{+0.07}_{-0.07}$	-1.22 $^{+0.07}_{-0.07}$	1415 $^{+648}_{-603}$	1104 $^{+515}_{-481}$	4.46 $^{+2.91}_{-1.48} \times 10^{-6}$	0.57 $^{+0.07}_{-0.07}$	-1.21 $^{+0.08}_{-0.08}$	-5.63 $^{+2.83}_{-2.83}$	1011 $^{+369}_{-360}$	4.54 $^{+2.33}_{-2.33} \times 10^{-6}$	0.1	0.2	0.6	
104.759~106.629	15.76	0.46 $^{+0.05}_{-0.05}$	-1.54 $^{+0.07}_{-0.07}$	2306 $^{+1427}_{-1358}$	1061 $^{+676}_{-650}$	1.50 $^{+0.79}_{-0.51} \times 10^{-6}$	0.47 $^{+0.06}_{-0.06}$	-1.54 $^{+0.07}_{-0.08}$	-5.85 $^{+2.79}_{-2.73}$	1030 $^{+622}_{-573}$	5.57 $^{+0.63}_{-0.46} \times 10^{-6}$	-0.0	1.3	1.2	
106.629~107.242	21.93	0.47 $^{+0.06}_{-0.06}$	-1.12 $^{+0.06}_{-0.06}$	1796 $^{+612}_{-619}$	1581 $^{+549}_{-555}$	7.29 $^{+4.12}_{-2.39} \times 10^{-6}$	0.47 $^{+0.06}_{-0.06}$	-1.11 $^{+0.06}_{-0.06}$	-6.16 $^{+2.71}_{-2.65}$	1494 $^{+443}_{-443}$	7.34 $^{+3.36}_{-2.25} \times 10^{-6}$	0.2	2.1	2.3	

Note—All columns are the same as Table A2 but for GRB 12071115.

Table A15. Time-resolved Spectral Fit Results of GRB 120728484

$t_{\text{start}} \sim t_{\text{stop}}$	S	Cutoff Power-Law Fitting						Band Fitting						Difference		
		K	α	E_c	E_p	F	K	α	β	E_p	F	ΔDIC	$p_{\text{DIC}}^{\text{CPL}}$	$p_{\text{DIC}}^{\text{Band}}$		
(1)	(2)	(3)	(4)	(5)	(6)	(7)	(8)	(9)	(10)	(11)	(12)	(13)	(14)	(15)		
Pulse 1																
-0.177~3.764	22.44	0.15 $^{+0.02}_{-0.02}$	-0.81 $^{+0.12}_{-0.12}$	168 $^{+36}_{-38}$	200 $^{+48}_{-49}$	0.60 $^{+0.34}_{-0.34}$	0.11 $^{+0.02}_{-0.02}$	0.45 $^{+0.41}_{-0.44}$	-2.05 $^{+0.04}_{-0.04}$	76 $^{+14}_{-13}$	1.04 $^{+0.90}_{-0.41} \times 10^{-6}$	-25.3	1.5	-5.5		
10.358~12.621	29.11	0.29 $^{+0.03}_{-0.03}$	-0.67 $^{+0.14}_{-0.14}$	92 $^{+17}_{-17}$	123 $^{+26}_{-26}$	0.77 $^{+0.41}_{-0.41}$	0.24 $^{+0.03}_{-0.03}$	0.66 $^{+0.26}_{-0.26}$	-2.16 $^{+0.08}_{-0.08}$	59 $^{+6}_{+6}$	1.28 $^{+0.41}_{-0.20} \times 10^{-6}$	-29.3	1.6	1.9		
12.621~15.450	52.23	0.52 $^{+0.03}_{-0.03}$	-0.93 $^{+0.06}_{-0.06}$	117 $^{+22}_{-22}$	189 $^{+26}_{-26}$	1.72 $^{+0.44}_{-0.44}$	0.36 $^{+0.03}_{-0.03}$	0.47 $^{+0.35}_{-0.33}$	-2.02 $^{+0.02}_{-0.02}$	67 $^{+8}_{-8}$	3.02 $^{+1.49}_{-1.49} \times 10^{-6}$	-69.6	2.6	-3.6		
15.450~16.538	43.39	0.63 $^{+0.06}_{-0.06}$	-0.83 $^{+0.08}_{-0.08}$	142 $^{+19}_{-19}$	167 $^{+25}_{-25}$	2.02 $^{+0.63}_{-0.45}$	0.50 $^{+0.30}_{-0.06}$	0.23 $^{+0.17}_{-0.28}$	-2.28 $^{+0.17}_{-0.12}$	100 $^{+17}_{-19}$	2.90 $^{+2.37}_{-1.11} \times 10^{-6}$	-15.2	2.5	-3.1		
16.538~17.118	39.84	0.92 $^{+0.08}_{-0.08}$	-0.95 $^{+0.08}_{-0.08}$	185 $^{+28}_{-29}$	194 $^{+34}_{-34}$	2.96 $^{+0.57}_{-0.66}$	0.89 $^{+0.10}_{-0.10}$	0.89 $^{+0.08}_{-0.12}$	-6.00 $^{+2.78}_{-2.66}$	181 $^{+24}_{-18}$	3.00 $^{+1.17}_{-0.76} \times 10^{-6}$	-0.4	2.5	2.0		
17.118~20.689	60.23	0.60 $^{+0.03}_{-0.03}$	-0.59 $^{+0.07}_{-0.07}$	71 $^{+5}_{-5}$	101 $^{+9}_{-9}$	1.35 $^{+0.29}_{-0.22}$	0.52 $^{+0.04}_{-0.04}$	0.87 $^{+0.11}_{-0.11}$	-2.23 $^{+0.05}_{-0.05}$	52 $^{+2}_{-2}$	2.11 $^{+0.41}_{-0.36} \times 10^{-6}$	-69.9	2.8	2.9		
20.689~22.369	55.38	0.71 $^{+0.05}_{-0.05}$	-0.46 $^{+0.09}_{-0.08}$	65 $^{+5}_{-5}$	100 $^{+10}_{-9}$	1.75 $^{+0.44}_{-0.34}$	0.63 $^{+0.05}_{-0.05}$	0.07 $^{+0.17}_{-0.17}$	-2.73 $^{+0.18}_{-0.16}$	81 $^{+6}_{-6}$	2.20 $^{+0.69}_{-0.46} \times 10^{-6}$	-17.6	2.8	3.7		
22.369~23.360	33.83	0.71 $^{+0.07}_{-0.07}$	-0.64 $^{+0.14}_{-0.14}$	63 $^{+9}_{-9}$	85 $^{+15}_{-15}$	1.21 $^{+0.53}_{-0.33}$	0.70 $^{+0.09}_{-0.09}$	0.77 $^{+0.19}_{-0.20}$	-2.32 $^{+0.09}_{-0.09}$	47 $^{+3}_{-4}$	1.76 $^{+0.72}_{-0.43} \times 10^{-6}$	-28.8	2.3	2.7		
23.360~23.781	31.19	0.79 $^{+0.10}_{-0.10}$	-0.78 $^{+0.13}_{-0.13}$	116 $^{+20}_{-21}$	141 $^{+29}_{-29}$	2.17 $^{+0.59}_{-0.59}$	0.74 $^{+0.11}_{-0.12}$	0.61 $^{+0.26}_{-0.24}$	-4.71 $^{+2.31}_{-2.31}$	123 $^{+21}_{-21}$	2.43 $^{+1.15}_{-0.84} \times 10^{-6}$	-4.8	2.1	-1.1		
23.781~25.046	68.22	1.01 $^{+0.06}_{-0.06}$	-0.67 $^{+0.07}_{-0.07}$	98 $^{+8}_{-8}$	131 $^{+13}_{-13}$	3.05 $^{+0.64}_{-0.64}$	0.80 $^{+0.06}_{-0.06}$	0.07 $^{+0.14}_{-0.14}$	-2.41 $^{+0.08}_{-0.08}$	89 $^{+6}_{-6}$	4.20 $^{+0.89}_{-0.82} \times 10^{-6}$	-57.9	2.8	3.6		
25.046~28.054	81.51	0.81 $^{+0.04}_{-0.04}$	-0.62 $^{+0.05}_{-0.05}$	86 $^{+5}_{-5}$	119 $^{+8}_{-9}$	2.24 $^{+0.35}_{-0.29}$	0.66 $^{+0.04}_{-0.04}$	0.04 $^{+0.14}_{-0.14}$	-2.38 $^{+0.07}_{-0.07}$	80 $^{+5}_{-5}$	3.15 $^{+0.81}_{-0.55} \times 10^{-6}$	-71.8	2.9	3.3		
28.054~29.854	53.08	0.84 $^{+0.05}_{-0.05}$	-0.65 $^{+0.09}_{-0.09}$	64 $^{+6}_{-6}$	86 $^{+10}_{-10}$	1.43 $^{+0.37}_{-0.26}$	0.77 $^{+0.06}_{-0.06}$	0.82 $^{+0.14}_{-0.15}$	-2.35 $^{+0.06}_{-0.06}$	48 $^{+2}_{-2}$	2.02 $^{+0.47}_{-0.35} \times 10^{-6}$	-57.5	2.7	3.0		
29.854~31.296	36.87	0.59 $^{+0.06}_{-0.05}$	-0.72 $^{+0.12}_{-0.12}$	78 $^{+11}_{-11}$	100 $^{+17}_{-16}$	1.17 $^{+0.45}_{-0.30}$	0.53 $^{+0.06}_{-0.06}$	0.54 $^{+0.37}_{-0.43}$	-2.29 $^{+0.11}_{-0.10}$	54 $^{+8}_{-7}$	1.67 $^{+0.99}_{-0.55} \times 10^{-6}$	-21.4	2.5	-1.6		
31.296~33.082	52.70	0.65 $^{+0.05}_{-0.05}$	-0.50 $^{+0.09}_{-0.09}$	66 $^{+6}_{-6}$	99 $^{+11}_{-11}$	1.53 $^{+0.41}_{-0.31}$	0.58 $^{+0.05}_{-0.05}$	0.08 $^{+0.21}_{-0.22}$	-2.66 $^{+0.19}_{-0.18}$	79 $^{+8}_{-8}$	1.95 $^{+0.78}_{-0.48} \times 10^{-6}$	-23.7	2.7	2.5		
33.082~34.792	72.96	0.98 $^{+0.05}_{-0.05}$	-0.65 $^{+0.06}_{-0.06}$	89 $^{+6}_{-6}$	120 $^{+10}_{-10}$	2.62 $^{+0.48}_{-0.40}$	0.85 $^{+0.05}_{-0.05}$	-0.50 $^{+0.11}_{-0.10}$	-2.62 $^{+0.11}_{-0.11}$	94 $^{+5}_{-5}$	3.29 $^{+0.63}_{-0.51} \times 10^{-6}$	-25.1	2.9	3.9		
34.792~35.936	67.95	1.05 $^{+0.07}_{-0.07}$	-0.46 $^{+0.07}_{-0.07}$	67 $^{+5}_{-5}$	103 $^{+9}_{-9}$	2.82 $^{+0.58}_{-0.52}$	0.90 $^{+0.07}_{-0.07}$	-0.03 $^{+0.15}_{-0.15}$	-2.76 $^{+0.14}_{-0.14}$	83 $^{+5}_{-5}$	3.37 $^{+0.77}_{-0.63} \times 10^{-6}$	-23.7	2.8	3.8		
35.936~37.102	52.30	1.00 $^{+0.07}_{-0.07}$	-0.45 $^{+0.10}_{-0.10}$	50 $^{+4}_{-4}$	78 $^{+8}_{-8}$	1.69 $^{+0.44}_{-0.32}$	0.95 $^{+0.08}_{-0.08}$	-0.17 $^{+0.25}_{-0.25}$	-3.79 $^{+0.96}_{-0.69}$	69 $^{+7}_{-7}$	1.85 $^{+0.67}_{-0.42} \times 10^{-6}$	-9.5	2.8	-1.9		
37.102~37.959	34.14	0.90 $^{+0.08}_{-0.08}$	-0.51 $^{+0.16}_{-0.16}$	46 $^{+7}_{-7}$	68 $^{+12}_{-12}$	1.21 $^{+0.51}_{-0.31}$	0.89 $^{+0.10}_{-0.11}$	0.71 $^{+0.23}_{-0.24}$	-2.55 $^{+0.13}_{-0.12}$	45 $^{+3}_{-3}$	1.51 $^{+0.48}_{-0.38} \times 10^{-6}$	-32.7	2.2	2.9		
37.959~39.308	23.40	0.48 $^{+0.06}_{-0.06}$	-0.51 $^{+0.24}_{-0.24}$	42 $^{+9}_{-8}$	62 $^{+16}_{-16}$	0.53 $^{+0.40}_{-0.18}$	0.56 $^{+0.10}_{-0.10}$	0.62 $^{+0.31}_{-0.32}$	-2.65 $^{+0.24}_{-0.16}$	41 $^{+4}_{-4}$	0.65 $^{+0.34}_{-0.20} \times 10^{-6}$	-11.5	1.7	2.3		
41.189~42.506	23.59	0.52 $^{+0.06}_{-0.06}$	-0.61 $^{+0.25}_{-0.24}$	45 $^{+11}_{-11}$	63 $^{+19}_{-18}$	0.57 $^{+0.44}_{-0.19}$	0.64 $^{+0.10}_{-0.10}$	0.78 $^{+0.18}_{-0.18}$	-2.53 $^{+0.14}_{-0.14}$	38 $^{+3}_{-3}$	0.69 $^{+0.26}_{-0.18} \times 10^{-6}$	-20.5	1.2	2.9		
42.506~48.146	29.35	0.34 $^{+0.03}_{-0.03}$	-0.08 $^{+0.22}_{-0.23}$	26 $^{+4}_{-4}$	49 $^{+9}_{-10}$	0.33 $^{+0.17}_{-0.12}$	0.47 $^{+0.06}_{-0.06}$	0.87 $^{+0.10}_{-0.10}$	-2.70 $^{+0.15}_{-0.15}$	35 $^{+2}_{-2}$	0.38 $^{+0.10}_{-0.08} \times 10^{-6}$	-25.5	1.9	2.9		
48.146~53.695	44.48	0.42 $^{+0.03}_{-0.03}$	-0.23 $^{+0.13}_{-0.13}$	34 $^{+3}_{-3}$	61 $^{+7}_{-7}$	0.54 $^{+0.17}_{-0.12}$	0.48 $^{+0.04}_{-0.04}$	0.93 $^{+0.06}_{-0.06}$	-2.61 $^{+0.09}_{-0.09}$	42 $^{+2}_{-2}$	0.68 $^{+0.11}_{-0.10} \times 10^{-6}$	-67.7	2.6	3.0		
53.695~57.165	20.60	0.25 $^{+0.03}_{-0.03}$	-0.38 $^{+0.27}_{-0.27}$	38 $^{+9}_{-9}$	62 $^{+18}_{-18}$	0.28 $^{+0.25}_{-0.11}$	0.34 $^{+0.05}_{-0.05}$	0.84 $^{+0.13}_{-0.13}$	-2.54 $^{+0.15}_{-0.15}$	38 $^{+3}_{-3}$	0.37 $^{+0.13}_{-0.10} \times 10^{-6}$	-24.0	0.7	3.0		
Pulse 2																
68.145~68.435	23.84	0.61 $^{+0.12}_{-0.12}$	-0.33 $^{+0.23}_{-0.23}$	60 $^{+12}_{-12}$	99 $^{+24}_{-24}$	1.69 $^{+1.36}_{-0.73}$	0.57 $^{+0.11}_{-0.11}$	-0.15 $^{+0.29}_{-0.30}$	-4.73 $^{+1.88}_{-2.78}$	90 $^{+10}_{-9}$	1.76 $^{+1.07}_{-0.58} \times 10^{-6}$	-1.3	1.1	1.5		
68.435~69.274	59.05	1.09 $^{+0.08}_{-0.08}$	-0.39 $^{+0.09}_{-0.09}$	59 $^{+5}_{-5}$	95 $^{+9}_{-9}$	2.72 $^{+0.73}_{-0.54}$	0.97 $^{+0.08}_{-0.08}$	-0.07 $^{+0.15}_{-0.15}$	-3.03 $^{+0.21}_{-0.20}$	82 $^{+5}_{-5}$	3.08 $^{+0.68}_{-0.57} \times 10^{-6}$	-13.3	2.8	3.9		
69.274~71.015	103.06	1.53 $^{+0.07}_{-0.07}$	-0.61 $^{+0.05}_{-0.05}$	78 $^{+4}_{-4}$	109 $^{+7}_{-7}$	3.81 $^{+1.04}_{-0.45}$	1.21 $^{+0.07}_{-0.07}$	0.99 $^{+0.12}_{-0.12}$	-2.52 $^{+0.06}_{-0.06}$	76 $^{+4}_{-4}$	4.88 $^{+0.93}_{-0.77} \times 10^{-6}$	-123.8	2.9	3.7		

Table A15 *continued on next page*

Table A15 (continued)

$t_{\text{start}} \sim t_{\text{stop}}$	S	Cutoff Power-Law Fitting						Band Fitting						ΔDIC	$p_{\text{DIC}}^{\text{Band}}$	$p_{\text{DIC}}^{\text{CPL}}$	Difference
		K	α	E_c	E_p	F	K	α	β	E_p	F	(13)	(14)	(15)			
71.015~71.665	56.60	1.19 ^{+0.10} _{-0.10}	-0.38 ^{+0.10} _{-0.10}	59 ⁺⁵ ₋₅	95 ⁺¹⁰ ₋₁₀	2.99 ^{+0.94} _{-0.61}	$1.06^{+0.10} \times 10^{-6}$	1.06 ^{+0.10} _{-0.10}	-0.04 ^{+0.17} _{-0.18}	-2.88 ^{+0.20} _{-0.19}	81 ⁺⁵ ₋₅	3.51 ^{+1.05} _{-0.73}	$\times 10^{-6}$	-18.0	2.6	3.8	
71.665~73.744	84.99	1.24 ^{+0.06} _{-0.06}	-0.55 ^{+0.06} _{-0.06}	61 ⁺⁴ ₋₄	89 ⁺⁶ ₋₆	2.43 ^{+0.38} _{-0.30}	$1.02^{+0.06} \times 10^{-6}$	0.54 ^{+0.29} _{-0.28}	-2.49 ^{+0.08} _{-0.08}	58 ⁺⁵ ₋₅	3.14 ^{+1.09} _{-0.68}	$\times 10^{-6}$	-74.6	2.9	1.2		
73.744~77.876	96.82	1.06 ^{+0.04} _{-0.04}	-0.31 ^{+0.06} _{-0.06}	42 ⁺² ₋₂	71 ⁺⁴ ₋₄	1.74 ^{+0.24} _{-0.20}	$1.00^{+0.04} \times 10^{-6}$	0.04 ^{+0.12} _{-0.12}	-3.11 ^{+0.13} _{-0.13}	62 ⁺² ₋₂	1.93 ^{+0.24} _{-0.21}	$\times 10^{-6}$	-35.5	2.9	3.9		
77.876~81.395	69.75	0.87 ^{+0.04} _{-0.04}	-0.21 ^{+0.08} _{-0.08}	35 ⁺² ₋₂	63 ⁺⁵ ₋₅	1.22 ^{+0.24} _{-0.20}	$0.83^{+0.05} \times 10^{-6}$	0.62 ^{+0.28} _{-0.29}	-2.93 ^{+0.14} _{-0.15}	50 ⁺³ ₋₃	1.39 ^{+0.37} _{-0.27}	$\times 10^{-6}$	-25.5	2.9	2.5		
81.395~84.068	48.62	0.83 ^{+0.05} _{-0.05}	-0.36 ^{+0.12} _{-0.12}	33 ⁺³ ₋₃	55 ⁺⁶ ₋₆	0.84 ^{+0.23} _{-0.15}	$1.02^{+0.09} \times 10^{-6}$	1.02 ^{+0.07} _{-0.09}	0.92 ^{+0.07} _{-0.07}	-2.69 ^{+0.09} _{-0.09}	37 ⁺² ₋₂	0.97 ^{+0.18} _{-0.15}	$\times 10^{-6}$	-40.8	2.7	3.0	
84.068~86.338	57.13	0.76 ^{+0.05} _{-0.05}	-0.44 ^{+0.09} _{-0.09}	52 ⁺⁴ ₋₄	81 ⁺⁸ ₋₈	1.37 ^{+0.31} _{-0.23}	$0.68^{+0.05} \times 10^{-6}$	0.27 ^{+0.28} _{-0.28}	-2.68 ^{+0.13} _{-0.13}	60 ⁺⁵ ₋₅	1.68 ^{+0.61} _{-0.39}	$\times 10^{-6}$	-26.2	2.8	2.8		
86.338~86.877	21.18	0.55 ^{+0.09} _{-0.09}	-0.26 ^{+0.23} _{-0.23}	43 ⁺⁷ ₋₇	74 ⁺¹⁶ ₋₁₆	0.96 ^{+0.66} _{-0.39}	$0.53^{+0.09} \times 10^{-6}$	0.17 ^{+0.25} _{-0.09}	-6.46 ^{+2.38} _{-2.38}	71 ⁺⁶ ₋₅	0.96 ^{+0.39} _{-0.24}	$\times 10^{-6}$	1.2	2.0	3.0		
86.877~87.677	39.56	0.70 ^{+0.07} _{-0.08}	-0.27 ^{+0.14} _{-0.14}	48 ⁺⁵ ₋₅	82 ⁺¹¹ ₋₁₁	1.51 ^{+0.60} _{-0.45}	$0.66^{+0.08} \times 10^{-6}$	0.66 ^{+0.21} _{-0.21}	-3.37 ^{+0.54} _{-0.26}	75 ⁺⁵ ₋₅	1.72 ^{+0.52} _{-0.39}	$\times 10^{-6}$	-7.6	2.5	3.1		
87.677~88.414	29.61	0.69 ^{+0.08} _{-0.08}	-0.47 ^{+0.17} _{-0.17}	50 ⁺⁷ ₋₇	77 ⁺¹⁴ ₋₁₄	1.15 ^{+0.58} _{-0.36}	$0.69^{+0.09} \times 10^{-6}$	0.33 ^{+0.58} _{-0.75}	-3.59 ^{+1.17} _{-1.97}	57 ⁺¹⁷ ₋₁₂	1.34 ^{+1.63} _{-0.60}	$\times 10^{-6}$	-27.8	2.4	-19.5		
88.414~89.905	26.41	0.51 ^{+0.06} _{-0.06}	-0.10 ^{+0.24} _{-0.24}	29 ⁺⁵ ₋₅	55 ⁺¹¹ ₋₁₁	0.57 ^{+0.36} _{-0.21}	$0.55^{+0.07} \times 10^{-6}$	0.75 ^{+0.20} _{-0.20}	-3.15 ^{+0.33} _{-0.18}	43 ⁺³ ₋₃	0.62 ^{+0.20} _{-0.14}	$\times 10^{-6}$	-11.4	1.9	2.5		

Note—All columns are the same as Table A2 but for GRB 120728484.

Table A16. Time-resolved Spectral Fit Results of GRB 121225417

$t_{\text{start}} \sim t_{\text{stop}}$	S	Cutoff Power-Law Fitting				Band Fitting				Difference				
		K	α	E_c	E_p	F	K	α	β	E_p	F	ΔDIC	$p_{\text{DIC}}^{\text{CPL}}$	$p_{\text{DIC}}^{\text{Band}}$
(1)	(2)	(3)	(4)	(5)	(6)	(7)	(8)	(9)	(10)	(11)	(12)	(13)	(14)	(15)
15.748~16.984	25.23	$0.24^{+0.02}_{-0.02}$	$-0.88^{+0.06}_{-0.06}$	515^{+101}_{-101}	577^{+118}_{-117}	$3.01^{+1.12 \times 10^{-6}}_{-0.52 \times 10^{-6}}$	$0.24^{+0.02}_{-0.02}$	$-0.86^{+0.06}_{-0.07}$	$-5.53^{+2.85}_{-3.03}$	55^{+86}_{-87}	$3.04^{+1.09 \times 10^{-6}}_{-0.69 \times 10^{-6}}$	-0.7	2.3	2.2
16.984~18.500	49.62	$0.45^{+0.02}_{-0.02}$	$-0.99^{+0.03}_{-0.02}$	1416^{+268}_{-271}	1430^{+274}_{-277}	$10.34^{+3.03 \times 10^{-6}}_{-2.18 \times 10^{-6}}$	$0.39^{+0.02}_{-0.02}$	$-0.89^{+0.04}_{-0.04}$	$-2.11^{+0.08}_{-0.08}$	814^{+99}_{-97}	$10.59^{+2.02 \times 10^{-6}}_{-1.83 \times 10^{-6}}$	-32.0	2.5	3.2
18.500~20.539	64.84	$0.60^{+0.02}_{-0.02}$	$-1.00^{+0.02}_{-0.02}$	788^{+86}_{-86}	788^{+86}_{-87}	$7.43^{+1.18 \times 10^{-6}}_{-1.00 \times 10^{-6}}$	$0.59^{+0.02}_{-0.02}$	$-0.98^{+0.03}_{-0.03}$	$-3.15^{+0.81}_{-0.31}$	700^{+75}_{-75}	$8.25^{+1.59 \times 10^{-6}}_{-1.29 \times 10^{-6}}$	-9.8	2.9	0.1
20.539~22.044	45.28	$0.48^{+0.02}_{-0.02}$	$-0.95^{+0.03}_{-0.03}$	439^{+31}_{-31}	461^{+35}_{-35}	$3.97^{+0.55 \times 10^{-6}}_{-0.43 \times 10^{-6}}$	$0.49^{+0.03}_{-0.03}$	$-0.96^{+0.04}_{-0.04}$	$-4.10^{+1.82}_{-1.82}$	470^{+61}_{-62}	$4.71^{+1.41 \times 10^{-6}}_{-1.02 \times 10^{-6}}$	-4.1	2.3	0.7
22.044~23.273	53.54	$0.53^{+0.03}_{-0.03}$	$-0.84^{+0.04}_{-0.03}$	378^{+35}_{-35}	438^{+43}_{-42}	$5.40^{+1.07 \times 10^{-6}}_{-0.83 \times 10^{-6}}$	$0.52^{+0.03}_{-0.03}$	$-0.82^{+0.04}_{-0.04}$	$-4.49^{+2.11}_{-2.11}$	418^{+35}_{-35}	$5.92^{+1.68 \times 10^{-6}}_{-1.11 \times 10^{-6}}$	-4.1	2.9	0.9
23.730~25.908	21.11	$0.29^{+0.03}_{-0.03}$	$-1.24^{+0.09}_{-0.09}$	439^{+154}_{-168}	334^{+124}_{-134}	$0.89^{+0.55 \times 10^{-6}}_{-0.29 \times 10^{-6}}$	$0.28^{+0.03}_{-0.03}$	$-1.21^{+0.09}_{-0.10}$	$-0.56^{+2.82}_{-2.93}$	280^{+74}_{-76}	$0.92^{+0.39 \times 10^{-6}}_{-0.23 \times 10^{-6}}$	1.3	-0.3	1.6
Pulse 1														
49.027~49.491	23.57	$0.22^{+0.03}_{-0.03}$	$-0.47^{+0.10}_{-0.10}$	192^{+28}_{-29}	294^{+47}_{-48}	$2.72^{+1.49 \times 10^{-6}}_{-0.84 \times 10^{-6}}$	$0.21^{+0.03}_{-0.03}$	$-0.45^{+0.10}_{-0.11}$	$-6.31^{+2.49}_{-2.50}$	286^{+28}_{-28}	$2.83^{+1.03 \times 10^{-6}}_{-0.72 \times 10^{-6}}$	0.5	2.2	2.8
50.150~50.951	30.79	$0.33^{+0.03}_{-0.03}$	$-0.56^{+0.08}_{-0.08}$	156^{+18}_{-18}	224^{+29}_{-29}	$2.31^{+0.75 \times 10^{-6}}_{-0.75 \times 10^{-6}}$	$0.31^{+0.03}_{-0.03}$	$-0.50^{+0.11}_{-0.10}$	$-4.00^{+1.68}_{-1.68}$	207^{+72}_{-72}	$2.82^{+1.25 \times 10^{-6}}_{-1.25 \times 10^{-6}}$	-5.2	2.5	0.2
51.415~51.697	24.07	$0.47^{+0.06}_{-0.06}$	$-0.58^{+0.11}_{-0.11}$	142^{+22}_{-22}	201^{+35}_{-35}	$2.71^{+1.33 \times 10^{-6}}_{-1.00 \times 10^{-6}}$	$0.46^{+0.06}_{-0.06}$	$-0.55^{+0.12}_{-0.12}$	$-5.92^{+2.87}_{-2.86}$	194^{+20}_{-20}	$2.96^{+1.15 \times 10^{-6}}_{-0.77 \times 10^{-6}}$	0.2	2.2	2.6
53.147~54.122	26.75	$0.30^{+0.03}_{-0.03}$	$-0.74^{+0.08}_{-0.08}$	193^{+27}_{-27}	244^{+37}_{-38}	$1.75^{+0.68 \times 10^{-6}}_{-0.68 \times 10^{-6}}$	$0.30^{+0.03}_{-0.03}$	$-0.73^{+0.08}_{-0.08}$	$-6.40^{+2.33}_{-2.37}$	240^{+22}_{-22}	$1.81^{+0.46 \times 10^{-6}}_{-0.32 \times 10^{-6}}$	0.6	2.5	3.0
54.483~54.893	20.76	$0.49^{+0.06}_{-0.06}$	$-0.80^{+0.12}_{-0.12}$	142^{+30}_{-30}	170^{+39}_{-40}	$1.66^{+0.88 \times 10^{-6}}_{-0.88 \times 10^{-6}}$	$0.46^{+0.06}_{-0.06}$	$-0.68^{+0.19}_{-0.19}$	$-4.42^{+2.15}_{-2.15}$	147^{+26}_{-26}	$1.84^{+1.07 \times 10^{-6}}_{-0.61 \times 10^{-6}}$	-3.2	1.6	0.3
54.893~55.123	27.67	$0.67^{+0.07}_{-0.07}$	$-0.80^{+0.07}_{-0.07}$	298^{+47}_{-47}	358^{+61}_{-60}	$5.60^{+2.13 \times 10^{-6}}_{-1.42 \times 10^{-6}}$	$0.66^{+0.07}_{-0.07}$	$-0.79^{+0.07}_{-0.07}$	$-5.98^{+2.73}_{-2.73}$	350^{+41}_{-41}	$5.83^{+1.79 \times 10^{-6}}_{-1.30 \times 10^{-6}}$	0.3	2.5	2.8
55.123~55.476	24.21	$0.73^{+0.07}_{-0.07}$	$-0.95^{+0.09}_{-0.09}$	207^{+42}_{-42}	217^{+47}_{-47}	$2.67^{+1.09 \times 10^{-6}}_{-0.73 \times 10^{-6}}$	$0.66^{+0.09}_{-0.09}$	$-0.72^{+0.23}_{-0.23}$	$-3.44^{+1.38}_{-1.38}$	161^{+48}_{-48}	$3.49^{+2.59 \times 10^{-6}}_{-1.51 \times 10^{-6}}$	-15.8	2.1	-8.2
55.915~56.143	23.49	$0.72^{+0.08}_{-0.08}$	$-0.90^{+0.08}_{-0.08}$	270^{+48}_{-50}	297^{+57}_{-59}	$4.03^{+1.54 \times 10^{-6}}_{-1.06 \times 10^{-6}}$	$0.72^{+0.08}_{-0.08}$	$-0.89^{+0.08}_{-0.08}$	$-6.56^{+2.40}_{-2.38}$	291^{+38}_{-38}	$4.00^{+1.23 \times 10^{-6}}_{-0.78 \times 10^{-6}}$	0.7	2.4	2.9
56.418~56.636	23.82	$0.42^{+0.06}_{-0.06}$	$-0.45^{+0.11}_{-0.11}$	138^{+22}_{+22}	214^{+37}_{-37}	$3.32^{+1.81 \times 10^{-6}}_{-1.14 \times 10^{-6}}$	$0.41^{+0.05}_{-0.05}$	$-0.38^{+0.12}_{-0.12}$	$-3.52^{+1.30}_{-1.30}$	192^{+24}_{-24}	$4.35^{+2.31 \times 10^{-6}}_{-1.47 \times 10^{-6}}$	-6.8	2.0	-0.1
58.457~59.386	22.83	$0.45^{+0.04}_{-0.04}$	$-0.82^{+0.13}_{-0.12}$	96^{+16}_{-17}	114^{+23}_{-23}	$0.93^{+0.41 \times 10^{-6}}_{-0.25 \times 10^{-6}}$	$0.45^{+0.04}_{-0.04}$	$-0.78^{+0.13}_{-0.13}$	$-5.47^{+2.52}_{-2.52}$	109^{+10}_{-10}	$0.99^{+0.26 \times 10^{-6}}_{-0.19 \times 10^{-6}}$	-0.2	2.1	2.5
59.386~62.911	30.33	$0.58^{+0.03}_{-0.03}$	$-1.13^{+0.10}_{-0.09}$	83^{+12}_{-12}	73^{+13}_{-13}	$0.62^{+0.14 \times 10^{-6}}_{-0.10 \times 10^{-6}}$	$0.58^{+0.03}_{-0.03}$	$-1.11^{+0.10}_{-0.10}$	$-6.09^{+2.52}_{-2.63}$	71^{+4}_{-4}	$0.62^{+0.07 \times 10^{-6}}_{-0.05 \times 10^{-6}}$	0.1	2.6	2.9
62.911~63.433	20.45	$0.77^{+0.07}_{-0.07}$	$-1.27^{+0.12}_{-0.12}$	195^{+59}_{-59}	143^{+49}_{-50}	$1.27^{+0.59 \times 10^{-6}}_{-0.56 \times 10^{-6}}$	$0.76^{+0.07}_{-0.07}$	$-1.24^{+0.12}_{-0.12}$	$-6.10^{+2.66}_{-2.66}$	131^{+21}_{-22}	$1.25^{+0.33 \times 10^{-6}}_{-0.21 \times 10^{-6}}$	1.5	1.0	2.7
63.433~67.779	28.57	$0.58^{+0.03}_{-0.03}$	$-1.46^{+0.10}_{-0.10}$	128^{+29}_{-30}	69^{+20}_{-21}	$0.54^{+0.12 \times 10^{-6}}_{-0.08 \times 10^{-6}}$	$0.57^{+0.03}_{-0.03}$	$-1.42^{+0.11}_{-0.11}$	$-5.85^{+2.71}_{-2.77}$	65^{+6}_{-6}	$0.55^{+0.05 \times 10^{-6}}_{-0.05 \times 10^{-6}}$	0.9	1.9	3.0

Note—All columns are the same as Table A2 but for GRB 121225417.

Table A17. Time-resolved Spectral Fit Results of GRB 130504978

$t_{\text{start}} \sim t_{\text{stop}}$	S	Cutoff Power-Law Fitting						Band Fitting						Difference			
		K	α	E_c	E_p	F	K	α	β	E_p	F	ΔDIC	$p_{\text{DIC}}^{\text{GPL}}$	$p_{\text{DIC}}^{\text{Band}}$			
(1)	(2)	(3)	(4)	(5)	(6)	(7)	(8)	(9)	(10)	(11)	(12)	(13)	(14)	(15)			
Pulse 1																	
2.418~8.809	20.81	0.09 $^{+0.01}_{-0.01}$	-1.02 $^{+0.08}_{-0.08}$	1.125 $^{+4.44}_{-4.42}$	11.03 $^{+4.45}_{-4.43}$	1.29 $^{+0.92}_{-0.91}$ $\times 10^{-6}$	0.09 $^{+0.01}_{-0.01}$	-1.01 $^{+0.08}_{-0.08}$	-5.33 $^{+2.78}_{-3.07}$	983 $^{+295}_{-297}$	1.26 $^{+0.79}_{-0.42}$ $\times 10^{-6}$	0.7	-1.1	0.3			
8.809~10.280	20.07	0.10 $^{+0.02}_{-0.02}$	-0.82 $^{+0.10}_{-0.09}$	787 $^{+232}_{-232}$	928 $^{+285}_{-283}$	2.35 $^{+2.10}_{-1.91}$ $\times 10^{-6}$	0.10 $^{+0.02}_{-0.02}$	-0.82 $^{+0.10}_{-0.10}$	-5.93 $^{+2.73}_{-2.74}$	917 $^{+219}_{-216}$	2.44 $^{+1.50}_{-0.83}$ $\times 10^{-6}$	0.9	0.4	1.3			
13.245~14.072	25.62	0.19 $^{+0.03}_{-0.03}$	-0.82 $^{+0.08}_{-0.08}$	711 $^{+179}_{-178}$	839 $^{+219}_{-219}$	3.90 $^{+2.50}_{-1.44}$ $\times 10^{-6}$	0.19 $^{+0.03}_{-0.03}$	-0.82 $^{+0.08}_{-0.08}$	-5.95 $^{+2.77}_{-2.77}$	808 $^{+157}_{-156}$	4.05 $^{+1.93}_{-1.21}$ $\times 10^{-6}$	0.3	1.3	1.8			
14.072~14.624	31.44	0.35 $^{+0.04}_{-0.04}$	-0.98 $^{+0.05}_{-0.05}$	1.826 $^{+4.36}_{-4.36}$	1863 $^{+454}_{-461}$	10.61 $^{+1.82}_{-2.96}$ $\times 10^{-6}$	0.34 $^{+0.03}_{-0.03}$	-0.97 $^{+0.05}_{-0.05}$	-4.86 $^{+2.51}_{-3.18}$	1716 $^{+373}_{-377}$	10.54 $^{+4.32}_{-2.97}$ $\times 10^{-6}$	-2.4	2.5	1.5			
14.624~15.677	67.16	0.48 $^{+0.03}_{-0.03}$	-0.82 $^{+0.04}_{-0.04}$	843 $^{+111}_{-111}$	994 $^{+138}_{-135}$	12.89 $^{+3.48}_{-2.55}$ $\times 10^{-6}$	0.42 $^{+0.03}_{-0.03}$	-0.72 $^{+0.04}_{-0.04}$	-2.10 $^{+0.07}_{-0.07}$	692 $^{+63}_{-64}$	16.14 $^{+3.29}_{-2.76}$ $\times 10^{-6}$	-51.3	2.5	3.2			
15.677~16.446	71.24	0.69 $^{+0.04}_{-0.04}$	-0.86 $^{+0.03}_{-0.03}$	916 $^{+103}_{-101}$	1044 $^{+120}_{-118}$	17.61 $^{+4.03}_{-2.82}$ $\times 10^{-6}$	0.62 $^{+0.04}_{-0.04}$	-0.77 $^{+0.04}_{-0.04}$	-2.19 $^{+0.10}_{-0.10}$	765 $^{+73}_{-71}$	20.94 $^{+3.78}_{-3.14}$ $\times 10^{-6}$	-34.9	2.7	3.8			
16.446~17.438	64.32	0.64 $^{+0.03}_{-0.03}$	-0.94 $^{+0.03}_{-0.03}$	936 $^{+113}_{-113}$	992 $^{+123}_{-123}$	11.88 $^{+2.51}_{-1.91}$ $\times 10^{-6}$	0.62 $^{+0.03}_{-0.03}$	-0.92 $^{+0.03}_{-0.03}$	-4.15 $^{+1.67}_{-2.83}$	908 $^{+108}_{-107}$	12.63 $^{+2.60}_{-2.27}$ $\times 10^{-6}$	-5.6	0.4	0.4			
17.438~19.097	59.27	0.53 $^{+0.03}_{-0.03}$	-0.99 $^{+0.03}_{-0.03}$	599 $^{+67}_{-68}$	605 $^{+70}_{-71}$	5.27 $^{+1.06}_{-0.82}$ $\times 10^{-6}$	0.53 $^{+0.03}_{-0.03}$	-0.98 $^{+0.04}_{-0.04}$	-4.48 $^{+2.15}_{-2.33}$	577 $^{+63}_{-63}$	5.81 $^{+1.51}_{-1.08}$ $\times 10^{-6}$	-3.4	2.8	1.4			
19.097~20.683	35.91	0.36 $^{+0.03}_{-0.03}$	-1.09 $^{+0.05}_{-0.05}$	724 $^{+154}_{-155}$	658 $^{+145}_{-146}$	2.89 $^{+0.92}_{-0.67}$ $\times 10^{-6}$	0.36 $^{+0.03}_{-0.03}$	-1.08 $^{+0.05}_{-0.05}$	-5.98 $^{+2.74}_{-2.68}$	637 $^{+106}_{-106}$	2.96 $^{+0.88}_{-0.57}$ $\times 10^{-6}$	0.3	2.2	2.6			
Pulse 2																	
20.683~24.672	32.54	0.23 $^{+0.02}_{-0.02}$	-1.06 $^{+0.06}_{-0.06}$	423 $^{+80}_{-82}$	397 $^{+79}_{-79}$	1.25 $^{+0.42}_{-0.28}$ $\times 10^{-6}$	0.23 $^{+0.02}_{-0.02}$	-1.05 $^{+0.06}_{-0.06}$	-5.44 $^{+2.80}_{-2.95}$	382 $^{+53}_{-54}$	1.30 $^{+0.37}_{-0.26}$ $\times 10^{-6}$	-0.3	2.2	2.4			
24.672~25.536	32.69	0.42 $^{+0.04}_{-0.04}$	-1.02 $^{+0.06}_{-0.06}$	537 $^{+111}_{-111}$	526 $^{+113}_{-117}$	3.17 $^{+1.28}_{-1.17}$ $\times 10^{-6}$	0.41 $^{+0.04}_{-0.04}$	-1.00 $^{+0.07}_{-0.07}$	-4.31 $^{+2.19}_{-2.19}$	486 $^{+89}_{-90}$	3.77 $^{+1.51}_{-1.51}$ $\times 10^{-6}$	-4.0	2.2	0.6			
25.536~28.190	43.48	0.50 $^{+0.03}_{-0.03}$	-1.27 $^{+0.05}_{-0.05}$	508 $^{+103}_{-103}$	371 $^{+80}_{-80}$	1.70 $^{+0.39}_{-0.31}$ $\times 10^{-6}$	0.49 $^{+0.03}_{-0.03}$	-1.26 $^{+0.05}_{-0.05}$	-5.46 $^{+2.98}_{-3.09}$	354 $^{+60}_{-61}$	1.78 $^{+0.48}_{-0.30}$ $\times 10^{-6}$	-0.7	2.4	2.2			
28.190~28.436	26.76	0.73 $^{+0.08}_{-0.08}$	-1.11 $^{+0.06}_{-0.06}$	1001 $^{+289}_{-289}$	891 $^{+256}_{-264}$	7.05 $^{+3.12}_{-2.12}$ $\times 10^{-6}$	0.72 $^{+0.08}_{-0.08}$	-1.10 $^{+0.06}_{-0.06}$	-6.20 $^{+2.60}_{-2.60}$	853 $^{+202}_{-203}$	7.18 $^{+2.47}_{-1.67}$ $\times 10^{-6}$	0.3	2.1	2.5			
28.436~28.969	64.01	1.13 $^{+0.06}_{-0.06}$	-1.08 $^{+0.03}_{-0.03}$	1342 $^{+229}_{-229}$	1234 $^{+214}_{-211}$	16.61 $^{+3.91}_{-2.87}$ $\times 10^{-6}$	1.08 $^{+0.07}_{-0.07}$	-1.04 $^{+0.04}_{-0.04}$	-3.13 $^{+0.90}_{-0.90}$	991 $^{+185}_{-185}$	17.32 $^{+4.46}_{-3.51}$ $\times 10^{-6}$	-9.6	2.7	0.0			
28.969~29.172	26.14	0.94 $^{+0.10}_{-0.10}$	-1.28 $^{+0.06}_{-0.06}$	4073 $^{+2887}_{-2853}$	2932 $^{+1736}_{-1711}$	11.79 $^{+7.26}_{-4.73}$ $\times 10^{-6}$	0.88 $^{+0.10}_{-0.10}$	-1.23 $^{+0.07}_{-0.07}$	-4.80 $^{+2.61}_{-2.61}$	1531 $^{+734}_{-662}$	10.03 $^{+3.36}_{-3.32}$ $\times 10^{-6}$	-3.2	0.9	-0.1			
29.172~30.574	37.51	0.47 $^{+0.03}_{-0.03}$	-1.16 $^{+0.05}_{-0.05}$	656 $^{+145}_{-150}$	551 $^{+126}_{-130}$	2.72 $^{+0.93}_{-0.64}$ $\times 10^{-6}$	0.47 $^{+0.04}_{-0.04}$	-1.15 $^{+0.05}_{-0.06}$	-5.27 $^{+2.78}_{-2.78}$	520 $^{+88}_{-94}$	2.87 $^{+0.88}_{-0.61}$ $\times 10^{-6}$	-1.0	2.1	2.0			
30.574~30.852	34.15	0.52 $^{+0.05}_{-0.05}$	-0.84 $^{+0.06}_{-0.06}$	695 $^{+116}_{-118}$	806 $^{+141}_{-143}$	10.51 $^{+3.71}_{-2.82}$ $\times 10^{-6}$	0.52 $^{+0.05}_{-0.05}$	-0.83 $^{+0.06}_{-0.06}$	-6.16 $^{+2.56}_{-2.61}$	798 $^{+106}_{-107}$	10.68 $^{+2.97}_{-2.28}$ $\times 10^{-6}$	0.2	2.5	2.7			
30.852~31.320	73.73	0.95 $^{+0.06}_{-0.06}$	-0.84 $^{+0.03}_{-0.03}$	753 $^{+84}_{-84}$	874 $^{+99}_{-100}$	21.22 $^{+4.79}_{-3.57}$ $\times 10^{-6}$	0.82 $^{+0.06}_{-0.06}$	-0.71 $^{+0.04}_{-0.04}$	-2.07 $^{+0.05}_{-0.05}$	587 $^{+55}_{-54}$	27.27 $^{+5.37}_{-5.37}$ $\times 10^{-6}$	-56.7	2.7	3.1			
31.320~31.802	62.69	1.10 $^{+0.07}_{-0.07}$	-0.97 $^{+0.04}_{-0.04}$	574 $^{+74}_{-73}$	591 $^{+79}_{-79}$	11.00 $^{+2.58}_{-2.08}$ $\times 10^{-6}$	1.03 $^{+0.07}_{-0.07}$	-0.89 $^{+0.06}_{-0.06}$	-2.32 $^{+0.25}_{-0.25}$	456 $^{+64}_{-65}$	14.30 $^{+3.84}_{-3.07}$ $\times 10^{-6}$	-13.1	2.7	2.9			
31.802~32.095	34.68	0.88 $^{+0.08}_{-0.08}$	-1.05 $^{+0.07}_{-0.07}$	433 $^{+93}_{-93}$	411 $^{+93}_{-94}$	5.14 $^{+1.81}_{-1.40}$ $\times 10^{-6}$	0.85 $^{+0.08}_{-0.09}$	-1.02 $^{+0.08}_{-0.09}$	-5.39 $^{+3.00}_{-3.09}$	381 $^{+66}_{-68}$	5.23 $^{+2.12}_{-1.23}$ $\times 10^{-6}$	-0.6	2.2	2.2			
32.095~32.793	34.34	0.71 $^{+0.06}_{-0.06}$	-1.25 $^{+0.07}_{-0.07}$	745 $^{+236}_{-206}$	558 $^{+195}_{-194}$	3.18 $^{+1.78}_{-1.57}$ $\times 10^{-6}$	0.69 $^{+0.06}_{-0.06}$	-1.22 $^{+0.07}_{-0.07}$	-5.05 $^{+2.78}_{-2.78}$	468 $^{+110}_{-112}$	3.33 $^{+1.25}_{-0.75}$ $\times 10^{-6}$	-0.1	-0.1	1.4			
32.793~33.445	20.13	0.42 $^{+0.05}_{-0.05}$	-1.16 $^{+0.11}_{-0.11}$	442 $^{+167}_{-174}$	371 $^{+149}_{-154}$	1.65 $^{+1.07}_{-0.62}$ $\times 10^{-6}$	0.39 $^{+0.06}_{-0.06}$	-1.07 $^{+0.15}_{-0.16}$	-4.77 $^{+2.59}_{-2.59}$	296 $^{+95}_{-99}$	1.72 $^{+1.15}_{-0.65}$ $\times 10^{-6}$	-2.6	-0.7	-1.7			
33.445~37.594	27.62	0.29 $^{+0.02}_{-0.02}$	-1.46 $^{+0.07}_{-0.07}$	1148 $^{+641}_{-558}$	620 $^{+356}_{-312}$	0.89 $^{+0.45}_{-0.26}$ $\times 10^{-6}$	0.29 $^{+0.02}_{-0.02}$	-1.46 $^{+0.07}_{-0.07}$	-5.87 $^{+2.89}_{-2.89}$	639 $^{+322}_{-294}$	0.90 $^{+0.43}_{-0.21}$ $\times 10^{-6}$	-0.2	-0.2	-0.4			
37.594~50.098	23.56	0.22 $^{+0.02}_{-0.02}$	-1.54 $^{+0.11}_{-0.11}$	274 $^{+106}_{-112}$	126 $^{+57}_{-60}$	0.26 $^{+0.10}_{-0.06}$ $\times 10^{-6}$	0.22 $^{+0.02}_{-0.02}$	-1.20 $^{+0.39}_{-0.38}$	-4.42 $^{+2.32}_{-2.32}$	86 $^{+33}_{-38}$	0.30 $^{+0.22}_{-0.10}$ $\times 10^{-6}$	-45.7	-0.4	-43.6			
Pulse 3	50.098~50.724	20.78	0.53 $^{+0.05}_{-0.05}$	-1.42 $^{+0.05}_{-0.06}$	3279 $^{+2079}_{-1537}$	1902 $^{+1217}_{-1083}$	3.16 $^{+1.63}_{-1.06}$	0.52 $^{+0.06}_{-0.06}$	-1.41 $^{+0.07}_{-0.07}$	-5.93 $^{+2.60}_{-2.71}$	1802 $^{+1167}_{-1044}$	3.18 $^{+1.62}_{-1.08}$ $\times 10^{-6}$	0.0	1.6	1.4		

Table A17 continued on next page

Table A17 (continued)

$t_{\text{start}} \sim t_{\text{stop}}$	S	Cutoff Power-Law Fitting						Band Fitting						Difference ΔDIC	
		K			E_p			K			E_p				
		(1)	(2)	(3)	(4)	(5)	(6)	(7)	(8)	(9)	(10)	(11)	(12)	(13)	(14)
50.724~51.699	50.98	0.72 $^{+0.04}_{-0.04}$	-1.13 $^{+0.04}_{-0.04}$	676 $^{+116}_{-115}$	588 $^{+105}_{-104}$	4.94 $^{+1.13}_{-0.94} \times 10^{-6}$	0.72 $^{+0.04}_{-0.04}$	-1.13 $^{+0.04}_{-0.04}$	-5.08 $^{+2.51}_{-3.05}$	571 $^{+76}_{-77}$	5.08 $^{+1.16}_{-0.87} \times 10^{-6}$	-1.2	2.5	2.2	
51.699~52.647	30.70	0.63 $^{+0.05}_{-0.05}$	-1.34 $^{+0.07}_{-0.07}$	720 $^{+238}_{-254}$	475 $^{+165}_{-175}$	2.17 $^{+0.89}_{-0.59} \times 10^{-6}$	0.63 $^{+0.05}_{-0.05}$	-1.33 $^{+0.07}_{-0.07}$	-6.05 $^{+2.78}_{-2.71}$	453 $^{+117}_{-127}$	2.17 $^{+0.73}_{-0.48} \times 10^{-6}$	0.8	1.1	1.9	
Pulse 4															
60.456~62.938	20.43	0.39 $^{+0.03}_{-0.03}$	-1.66 $^{+0.07}_{-0.07}$	1307 $^{+850}_{-756}$	444 $^{+303}_{-273}$	0.71 $^{+0.27}_{-0.18} \times 10^{-6}$	0.39 $^{+0.03}_{-0.03}$	-1.65 $^{+0.09}_{-0.09}$	-5.78 $^{+2.89}_{-2.84}$	478 $^{+355}_{-285}$	0.75 $^{+0.28}_{-0.19} \times 10^{-6}$	-1.1	1.1	-0.1	
62.938~63.454	20.45	0.47 $^{+0.06}_{-0.06}$	-1.21 $^{+0.11}_{-0.11}$	648 $^{+292}_{-286}$	512 $^{+241}_{-247}$	2.05 $^{+1.42}_{-1.73} \times 10^{-6}$	0.46 $^{+0.06}_{-0.06}$	-1.20 $^{+0.11}_{-0.11}$	-6.11 $^{+2.77}_{-2.69}$	472 $^{+153}_{-162}$	2.06 $^{+1.11}_{-0.56} \times 10^{-6}$	1.1	-0.8	0.4	
63.454~64.026	33.88	0.63 $^{+0.05}_{-0.05}$	-1.15 $^{+0.05}_{-0.05}$	867 $^{+199}_{-202}$	737 $^{+175}_{-177}$	4.78 $^{+1.69}_{-1.20} \times 10^{-6}$	0.63 $^{+0.05}_{-0.05}$	-1.15 $^{+0.05}_{-0.05}$	-6.43 $^{+2.48}_{-2.48}$	720 $^{+125}_{-130}$	4.75 $^{+1.37}_{-0.89} \times 10^{-6}$	0.4	2.4	2.8	
64.026~64.821	50.52	0.94 $^{+0.05}_{-0.05}$	-1.23 $^{+0.04}_{-0.04}$	985 $^{+186}_{-189}$	758 $^{+149}_{-151}$	6.17 $^{+1.50}_{-1.20} \times 10^{-6}$	0.94 $^{+0.05}_{-0.05}$	-1.23 $^{+0.03}_{-0.04}$	-6.36 $^{+2.43}_{-2.48}$	754 $^{+114}_{-116}$	6.14 $^{+1.07}_{-0.91} \times 10^{-6}$	0.4	2.6	2.9	
64.821~65.261	22.99	0.73 $^{+0.07}_{-0.07}$	-1.40 $^{+0.07}_{-0.07}$	1398 $^{+748}_{-694}$	839 $^{+459}_{-428}$	2.99 $^{+1.69}_{-0.95} \times 10^{-6}$	0.73 $^{+0.07}_{-0.08}$	-1.39 $^{+0.07}_{-0.07}$	-6.27 $^{+2.56}_{-2.58}$	808 $^{+358}_{-353}$	2.93 $^{+1.40}_{-0.74} \times 10^{-6}$	0.5	0.9	1.3	
Pulse 5															
65.261~67.264	29.01	0.45 $^{+0.04}_{-0.04}$	-1.40 $^{+0.07}_{-0.07}$	799 $^{+308}_{-311}$	479 $^{+193}_{-195}$	1.38 $^{+0.61}_{-0.36} \times 10^{-6}$	0.45 $^{+0.04}_{-0.04}$	-1.39 $^{+0.07}_{-0.07}$	-6.05 $^{+2.65}_{-2.63}$	446 $^{+135}_{-138}$	1.40 $^{+0.43}_{-0.30} \times 10^{-6}$	1.0	0.6	1.6	
67.264~67.529	27.06	0.54 $^{+0.07}_{-0.07}$	-0.89 $^{+0.09}_{-0.09}$	367 $^{+79}_{-80}$	407 $^{+94}_{-95}$	4.35 $^{+2.27}_{-2.39} \times 10^{-6}$	0.53 $^{+0.07}_{-0.07}$	-0.88 $^{+0.09}_{-0.09}$	-6.18 $^{+2.53}_{-2.59}$	397 $^{+59}_{-61}$	4.36 $^{+1.73}_{-1.08} \times 10^{-6}$	0.7	1.8	2.5	
67.529~68.236	28.76	0.55 $^{+0.05}_{-0.05}$	-1.11 $^{+0.08}_{-0.08}$	365 $^{+81}_{-82}$	324 $^{+78}_{-82}$	2.13 $^{+0.82}_{-0.82} \times 10^{-6}$	0.54 $^{+0.05}_{-0.05}$	-1.10 $^{+0.08}_{-0.08}$	-6.25 $^{+2.62}_{-2.62}$	308 $^{+46}_{-46}$	2.16 $^{+0.62}_{-0.43} \times 10^{-6}$	0.8	2.0	2.8	
68.236~68.345	23.62	0.52 $^{+0.05}_{-0.05}$	-1.44 $^{+0.08}_{-0.08}$	1152 $^{+710}_{-690}$	645 $^{+408}_{-348}$	1.65 $^{+0.97}_{-0.52} \times 10^{-6}$	0.43 $^{+0.05}_{-0.05}$	-0.96 $^{+0.05}_{-0.05}$	-2.10 $^{+0.09}_{-0.09}$	135 $^{+23}_{-18}$	1.73 $^{+0.60}_{-0.46} \times 10^{-6}$	-9.2	-0.2	-10.2	
69.345~69.522	23.06	0.22 $^{+0.05}_{-0.05}$	-0.45 $^{+0.11}_{-0.11}$	370 $^{+63}_{-63}$	573 $^{+105}_{-106}$	7.41 $^{+5.86}_{-2.85} \times 10^{-6}$	0.21 $^{+0.04}_{-0.04}$	-0.45 $^{+0.11}_{-0.10}$	-6.81 $^{+2.26}_{-2.25}$	561 $^{+61}_{-63}$	7.56 $^{+3.83}_{-2.26} \times 10^{-6}$	1.0	1.3	2.3	
69.522~70.045	56.87	0.69 $^{+0.05}_{-0.05}$	-0.83 $^{+0.04}_{-0.04}$	605 $^{+66}_{-67}$	707 $^{+81}_{-82}$	12.20 $^{+2.74}_{-2.12} \times 10^{-6}$	0.69 $^{+0.05}_{-0.05}$	-0.83 $^{+0.04}_{-0.04}$	-6.03 $^{+2.58}_{-2.58}$	693 $^{+57}_{-59}$	12.40 $^{+2.27}_{-1.89} \times 10^{-6}$	-0.0	2.7	2.9	
70.045~70.559	44.95	0.74 $^{+0.06}_{-0.06}$	-0.98 $^{+0.05}_{-0.05}$	524 $^{+84}_{-88}$	534 $^{+89}_{-88}$	6.48 $^{+1.89}_{-1.37} \times 10^{-6}$	0.74 $^{+0.06}_{-0.06}$	-0.98 $^{+0.05}_{-0.05}$	-5.69 $^{+2.64}_{-2.88}$	521 $^{+63}_{-63}$	6.67 $^{+1.48}_{-1.25} \times 10^{-6}$	-0.4	2.6	2.6	
70.559~70.903	28.30	0.69 $^{+0.08}_{-0.08}$	-1.02 $^{+0.09}_{-0.09}$	283 $^{+63}_{-65}$	277 $^{+67}_{-69}$	2.80 $^{+1.37}_{-0.81} \times 10^{-6}$	0.68 $^{+0.08}_{-0.08}$	-0.99 $^{+0.10}_{-0.10}$	-6.06 $^{+2.74}_{-2.71}$	257 $^{+39}_{-38}$	2.85 $^{+1.06}_{-0.66} \times 10^{-6}$	0.7	1.9	2.7	
70.903~71.772	29.85	0.48 $^{+0.05}_{-0.05}$	-1.12 $^{+0.08}_{-0.08}$	360 $^{+88}_{-90}$	317 $^{+82}_{-84}$	1.86 $^{+0.79}_{-0.51} \times 10^{-6}$	0.48 $^{+0.05}_{-0.05}$	-1.11 $^{+0.09}_{-0.08}$	-6.06 $^{+2.74}_{-2.74}$	299 $^{+49}_{-52}$	1.88 $^{+0.61}_{-0.35} \times 10^{-6}$	0.7	1.8	2.5	
Pulse 6															
75.336~77.703	32.49	0.46 $^{+0.03}_{-0.03}$	-1.25 $^{+0.08}_{-0.08}$	215 $^{+44}_{-45}$	162 $^{+37}_{-38}$	0.85 $^{+0.25}_{-0.18} \times 10^{-6}$	0.45 $^{+0.03}_{-0.03}$	-1.23 $^{+0.08}_{-0.08}$	-6.37 $^{+2.55}_{-2.52}$	156 $^{+19}_{-19}$	0.86 $^{+0.15}_{-0.11} \times 10^{-6}$	0.8	2.1	3.0	
77.703~78.987	38.54	0.70 $^{+0.06}_{-0.05}$	-1.30 $^{+0.06}_{-0.05}$	399 $^{+89}_{-92}$	279 $^{+67}_{-69}$	1.80 $^{+0.56}_{-0.35} \times 10^{-6}$	0.69 $^{+0.04}_{-0.05}$	-1.30 $^{+0.06}_{-0.06}$	-6.00 $^{+2.65}_{-2.68}$	267 $^{+39}_{-40}$	1.83 $^{+0.25}_{-0.25} \times 10^{-6}$	0.5	2.2	2.8	

Note—All columns are the same as Table A2 but for GRB 130504978.

Table A18. Time-resolved Spectral Fit Results of GRB 130606497

$t_{\text{start}} \sim t_{\text{stop}}$	S	Cutoff Power-Law Fitting						Band Fitting						Difference			
		K	α	E_c	E_p	F	K	α	β	E_p	F	ΔDIC	$p_{\text{CPL}}^{\text{Band}}$	$p_{\text{DIC}}^{\text{Band}}$			
(1)	(2)	(3)	(4)	(5)	(6)	(7)	(8)	(9)	(10)	(11)	(12)	(13)	(14)	(15)			
Pulse 1																	
2.568~5.174	41.00	$0.20^{+0.02}_{-0.02}$	$-0.78^{+0.05}_{-0.05}$	545^{+69}_{-68}	665^{+89}_{-88}	$3.82^{+1.19}_{-0.81} \times 10^{-6}$	$0.18^{+0.02}_{-0.02}$	$-0.67^{+0.07}_{-0.07}$	$-2.30^{+0.21}_{-0.10}$	512^{+64}_{-64}	$4.97^{+1.75}_{-1.16} \times 10^{-6}$	-15.0	2.6	2.6			
5.174~5.687	28.66	$0.45^{+0.05}_{-0.05}$	$-0.98^{+0.06}_{-0.06}$	784^{+175}_{-176}	800^{+185}_{-185}	$5.87^{+2.71}_{-2.71} \times 10^{-6}$	$0.44^{+0.05}_{-0.05}$	$-0.96^{+0.07}_{-0.07}$	$-5.35^{+2.85}_{-2.85}$	746^{+147}_{-147}	$6.17^{+2.60}_{-2.60} \times 10^{-6}$	-0.8	2.3	2.1			
5.687~7.664	38.79	$0.24^{+0.02}_{-0.02}$	$-0.72^{+0.06}_{-0.06}$	209^{+34}_{-34}	383^{+47}_{-47}	$2.67^{+0.78}_{-0.59} \times 10^{-6}$	$0.23^{+0.02}_{-0.02}$	$-0.68^{+0.07}_{-0.07}$	$-3.90^{+1.53}_{-2.51}$	355^{+36}_{-37}	$3.07^{+1.10}_{-0.78} \times 10^{-6}$	-5.8	2.6	0.2			
7.664~8.092	31.22	$0.45^{+0.05}_{-0.05}$	$-0.83^{+0.07}_{-0.07}$	497^{+103}_{-103}	582^{+125}_{-125}	$6.06^{+2.95}_{-1.83} \times 10^{-6}$	$0.37^{+0.06}_{-0.06}$	$-0.65^{+0.11}_{-0.11}$	$-2.14^{+0.11}_{-0.10}$	384^{+62}_{-63}	$8.48^{+3.67}_{-2.59} \times 10^{-6}$	-16.9	2.0	2.1			
8.092~8.845	55.95	$0.64^{+0.04}_{-0.04}$	$-0.82^{+0.04}_{-0.04}$	467^{+47}_{-46}	551^{+58}_{-58}	$8.88^{+2.05}_{-1.58} \times 10^{-6}$	$0.59^{+0.05}_{-0.05}$	$-0.74^{+0.05}_{-0.05}$	$-2.31^{+0.14}_{-0.14}$	448^{+47}_{-47}	$11.75^{+2.89}_{-2.53} \times 10^{-6}$	-16.2	2.8	3.7			
8.845~9.090	43.37	$1.23^{+0.09}_{-0.09}$	$-1.07^{+0.03}_{-0.03}$	1896^{+319}_{-323}	1764^{+302}_{-302}	$25.95^{+7.36}_{-4.98} \times 10^{-6}$	$1.01^{+0.09}_{-0.09}$	$-0.92^{+0.05}_{-0.05}$	$-2.13^{+0.10}_{-0.10}$	840^{+135}_{-135}	$24.49^{+6.90}_{-4.99} \times 10^{-6}$	-23.2	2.9	3.1			
9.090~9.280	55.66	$1.81^{+0.11}_{-0.11}$	$-1.05^{+0.02}_{-0.03}$	2750^{+376}_{-376}	2613^{+361}_{-364}	$58.34^{+11.42}_{-9.55} \times 10^{-6}$	$1.58^{+0.12}_{-0.12}$	$-0.97^{+0.04}_{-0.04}$	$-2.12^{+0.09}_{-0.09}$	1502^{+232}_{-231}	$53.48^{+11.80}_{-9.19} \times 10^{-6}$	-37.3	2.9	3.1			
9.280~9.738	73.73	$1.57^{+0.07}_{-0.06}$	$-1.05^{+0.02}_{-0.02}$	2389^{+204}_{-204}	2270^{+200}_{-199}	$45.53^{+5.43}_{-5.56} \times 10^{-6}$	$1.25^{+0.07}_{-0.07}$	$-0.88^{+0.03}_{-0.03}$	$-2.04^{+0.03}_{-0.03}$	938^{+94}_{-94}	$40.13^{+6.50}_{-5.88} \times 10^{-6}$	-65.4	3.0	3.0			
9.738~9.907	58.77	$1.87^{+0.11}_{-0.12}$	$-0.98^{+0.03}_{-0.03}$	1887^{+206}_{-207}	1924^{+218}_{-219}	$60.03^{+12.18}_{-9.00} \times 10^{-6}$	$1.55^{+0.13}_{-0.13}$	$-0.85^{+0.05}_{-0.05}$	$-2.23^{+0.13}_{-0.13}$	1062^{+171}_{-172}	$55.07^{+15.92}_{-11.84} \times 10^{-6}$	-23.0	3.0	3.2			
9.907~10.355	74.79	$1.52^{+0.07}_{-0.07}$	$-1.00^{+0.02}_{-0.02}$	1333^{+145}_{-145}	1333^{+147}_{-147}	$31.87^{+5.71}_{-4.53} \times 10^{-6}$	$1.23^{+0.07}_{-0.07}$	$-0.83^{+0.04}_{-0.04}$	$-2.07^{+0.05}_{-0.05}$	668^{+62}_{-64}	$33.21^{+6.09}_{-4.70} \times 10^{-6}$	-78.1	2.9	3.3			
10.355~11.526	88.92	$0.96^{+0.04}_{-0.04}$	$-0.87^{+0.02}_{-0.02}$	527^{+37}_{-37}	596^{+43}_{-43}	$12.75^{+1.79}_{-1.46} \times 10^{-6}$	$0.87^{+0.04}_{-0.04}$	$-0.77^{+0.03}_{-0.03}$	$-2.29^{+0.09}_{-0.09}$	458^{+31}_{-31}	$16.19^{+2.55}_{-2.11} \times 10^{-6}$	-42.1	2.9	3.9			
Pulse 2																	
11.526~12.552	76.16	$0.88^{+0.04}_{-0.04}$	$-0.90^{+0.03}_{-0.03}$	597^{+49}_{-50}	657^{+57}_{-57}	$11.92^{+1.89}_{-1.49} \times 10^{-6}$	$0.82^{+0.04}_{-0.04}$	$-0.84^{+0.03}_{-0.03}$	$-2.33^{+0.12}_{-0.11}$	548^{+43}_{-43}	$15.04^{+2.41}_{-2.09} \times 10^{-6}$	-25.0	2.9	3.9			
12.552~12.788	46.17	$1.33^{+0.09}_{-0.09}$	$-1.04^{+0.03}_{-0.03}$	1857^{+277}_{-277}	1783^{+272}_{-272}	$32.02^{+7.68}_{-7.68} \times 10^{-6}$	$1.11^{+0.10}_{-0.09}$	$-0.90^{+0.05}_{-0.05}$	$-2.09^{+0.07}_{-0.07}$	903^{+133}_{-133}	$31.02^{+7.23}_{-6.52} \times 10^{-6}$	-36.4	2.9	3.0			
12.788~12.988	51.73	$1.78^{+0.10}_{-0.10}$	$-1.11^{+0.02}_{-0.02}$	4005^{+510}_{-510}	3565^{+460}_{-461}	$57.67^{+9.81}_{-7.98} \times 10^{-6}$	$1.42^{+0.11}_{-0.11}$	$-0.96^{+0.04}_{-0.04}$	$-2.04^{+0.03}_{-0.03}$	1309^{+206}_{-206}	$45.01^{+11.48}_{-8.09} \times 10^{-6}$	-32.3	3.0	2.8			
12.988~13.173	36.90	$1.11^{+0.09}_{-0.09}$	$-0.99^{+0.04}_{-0.04}$	1644^{+275}_{-279}	1661^{+286}_{-289}	$30.47^{+8.70}_{-7.41} \times 10^{-6}$	$0.92^{+0.10}_{-0.10}$	$-0.86^{+0.06}_{-0.06}$	$-2.20^{+0.15}_{-0.15}$	943^{+175}_{-175}	$28.77^{+9.80}_{-6.66} \times 10^{-6}$	-17.4	2.8	3.0			
13.173~14.069	99.58	$1.66^{+0.05}_{-0.05}$	$-1.10^{+0.01}_{-0.01}$	2366^{+187}_{-186}	2129^{+170}_{-169}	$38.69^{+4.29}_{-3.79} \times 10^{-6}$	$1.34^{+0.05}_{-0.05}$	$-0.94^{+0.02}_{-0.02}$	$-2.01^{+0.01}_{-0.01}$	887^{+63}_{-64}	$35.09^{+3.66}_{-3.56} \times 10^{-6}$	-178.7	3.0	3.0			
14.069~14.542	85.50	$2.42^{+0.08}_{-0.08}$	$-1.21^{+0.01}_{-0.01}$	4671^{+469}_{-469}	3690^{+379}_{-373}	$52.49^{+5.56}_{-4.79} \times 10^{-6}$	$2.21^{+0.09}_{-0.09}$	$-1.15^{+0.02}_{-0.02}$	$-2.06^{+0.05}_{-0.05}$	1889^{+235}_{-233}	$45.57^{+5.41}_{-5.18} \times 10^{-6}$	-42.7	3.0	3.1			
14.542~15.395	89.33	$2.03^{+0.06}_{-0.06}$	$-1.26^{+0.01}_{-0.01}$	3590^{+402}_{-402}	2657^{+299}_{-305}	$30.08^{+3.12}_{-2.79} \times 10^{-6}$	$1.87^{+0.07}_{-0.07}$	$-1.19^{+0.02}_{-0.02}$	$-2.06^{+0.05}_{-0.05}$	1365^{+166}_{-167}	$27.25^{+2.98}_{-2.87} \times 10^{-6}$	-50.0	2.9	3.1			
15.395~16.264	72.02	$1.69^{+0.07}_{-0.07}$	$-1.30^{+0.02}_{-0.02}$	1670^{+255}_{-255}	1169^{+182}_{-183}	$12.45^{+2.00}_{-1.70} \times 10^{-6}$	$1.68^{+0.07}_{-0.07}$	$-1.29^{+0.02}_{-0.02}$	$-4.41^{+1.93}_{-2.94} \times 10^{-6}$	1111^{+158}_{-159}	$12.69^{+1.93}_{-1.56} \times 10^{-6}$	-3.6	2.9	1.5			
16.264~17.499	73.58	$1.67^{+0.06}_{-0.06}$	$-1.37^{+0.02}_{-0.02}$	1205^{+185}_{-186}	759^{+119}_{-120}	$7.68^{+1.11}_{-0.94} \times 10^{-6}$	$1.67^{+0.06}_{-0.06}$	$-1.37^{+0.02}_{-0.02}$	$-6.61^{+2.39}_{-2.39}$	752^{+93}_{-94}	$7.68^{+0.85}_{-0.70} \times 10^{-6}$	0.2	2.8	3.0			
17.499~19.230	69.49	$1.42^{+0.05}_{-0.05}$	$-1.43^{+0.03}_{-0.03}$	979^{+173}_{-174}	558^{+103}_{-103}	$4.62^{+0.70}_{-0.52} \times 10^{-6}$	$1.42^{+0.05}_{-0.05}$	$-1.43^{+0.03}_{-0.03}$	$-6.34^{+2.43}_{-2.47}$	547^{+74}_{-75}	$4.66^{+0.47}_{-0.47} \times 10^{-6}$	0.2	2.8	3.0			
19.230~20.785	43.21	$1.18^{+0.06}_{-0.06}$	$-1.59^{+0.06}_{-0.06}$	410^{+107}_{-111}	168^{+50}_{-52}	$1.66^{+0.25}_{-0.25} \times 10^{-6}$	$1.18^{+0.06}_{-0.06}$	$-1.58^{+0.06}_{-0.06}$	$-6.46^{+2.48}_{-2.44}$	160^{+25}_{-26}	$1.66^{+0.16}_{-0.16} \times 10^{-6}$	0.8	2.2	3.0			
20.785~23.209	37.31	$1.06^{+0.05}_{-0.05}$	$-1.87^{+0.06}_{-0.06}$	1060^{+722}_{-589}	138^{+113}_{-100}	$1.23^{+0.25}_{-0.19} \times 10^{-6}$	$0.02^{+0.00}_{-0.00}$	$-1.81^{+0.08}_{-0.08}$	$-5.57^{+3.03}_{-3.05}$	98^{+28}_{-25}	$1.18^{+0.41}_{-0.31} \times 10^{-6}$	-3.8	0.6	1.3			
Pulse 3																	
23.209~28.671	38.24	$0.70^{+0.03}_{-0.03}$	$-1.67^{+0.08}_{-0.08}$	256^{+77}_{-83}	84^{+33}_{-34}	$0.71^{+0.16}_{-0.11} \times 10^{-6}$	$0.01^{+0.00}_{-0.00}$	$-1.75^{+0.06}_{-0.06}$	$-6.13^{+2.65}_{-2.65}$	111^{+18}_{-9}	$0.80^{+0.15}_{-0.13} \times 10^{-6}$	2.7	0.9	1.6			
28.671~31.747	38.17	$0.56^{+0.03}_{-0.03}$	$-1.45^{+0.05}_{-0.05}$	589^{+151}_{-153}	324^{+88}_{-92}	$1.27^{+0.31}_{-0.22} \times 10^{-6}$	$0.55^{+0.03}_{-0.03}$	$-1.44^{+0.05}_{-0.05}$	$-6.36^{+2.49}_{-2.46}$	314^{+57}_{-61}	$1.28^{+0.18}_{-0.18} \times 10^{-6}$	0.7	2.3	2.9			

Table A18 continued on next page

Table A18 (continued)

$t_{\text{start}} \sim t_{\text{stop}}$	S	Cutoff Power-Law Fitting						Band Fitting						Difference	
		K	α	E_c	E_p	F	K	α	β	E_p	F	ΔDIC	p_{CPL}	p_{Band}	
(1)	(2)	(3)	(4)	(5)	(6)	(7)	(8)	(9)	(10)	(11)	(12)	(13)	(14)	(15)	
31.747~36.141	33.76	$0.47^{+0.03}_{-0.03}$	$-1.43^{+0.08}_{-0.08}$	278^{+69}_{-73}	158^{+45}_{-47}	$0.72^{+0.19}_{-0.14} \times 10^{-6}$	$0.46^{+0.03}_{-0.03}$	$-1.38^{+0.10}_{-0.11}$	$-5.04^{+2.80}_{-3.24}$	138^{+27}_{-29}	$0.75^{+0.28}_{-0.15} \times 10^{-6}$	-1.5	1.9	1.4	
36.141~37.288	36.11	$0.54^{+0.04}_{-0.04}$	$-1.09^{+0.05}_{-0.05}$	457^{+74}_{-76}	416^{+71}_{-71}	$2.96^{+0.76}_{-0.63} \times 10^{-6}$	$0.54^{+0.04}_{-0.04}$	$-1.09^{+0.05}_{-0.05}$	$-6.42^{+2.49}_{-2.48}$	407^{+49}_{-48}	$2.93^{+0.56}_{-0.48} \times 10^{-6}$	0.3	2.7	3.0	
37.288~38.214	51.42	$0.65^{+0.04}_{-0.04}$	$-0.92^{+0.04}_{-0.04}$	462^{+47}_{-48}	499^{+54}_{-55}	$6.18^{+1.35}_{-1.00} \times 10^{-6}$	$0.65^{+0.04}_{-0.04}$	$-0.92^{+0.04}_{-0.04}$	$-6.40^{+2.33}_{-2.40}$	495^{+37}_{-36}	$6.29^{+1.02}_{-0.81} \times 10^{-6}$	0.3	2.9	3.0	
38.214~39.561	47.89	$0.53^{+0.04}_{-0.04}$	$-0.92^{+0.04}_{-0.04}$	369^{+45}_{-40}	399^{+45}_{-46}	$4.01^{+0.88}_{-0.66} \times 10^{-6}$	$0.53^{+0.04}_{-0.04}$	$-0.91^{+0.04}_{-0.05}$	$-5.99^{+2.65}_{-2.68}$	394^{+31}_{-31}	$4.08^{+0.77}_{-0.54} \times 10^{-6}$	0.1	2.8	3.0	
39.561~40.154	51.76	$0.74^{+0.05}_{-0.05}$	$-0.84^{+0.04}_{-0.04}$	408^{+45}_{-45}	474^{+54}_{-54}	$8.11^{+1.97}_{-1.52} \times 10^{-6}$	$0.69^{+0.06}_{-0.06}$	$-0.75^{+0.06}_{-0.06}$	$-2.38^{+0.20}_{-0.14}$	388^{+41}_{-41}	$10.74^{+2.65}_{-2.26} \times 10^{-6}$	-12.2	2.8	3.5	
40.154~40.691	39.02	$0.72^{+0.06}_{-0.06}$	$-0.85^{+0.07}_{-0.07}$	236^{+32}_{-32}	271^{+40}_{-40}	$4.00^{+1.32}_{-0.89} \times 10^{-6}$	$0.66^{+0.06}_{-0.06}$	$-0.71^{+0.07}_{-0.09}$	$-2.34^{+0.24}_{-0.12}$	214^{+26}_{-26}	$5.88^{+1.94}_{-1.51} \times 10^{-6}$	-11.0	2.6	3.1	
40.691~42.885	65.04	$0.71^{+0.03}_{-0.03}$	$-0.96^{+0.04}_{-0.04}$	232^{+22}_{-19}	241^{+22}_{-19}	$2.91^{+0.47}_{-0.37} \times 10^{-6}$	$0.71^{+0.04}_{-0.04}$	$-0.95^{+0.04}_{-0.04}$	$-5.49^{+2.39}_{-2.83}$	238^{+13}_{-13}	$3.02^{+0.37}_{-0.31} \times 10^{-6}$	-1.1	2.9	2.5	
42.885~49.746	81.33	$0.54^{+0.02}_{-0.02}$	$-0.91^{+0.03}_{-0.03}$	162^{+10}_{-10}	176^{+12}_{-12}	$1.73^{+0.21}_{-0.18} \times 10^{-6}$	$0.54^{+0.02}_{-0.02}$	$-0.90^{+0.04}_{-0.04}$	$-5.19^{+2.12}_{-2.89}$	174^{+7}_{-7}	$1.78^{+0.20}_{-0.14} \times 10^{-6}$	-2.3	2.9	1.8	
Pulse 4															
49.746~51.162	76.37	$0.12^{+0.00}_{-0.00}$	$-0.82^{+0.03}_{-0.03}$	294^{+20}_{-20}	347^{+25}_{-25}	$6.18^{+0.59}_{-0.56} \times 10^{-6}$	$0.72^{+0.04}_{-0.04}$	$-0.75^{+0.05}_{-0.05}$	$-2.81^{+0.41}_{-0.09}$	305^{+24}_{-23}	$7.25^{+1.51}_{-1.21} \times 10^{-6}$	-9.4	2.9	1.9	
51.162~52.078	78.76	$0.18^{+0.01}_{-0.01}$	$-0.70^{+0.03}_{-0.03}$	233^{+14}_{-14}	303^{+19}_{-19}	$7.69^{+0.71}_{-0.65} \times 10^{-6}$	$0.88^{+0.05}_{-0.05}$	$-0.67^{+0.05}_{-0.05}$	$-4.16^{+1.49}_{-2.47}$	287^{+19}_{-20}	$8.31^{+1.75}_{-1.31} \times 10^{-6}$	-4.9	3.0	-0.3	
52.078~52.769	52.08	$0.13^{+0.01}_{-0.01}$	$-0.78^{+0.05}_{-0.05}$	220^{+20}_{-20}	268^{+27}_{-27}	$4.98^{+0.67}_{-0.67} \times 10^{-6}$	$0.79^{+0.05}_{-0.05}$	$-0.77^{+0.05}_{-0.05}$	$-5.66^{+2.62}_{-2.97}$	261^{+17}_{-17}	$5.09^{+1.01}_{-0.70} \times 10^{-6}$	0.4	2.8	2.4	
52.769~55.034	67.36	$0.09^{+0.00}_{-0.00}$	$-0.83^{+0.04}_{-0.04}$	229^{+17}_{-17}	268^{+22}_{-21}	$3.37^{+0.36}_{-0.33} \times 10^{-6}$	$0.59^{+0.03}_{-0.03}$	$-0.82^{+0.04}_{-0.04}$	$-5.21^{+2.31}_{-2.88}$	261^{+14}_{-14}	$3.56^{+0.60}_{-0.41} \times 10^{-6}$	-0.2	2.9	2.1	
55.034~57.681	50.38	$0.07^{+0.01}_{-0.01}$	$-0.89^{+0.06}_{-0.06}$	148^{+14}_{-13}	164^{+18}_{-17}	$1.55^{+0.21}_{-0.19} \times 10^{-6}$	$0.51^{+0.03}_{-0.03}$	$-0.88^{+0.06}_{-0.05}$	$-6.48^{+2.31}_{-2.35}$	163^{+8}_{-8}	$1.55^{+0.18}_{-0.16} \times 10^{-6}$	2.1	2.8	3.1	
57.681~59.514	32.25	$0.05^{+0.01}_{-0.01}$	$-0.98^{+0.09}_{-0.09}$	132^{+20}_{-20}	135^{+24}_{-24}	$0.99^{+0.27}_{-0.18} \times 10^{-6}$	$0.46^{+0.04}_{-0.04}$	$-0.97^{+0.10}_{-0.11}$	$-5.82^{+2.79}_{-2.81}$	130^{+13}_{-12}	$1.02^{+0.24}_{-0.17} \times 10^{-6}$	2.4	2.1	2.7	
59.514~62.237	30.08	$0.04^{+0.01}_{-0.01}$	$-1.01^{+0.13}_{-0.13}$	98^{+19}_{-23}	97^{+22}_{-23}	$0.63^{+0.27}_{-0.17} \times 10^{-6}$	$0.39^{+0.04}_{-0.04}$	$-0.60^{+0.27}_{-0.27}$	$-2.64^{+0.35}_{-0.06}$	71^{+10}_{-10}	$0.80^{+0.37}_{-0.23} \times 10^{-6}$	-5.6	-0.7	2.0	

Note—All columns are the same as Table A2 but for GRB 130606497.

Table A19. Time-resolved Spectral Fit Results of GRB 131014215

$t_{\text{start}} \sim t_{\text{stop}}$	S	Cutoff Power-Law Fitting						Band Fitting						Difference	
		K	α	E_c	E_p	F	K	α	β	E_p	F	ΔDIC	$p_{\text{DIC}}^{\text{CPL}}$	$p_{\text{DIC}}^{\text{Band}}$	
(1)	(2)	(3)	(4)	(5)	(6)	(7)	(8)	(9)	(10)	(11)	(12)	(13)	(14)	(15)	
Pulse 1															
0.064~0.274	27.86	$0.07^{+0.02}_{-0.02}$	$0.14^{+0.11}_{-0.04}$	287^{+32}_{-32}	614^{+76}_{-75}	$14.26^{+9.25}_{-9.25} \times 10^{-6}$	$0.07^{+0.02}_{-0.02}$	$0.15^{+0.11}_{-0.11}$	$-6.57^{+2.38}_{-2.32}$	605^{+43}_{-43}	$14.03^{+8.58}_{-4.48} \times 10^{-6}$	0.7	0.5	1.0	
0.274~0.966	73.93	$0.43^{+0.03}_{-0.03}$	$0.09^{+0.04}_{-0.04}$	125^{+6}_{-6}	238^{+12}_{-12}	$8.06^{+1.38}_{-1.16} \times 10^{-6}$	$0.39^{+0.03}_{-0.03}$	$0.02^{+0.06}_{-0.06}$	$-2.81^{+0.21}_{-0.20}$	2.15^{+9}_{-9}	$9.92^{+2.26}_{-1.63} \times 10^{-6}$	-17.0	2.8	3.8	
0.966~1.101	53.68	$0.76^{+0.07}_{-0.07}$	$-0.22^{+0.06}_{-0.06}$	184^{+13}_{-13}	327^{+25}_{-25}	$20.01^{+5.43}_{-5.36} \times 10^{-6}$	$0.75^{+0.07}_{-0.07}$	$-0.20^{+0.06}_{-0.06}$	$-6.16^{+2.56}_{-2.62}$	321^{+17}_{-16}	$20.63^{+3.84}_{-3.84} \times 10^{-6}$	-0.1	2.8	2.8	
1.101~1.210	60.68	$0.87^{+0.08}_{-0.07}$	$-0.11^{+0.06}_{-0.06}$	171^{+11}_{-11}	324^{+23}_{-22}	$28.39^{+7.14}_{-5.92} \times 10^{-6}$	$0.92^{+0.05}_{-0.05}$	$-0.14^{+0.03}_{-0.03}$	$-4.16^{+1.27}_{-1.14}$	318^{+13}_{-13}	$31.77^{+4.91}_{-4.49} \times 10^{-6}$	-7.4	2.8	-0.3	
1.210~1.281	63.90	$1.04^{+0.09}_{-0.09}$	$-0.17^{+0.05}_{-0.05}$	248^{+16}_{-16}	454^{+31}_{-31}	$53.79^{+13.76}_{-10.77} \times 10^{-6}$	$1.03^{+0.10}_{-0.10}$	$-0.17^{+0.05}_{-0.05}$	$-6.15^{+2.36}_{-2.52}$	448^{+21}_{-21}	$55.47^{+11.87}_{-9.38} \times 10^{-6}$	-0.1	2.7	2.7	
1.283~1.339	57.43	$1.11^{+0.11}_{-0.11}$	$-0.13^{+0.06}_{-0.06}$	206^{+14}_{-14}	385^{+29}_{-29}	$48.36^{+14.79}_{-10.74} \times 10^{-6}$	$1.08^{+0.11}_{-0.11}$	$-0.11^{+0.06}_{-0.06}$	$-5.75^{+2.48}_{-2.82}$	376^{+21}_{-20}	$49.76^{+13.44}_{-9.39} \times 10^{-6}$	-1.2	2.7	2.1	
1.339~1.448	65.48	$1.12^{+0.08}_{-0.08}$	$-0.28^{+0.05}_{-0.05}$	235^{+15}_{-15}	404^{+28}_{-27}	$36.72^{+8.45}_{-6.87} \times 10^{-6}$	$1.00^{+0.09}_{-0.09}$	$-0.17^{+0.07}_{-0.07}$	$-2.59^{+0.18}_{-0.18}$	345^{+22}_{-22}	$45.99^{+12.27}_{-8.88} \times 10^{-6}$	-13.9	2.8	3.7	
1.448~1.506	73.77	$1.22^{+0.10}_{-0.10}$	$-0.19^{+0.04}_{-0.04}$	345^{+20}_{-20}	624^{+38}_{-38}	$109.70^{+25.73}_{-20.31} \times 10^{-6}$	$1.19^{+0.11}_{-0.11}$	$-0.17^{+0.05}_{-0.05}$	$-5.29^{+2.04}_{-2.04}$	608^{+29}_{-29}	$114.50^{+21.76}_{-19.39} \times 10^{-6}$	-2.4	2.8	1.7	
1.506~1.612	128.93	$1.25^{+0.07}_{-0.07}$	$-0.04^{+0.03}_{-0.03}$	323^{+10}_{-10}	632^{+22}_{-23}	$174.90^{+24.64}_{-20.02} \times 10^{-6}$	$1.24^{+0.07}_{-0.07}$	$-0.04^{+0.03}_{-0.03}$	$-6.48^{+2.03}_{-2.31}$	627^{+14}_{-14}	$177.60^{+20.22}_{-18.47} \times 10^{-6}$	-0.5	2.9	2.7	
1.612~1.876	235.76	$2.03^{+0.06}_{-0.06}$	$-0.12^{+0.01}_{-0.01}$	308^{+6}_{-6}	579^{+12}_{-12}	$194.80^{+14.34}_{-13.90} \times 10^{-6}$	$1.71^{+0.06}_{-0.06}$	$0.01^{+0.02}_{-0.02}$	$-2.67^{+0.05}_{-0.05}$	492^{+9}_{-9}	$232.70^{+17.53}_{-17.48} \times 10^{-6}$	-261.0	3.0	3.9	
1.876~2.226	231.08	$2.23^{+0.06}_{-0.06}$	$-0.11^{+0.01}_{-0.01}$	202^{+4}_{-4}	382^{+7}_{-7}	$101.50^{+6.76}_{-6.81} \times 10^{-6}$	$2.06^{+0.06}_{-0.06}$	$-0.04^{+0.02}_{-0.02}$	$-3.11^{+0.10}_{-0.10}$	354^{+6}_{-6}	$113.30^{+22.27}_{-7.85} \times 10^{-6}$	-57.8	2.9	4.0	
2.226~2.301	88.35	$2.55^{+0.15}_{-0.15}$	$-0.23^{+0.04}_{-0.04}$	170^{+8}_{-8}	300^{+16}_{-16}	$56.95^{+8.24}_{-8.52} \times 10^{-6}$	$2.44^{+0.18}_{-0.18}$	$-0.19^{+0.06}_{-0.06}$	$-4.90^{+1.89}_{-2.97}$	287^{+15}_{-15}	$59.02^{+12.50}_{-10.76} \times 10^{-6}$	-5.2	2.9	-0.3	
2.301~2.343	53.97	$2.39^{+0.22}_{-0.22}$	$-0.21^{+0.07}_{-0.07}$	124^{+10}_{-10}	221^{+19}_{-19}	$30.82^{+9.50}_{-6.38} \times 10^{-6}$	$2.10^{+0.24}_{-0.24}$	$-0.04^{+0.11}_{-0.11}$	$-2.79^{+0.30}_{-0.22}$	189^{+14}_{-14}	$38.19^{+14.60}_{-9.08} \times 10^{-6}$	-10.6	2.7	3.7	
2.343~2.404	45.12	$2.15^{+0.20}_{-0.20}$	$-0.23^{+0.08}_{-0.08}$	86^{+7}_{-7}	153^{+15}_{-15}	$14.02^{+3.99}_{-3.52} \times 10^{-6}$	$1.99^{+0.21}_{-0.21}$	$-0.09^{+0.13}_{-0.13}$	$-3.47^{+0.81}_{-0.81}$	137^{+11}_{-11}	$16.19^{+5.61}_{-4.21} \times 10^{-6}$	-8.2	2.8	0.9	
2.404~2.484	41.79	$1.93^{+0.17}_{-0.18}$	$-0.18^{+0.10}_{-0.10}$	68^{+6}_{-6}	125^{+13}_{-13}	$9.43^{+3.11}_{-2.28} \times 10^{-6}$	$1.59^{+0.18}_{-0.17}$	$0.23^{+0.15}_{-0.16}$	$-2.74^{+0.16}_{-0.16}$	100^{+6}_{-6}	$11.66^{+3.38}_{-2.83} \times 10^{-6}$	-19.7	2.7	3.8	
Pulse 2															
2.484~2.546	55.96	$1.71^{+0.16}_{-0.16}$	$-0.02^{+0.07}_{-0.07}$	91^{+6}_{-6}	180^{+13}_{-13}	$21.36^{+6.45}_{-4.79} \times 10^{-6}$	$1.69^{+0.16}_{-0.16}$	$-0.00^{+0.08}_{-0.08}$	$-6.32^{+2.24}_{-2.41}$	178^{+6}_{-6}	$21.49^{+4.16}_{-3.34} \times 10^{-6}$	-0.3	2.8	2.7	
2.546~2.594	68.09	$2.35^{+0.18}_{-0.18}$	$-0.18^{+0.05}_{-0.05}$	161^{+10}_{-10}	292^{+20}_{-20}	$54.71^{+11.73}_{-10.40} \times 10^{-6}$	$2.14^{+0.19}_{-0.19}$	$-0.08^{+0.07}_{-0.07}$	$-3.09^{+0.33}_{-0.20}$	264^{+14}_{-14}	$62.88^{+12.77}_{-12.77} \times 10^{-6}$	-10.0	2.8	3.5	
2.594~2.705	120.28	$2.68^{+0.12}_{-0.12}$	$-0.25^{+0.03}_{-0.03}$	212^{+8}_{-8}	370^{+15}_{-15}	$80.45^{+11.69}_{-8.74} \times 10^{-6}$	$2.13^{+0.14}_{-0.14}$	$-0.02^{+0.05}_{-0.05}$	$-2.52^{+0.08}_{-0.08}$	287^{+12}_{-12}	$102.50^{+16.04}_{-15.93} \times 10^{-6}$	-68.1	2.9	3.8	
2.705~3.054	179.52	$2.99^{+0.08}_{-0.08}$	$-0.27^{+0.02}_{-0.02}$	144^{+3}_{-3}	249^{+7}_{-7}	$44.42^{+3.66}_{-3.10} \times 10^{-6}$	$2.70^{+0.09}_{-0.09}$	$-0.14^{+0.03}_{-0.03}$	$-2.86^{+0.09}_{-0.09}$	220^{+5}_{-5}	$52.13^{+4.08}_{-4.08} \times 10^{-6}$	-69.6	3.0	4.0	
3.054~3.315	134.79	$2.81^{+0.10}_{-0.10}$	$-0.29^{+0.03}_{-0.03}$	128^{+4}_{-4}	219^{+8}_{-8}	$31.78^{+3.23}_{-2.85} \times 10^{-6}$	$2.64^{+0.10}_{-0.10}$	$-0.21^{+0.04}_{-0.04}$	$-3.13^{+0.18}_{-0.18}$	202^{+5}_{-5}	$35.37^{+3.64}_{-3.03} \times 10^{-6}$	-22.1	3.0	4.0	
3.315~3.377	76.64	$2.61^{+0.17}_{-0.17}$	$-0.35^{+0.04}_{-0.04}$	221^{+12}_{-13}	365^{+22}_{-23}	$61.24^{+10.98}_{-9.71} \times 10^{-6}$	$2.60^{+0.17}_{-0.17}$	$-0.35^{+0.04}_{-0.04}$	$-6.30^{+2.44}_{-2.44}$	361^{+14}_{-14}	$61.63^{+9.79}_{-9.79} \times 10^{-6}$	-0.4	2.9	2.8	
3.377~3.482	81.16	$2.35^{+0.14}_{-0.14}$	$-0.27^{+0.04}_{-0.04}$	140^{+7}_{-7}	242^{+13}_{-13}	$32.89^{+5.67}_{-4.81} \times 10^{-6}$	$2.22^{+0.15}_{-0.15}$	$-0.20^{+0.06}_{-0.06}$	$-3.67^{+0.76}_{-0.76}$	226^{+12}_{-12}	$35.65^{+6.94}_{-5.90} \times 10^{-6}$	-7.3	2.9	1.6	
3.482~3.652	135.61	$2.78^{+0.11}_{-0.11}$	$-0.23^{+0.03}_{-0.03}$	166^{+5}_{-5}	293^{+10}_{-10}	$58.55^{+6.45}_{-6.51} \times 10^{-6}$	$2.50^{+0.11}_{-0.11}$	$-0.12^{+0.03}_{-0.03}$	$-2.83^{+0.11}_{-0.11}$	259^{+7}_{-7}	$68.26^{+8.13}_{-6.82} \times 10^{-6}$	-50.2	3.0	4.0	
3.652~3.933	136.78	$3.55^{+0.11}_{-0.11}$	$-0.48^{+0.02}_{-0.02}$	150^{+5}_{-5}	227^{+8}_{-8}	$30.93^{+2.97}_{-2.49} \times 10^{-6}$	$3.22^{+0.12}_{-0.12}$	$-0.34^{+0.04}_{-0.04}$	$-2.68^{+0.10}_{-0.10}$	194^{+7}_{-7}	$37.50^{+4.31}_{-3.73} \times 10^{-6}$	-41.3	3.0	4.0	
3.933~4.128	87.98	$2.94^{+0.13}_{-0.13}$	$-0.55^{+0.04}_{-0.04}$	143^{+8}_{-8}	207^{+13}_{-13}	$19.40^{+2.94}_{-2.29} \times 10^{-6}$	$2.62^{+0.14}_{-0.14}$	$-0.36^{+0.06}_{-0.06}$	$-2.52^{+0.11}_{-0.11}$	168^{+9}_{-9}	$25.55^{+3.99}_{-3.73} \times 10^{-6}$	-35.3	2.9	3.9	
4.128~4.273	56.15	$2.95^{+0.17}_{-0.17}$	$-0.64^{+0.06}_{-0.06}$	101^{+8}_{-8}	138^{+12}_{-12}	$9.67^{+2.07}_{-1.70} \times 10^{-6}$	$2.88^{+0.18}_{-0.18}$	$-0.59^{+0.08}_{-0.08}$	$-4.68^{+2.82}_{-2.82}$	131^{+8}_{-9}	$10.14^{+1.59}_{-1.59} \times 10^{-6}$	-4.5	2.9	0.7	
4.273~4.513	54.85	$2.50^{+0.13}_{-0.13}$	$-0.58^{+0.07}_{-0.07}$	71^{+5}_{-5}	100^{+8}_{-8}	$5.66^{+1.04}_{-1.04} \times 10^{-6}$	$2.45^{+0.15}_{-0.15}$	$-0.51^{+0.11}_{-0.11}$	$-5.10^{+2.02}_{-2.02}$	96^{+5}_{-5}	$5.84^{+1.10}_{-0.84} \times 10^{-6}$	-3.2	2.8	0.6	
4.513~5.467	62.78	$1.90^{+0.07}_{-0.07}$	$-1.04^{+0.05}_{-0.05}$	102^{+8}_{-8}	97^{+9}_{-9}	$2.81^{+0.37}_{-0.32} \times 10^{-6}$	$1.79^{+0.08}_{-0.08}$	$-0.68^{+0.21}_{-0.21}$	$-2.74^{+0.45}_{-0.45}$	72^{+11}_{-10}	$3.63^{+2.12}_{-2.09} \times 10^{-6}$	-28.3	2.9	-13.5	
5.467~6.000	29.21	$1.22^{+0.08}_{-0.08}$	$-1.06^{+0.10}_{-0.10}$	88^{+14}_{-14}	82^{+16}_{-16}	$1.51^{+0.38}_{-0.30} \times 10^{-6}$	$1.21^{+0.08}_{-0.08}$	$-1.03^{+0.11}_{-0.11}$	$-5.90^{+2.66}_{-2.73}$	80^{+6}_{-5}	$1.55^{+0.24}_{-0.18} \times 10^{-6}$	0.2	2.4	2.9	

Note—All columns are the same as Table A2 but for GRB 131014215.

Table A20. Time-resolved Spectral Fit Results of GRB 131127592

$t_{\text{start}} \sim t_{\text{stop}}$	S	Cutoff Power-Law Fitting				Band Fitting				Difference				
		K	α	E_c	E_p	F	K	α	β	E_p	F	ΔDIC	$p_{\text{DIC}}^{\text{CPL}}$	$p_{\text{DIC}}^{\text{Band}}$
(1)	(2)	(3)	(4)	(5)	(6)	(7)	(8)	(9)	(10)	(11)	(12)	(13)	(14)	(15)
Pulse 1														
0.664~1.947	21.93	$0.32^{+0.03}_{-0.03}$	$-1.11^{+0.10}_{-0.10}$	247^{+64}_{-64}	220^{+62}_{-64}	$0.90^{+0.39}_{-0.25} \times 10^{-6}$	$0.31^{+0.04}_{-0.04}$	$-1.04^{+0.15}_{-0.15}$	$-4.82^{+2.62}_{-3.24}$	190^{+44}_{-49}	$1.00^{+0.56}_{-0.31} \times 10^{-6}$	-2.6	1.1	0.0
1.947~2.420	27.62	$0.47^{+0.05}_{-0.05}$	$-0.96^{+0.07}_{-0.07}$	322^{+58}_{-65}	$2.65^{+0.93}_{-0.72} \times 10^{-6}$	$0.46^{+0.05}_{-0.05}$	$-0.96^{+0.08}_{-0.07}$	$-6.27^{+2.44}_{-2.51}$	329^{+43}_{-43}	$2.63^{+0.63}_{-0.51} \times 10^{-6}$	0.6	2.4	2.9	
2.420~3.429	59.89	$0.81^{+0.04}_{-0.04}$	$-1.06^{+0.03}_{-0.03}$	476^{+52}_{-51}	448^{+51}_{-51}	$5.06^{+0.86}_{-0.70} \times 10^{-6}$	$0.81^{+0.04}_{-0.04}$	$-1.06^{+0.03}_{-0.03}$	$-6.34^{+2.49}_{-2.49}$	443^{+36}_{-36}	$5.13^{+0.60}_{-0.55} \times 10^{-6}$	0.2	2.8	3.0
3.429~4.358	47.63	$0.76^{+0.04}_{-0.04}$	$-1.09^{+0.04}_{-0.04}$	387^{+51}_{-51}	352^{+49}_{-49}	$3.46^{+0.75}_{-0.52} \times 10^{-6}$	$0.76^{+0.04}_{-0.04}$	$-1.09^{+0.04}_{-0.04}$	$-5.86^{+2.69}_{-2.74}$	344^{+36}_{-35}	$3.57^{+0.67}_{-0.49} \times 10^{-6}$	-0.0	2.7	2.8
Pulse 2														
4.358~5.740	42.75	$0.62^{+0.03}_{-0.03}$	$-1.12^{+0.05}_{-0.05}$	340^{+49}_{-50}	299^{+46}_{-47}	$2.34^{+0.50}_{-0.38} \times 10^{-6}$	$0.57^{+0.04}_{-0.04}$	$-0.97^{+0.09}_{-0.10}$	$-2.67^{+0.64}_{-0.37}$	208^{+42}_{-37}	$3.26^{+1.14}_{-0.64} \times 10^{-6}$	-23.0	2.6	-8.9
5.740~5.862	20.56	$0.43^{+0.08}_{-0.08}$	$-0.69^{+0.11}_{-0.12}$	338^{+83}_{-82}	443^{+114}_{-115}	$5.63^{+4.02}_{-2.28} \times 10^{-6}$	$0.43^{+0.07}_{-0.07}$	$-0.68^{+0.11}_{-0.11}$	$-5.67^{+2.84}_{-2.95}$	41.4^{+67}_{-67}	$5.91^{+3.19}_{-1.91} \times 10^{-6}$	0.3	1.1	2.0
5.862~6.384	69.07	$1.07^{+0.05}_{-0.05}$	$-0.81^{+0.03}_{-0.03}$	295^{+22}_{-22}	352^{+22}_{-28}	$8.76^{+1.32}_{-1.22} \times 10^{-6}$	$0.99^{+0.06}_{-0.06}$	$-0.71^{+0.05}_{-0.05}$	$-2.55^{+2.24}_{-0.09}$	285^{+24}_{-24}	$10.94^{+2.41}_{-1.93} \times 10^{-6}$	-14.4	2.9	3.5
6.384~6.568	34.22	$1.16^{+0.11}_{-0.11}$	$-0.88^{+0.08}_{-0.08}$	199^{+31}_{-31}	223^{+39}_{-39}	$4.82^{+1.68}_{-1.13} \times 10^{-6}$	$1.13^{+0.11}_{-0.11}$	$-0.84^{+0.09}_{-0.10}$	$-5.52^{+2.78}_{-2.96}$	208^{+25}_{-23}	$4.99^{+1.88}_{-1.19} \times 10^{-6}$	-0.9	2.4	2.0
6.568~6.889	34.13	$1.25^{+0.09}_{-0.09}$	$-1.23^{+0.06}_{-0.06}$	386^{+82}_{-85}	297^{+67}_{-70}	$3.86^{+1.15}_{-0.83} \times 10^{-6}$	$1.19^{+0.12}_{-0.12}$	$-1.11^{+0.15}_{-0.15}$	$-4.45^{+3.75}_{-3.38}$	236^{+75}_{-75}	$4.25^{+1.67}_{-1.67} \times 10^{-6}$	-13.3	2.3	-8.4
6.889~7.464	34.47	$1.11^{+0.07}_{-0.07}$	$-1.34^{+0.07}_{-0.07}$	304^{+77}_{-77}	201^{+54}_{-55}	$2.16^{+0.64}_{-0.44} \times 10^{-6}$	$0.99^{+0.07}_{-0.07}$	$-1.01^{+0.14}_{-0.15}$	$-2.16^{+0.12}_{-0.19}$	107^{+18}_{-19}	$3.04^{+1.00}_{-0.67} \times 10^{-6}$	-13.5	1.7	1.8
7.464~8.885	42.52	$0.85^{+0.04}_{-0.04}$	$-1.29^{+0.06}_{-0.06}$	238^{+39}_{-39}	169^{+31}_{-31}	$1.59^{+0.33}_{-0.23} \times 10^{-6}$	$0.77^{+0.05}_{-0.05}$	$-0.96^{+0.15}_{-0.15}$	$-2.23^{+0.20}_{-0.15}$	97^{+15}_{-15}	$2.36^{+0.67}_{-0.64} \times 10^{-6}$	-21.3	2.4	0.5
Pulse 3														
8.885~9.115	33.90	$0.70^{+0.07}_{-0.07}$	$-0.66^{+0.08}_{-0.08}$	165^{+20}_{-20}	221^{+30}_{-30}	$4.14^{+1.47}_{-0.97} \times 10^{-6}$	$0.69^{+0.07}_{-0.07}$	$-0.66^{+0.08}_{-0.08}$	$-6.48^{+2.39}_{-2.42}$	219^{+16}_{-16}	$4.18^{+0.97}_{-0.73} \times 10^{-6}$	0.4	2.6	3.0
9.115~9.403	22.68	$0.89^{+0.09}_{-0.09}$	$-0.59^{+0.11}_{-0.11}$	132^{+26}_{-25}	133^{+30}_{-29}	$1.85^{+0.77}_{-0.47} \times 10^{-6}$	$0.88^{+0.09}_{-0.09}$	$-0.96^{+0.12}_{-0.12}$	$-6.02^{+2.68}_{-2.70}$	126^{+14}_{-14}	$1.89^{+0.49}_{-0.38} \times 10^{-6}$	0.6	2.1	2.8
9.403~9.668	32.26	$1.03^{+0.09}_{-0.09}$	$-0.84^{+0.09}_{-0.09}$	128^{+17}_{-17}	149^{+23}_{-23}	$2.86^{+0.92}_{-0.68} \times 10^{-6}$	$1.01^{+0.09}_{-0.09}$	$-0.80^{+0.13}_{-0.11}$	$-5.20^{+2.43}_{-2.43}$	141^{+13}_{-14}	$3.02^{+0.84}_{-0.58} \times 10^{-6}$	-1.1	2.4	2.0
9.668~10.349	29.80	$0.91^{+0.06}_{-0.06}$	$-1.35^{+0.08}_{-0.08}$	225^{+53}_{-54}	146^{+39}_{-39}	$1.40^{+0.40}_{-0.26} \times 10^{-6}$	$0.88^{+0.07}_{-0.07}$	$-1.22^{+0.17}_{-0.19}$	$-5.03^{+2.82}_{-3.24}$	123^{+30}_{-36}	$1.51^{+0.83}_{-0.38} \times 10^{-6}$	-8.3	2.0	-5.3
Pulse 4														
10.349~11.673	22.22	$0.55^{+0.04}_{-0.04}$	$-1.48^{+0.10}_{-0.10}$	289^{+101}_{-104}	150^{+60}_{-61}	$0.78^{+0.30}_{-0.18} \times 10^{-6}$	$0.54^{+0.04}_{-0.04}$	$-1.45^{+0.11}_{-0.11}$	$-6.04^{+2.69}_{-2.67}$	133^{+25}_{-25}	$0.77^{+0.18}_{-0.11} \times 10^{-6}$	1.9	0.5	2.6
11.673~12.126	36.18	$0.97^{+0.07}_{-0.07}$	$-0.59^{+0.08}_{-0.08}$	149^{+21}_{-21}	151^{+24}_{-25}	$2.33^{+0.59}_{-0.48} \times 10^{-6}$	$0.93^{+0.08}_{-0.08}$	$-0.88^{+0.14}_{-0.13}$	$-4.07^{+1.80}_{-1.80}$	131^{+20}_{-20}	$2.74^{+1.10}_{-0.78} \times 10^{-6}$	-7.1	2.5	-1.5
Pulse 5														
15.851~16.617	26.07	$0.65^{+0.05}_{-0.05}$	$-1.12^{+0.11}_{-0.10}$	143^{+28}_{-30}	126^{+29}_{-30}	$1.10^{+0.40}_{-0.24} \times 10^{-6}$	$0.60^{+0.06}_{-0.06}$	$-0.75^{+0.38}_{-0.38}$	$-3.69^{+1.55}_{-2.09}$	91^{+29}_{-29}	$1.37^{+1.19}_{-0.56} \times 10^{-6}$	-26.6	2.0	-20.6
17.425~17.630	30.88	$1.04^{+0.10}_{-0.10}$	$-0.75^{+0.10}_{-0.10}$	120^{+17}_{-17}	150^{+24}_{-24}	$3.25^{+1.22}_{-0.79} \times 10^{-6}$	$1.03^{+0.10}_{-0.10}$	$-0.71^{+0.11}_{-0.11}$	$-5.16^{+2.35}_{-2.35}$	144^{+13}_{-13}	$3.53^{+1.02}_{-0.76} \times 10^{-6}$	-1.6	2.4	1.9
17.630~18.124	62.58	$1.17^{+0.06}_{-0.06}$	$-0.63^{+0.05}_{-0.05}$	117^{+8}_{-8}	160^{+12}_{-12}	$4.76^{+0.85}_{-0.74} \times 10^{-6}$	$1.13^{+0.07}_{-0.07}$	$-0.56^{+0.08}_{-0.08}$	$-4.30^{+1.56}_{-1.56}$	150^{+11}_{-11}	$5.19^{+1.19}_{-0.92} \times 10^{-6}$	-7.6	2.9	-1.4
18.124~18.582	39.28	$1.31^{+0.09}_{-0.09}$	$-0.90^{+0.09}_{-0.09}$	90^{+11}_{-11}	99^{+15}_{-15}	$2.20^{+0.55}_{-0.40} \times 10^{-6}$	$1.18^{+0.08}_{-0.08}$	$-0.49^{+0.17}_{-0.17}$	$-2.50^{+0.13}_{-0.13}$	74^{+6}_{-6}	$2.75^{+0.72}_{-0.52} \times 10^{-6}$	-21.8	2.6	3.7
18.582~19.244	27.07	$0.79^{+0.06}_{-0.06}$	$-1.21^{+0.10}_{-0.10}$	152^{+31}_{-31}	120^{+29}_{-29}	$1.22^{+0.40}_{-0.24} \times 10^{-6}$	$0.78^{+0.06}_{-0.06}$	$-1.18^{+0.10}_{-0.10}$	$-6.45^{+2.47}_{-2.47}$	116^{+12}_{-12}	$1.24^{+0.22}_{-0.17} \times 10^{-6}$	1.0	2.2	3.0

Note—All columns are the same as Table A2 but for GRB 131127592.

Table A21. Time-resolved Spectral Fit Results of GRB 140206275

$t_{\text{start}} \sim t_{\text{stop}}$	S	Cutoff Power-Law Fitting						Band Fitting						Difference	
		K	α	E_c	E_p	F	K	α	β	E_p	F	ΔDIC	$p_{\text{DIC}}^{\text{CPL}}$	$p_{\text{DIC}}^{\text{Band}}$	
(1)	(2)	(3)	(4)	(5)	(6)	(7)	(8)	(9)	(10)	(11)	(12)	(13)	(14)	(15)	
Pulse 1															
7.311~8.264	21.37	$0.02^{+0.00}_{-0.00}$	$-0.89^{+0.04}_{-0.04}$	2302^{+467}_{-463}	2555^{+527}_{-522}	$8.58^{+2.23 \times 10^{-6}}_{-1.83 \times 10^{-6}}$	$0.02^{+0.00}_{-0.00}$	$-0.78^{+0.10}_{-0.10}$	$3.10^{+1.05}_{-1.05}$	1648^{+729}_{-601}	$7.30^{+4.46 \times 10^{-6}}_{-2.48 \times 10^{-6}}$	-14.2	2.9	-5.2	
8.264~9.521	36.16	$0.04^{+0.00}_{-0.00}$	$-0.70^{+0.05}_{-0.05}$	734^{+97}_{-98}	954^{+131}_{-133}	$6.68^{+1.15 \times 10^{-6}}_{-1.15 \times 10^{-6}}$	$0.04^{+0.00}_{-0.00}$	$-0.62^{+0.06}_{-0.06}$	$-2.36^{+0.25}_{-0.25}$	745^{+93}_{-94}	$7.96^{+1.85 \times 10^{-6}}_{-1.48 \times 10^{-6}}$	-12.2	2.7	3.2	
9.521~11.860	60.59	$0.05^{+0.00}_{-0.00}$	$-0.88^{+0.03}_{-0.03}$	579^{+56}_{-55}	648^{+65}_{-64}	$5.12^{+0.64 \times 10^{-6}}_{-0.51 \times 10^{-6}}$	$0.06^{+0.00}_{-0.00}$	$-0.77^{+0.04}_{-0.04}$	$-2.04^{+0.03}_{-0.03}$	458^{+36}_{-36}	$7.35^{+0.73 \times 10^{-6}}_{-0.68 \times 10^{-6}}$	-60.9	2.9	2.9	
11.860~12.546	42.90	$0.06^{+0.00}_{-0.00}$	$-0.93^{+0.03}_{-0.03}$	749^{+91}_{-93}	802^{+100}_{-102}	$7.91^{+1.30 \times 10^{-6}}_{-1.06 \times 10^{-6}}$	$0.06^{+0.00}_{-0.00}$	$-0.93^{+0.03}_{-0.03}$	$-6.55^{+2.23}_{-2.35}$	796^{+79}_{-79}	$7.91^{+1.05 \times 10^{-6}}_{-0.80 \times 10^{-6}}$	0.4	2.9	3.1	
12.546~13.139	52.72	$0.11^{+0.00}_{-0.00}$	$-0.59^{+0.04}_{-0.04}$	327^{+24}_{-24}	461^{+37}_{-37}	$8.49^{+1.13 \times 10^{-6}}_{-0.92 \times 10^{-6}}$	$0.11^{+0.00}_{-0.00}$	$-0.58^{+0.04}_{-0.04}$	$-5.79^{+2.49}_{-2.49}$	455^{+25}_{-25}	$8.69^{+0.81 \times 10^{-6}}_{-0.81 \times 10^{-6}}$	-0.7	3.0	2.6	
13.139~14.776	109.21	$0.15^{+0.00}_{-0.00}$	$-0.69^{+0.02}_{-0.02}$	314^{+12}_{-13}	411^{+18}_{-18}	$10.00^{+0.57 \times 10^{-6}}_{-0.58 \times 10^{-6}}$	$0.18^{+0.01}_{-0.01}$	$-0.59^{+0.03}_{-0.03}$	$-2.33^{+0.08}_{-0.08}$	337^{+15}_{-15}	$13.45^{+1.12 \times 10^{-6}}_{-1.10 \times 10^{-6}}$	-51.3	3.0	3.9	
14.776~15.643	71.92	$0.13^{+0.00}_{-0.00}$	$-0.82^{+0.03}_{-0.03}$	315^{+21}_{-21}	371^{+26}_{-27}	$7.36^{+0.67 \times 10^{-6}}_{-0.64 \times 10^{-6}}$	$0.14^{+0.01}_{-0.01}$	$-0.77^{+0.05}_{-0.05}$	$-3.93^{+1.60}_{-1.60}$	332^{+40}_{-38}	$8.56^{+2.17 \times 10^{-6}}_{-2.00 \times 10^{-6}}$	-11.3	2.9	-5.0	
15.643~16.919	75.17	$0.12^{+0.00}_{-0.00}$	$-0.80^{+0.03}_{-0.03}$	246^{+16}_{-16}	295^{+20}_{-20}	$5.12^{+0.47 \times 10^{-6}}_{-0.42 \times 10^{-6}}$	$0.19^{+0.02}_{-0.02}$	$-0.50^{+0.06}_{-0.06}$	$-2.08^{+0.05}_{-0.05}$	184^{+12}_{-12}	$8.24^{+1.23 \times 10^{-6}}_{-1.18 \times 10^{-6}}$	-54.3	2.9	2.9	
16.919~18.618	69.69	$0.09^{+0.00}_{-0.00}$	$-0.98^{+0.03}_{-0.03}$	256^{+20}_{-20}	261^{+21}_{-21}	$3.54^{+0.36 \times 10^{-6}}_{-0.36 \times 10^{-6}}$	$0.14^{+0.01}_{-0.01}$	$-0.72^{+0.06}_{-0.06}$	$-0.09^{+0.05}_{-0.05}$	163^{+12}_{-12}	$5.55^{+0.93 \times 10^{-6}}_{-0.93 \times 10^{-6}}$	-40.7	2.9	3.1	
18.618~19.752	42.27	$0.06^{+0.00}_{-0.00}$	$-1.01^{+0.05}_{-0.05}$	253^{+34}_{-34}	250^{+36}_{-36}	$2.33^{+0.39 \times 10^{-6}}_{-0.33 \times 10^{-6}}$	$0.09^{+0.01}_{-0.01}$	$-0.74^{+0.01}_{-0.01}$	$-0.21^{+0.08}_{-0.08}$	157^{+17}_{-17}	$3.62^{+0.97 \times 10^{-6}}_{-0.97 \times 10^{-6}}$	-22.2	2.5	1.6	
19.752~25.143	71.23	$0.04^{+0.00}_{-0.00}$	$-1.25^{+0.03}_{-0.03}$	261^{+25}_{-25}	196^{+20}_{-20}	$1.56^{+0.15 \times 10^{-6}}_{-0.13 \times 10^{-6}}$	$0.06^{+0.01}_{-0.01}$	$-1.05^{+0.05}_{-0.05}$	$-2.10^{+0.05}_{-0.05}$	128^{+10}_{-10}	$2.42^{+0.35 \times 10^{-6}}_{-0.35 \times 10^{-6}}$	-47.0	2.7	3.2	
25.143~27.733	44.38	$0.03^{+0.00}_{-0.00}$	$-1.26^{+0.05}_{-0.05}$	262^{+37}_{-38}	194^{+31}_{-31}	$1.33^{+0.20 \times 10^{-6}}_{-0.17 \times 10^{-6}}$	$0.05^{+0.01}_{-0.01}$	$-1.11^{+0.09}_{-0.09}$	$2.42^{+0.35}_{-0.34}$	139^{+21}_{-21}	$1.85^{+0.54 \times 10^{-6}}_{-0.45 \times 10^{-6}}$	-13.5	2.5	-1.6	
Pulse 2															
27.763~28.941	39.98	$0.07^{+0.01}_{-0.01}$	$-0.84^{+0.06}_{-0.06}$	163^{+16}_{-17}	189^{+21}_{-22}	$1.93^{+0.31 \times 10^{-6}}_{-0.36 \times 10^{-6}}$	$0.08^{+0.01}_{-0.01}$	$-0.82^{+0.07}_{-0.07}$	$-5.51^{+2.68}_{-2.68}$	183^{+14}_{-14}	$2.00^{+0.47 \times 10^{-6}}_{-0.33 \times 10^{-6}}$	-0.8	2.7	2.3	
28.941~31.021	67.73	$0.09^{+0.00}_{-0.00}$	$-0.92^{+0.04}_{-0.04}$	169^{+11}_{-11}	182^{+14}_{-14}	$2.44^{+0.23 \times 10^{-6}}_{-0.21 \times 10^{-6}}$	$0.09^{+0.01}_{-0.01}$	$-0.91^{+0.04}_{-0.04}$	$-5.35^{+2.30}_{-2.30}$	178^{+8}_{-8}	$2.50^{+0.33 \times 10^{-6}}_{-0.33 \times 10^{-6}}$	-1.6	2.8	2.1	
31.021~33.597	58.68	$0.05^{+0.00}_{-0.00}$	$-1.22^{+0.04}_{-0.04}$	210^{+21}_{-21}	164^{+18}_{-19}	$1.68^{+0.19 \times 10^{-6}}_{-0.16 \times 10^{-6}}$	$0.05^{+0.01}_{-0.01}$	$-1.18^{+0.06}_{-0.06}$	$-4.73^{+2.31}_{-2.31}$	154^{+15}_{-16}	$1.80^{+0.49 \times 10^{-6}}_{-0.30 \times 10^{-6}}$	-4.0	2.8	0.3	
33.597~37.804	46.57	$0.04^{+0.00}_{-0.00}$	$-1.17^{+0.05}_{-0.05}$	161^{+18}_{-18}	1.34^{+17}_{-17}	$0.94^{+0.13 \times 10^{-6}}_{-0.11 \times 10^{-6}}$	$0.04^{+0.00}_{-0.00}$	$-1.14^{+0.06}_{-0.06}$	$-4.86^{+2.26}_{-2.26}$	127^{+10}_{-10}	$0.98^{+0.20 \times 10^{-6}}_{-0.15 \times 10^{-6}}$	-2.8	2.6	1.1	
37.804~43.255	37.31	$0.02^{+0.00}_{-0.00}$	$-1.38^{+0.07}_{-0.07}$	128^{+20}_{-21}	79^{+15}_{-16}	$0.56^{+0.12 \times 10^{-6}}_{-0.10 \times 10^{-6}}$	$0.03^{+0.00}_{-0.00}$	$-1.33^{+0.09}_{-0.09}$	$-4.60^{+2.00}_{-2.00}$	74^{+6}_{-6}	$0.57^{+0.21 \times 10^{-6}}_{-0.13 \times 10^{-6}}$	-4.4	1.7	-0.7	

Note—All columns are the same as Table A2 but for GRB 140206275.

Table A22. Time-resolved Spectral Fit Results of GRB 140213807

$t_{\text{start}} \sim t_{\text{stop}}$	S	Cutoff Power-Law Fitting				Band Fitting				Difference				
		K	α	E_c	E_p	F	K	α	β	E_p	F	ΔDIC	$p_{\text{DIC}}^{\text{CPL}}$	
(1)	(2)	(3)	(4)	(5)	(6)	(7)	(8)	(9)	(10)	(11)	(12)	(13)	(14)	(15)
Pulse 1														
0.432~1.161	44.05	$0.05^{+0.00}_{-0.00}$	$-1.38^{+0.05}_{-0.05}$	433^{+101}_{-107}	$2.49^{+0.49}_{-0.42} \times 10^{-6}$	$1.08^{+0.06}_{-0.06}$	$-1.33^{+0.08}_{-0.08}$	$-3.95^{+11.87}_{-3.20}$	2.16^{+53}_{-56}	$2.89^{+0.96}_{-0.77} \times 10^{-6}$	-4.0	2.0	-1.3	
1.161~2.136	65.21	$0.07^{+0.00}_{-0.00}$	$-1.20^{+0.03}_{-0.03}$	411^{+41}_{-49}	329^{+41}_{-41}	$4.06^{+0.50}_{-0.38} \times 10^{-6}$	$1.13^{+0.04}_{-0.04}$	$-1.20^{+0.03}_{-0.03}$	$-6.13^{+2.60}_{-2.63}$	326^{+29}_{-29}	$4.13^{+0.49}_{-0.38} \times 10^{-6}$	2.7	2.9	3.0
2.136~2.871	49.72	$0.08^{+0.01}_{-0.01}$	$-0.99^{+0.05}_{-0.05}$	250^{+30}_{-30}	252^{+33}_{-33}	$3.10^{+0.50}_{-0.39} \times 10^{-6}$	$0.74^{+0.05}_{-0.05}$	$-0.91^{+0.10}_{-0.09}$	$-3.74^{+1.61}_{-1.61}$	215^{+39}_{-41}	$3.83^{+1.88}_{-1.88} \times 10^{-6}$	-7.9	2.7	-3.2
2.880~4.206	54.78	$0.11^{+0.01}_{-0.01}$	$-0.80^{+0.06}_{-0.06}$	99^{+8}_{-9}	118^{+12}_{-12}	$1.56^{+0.26}_{-0.21} \times 10^{-6}$	$0.65^{+0.03}_{-0.03}$	$-0.61^{+0.10}_{-0.10}$	$-2.52^{+0.17}_{-0.14}$	98^{+7}_{-7}	$2.03^{+0.44}_{-0.34} \times 10^{-6}$	-11.7	2.6	3.8
4.206~5.332	38.06	$0.08^{+0.02}_{-0.02}$	$-0.98^{+0.09}_{-0.10}$	69^{+9}_{-9}	70^{+11}_{-11}	$0.89^{+0.24}_{-0.20} \times 10^{-6}$	$0.79^{+0.04}_{-0.04}$	$-0.95^{+0.11}_{-0.11}$	$-5.67^{+2.32}_{-2.87}$	68^{+4}_{-4}	$0.89^{+0.11}_{-0.09} \times 10^{-6}$	2.3	1.4	2.3
Pulse 2														
5.332~6.038	54.82	$0.21^{+0.03}_{-0.03}$	$-0.90^{+0.08}_{-0.08}$	61^{+5}_{-5}	67^{+8}_{-8}	$1.82^{+0.37}_{-0.32} \times 10^{-6}$	$1.63^{+0.07}_{-0.07}$	$-0.87^{+0.09}_{-0.09}$	$-5.46^{+2.21}_{-2.21}$	66^{+3}_{-3}	$1.84^{+0.18}_{-0.14} \times 10^{-6}$	0.6	2.1	1.9
6.038~7.278	94.15	$0.22^{+0.02}_{-0.02}$	$-0.95^{+0.04}_{-0.04}$	85^{+5}_{-5}	90^{+6}_{-6}	$2.84^{+0.27}_{-0.27} \times 10^{-6}$	$1.89^{+0.06}_{-0.06}$	$-0.87^{+0.05}_{-0.06}$	$-3.22^{+0.37}_{-0.37}$	83^{+3}_{-3}	$3.09^{+0.26}_{-0.25} \times 10^{-6}$	-7.9	2.8	2.3
7.278~7.694	44.94	$0.22^{+0.04}_{-0.04}$	$-0.85^{+0.09}_{-0.09}$	67^{+8}_{-8}	77^{+11}_{-11}	$2.03^{+0.54}_{-0.42} \times 10^{-6}$	$1.48^{+0.09}_{-0.09}$	$-0.49^{+0.20}_{-0.20}$	$-2.69^{+0.19}_{-0.18}$	62^{+6}_{-6}	$2.41^{+0.57}_{-0.44} \times 10^{-6}$	-11.4	1.5	3.6
7.694~9.423	60.99	$0.11^{+0.01}_{-0.01}$	$-1.09^{+0.06}_{-0.06}$	64^{+5}_{-5}	58^{+6}_{-6}	$1.24^{+0.20}_{-0.19} \times 10^{-6}$	$1.35^{+0.04}_{-0.04}$	$-0.97^{+0.12}_{-0.12}$	$-3.78^{+0.99}_{-1.03}$	55^{+3}_{-3}	$1.30^{+0.17}_{-0.13} \times 10^{-6}$	-7.2	2.2	-2.3
9.423~10.015	26.33	$0.05^{+0.01}_{-0.02}$	$-1.34^{+0.14}_{-0.14}$	78^{+8}_{-8}	52^{+16}_{-16}	$0.89^{+0.42}_{-0.29} \times 10^{-6}$	$1.12^{+0.08}_{-0.08}$	$-1.28^{+0.16}_{-0.16}$	$-5.72^{+2.60}_{-2.80}$	48^{+4}_{-4}	$0.88^{+0.11}_{-0.09} \times 10^{-6}$	7.4	-2.3	2.6
10.015~11.505	25.79	$0.03^{+0.01}_{-0.01}$	$-1.60^{+0.16}_{-0.16}$	68^{+18}_{-19}	27^{+13}_{-13}	$0.60^{+0.33}_{-0.23} \times 10^{-6}$	$0.99^{+0.05}_{-0.06}$	$-1.51^{+0.17}_{-0.19}$	$-5.97^{+2.73}_{-2.69}$	26^{+4}_{-4}	$0.56^{+0.11}_{-0.12} \times 10^{-6}$	15.6	-10.4	2.1

Note—All columns are the same as Table A2 but for GRB 140213807.

Table A23. Time-resolved Spectral Fit Results of GRB 140416060

$t_{\text{start}} \sim t_{\text{stop}}$	S	Cutoff Power-Law Fitting						Band Fitting						Difference					
		K		E_c		E_p		F		K		α		β	E_p	F	ΔDIC	$p_{\text{DIC}}^{\text{CPL}}$	$p_{\text{DIC}}^{\text{Band}}$
		(1)	(2)	(3)	(4)	(5)	(6)	(7)	(8)	(9)	(10)	(11)	(12)	(13)	(14)	(15)			
Pulse 1																			
-0.184~0.546	25.79	1.13 $^{+0.15}_{-0.15}$	-1.25 $^{+0.14}_{-0.14}$	205 $^{+57}_{-63}$	154 $^{+52}_{-55}$	1.97 $^{+0.97}_{-0.58}$ $\times 10^{-6}$	3.04 $^{+1.95}_{-1.74}$	0.46 $^{+0.34}_{-0.34}$	-2.09 $^{+0.06}_{-0.06}$	47 $^{+2}_{-3}$	2.93 $^{+3.85}_{-6.65}$ $\times 10^{-6}$	-7.7	0.6	-17.9					
0.546~1.544	42.07	1.53 $^{+0.13}_{-0.14}$	-1.10 $^{+0.10}_{-0.10}$	133 $^{+22}_{-22}$	119 $^{+24}_{-24}$	2.59 $^{+0.81}_{-0.60}$ $\times 10^{-6}$	1.22 $^{+0.14}_{-0.14}$	-0.55 $^{+0.20}_{-0.20}$	-2.49 $^{+0.13}_{-0.13}$	80 $^{+8}_{-8}$	3.10 $^{+0.98}_{-0.72}$ $\times 10^{-6}$	-14.2	2.3	3.7					
1.544~3.726	50.93	0.08 $^{+0.01}_{-0.01}$	-1.29 $^{+0.08}_{-0.08}$	145 $^{+23}_{-23}$	103 $^{+20}_{-20}$	2.06 $^{+0.48}_{-0.32}$ $\times 10^{-6}$	1.37 $^{+0.11}_{-0.11}$	-0.72 $^{+0.23}_{-0.23}$	2.40 $^{+0.11}_{-0.10}$	67 $^{+8}_{-8}$	2.54 $^{+0.69}_{-0.52}$ $\times 10^{-6}$	-16.8	1.8	2.8					
4.350~6.121	22.81	0.04 $^{+0.01}_{-0.01}$	-1.36 $^{+0.21}_{-0.21}$	148 $^{+55}_{-62}$	95 $^{+47}_{-50}$	0.94 $^{+0.72}_{-0.37}$ $\times 10^{-6}$	0.81 $^{+0.12}_{-0.12}$	-1.11 $^{+0.33}_{-0.35}$	4.29 $^{+1.88}_{-3.10}$	71 $^{+14}_{-15}$	0.96 $^{+0.12}_{-0.24}$ $\times 10^{-6}$	12.7	-13.1	-0.7					
Pulse 2																			
6.604~6.752	21.41	0.09 $^{+0.01}_{-0.01}$	-1.30 $^{+0.12}_{-0.12}$	528 $^{+206}_{-217}$	369 $^{+158}_{-164}$	5.54 $^{+2.68}_{-1.56}$ $\times 10^{-6}$	1.81 $^{+0.32}_{-0.32}$	-1.26 $^{+0.11}_{-0.14}$	5.98 $^{+2.65}_{-2.73}$	307 $^{+87}_{-74}$	5.34 $^{+2.42}_{-1.48}$ $\times 10^{-6}$	3.3	0.6	1.5					
6.752~6.838	28.27	0.26 $^{+0.03}_{-0.03}$	-0.92 $^{+0.11}_{-0.11}$	267 $^{+52}_{-53}$	289 $^{+63}_{-64}$	11.07 $^{+3.61}_{-2.39}$ $\times 10^{-6}$	2.19 $^{+0.35}_{-0.36}$	-0.93 $^{+0.11}_{-0.11}$	-6.91 $^{+2.23}_{-2.18}$	283 $^{+35}_{-35}$	10.93 $^{+3.77}_{-2.65}$ $\times 10^{-6}$	2.5	2.4	2.8					
6.838~7.390	93.49	0.42 $^{+0.02}_{-0.02}$	-0.85 $^{+0.04}_{-0.04}$	205 $^{+14}_{-14}$	236 $^{+18}_{-18}$	14.10 $^{+1.45}_{-1.27}$ $\times 10^{-6}$	2.91 $^{+0.18}_{-0.18}$	-0.83 $^{+0.05}_{-0.05}$	-5.83 $^{+2.57}_{-2.78}$	230 $^{+12}_{-12}$	14.54 $^{+1.99}_{-1.72}$ $\times 10^{-6}$	0.9	2.9	2.3					
7.390~7.724	48.39	0.28 $^{+0.05}_{-0.05}$	-1.05 $^{+0.12}_{-0.12}$	129 $^{+25}_{-25}$	122 $^{+28}_{-29}$	5.65 $^{+2.02}_{-1.40}$ $\times 10^{-6}$	2.46 $^{+0.30}_{-0.30}$	-0.51 $^{+0.20}_{-0.20}$	-2.50 $^{+0.11}_{-0.11}$	83 $^{+7}_{-7}$	6.73 $^{+2.23}_{-1.52}$ $\times 10^{-6}$	-21.0	0.2	3.8					
7.724~8.128	41.14	0.30 $^{+0.07}_{-0.07}$	-0.92 $^{+0.14}_{-0.14}$	83 $^{+14}_{-14}$	89 $^{+19}_{-19}$	3.54 $^{+1.43}_{-0.96}$ $\times 10^{-6}$	2.21 $^{+0.28}_{-0.27}$	-0.60 $^{+0.22}_{-0.22}$	3.06 $^{+0.40}_{-0.40}$	74 $^{+7}_{-7}$	3.95 $^{+1.17}_{-1.17}$ $\times 10^{-6}$	-4.2	-0.1	3.2					
8.128~8.422	43.98	0.81 $^{+0.21}_{-0.21}$	-0.55 $^{+0.15}_{-0.15}$	52 $^{+6}_{-6}$	76 $^{+12}_{-12}$	4.28 $^{+1.68}_{-1.15}$ $\times 10^{-6}$	2.79 $^{+0.32}_{-0.32}$	-0.51 $^{+0.16}_{-0.16}$	-5.57 $^{+2.00}_{-2.67}$	73 $^{+3}_{-3}$	4.33 $^{+0.84}_{-0.69}$ $\times 10^{-6}$	1.3	0.6	2.1					
8.422~8.969	36.96	0.38 $^{+0.11}_{-0.12}$	-0.81 $^{+0.17}_{-0.17}$	53 $^{+8}_{-8}$	63 $^{+13}_{-13}$	2.49 $^{+1.31}_{-0.88}$ $\times 10^{-6}$	2.24 $^{+0.25}_{-0.25}$	-0.59 $^{+0.26}_{-0.26}$	-3.69 $^{+0.76}_{-0.44}$	57 $^{+4}_{-4}$	2.49 $^{+0.61}_{-0.43}$ $\times 10^{-6}$	0.3	-1.6	2.3					
8.969~9.326	43.68	0.60 $^{+0.15}_{-0.16}$	-0.67 $^{+0.15}_{-0.15}$	58 $^{+8}_{-8}$	77 $^{+14}_{-14}$	3.95 $^{+1.74}_{-1.11}$ $\times 10^{-6}$	2.58 $^{+0.30}_{-0.30}$	-0.44 $^{+0.21}_{-0.21}$	3.39 $^{+0.49}_{-0.49}$	69 $^{+5}_{-5}$	4.18 $^{+1.07}_{-0.81}$ $\times 10^{-6}$	-3.2	-0.2	3.4					
9.326~10.226	56.34	0.38 $^{+0.07}_{-0.07}$	-0.87 $^{+0.11}_{-0.11}$	58 $^{+6}_{-6}$	65 $^{+9}_{-9}$	2.96 $^{+0.89}_{-0.70}$ $\times 10^{-6}$	2.72 $^{+0.19}_{-0.19}$	-0.81 $^{+0.13}_{-0.13}$	-5.03 $^{+1.70}_{-2.58}$	63 $^{+3}_{-3}$	3.00 $^{+0.37}_{-0.32}$ $\times 10^{-6}$	-0.5	1.6	1.3					
10.226~10.500	22.60	0.13 $^{+0.06}_{-0.06}$	-1.36 $^{+0.27}_{-0.28}$	111 $^{+49}_{-49}$	71 $^{+43}_{-43}$	2.58 $^{+2.61}_{-2.61}$ $\times 10^{-6}$	2.61 $^{+0.39}_{-0.39}$	-1.23 $^{+0.32}_{-0.32}$	-5.35 $^{+2.45}_{-2.95}$	57 $^{+8}_{-8}$	2.37 $^{+0.56}_{-0.46}$ $\times 10^{-6}$	24.3	-20.2	2.2					
10.500~12.542	27.53	0.03 $^{+0.01}_{-0.01}$	-1.74 $^{+0.19}_{-0.18}$	205 $^{+109}_{-103}$	53 $^{+48}_{-46}$	1.17 $^{+0.71}_{-0.43}$ $\times 10^{-6}$	1.35 $^{+0.12}_{-0.14}$	-1.56 $^{+0.22}_{-0.24}$	-4.33 $^{+1.86}_{-2.97}$	41 $^{+8}_{-8}$	1.10 $^{+0.26}_{-0.19}$ $\times 10^{-6}$	14.2	-13.0	-0.2					
Pulse 3																			
12.542~13.015	32.14	0.20 $^{+0.05}_{-0.05}$	-0.96 $^{+0.15}_{-0.15}$	88 $^{+16}_{-16}$	92 $^{+21}_{-22}$	2.52 $^{+1.06}_{-0.68}$ $\times 10^{-6}$	1.73 $^{+0.21}_{-0.22}$	-0.92 $^{+0.17}_{-0.17}$	-5.83 $^{+2.67}_{-2.74}$	87 $^{+7}_{-7}$	2.57 $^{+0.68}_{-0.44}$ $\times 10^{-6}$	4.1	0.4	2.8					
13.015~13.501	42.76	0.15 $^{+0.02}_{-0.02}$	-1.08 $^{+0.09}_{-0.09}$	174 $^{+28}_{-28}$	160 $^{+30}_{-31}$	4.23 $^{+1.00}_{-0.79}$ $\times 10^{-6}$	1.84 $^{+0.19}_{-0.19}$	-1.05 $^{+0.11}_{-0.12}$	-5.75 $^{+2.84}_{-2.88}$	152 $^{+17}_{-16}$	4.23 $^{+1.16}_{-1.16}$ $\times 10^{-6}$	2.4	2.1	2.5					
13.501~14.011	26.43	0.07 $^{+0.02}_{-0.02}$	-1.50 $^{+0.18}_{-0.19}$	166 $^{+60}_{-60}$	83 $^{+42}_{-46}$	2.17 $^{+1.37}_{-0.81}$ $\times 10^{-6}$	2.13 $^{+0.26}_{-0.26}$	-1.43 $^{+0.19}_{-0.19}$	-5.51 $^{+2.77}_{-3.00}$	67 $^{+10}_{-10}$	2.09 $^{+0.46}_{-0.33}$ $\times 10^{-6}$	12.4	-7.3	2.8					
14.608~21.034	25.53	0.01 $^{+0.00}_{-0.00}$	-1.84 $^{+0.05}_{-0.05}$	83 $^{+3}_{-3}$	13 $^{+4}_{-4}$	0.70 $^{+0.10}_{-0.11}$ $\times 10^{-6}$	0.92 $^{+0.08}_{-0.09}$	-1.21 $^{+0.26}_{-0.27}$	6.02 $^{+2.32}_{-2.50}$	29 $^{+4}_{-4}$	0.48 $^{+0.09}_{-0.09}$ $\times 10^{-6}$	-84.8	1.3	2.5					
Pulse 4																			
21.034~22.305	42.08	0.17 $^{+0.04}_{-0.04}$	-1.18 $^{+0.13}_{-0.13}$	55 $^{+8}_{-10}$	45 $^{+10}_{-10}$	1.78 $^{+0.69}_{-0.68}$ $\times 10^{-6}$	2.49 $^{+0.18}_{-0.18}$	-1.17 $^{+0.14}_{-0.14}$	-6.72 $^{+2.20}_{-2.21}$	44 $^{+3}_{-3}$	1.77 $^{+0.18}_{-0.15}$ $\times 10^{-6}$	5.4	0.2	3.1					
22.305~22.460	24.88	0.09 $^{+0.03}_{-0.03}$	-1.67 $^{+0.16}_{-0.16}$	361 $^{+22}_{-189}$	119 $^{+93}_{-85}$	4.87 $^{+2.57}_{-1.63}$ $\times 10^{-6}$	0.24 $^{+0.03}_{-0.03}$	-1.05 $^{+0.04}_{-0.04}$	-5.67 $^{+2.26}_{-2.21}$	86 $^{+5}_{-5}$	3.66 $^{+0.61}_{-0.61}$ $\times 10^{-6}$	14.2	-3.8	1.2					
22.460~23.963	117.20	0.25 $^{+0.01}_{-0.01}$	-1.20 $^{+0.03}_{-0.03}$	204 $^{+14}_{-14}$	163 $^{+13}_{-13}$	7.96 $^{+0.58}_{-0.58}$ $\times 10^{-6}$	3.73 $^{+0.25}_{-0.26}$	-1.09 $^{+0.14}_{-0.14}$	-4.48 $^{+2.05}_{-2.05}$	142 $^{+22}_{-25}$	8.79 $^{+2.49}_{-1.93}$ $\times 10^{-6}$	-19.1	2.9	-15.7					
23.963~24.680	71.54	0.26 $^{+0.03}_{-0.03}$	-1.08 $^{+0.06}_{-0.06}$	144 $^{+15}_{-15}$	133 $^{+16}_{-16}$	6.00 $^{+0.86}_{-0.78}$ $\times 10^{-6}$	2.71 $^{+0.22}_{-0.22}$	-0.81 $^{+0.14}_{-0.14}$	-2.69 $^{+0.23}_{-0.23}$	104 $^{+10}_{-10}$	7.13 $^{+1.76}_{-1.43}$ $\times 10^{-6}$	-7.0	2.6	2.9					
24.680~25.163	45.85	0.13 $^{+0.02}_{-0.02}$	-1.40 $^{+0.10}_{-0.11}$	224 $^{+60}_{-62}$	134 $^{+42}_{-44}$	4.65 $^{+1.44}_{-1.08}$ $\times 10^{-6}$	2.57 $^{+0.28}_{-0.28}$	-0.79 $^{+0.24}_{-0.24}$	-2.33 $^{+0.11}_{-0.10}$	74 $^{+10}_{-10}$	5.48 $^{+1.88}_{-1.32}$ $\times 10^{-6}$	-13.0	-0.2	3.0					
25.163~25.706	33.34	0.12 $^{+0.03}_{-0.03}$	-1.15 $^{+0.14}_{-0.15}$	139 $^{+34}_{-36}$	118 $^{+34}_{-36}$	2.64 $^{+0.75}_{-0.75}$ $\times 10^{-6}$	1.45 $^{+0.21}_{-0.21}$	-0.78 $^{+0.28}_{-0.28}$	-3.04 $^{+0.06}_{-0.06}$	87 $^{+15}_{-15}$	3.12 $^{+1.62}_{-0.98}$ $\times 10^{-6}$	-5.4	-1.0	-1.0					
25.706~26.810	25.72	0.07 $^{+0.03}_{-0.03}$	-1.22 $^{+0.22}_{-0.23}$	109 $^{+38}_{-40}$	85 $^{+40}_{-40}$	1.28 $^{+0.94}_{-0.94}$ $\times 10^{-6}$	0.09 $^{+0.01}_{-0.01}$	-1.01 $^{+0.07}_{-0.07}$	-4.63 $^{+1.79}_{-2.59}$	83 $^{+2}_{-2}$	1.22 $^{+0.24}_{-0.22}$ $\times 10^{-6}$	18.8	-17.1	-0.1					

Note—All columns are the same as Table A2 but for GRB 140416060.

Table A24. Time-resolved Spectral Fit Results of GRB 140508128

$t_{\text{start}} \sim t_{\text{stop}}$	S	Cutoff Power-Law Fitting				Band Fitting				Difference				
		K	α	E_c	E_p	F	K	α	β	E_p	F	ΔDIC	$p_{\text{DIC}}^{\text{CPL}}$	$p_{\text{DIC}}^{\text{Band}}$
(1)	(2)	(3)	(4)	(5)	(6)	(7)	(8)	(9)	(10)	(11)	(12)	(13)	(14)	(15)
Pulse 1														
2.465~4.213	51.95	$0.05^{+0.00}_{-0.00}$	$-1.08^{+0.04}_{-0.04}$	492^{+68}_{-68}	452^{+65}_{-66}	$3.76^{+0.57}_{-0.45} \times 10^{-6}$	$0.64^{+0.04}_{-0.04}$	$-1.09^{+0.04}_{-0.05}$	$-6.11^{+2.57}_{-2.62}$	451^{+48}_{-48}	$3.88^{+0.69}_{-0.60} \times 10^{-6}$	2.3	2.8	2.9
4.213~4.473	30.21	$0.12^{+0.02}_{-0.02}$	$-0.70^{+0.11}_{-0.11}$	235^{+45}_{-45}	306^{+64}_{-64}	$5.02^{+1.95}_{-1.35} \times 10^{-6}$	$0.60^{+0.10}_{-0.10}$	$-0.68^{+0.12}_{-0.12}$	$-5.87^{+2.69}_{-2.75}$	297^{+39}_{-39}	$5.17^{+2.52}_{-1.52} \times 10^{-6}$	1.5	2.2	2.4
4.473~4.710	49.94	$0.20^{+0.01}_{-0.01}$	$-0.67^{+0.06}_{-0.06}$	369^{+49}_{-49}	491^{+69}_{-68}	$16.08^{+3.42}_{-2.93} \times 10^{-6}$	$0.76^{+0.10}_{-0.10}$	$-0.49^{+0.09}_{-0.09}$	$-2.27^{+0.12}_{-0.12}$	360^{+39}_{-39}	$21.58^{+8.16}_{-5.76} \times 10^{-6}$	-24.6	2.7	3.4
4.710~5.033	73.38	$0.28^{+0.01}_{-0.01}$	$-0.55^{+0.04}_{-0.04}$	322^{+24}_{-24}	467^{+37}_{-37}	$20.97^{+3.00}_{-2.72} \times 10^{-6}$	$0.88^{+0.08}_{-0.08}$	$-0.45^{+0.06}_{-0.06}$	$-2.51^{+0.12}_{-0.12}$	392^{+26}_{-26}	$26.42^{+6.01}_{-4.75} \times 10^{-6}$	-25.4	2.9	3.8
5.033~5.328	81.12	$0.34^{+0.01}_{-0.01}$	$-0.65^{+0.04}_{-0.04}$	327^{+24}_{-24}	441^{+35}_{-35}	$23.84^{+2.89}_{-2.81} \times 10^{-6}$	$1.41^{+0.11}_{-0.11}$	$-0.58^{+0.05}_{-0.05}$	$-2.73^{+0.18}_{-0.18}$	391^{+23}_{-23}	$27.79^{+5.06}_{-4.77} \times 10^{-6}$	-13.5	2.9	3.9
5.328~5.431	38.62	$0.19^{+0.02}_{-0.02}$	$-0.96^{+0.08}_{-0.08}$	559^{+130}_{-131}	581^{+143}_{-144}	$16.66^{+6.37}_{-6.32} \times 10^{-6}$	$1.62^{+0.25}_{-0.25}$	$-0.87^{+0.13}_{-0.13}$	$-3.73^{+1.57}_{-1.57}$	466^{+126}_{-132}	$18.82^{+4.26}_{-7.03} \times 10^{-6}$	-6.0	2.3	-1.7
5.431~5.614	35.44	$0.13^{+0.01}_{-0.01}$	$-0.97^{+0.08}_{-0.08}$	387^{+79}_{-80}	399^{+87}_{-88}	$8.27^{+2.63}_{-1.81} \times 10^{-6}$	$1.25^{+0.15}_{-0.15}$	$-0.97^{+0.08}_{-0.08}$	$-6.15^{+2.67}_{-2.62}$	395^{+53}_{-55}	$8.34^{+2.44}_{-1.88} \times 10^{-6}$	2.1	2.5	2.7
5.614~6.580	56.73	$0.09^{+0.01}_{-0.01}$	$-1.02^{+0.05}_{-0.05}$	326^{+42}_{-42}	319^{+44}_{-44}	$4.58^{+0.81}_{-0.58} \times 10^{-6}$	$0.96^{+0.07}_{-0.07}$	$-1.01^{+0.06}_{-0.06}$	$-4.63^{+2.17}_{-2.17}$	302^{+31}_{-31}	$5.02^{+1.36}_{-0.95} \times 10^{-6}$	-1.1	2.7	1.4
6.580~7.289	28.51	$0.05^{+0.01}_{-0.01}$	$-0.99^{+0.11}_{-0.11}$	273^{+72}_{-72}	276^{+76}_{-76}	$2.22^{+0.57}_{-0.57} \times 10^{-6}$	$0.52^{+0.07}_{-0.07}$	$-0.96^{+0.12}_{-0.12}$	$-4.67^{+2.33}_{-2.33}$	248^{+43}_{-44}	$2.42^{+0.66}_{-0.70} \times 10^{-6}$	0.4	1.1	1.2
7.289~10.165	35.54	$0.03^{+0.00}_{-0.00}$	$-1.10^{+0.08}_{-0.08}$	222^{+44}_{-44}	200^{+44}_{-43}	$1.14^{+0.23}_{-0.23} \times 10^{-6}$	$0.41^{+0.04}_{-0.04}$	$-1.09^{+0.09}_{-0.09}$	$-5.62^{+2.80}_{-2.90}$	193^{+25}_{-24}	$1.13^{+0.33}_{-0.19} \times 10^{-6}$	2.3	2.1	2.6
Pulse 2														
24.711~25.282	46.72	$0.14^{+0.01}_{-0.01}$	$-0.67^{+0.07}_{-0.07}$	217^{+27}_{-27}	289^{+40}_{-40}	$5.30^{+1.17}_{-0.93} \times 10^{-6}$	$0.56^{+0.07}_{-0.07}$	$-0.52^{+0.11}_{-0.11}$	$-2.89^{+0.55}_{-0.55}$	235^{+27}_{-26}	$6.46^{+2.61}_{-1.78} \times 10^{-6}$	-9.4	2.6	0.9
25.282~26.413	90.28	$0.28^{+0.02}_{-0.02}$	$-0.48^{+0.04}_{-0.04}$	140^{+18}_{-18}	213^{+13}_{-13}	$6.59^{+0.73}_{-0.63} \times 10^{-6}$	$0.83^{+0.05}_{-0.05}$	$-0.45^{+0.06}_{-0.06}$	$-4.46^{+1.39}_{-2.21}$	205^{+10}_{-10}	$6.95^{+1.13}_{-0.91} \times 10^{-6}$	-4.4	2.9	0.5
26.413~26.613	26.51	$0.12^{+0.03}_{-0.03}$	$-1.04^{+0.16}_{-0.16}$	152^{+41}_{-43}	146^{+46}_{-48}	$2.87^{+1.37}_{-0.86} \times 10^{-6}$	$1.28^{+0.22}_{-0.23}$	$-0.83^{+0.07}_{-0.07}$	$-5.75^{+3.03}_{-2.97}$	126^{+26}_{-20}	$2.75^{+1.87}_{-0.96} \times 10^{-6}$	-6.2	0.3	-8.1
26.613~26.961	21.78	$0.08^{+0.03}_{-0.03}$	$-1.00^{+0.21}_{-0.22}$	150^{+52}_{-58}	150^{+61}_{-66}	$1.64^{+1.37}_{-0.72} \times 10^{-6}$	$0.75^{+0.13}_{-0.13}$	$-0.95^{+0.24}_{-0.25}$	$-4.83^{+2.46}_{-3.13}$	129^{+28}_{-31}	$1.75^{+1.24}_{-0.61} \times 10^{-6}$	8.9	-7.1	0.7
Pulse 3														
38.914~39.669	56.66	$0.10^{+0.01}_{-0.01}$	$-1.10^{+0.06}_{-0.06}$	278^{+41}_{-42}	250^{+40}_{-41}	$4.27^{+0.83}_{-0.61} \times 10^{-6}$	$1.26^{+0.10}_{-0.10}$	$-1.04^{+0.09}_{-0.09}$	$-3.88^{+1.60}_{-2.81}$	220^{+33}_{-35}	$4.90^{+1.88}_{-1.19} \times 10^{-6}$	-4.6	2.6	-0.6
39.669~39.877	21.85	$0.10^{+0.03}_{-0.03}$	$-1.11^{+0.19}_{-0.19}$	149^{+47}_{-51}	133^{+51}_{-54}	$2.23^{+1.36}_{-0.82} \times 10^{-6}$	$1.24^{+0.21}_{-0.20}$	$-1.12^{+0.19}_{-0.19}$	$-6.36^{+2.46}_{-2.48}$	125^{+17}_{-23}	$2.15^{+0.84}_{-0.51} \times 10^{-6}$	6.9	-1.8	2.7
39.877~41.506	29.75	$0.04^{+0.01}_{-0.01}$	$-1.18^{+0.13}_{-0.13}$	148^{+39}_{-40}	121^{+37}_{-38}	$0.94^{+0.33}_{-0.33} \times 10^{-6}$	$0.59^{+0.06}_{-0.06}$	$-1.15^{+0.15}_{-0.16}$	$-5.33^{+2.46}_{-2.68}$	111^{+17}_{-16}	$0.95^{+0.94}_{-0.19} \times 10^{-6}$	3.9	0.2	2.3

Note—All columns are the same as Table A2 but for GRB 140508128.

Table A25. Time-resolved Spectral Fit Results of GRB 140523129

$t_{\text{start}} \sim t_{\text{stop}}$	S	Cutoff Power-Law Fitting						Band Fitting						Difference	
		K	α	E_c	E_p	F	K	α	β	E_p	F	ΔDIC	$p_{\text{DIC}}^{\text{CPL}}$	$p_{\text{DIC}}^{\text{Band}}$	
(1)	(2)	(3)	(4)	(5)	(6)	(7)	(8)	(9)	(10)	(11)	(12)	(13)	(14)	(15)	
Pulse 1															
-0.009~0.668	29.99	0.22+0.03 -0.62+0.08	298+44 -0.94	411+65 -66	3.31+1.58 -3.31	10^{-6}	0.06+0.01 -0.49	+0.15 -0.14	-4.17+1.93 -2.33	346+66 -68	3.91+1.88 -1.68	-8.5	2.1	-2.7	
0.668~1.024	60.87	0.37+0.03 -0.35+0.04	333+22 -0.39	550+37 -3.04	16.82+3.75 -3.04	10^{-6}	0.37+0.03 -0.35	+0.04 -0.04	-5.92+2.33 -2.63	544+25 -2.63	17.42+3.05 -2.70	-0.8	2.8	2.6	
1.024~1.317	36.47	0.46+0.05 -0.54+0.08	194+23 -0.16	283+37 -0.14	4.82+1.84 -1.84	10^{-6}	0.33+0.05 -0.11	+0.16 -0.10	-2.16+1.11 -1.79	1.79+1.19 -1.19	7.56+3.87 -2.32	-15.4	2.5	2.0	
1.317~1.661	22.96	0.56+0.07 -0.77+0.15	112+23 -0.15	138+33 -0.14	1.54+0.85 -0.53	10^{-6}	0.49+0.08 -0.41	+0.26 -0.27	-2.80+0.59 -0.02	102+1.6 -0.16	2.10+1.30 -0.79	-8.6	1.1	0.5	
Pulse 2															
3.275~3.800	21.97	0.21+0.03 -0.72+0.11	304+62 -0.89	389+87 -0.89	2.31+1.59 -2.31	10^{-6}	0.20+0.03 -0.70	+0.11 -0.11	-6.57+2.47 -2.42	375+52 -54	2.23+0.94 -0.64	-1.0	1.4	2.4	
3.800~4.304	36.29	0.36+0.04 -0.74+0.06	409+55 -0.84	515+74 -0.84	5.35+1.92 -5.35	10^{-6}	0.36+0.04 -0.73	+0.06 -0.06	-5.53+2.54 -2.48	506+48 -48	5.69+1.58 -1.66	-0.6	2.5	2.5	
4.304~4.438	28.24	0.25+0.05 -0.28+0.10	249+32 -0.28	428+61 -0.30	8.65+5.00 -8.65	10^{-6}	0.25+0.05 -0.24	+0.10 -0.10	-6.57+2.28 -2.34	419+34 -33	8.89+3.62 -2.53	0.5	1.8	2.4	
4.438~4.949	68.87	0.19+0.01 -0.39+0.04	233+14 -0.39	375+24 -0.39	10.53+1.11 -1.01	10^{-6}	0.47+0.03 -0.39	+0.04 -0.04	-7.21+1.90 -1.93	373+13 -1.23	10.57+1.59 -1.05	1.4	2.9	3.2	
5.183~5.423	49.82	0.18+0.01 -0.46+0.05	291+26 -0.46	449+42 -0.46	12.93+2.33 -2.33	10^{-6}	0.47+0.05 -0.37	+0.08 -0.08	-2.79+0.47 -0.11	390+39 -33	15.48+6.16 -3.79	-8.3	2.8	2.0	
5.423~5.635	38.62	0.18+0.02 -0.52+0.07	201+22 -0.52	298+36 -0.52	6.95+1.53 -1.13	10^{-6}	0.52+0.08 -0.36	+0.17 -0.16	-3.33+1.26 -0.16	246+45 -44	8.33+5.94 -3.05	-10.1	2.6	-3.5	
Pulse 3															
7.240~7.384	42.99	0.20+0.01 -0.57+0.06	274+30 -0.66	392+46 -0.66	11.55+2.27 -1.75	10^{-6}	0.72+0.08 -0.56	+0.07 -0.07	-5.74+2.56 -2.47	386+31 -31	11.96+3.58 -2.47	-0.9	2.7	2.7	
7.384~8.371	87.11	0.23+0.01 -0.51+0.04	152+7 -0.04	226+12 -0.04	5.92+0.53 -0.53	10^{-6}	0.23+0.02 -0.48	+0.05 -0.05	-4.88+1.85 -1.85	220+10 -10	6.24+0.87 -0.67	-3.6	2.9	1.1	
8.371~8.894	52.99	0.22+0.02 -0.56+0.07	105+9 -0.05	151+15 -0.15	3.32+0.58 -0.58	10^{-6}	0.67+0.06 -0.26	+0.12 -0.11	-2.44+0.12 -0.12	11.3+8 -8	4.46+1.24 -0.67	-22.4	2.5	3.8	
8.894~9.448	36.62	0.12+0.02 -0.82+0.09	98+12 -0.09	115+17 -0.17	1.70+0.46 -0.46	10^{-6}	0.80+0.07 -0.79	+0.12 -0.12	-5.32+2.48 -2.48	11.0+9 -9	1.81+0.50 -0.50	0.8	1.9	1.9	
9.720~10.034	43.23	0.13+0.01 -0.83+0.06	239+28 -0.06	280+36 -0.06	5.28+0.98 -0.81	10^{-6}	0.88+0.07 -0.83	+0.06 -0.06	-6.23+2.43 -2.43	275+22 -21	5.38+1.32 -0.89	2.1	2.7	3.0	
10.034~10.426	34.02	0.08+0.01 -1.10+0.08	200+34 -0.08	180+35 -0.08	2.54+0.58 -0.45	10^{-6}	1.04+0.08 -1.10	+0.08 -0.08	-6.40+2.50 -2.46	176+19 -19	2.55+0.48 -0.38	3.2	2.1	3.0	
Pulse 4															
12.914~14.037	45.10	0.08+0.01 -1.04	+0.07 131+16	126+18 -18	1.59+0.28 -0.24	10^{-6}	0.82+0.05 -0.98	+0.10 -0.10	-5.04+2.48 -3.23	117+12 -13	1.67+0.52 -0.28	-0.4	2.4	1.0	
Pulse 5															
15.540~16.452	29.85	0.06+0.01 -1.08	+0.10 113+19	104+21 -19	1.08+0.30 -0.25	10^{-6}	0.69+0.06 -0.05	-1.07	+0.11 -0.11	6.24+2.54 -2.55	102+8 -8	1.07+0.16 -0.14	-3.7	1.5	3.0
16.452~16.585	25.41	0.13+0.03 -0.95	+0.13 183+45	192+53 -53	3.49+1.63 -0.98	10^{-6}	0.96+0.16 -0.15	-0.49	+0.35 -0.35	2.86+0.73 -0.73	11.6+32 -32	4.81+1.91 -2.15	-13.8	-1.4	-7.4
16.585~17.194	75.75	0.41+0.03 -0.51	+0.05 83+5	124+8 -5	4.38+0.59 -0.52	10^{-6}	1.21+0.06 -0.06	-0.30	+0.07 -0.07	-2.84+0.14 -0.14	107+4 -4	5.12+0.75 -0.73	-18.6	2.8	4.0
17.194~17.388	30.49	0.19+0.04 -0.93	+0.13 86+15	92+20 -20	2.42+0.89 -0.49	10^{-6}	1.59+0.15 -0.15	-0.90	+0.14 -0.14	-5.43+2.40 -2.40	88+7 -7	2.46+0.37 -0.37	2.9	0.3	2.2
17.388~17.724	24.07	0.10+0.03 -1.12	+0.18 79+18	69+21 -21	1.23+0.66 -0.42	10^{-6}	1.17+0.12 -0.11	-0.86	+0.34 -0.34	-4.09+2.65 -2.65	58+10 -10	1.27+0.52 -0.52	1.4	-4.1	-1.8
18.011~18.691	39.22	0.16+0.03 -0.91	+0.11 60+7	66+10 -10	1.35+0.40 -0.29	10^{-6}	1.25+0.08 -0.08	-0.90	+0.11 -0.12	-6.27+2.54 -2.54	65+3 -3	1.35+0.14 -0.13	3.1	1.3	2.8
18.691~19.235	26.46	0.10+0.03 -1.13	+0.16 56+11	49+13 -13	1.01+0.54 -0.35	10^{-6}	1.33+0.10 -0.10	-1.11	+0.18 -0.18	-6.46+2.52 -2.52	47+3 -3	0.98+0.10 -0.10	8.7	-3.5	3.0
19.235~21.500	35.76	0.06+0.02 -1.22	+0.13 50+8	39+9 -9	0.62+0.30 -0.18	10^{-6}	1.01+0.05 -0.05	-1.06	+0.22 -0.22	-4.60+1.66 -1.66	37+2 -2	0.63+0.07 -0.07	3.4	-4.0	-0.7
21.500~21.900	25.55	0.08+0.02 -1.14	+0.16 96+22	82+24 -24	1.24+0.60 -0.42	10^{-6}	1.03+0.10 -0.10	-1.05	+0.18 -0.20	-5.40+2.62 -2.62	74+9 -9	1.25+0.22 -0.22	5.3	-1.9	1.9

Note—All columns are the same as Table A2 but for GRB 140523129.

Table A26. Time-resolved Spectral Fit Results of GRB 140810782

$t_{\text{start}} \sim t_{\text{stop}}$	S	Cutoff Power-Law Fitting				Band Fitting				Difference				
		K	α	E_c	E_p	F	K	α	β	E_p	F	ΔDIC	$p_{\text{DIC}}^{\text{CPL}}$	
(1)	(2)	(3)	(4)	(5)	(6)	(7)	(8)	(9)	(10)	(11)	(12)	(13)	(14)	(15)
Pulse 1														
7.394~8.677	31.30	$0.04^{+0.00}_{-0.00}$	$-0.82^{+0.06}_{-0.06}$	520^{+83}_{-84}	614^{+102}_{-104}	$4.37^{+1.19}_{-0.81} \times 10^{-6}$	$0.29^{+0.03}_{-0.03}$	$-0.82^{+0.06}_{-0.06}$	$-6.26^{+2.53}_{-2.53}$	609^{+72}_{-72}	$4.46^{+1.21}_{-0.91} \times 10^{-6}$	1.7	2.7	2.8
Pulse 2														
24.323~25.340	32.64	$0.05^{+0.00}_{-0.00}$	$-0.57^{+0.07}_{-0.07}$	450^{+61}_{-62}	644^{+93}_{-94}	$6.25^{+1.43}_{-1.29} \times 10^{-6}$	$0.19^{+0.02}_{-0.02}$	$-0.57^{+0.07}_{-0.07}$	$-6.18^{+2.64}_{-2.59}$	632^{+65}_{-64}	$6.38^{+2.11}_{-1.48} \times 10^{-6}$	1.0	2.7	2.6
25.340~27.759	56.62	$0.07^{+0.00}_{-0.00}$	$-0.69^{+0.03}_{-0.04}$	450^{+36}_{-36}	590^{+49}_{-50}	$6.78^{+0.85}_{-0.74} \times 10^{-6}$	$0.32^{+0.02}_{-0.02}$	$-0.68^{+0.03}_{-0.03}$	$-5.58^{+2.53}_{-2.53}$	582^{+36}_{-35}	$7.05^{+1.15}_{-0.99} \times 10^{-6}$	0.1	2.9	2.4
27.759~28.108	30.81	$0.08^{+0.00}_{-0.00}$	$-0.62^{+0.07}_{-0.07}$	572^{+93}_{-93}	790^{+134}_{-134}	$12.11^{+3.48}_{-2.50} \times 10^{-6}$	$0.33^{+0.04}_{-0.04}$	$-0.62^{+0.07}_{-0.07}$	$-6.18^{+2.66}_{-2.63}$	778^{+98}_{-97}	$12.19^{+4.41}_{-3.23} \times 10^{-6}$	1.0	2.6	2.5
28.108~29.071	34.03	$0.07^{+0.00}_{-0.00}$	$-0.67^{+0.07}_{-0.06}$	322^{+42}_{-43}	429^{+60}_{-60}	$4.68^{+1.06}_{-0.81} \times 10^{-6}$	$0.32^{+0.03}_{-0.03}$	$-0.66^{+0.07}_{-0.07}$	$-5.44^{+2.67}_{-2.99}$	418^{+40}_{-39}	$5.01^{+1.41}_{-1.12} \times 10^{-6}$	0.3	2.6	2.3
Pulse 3														
29.071~30.840	20.63	$0.05^{+0.01}_{-0.01}$	$-0.59^{+0.13}_{-0.13}$	124^{+22}_{-22}	174^{+35}_{-35}	$0.99^{+0.40}_{-0.25} \times 10^{-6}$	$0.21^{+0.03}_{-0.03}$	$-0.57^{+0.15}_{-0.15}$	$-5.95^{+4.28}_{-2.83}$	166^{+19}_{-18}	$1.03^{+0.50}_{-0.28} \times 10^{-6}$	2.4	0.9	2.3
30.840~31.783	35.49	$0.07^{+0.00}_{-0.00}$	$-0.72^{+0.06}_{-0.06}$	337^{+45}_{-45}	432^{+61}_{-61}	$4.51^{+0.89}_{-0.75} \times 10^{-6}$	$0.35^{+0.04}_{-0.04}$	$-0.71^{+0.06}_{-0.07}$	$-5.74^{+3.00}_{-2.96}$	416^{+48}_{-48}	$4.76^{+1.63}_{-1.17} \times 10^{-6}$	1.1	2.6	2.4
31.783~33.129	29.86	$0.06^{+0.01}_{-0.01}$	$-0.75^{+0.08}_{-0.08}$	219^{+33}_{-34}	273^{+45}_{-45}	$2.17^{+0.49}_{-0.40} \times 10^{-6}$	$0.32^{+0.04}_{-0.04}$	$-0.69^{+0.13}_{-0.13}$	$-4.92^{+2.58}_{-2.40}$	249^{+45}_{-45}	$2.31^{+1.66}_{-1.66} \times 10^{-6}$	-1.7	2.3	-0.2
33.129~33.897	44.92	$0.09^{+0.00}_{-0.00}$	$-0.63^{+0.05}_{-0.05}$	436^{+44}_{-44}	597^{+64}_{-64}	$9.67^{+1.76}_{-1.41} \times 10^{-6}$	$0.39^{+0.03}_{-0.03}$	$-0.63^{+0.05}_{-0.05}$	$-5.35^{+2.56}_{-3.12}$	587^{+46}_{-44}	$10.20^{+2.61}_{-2.61} \times 10^{-6}$	-0.4	2.8	2.1
33.897~35.883	49.74	$0.07^{+0.00}_{-0.00}$	$-0.79^{+0.05}_{-0.05}$	317^{+33}_{-33}	383^{+43}_{-43}	$4.07^{+0.70}_{-0.60} \times 10^{-6}$	$0.40^{+0.03}_{-0.03}$	$-0.73^{+0.06}_{-0.06}$	$-3.15^{+0.95}_{-0.88}$	335^{+38}_{-38}	$5.30^{+1.64}_{-1.64} \times 10^{-6}$	-10.0	2.8	-2.4
35.883~40.114	26.96	$0.04^{+0.01}_{-0.01}$	$-0.82^{+0.09}_{-0.09}$	140^{+21}_{-22}	166^{+28}_{-28}	$0.83^{+0.21}_{-0.16} \times 10^{-6}$	$0.25^{+0.03}_{-0.03}$	$-0.76^{+0.13}_{-0.12}$	$-4.48^{+2.17}_{-2.22}$	153^{+18}_{-19}	$0.97^{+0.44}_{-0.27} \times 10^{-6}$	-1.0	1.9	1.1
Pulse 4														
44.814~47.047	43.94	$0.07^{+0.00}_{-0.00}$	$-0.84^{+0.05}_{-0.05}$	218^{+24}_{-24}	253^{+30}_{-30}	$2.42^{+0.37}_{-0.32} \times 10^{-6}$	$0.43^{+0.04}_{-0.04}$	$-0.72^{+0.13}_{-0.13}$	$-3.32^{+1.24}_{-2.20}$	206^{+44}_{-39}	$3.25^{+1.77}_{-1.19} \times 10^{-6}$	-13.6	2.7	-7.0
47.047~48.370	58.51	$0.14^{+0.01}_{-0.01}$	$-0.70^{+0.05}_{-0.05}$	170^{+13}_{-13}	221^{+19}_{-19}	$4.09^{+0.58}_{-0.47} \times 10^{-6}$	$0.59^{+0.05}_{-0.05}$	$-0.38^{+0.10}_{-0.10}$	$-2.29^{+0.11}_{-0.09}$	155^{+12}_{-13}	$5.87^{+1.68}_{-1.24} \times 10^{-6}$	-10.6	2.9	3.4
48.370~50.060	76.50	$0.14^{+0.01}_{-0.01}$	$-0.81^{+0.03}_{-0.03}$	231^{+16}_{-16}	274^{+21}_{-21}	$5.58^{+0.58}_{-0.56} \times 10^{-6}$	$0.84^{+0.06}_{-0.06}$	$-0.70^{+0.08}_{-0.08}$	$-2.99^{+0.14}_{-0.14}$	231^{+31}_{-28}	$6.86^{+2.21}_{-1.72} \times 10^{-6}$	-11.7	2.9	-4.0
50.060~50.716	30.45	$0.09^{+0.01}_{-0.01}$	$-0.94^{+0.09}_{-0.09}$	163^{+28}_{-28}	173^{+33}_{-34}	$2.25^{+0.62}_{-0.44} \times 10^{-6}$	$0.78^{+0.07}_{-0.07}$	$-0.92^{+0.10}_{-0.10}$	$-5.80^{+0.72}_{-0.72}$	167^{+19}_{-19}	$2.35^{+0.72}_{-0.49} \times 10^{-6}$	2.6	1.8	2.7
50.716~51.734	20.92	$0.06^{+0.01}_{-0.01}$	$-0.92^{+0.15}_{-0.15}$	132^{+33}_{-35}	142^{+41}_{-42}	$1.04^{+0.49}_{-0.32} \times 10^{-6}$	$0.40^{+0.06}_{-0.06}$	$-0.56^{+0.30}_{-0.30}$	$-2.89^{+0.78}_{-0.78}$	101^{+21}_{-21}	$1.37^{+1.14}_{-0.55} \times 10^{-6}$	-5.2	-2.1	-2.1

Note—All columns are the same as Table A2 but for GRB 140810782.

Table A27. Time-resolved Spectral Fit Results of GRB 141222691

$t_{\text{start}} \sim t_{\text{stop}}$	S	Cutoff Power-Law Fitting						Band Fitting						Difference		
		K	α	E_c	E_p	F	K	α	β	E_p	F	ΔDIC	$p_{\text{DIC}}^{\text{CPL}}$	$p_{\text{DIC}}^{\text{Band}}$		
Pulse 1																
0.640~2.116	28.38	0.02 ^{+0.00} _{-0.00}	-1.19 ^{+0.06} _{-0.06}	710 ⁺²¹⁴ ₋₂₂₃	575 ⁺¹⁷⁸ ₋₁₈₅	1.79 ^{+0.59} _{-0.39}	$\times 10^{-6}$	0.33 ^{+0.03} _{-0.03}	-1.18 ^{+0.07} _{-0.07}	-5.91 ^{+2.71} _{-2.72}	542 ⁺¹³² ₋₁₃₇	1.81 ^{+0.64} _{-0.42}	$\times 10^{-6}$	3.0	1.5	2.0
2.116~3.014	31.12	0.04 ^{+0.00} _{-0.00}	-1.05 ^{+0.08} _{-0.08}	335 ⁺⁸⁰ ₋₈₃	318 ⁺⁸¹ ₋₈₃	1.88 ^{+0.40} _{-0.40}	$\times 10^{-6}$	0.40 ^{+0.04} _{-0.04}	-0.94 ^{+0.12} _{-0.12}	-3.07 ^{+1.02} _{-1.27}	241 ⁺⁵¹ ₋₅₁	2.52 ^{+0.86} _{-0.86}	$\times 10^{-6}$	-8.9	1.2	-3.0
3.014~4.887	60.17	0.07 ^{+0.00} _{-0.00}	-0.78 ^{+0.04} _{-0.04}	228 ⁺¹⁹ ₋₁₉	278 ⁺²⁵ ₋₂₅	2.84 ^{+0.33} _{-0.32}	$\times 10^{-6}$	0.42 ^{+0.03} _{-0.03}	-0.73 ^{+0.05} _{-0.05}	-3.18 ^{+0.86} _{-0.28}	252 ⁺²¹ ₋₂₀	3.47 ^{+0.85} _{-0.72}	$\times 10^{-6}$	-8.3	2.9	-0.8
4.887~5.798	26.37	0.06 ^{+0.01} _{-0.01}	-0.73 ^{+0.10} _{-0.10}	134 ⁺²¹ ₋₂₁	170 ⁺³⁰ ₋₃₁	1.26 ^{+0.37} _{-0.29}	$\times 10^{-6}$	0.28 ^{+0.04} _{-0.04}	-0.34 ^{+0.26} _{-0.26}	-2.28 ^{+0.23} _{-0.13}	117 ⁺²² ₋₂₂	1.98 ^{+1.39} _{-0.72}	$\times 10^{-6}$	-13.4	1.6	-1.1
5.798~9.086	25.78	0.03 ^{+0.00} _{-0.00}	-0.92 ^{+0.10} _{-0.10}	130 ⁺²² ₋₂₂	141 ⁺²⁷ ₋₂₇	0.56 ^{+0.16} _{-0.11}	$\times 10^{-6}$	0.23 ^{+0.02} _{-0.02}	-0.90 ^{+0.10} _{-0.11}	-5.96 ^{+2.75} _{-2.77}	136 ⁺¹³ ₋₁₂	0.57 ^{+0.15} _{-0.10}	$\times 10^{-6}$	2.7	1.7	2.8
Pulse 2																
14.378~16.037	30.11	0.05 ^{+0.01} _{-0.01}	-0.97 ^{+0.10} _{-0.10}	105 ⁺¹⁶ ₋₁₆	108 ⁺²⁰ ₋₂₀	0.77 ^{+0.20} _{-0.16}	$\times 10^{-6}$	0.44 ^{+0.04} _{-0.04}	-0.94 ^{+0.12} _{-0.12}	-5.73 ^{+2.67} _{-2.85}	103 ⁺⁹ ₋₉	0.78 ^{+0.16} _{-0.12}	$\times 10^{-6}$	2.5	1.5	2.5
16.037~18.191	25.61	0.03 ^{+0.01} _{-0.01}	-1.06 ^{+0.11} _{-0.11}	112 ⁺²¹ ₋₂₂	105 ⁺²³ ₋₂₄	0.55 ^{+0.19} _{-0.13}	$\times 10^{-6}$	0.36 ^{+0.03} _{-0.03}	-1.06 ^{+0.12} _{-0.12}	-6.29 ^{+2.70} _{-2.60}	101 ⁺¹⁰ ₋₉	0.56 ^{+0.11} _{-0.08}	$\times 10^{-6}$	4.3	0.8	3.0
18.191~20.566	47.81	0.05 ^{+0.00} _{-0.00}	-1.13 ^{+0.06} _{-0.06}	142 ⁺¹⁵ ₋₁₆	123 ⁺¹⁶ ₋₁₆	1.14 ^{+0.16} _{-0.14}	$\times 10^{-6}$	0.66 ^{+0.03} _{-0.03}	-1.12 ^{+0.06} _{-0.06}	-6.45 ^{+2.39} _{-2.38}	122 ⁺⁷ ₋₇	1.15 ^{+0.12} _{-0.11}	$\times 10^{-6}$	3.0	2.6	3.2
20.566~22.331	31.00	0.03 ^{+0.01} _{-0.01}	-1.33 ^{+0.11} _{-0.11}	128 ⁺²⁸ ₋₂₉	86 ⁺²⁴ ₋₂₄	0.70 ^{+0.26} _{-0.17}	$\times 10^{-6}$	0.62 ^{+0.04} _{-0.04}	-1.04 ^{+0.36} _{-0.33}	-4.14 ^{+1.88} _{-3.05}	69 ⁺¹⁶ ₋₂₀	0.78 ^{+0.37} _{-0.21}	$\times 10^{-6}$	-12.1	-0.0	-12.8
22.331~26.068	29.38	0.02 ^{+0.00} _{-0.00}	-1.46 ^{+0.12} _{-0.12}	92 ⁺²⁰ ₋₂₁	50 ⁺¹⁶ ₋₁₆	0.45 ^{+0.17} _{-0.12}	$\times 10^{-6}$	0.57 ^{+0.03} _{-0.03}	-1.42 ^{+0.12} _{-0.14}	-5.97 ^{+2.67} _{-2.72}	47 ⁺⁴ ₋₄	0.44 ^{+0.04} _{-0.04}	$\times 10^{-6}$	6.7	-0.8	3.0
26.068~32.663	24.00	0.01 ^{+0.00} _{-0.00}	-1.73 ^{+0.14} _{-0.14}	135 ⁺⁴⁹ ₋₄₉	36 ⁺²³ ₋₂₃	0.31 ^{+0.14} _{-0.10}	$\times 10^{-6}$	0.01 ^{+0.01} _{-0.00}	-1.56 ^{+0.24} _{-0.18}	-5.43 ^{+2.83} _{-3.01}	33 ⁺⁵ ₋₅	0.29 ^{+0.28} _{-0.14}	$\times 10^{-6}$	-5.1	-4.2	-9.1
Pulse 3																
32.663~34.125	20.81	0.01 ^{+0.00} _{-0.00}	-1.62 ^{+0.12} _{-0.12}	341 ⁺¹⁸⁹ ₋₁₆₃	130 ⁺¹⁸³ ₋₇₄	0.65 ^{+0.26} _{-0.19}	$\times 10^{-6}$	0.55 ^{+0.05} _{-0.05}	-1.60 ^{+0.13} _{-0.14}	-6.09 ^{+2.70} _{-2.67}	115 ⁺²⁶ ₋₃₃	0.64 ^{+0.14} _{-0.09}	$\times 10^{-6}$	7.8	-2.7	1.7

Note—All columns are the same as Table A2 but for GRB 141222691.

Table A28. Time-resolved Spectral Fit Results of GRB 150118409

$t_{\text{start}} \sim t_{\text{stop}}$	S	Cutoff Power-Law Fitting						Band Fitting						Difference	
		K	α	E_c	E_p	F	K	α	β	E_p	F	ΔDIC	$p_{\text{DIC}}^{\text{CPL}}$	$p_{\text{DIC}}^{\text{Band}}$	
(1)	(2)	(3)	(4)	(5)	(6)	(7)	(8)	(9)	(10)	(11)	(12)	(13)	(14)	(15)	
Pulse 1															
5.671~7.763	27.61	0.03 $^{+0.00}_{-0.01}$	-0.91 $^{+0.10}_{-0.10}$	1.56 $^{+0.28}_{-0.28}$	170 $^{+34}_{-34}$	0.81 $^{+0.24}_{-0.17} \times 10^{-6}$	0.26 $^{+0.03}_{-0.03}$	-0.84 $^{+0.12}_{-0.12}$	-3.72 $^{+1.49}_{-2.59}$	152 $^{+21}_{-21}$	1.00 $^{+0.41}_{-0.29} \times 10^{-6}$	-3.6	1.4	-0.2	
7.763~8.655	24.51	0.05 $^{+0.01}_{-0.01}$	-0.89 $^{+0.10}_{-0.10}$	143 $^{+26}_{-26}$	158 $^{+32}_{-32}$	1.15 $^{+0.36}_{-0.26} \times 10^{-6}$	0.38 $^{+0.05}_{-0.05}$	-0.75 $^{+0.19}_{-0.19}$	-4.30 $^{+2.09}_{-3.30}$	137 $^{+25}_{-27}$	1.31 $^{+0.43}_{-0.43} \times 10^{-6}$	-3.8	1.5	-1.8	
9.631~9.965	28.83	0.07 $^{+0.01}_{-0.01}$	-0.69 $^{+0.07}_{-0.07}$	322 $^{+47}_{-47}$	422 $^{+65}_{-65}$	4.82 $^{+1.18}_{-0.97} \times 10^{-6}$	0.36 $^{+0.04}_{-0.04}$	-0.69 $^{+0.07}_{-0.07}$	-6.40 $^{+2.40}_{-2.42}$	423 $^{+44}_{-45}$	4.92 $^{+1.44}_{-1.06} \times 10^{-6}$	1.7	2.7	2.9	
9.965~10.672	21.52	0.04 $^{+0.01}_{-0.01}$	-1.00 $^{+0.12}_{-0.12}$	175 $^{+47}_{-45}$	175 $^{+47}_{-45}$	1.13 $^{+0.48}_{-0.48} \times 10^{-6}$	0.41 $^{+0.05}_{-0.05}$	-0.92 $^{+0.17}_{-0.17}$	-4.71 $^{+2.43}_{-2.43}$	15 $^{+29}_{-29}$	1.25 $^{+0.68}_{-0.68} \times 10^{-6}$	1.1	-0.1	0.5	
10.672~10.848	21.72	0.07 $^{+0.01}_{-0.01}$	-0.77 $^{+0.11}_{-0.11}$	329 $^{+78}_{-78}$	404 $^{+103}_{-105}$	4.32 $^{+1.85}_{-1.10} \times 10^{-6}$	0.45 $^{+0.07}_{-0.07}$	-0.78 $^{+0.11}_{-0.11}$	-4.79 $^{+2.54}_{-3.29}$	396 $^{+71}_{-72}$	5.01 $^{+3.00}_{-1.65} \times 10^{-6}$	-0.4	1.8	1.2	
10.848~12.278	37.74	0.07 $^{+0.01}_{-0.01}$	-0.74 $^{+0.07}_{-0.07}$	139 $^{+16}_{-16}$	176 $^{+22}_{-22}$	1.59 $^{+0.29}_{-0.27} \times 10^{-6}$	0.34 $^{+0.03}_{-0.03}$	-0.41 $^{+0.12}_{-0.12}$	-2.21 $^{+0.10}_{-0.10}$	123 $^{+10}_{-10}$	2.48 $^{+0.78}_{-0.55} \times 10^{-6}$	-19.8	2.4	3.5	
12.278~13.559	26.69	0.05 $^{+0.01}_{-0.01}$	-0.94 $^{+0.10}_{-0.10}$	135 $^{+25}_{-25}$	143 $^{+29}_{-29}$	0.93 $^{+0.29}_{-0.20} \times 10^{-6}$	0.38 $^{+0.04}_{-0.04}$	-0.88 $^{+0.15}_{-0.14}$	-4.66 $^{+2.26}_{-3.15}$	13 $^{+19}_{-19}$	1.04 $^{+0.46}_{-0.27} \times 10^{-6}$	0.1	1.3	1.0	
13.559~14.004	30.81	0.08 $^{+0.01}_{-0.01}$	-0.59 $^{+0.08}_{-0.08}$	240 $^{+32}_{-32}$	339 $^{+50}_{-50}$	3.92 $^{+0.98}_{-0.70} \times 10^{-6}$	0.32 $^{+0.04}_{-0.04}$	-0.58 $^{+0.09}_{-0.09}$	-5.49 $^{+2.79}_{-3.02}$	325 $^{+35}_{-35}$	4.12 $^{+1.86}_{-1.00} \times 10^{-6}$	0.6	2.5	2.3	
14.004~14.851	22.82	0.05 $^{+0.01}_{-0.01}$	-0.87 $^{+0.10}_{-0.10}$	162 $^{+30}_{-30}$	183 $^{+38}_{-37}$	1.17 $^{+0.37}_{-0.27} \times 10^{-6}$	0.34 $^{+0.04}_{-0.04}$	-0.87 $^{+0.10}_{-0.10}$	-6.35 $^{+2.44}_{-2.45}$	180 $^{+19}_{-20}$	1.17 $^{+0.30}_{-0.22} \times 10^{-6}$	2.9	1.9	2.9	
14.851~15.068	30.99	0.14 $^{+0.01}_{-0.01}$	-0.46 $^{+0.07}_{-0.07}$	220 $^{+25}_{-25}$	339 $^{+42}_{-42}$	6.66 $^{+1.68}_{-1.09} \times 10^{-6}$	0.42 $^{+0.05}_{-0.05}$	-0.46 $^{+0.08}_{-0.08}$	-6.63 $^{+2.31}_{-2.28}$	336 $^{+26}_{-26}$	6.79 $^{+1.87}_{-1.38} \times 10^{-6}$	1.4	2.7	3.0	
15.068~15.421	22.33	0.14 $^{+0.03}_{-0.03}$	-0.63 $^{+0.16}_{-0.16}$	87 $^{+16}_{-16}$	119 $^{+25}_{-25}$	1.48 $^{+0.76}_{-0.60} \times 10^{-6}$	0.20 $^{+0.04}_{-0.05}$	-0.44 $^{+0.11}_{-0.12}$	-2.75 $^{+0.46}_{-0.46}$	98 $^{+9}_{-9}$	2.08 $^{+0.89}_{-0.65} \times 10^{-6}$	-7.5	-1.0	1.4	
15.779~16.232	28.49	0.10 $^{+0.01}_{-0.01}$	-0.66 $^{+0.10}_{-0.10}$	134 $^{+20}_{-20}$	180 $^{+30}_{-30}$	2.05 $^{+0.57}_{-0.57} \times 10^{-6}$	0.45 $^{+0.05}_{-0.05}$	-0.64 $^{+0.11}_{-0.12}$	-5.88 $^{+2.80}_{-2.79}$	174 $^{+18}_{-17}$	2.10 $^{+0.81}_{-0.47} \times 10^{-6}$	1.7	2.0	2.5	
16.500~16.854	32.50	0.11 $^{+0.01}_{-0.01}$	-0.73 $^{+0.07}_{-0.07}$	203 $^{+26}_{-26}$	258 $^{+36}_{-36}$	3.89 $^{+0.84}_{-0.70} \times 10^{-6}$	0.59 $^{+0.06}_{-0.06}$	-0.72 $^{+0.07}_{-0.07}$	-6.09 $^{+2.55}_{-2.59}$	255 $^{+22}_{-22}$	3.96 $^{+0.93}_{-0.70} \times 10^{-6}$	1.8	2.6	2.9	
16.854~19.838	30.96	0.04 $^{+0.01}_{-0.01}$	-1.01 $^{+0.09}_{-0.09}$	98 $^{+16}_{-14}$	97 $^{+16}_{-16}$	0.60 $^{+0.14}_{-0.12} \times 10^{-6}$	0.39 $^{+0.03}_{-0.03}$	-0.95 $^{+0.11}_{-0.12}$	-4.52 $^{+1.93}_{-2.8}$	92 $^{+8}_{-8}$	0.66 $^{+0.17}_{-0.11} \times 10^{-6}$	-1.1	1.6	0.8	
Pulse 2															
19.838~20.287	21.03	0.04 $^{+0.01}_{-0.01}$	-1.14 $^{+0.10}_{-0.10}$	301 $^{+86}_{-93}$	259 $^{+80}_{-85}$	1.71 $^{+0.65}_{-0.45} \times 10^{-6}$	0.55 $^{+0.06}_{-0.06}$	-1.13 $^{+0.11}_{-0.12}$	-6.01 $^{+2.76}_{-2.76}$	243 $^{+53}_{-53}$	1.72 $^{+0.63}_{-0.44} \times 10^{-6}$	3.5	0.8	2.0	
20.287~20.863	35.54	0.06 $^{+0.00}_{-0.00}$	-0.89 $^{+0.05}_{-0.05}$	579 $^{+85}_{-85}$	642 $^{+99}_{-98}$	6.02 $^{+0.98}_{-0.98} \times 10^{-6}$	0.45 $^{+0.03}_{-0.03}$	-0.89 $^{+0.05}_{-0.05}$	-6.82 $^{+2.21}_{-2.21}$	639 $^{+73}_{-73}$	6.01 $^{+1.26}_{-1.26} \times 10^{-6}$	2.0	2.8	3.0	
20.863~21.129	31.34	0.07 $^{+0.00}_{-0.00}$	-0.72 $^{+0.12}_{-0.12}$	880 $^{+126}_{-126}$	1127 $^{+167}_{-167}$	15.66 $^{+3.87}_{-2.94} \times 10^{-6}$	0.07 $^{+0.00}_{-0.00}$	-0.72 $^{+0.05}_{-0.05}$	-6.70 $^{+2.27}_{-2.27}$	1117 $^{+128}_{-128}$	15.60 $^{+2.70}_{-2.19} \times 10^{-6}$	0.4	2.9	3.1	
21.129~21.448	21.83	0.04 $^{+0.00}_{-0.00}$	-0.98 $^{+0.07}_{-0.07}$	620 $^{+126}_{-126}$	633 $^{+158}_{-161}$	4.20 $^{+1.49}_{-0.97} \times 10^{-6}$	0.42 $^{+0.05}_{-0.05}$	-0.99 $^{+0.08}_{-0.08}$	-6.35 $^{+2.52}_{-2.50}$	623 $^{+128}_{-129}$	4.15 $^{+1.66}_{-1.66} \times 10^{-6}$	2.5	2.3	2.7	
21.448~22.748	59.86	0.06 $^{+0.00}_{-0.00}$	-0.69 $^{+0.02}_{-0.02}$	952 $^{+66}_{-66}$	1247 $^{+89}_{-88}$	16.00 $^{+1.87}_{-1.54} \times 10^{-6}$	0.29 $^{+0.02}_{-0.02}$	-0.69 $^{+0.02}_{-0.02}$	-6.20 $^{+2.25}_{-2.47}$	1240 $^{+70}_{-69}$	16.06 $^{+2.22}_{-1.84} \times 10^{-6}$	0.9	3.0	2.8	
22.748~28.687	103.91	0.05 $^{+0.00}_{-0.00}$	-0.57 $^{+0.02}_{-0.02}$	733 $^{+27}_{-27}$	1048 $^{+41}_{-41}$	12.71 $^{+0.84}_{-0.77} \times 10^{-6}$	0.19 $^{+0.01}_{-0.01}$	-0.57 $^{+0.02}_{-0.02}$	-6.69 $^{+2.06}_{-2.06}$	1049 $^{+29}_{-28}$	12.76 $^{+0.98}_{-0.92} \times 10^{-6}$	0.9	3.0	2.9	
28.687~32.214	61.28	0.04 $^{+0.00}_{-0.00}$	-0.63 $^{+0.03}_{-0.03}$	608 $^{+37}_{-37}$	833 $^{+55}_{-54}$	6.85 $^{+0.72}_{-0.61} \times 10^{-6}$	0.17 $^{+0.01}_{-0.01}$	-0.63 $^{+0.03}_{-0.03}$	-6.99 $^{+2.12}_{-2.12}$	834 $^{+39}_{-39}$	6.83 $^{+0.82}_{-0.77} \times 10^{-6}$	1.5	3.0	3.1	
32.283~35.209	63.13	0.05 $^{+0.00}_{-0.00}$	-0.77 $^{+0.03}_{-0.03}$	418 $^{+30}_{-30}$	515 $^{+39}_{-39}$	4.30 $^{+0.47}_{-0.40} \times 10^{-6}$	0.31 $^{+0.01}_{-0.01}$	-0.77 $^{+0.03}_{-0.03}$	-5.41 $^{+2.53}_{-2.53}$	507 $^{+29}_{-29}$	4.51 $^{+0.77}_{-0.77} \times 10^{-6}$	0.1	3.0	2.4	
35.209~36.175	29.99	0.04 $^{+0.00}_{-0.00}$	-0.91 $^{+0.07}_{-0.07}$	271 $^{+48}_{-48}$	295 $^{+55}_{-55}$	2.01 $^{+0.49}_{-0.41} \times 10^{-6}$	0.33 $^{+0.04}_{-0.04}$	-0.75 $^{+0.14}_{-0.14}$	-2.92 $^{+0.89}_{-0.89}$	223 $^{+50}_{-44}$	2.82 $^{+1.55}_{-1.04} \times 10^{-6}$	-13.9	2.3	-5.7	
Pulse 3															
45.031~45.690	37.45	0.06 $^{+0.00}_{-0.00}$	-0.58 $^{+0.05}_{-0.04}$	491 $^{+47}_{-45}$	698 $^{+72}_{-71}$	8.43 $^{+1.53}_{-1.22} \times 10^{-6}$	0.24 $^{+0.02}_{-0.02}$	-0.59 $^{+0.05}_{-0.05}$	-6.76 $^{+2.12}_{-2.19}$	696 $^{+51}_{-51}$	8.54 $^{+1.79}_{-1.53} \times 10^{-6}$	1.5	2.9	3.0	
45.690~46.088	47.22	0.11 $^{+0.00}_{-0.00}$	-0.51 $^{+0.04}_{-0.04}$	547 $^{+45}_{-44}$	815 $^{+70}_{-69}$	18.66 $^{+3.31}_{-2.26} \times 10^{-6}$	0.34 $^{+0.03}_{-0.03}$	-0.51 $^{+0.04}_{-0.04}$	-6.26 $^{+2.35}_{-2.49}$	816 $^{+50}_{-50}$	19.02 $^{+3.83}_{-3.11} \times 10^{-6}$	0.8	2.9	2.8	
46.088~46.736	70.22	0.12 $^{+0.00}_{-0.00}$	-0.73 $^{+0.02}_{-0.02}$	773 $^{+49}_{-49}$	981 $^{+64}_{-64}$	22.70 $^{+2.18}_{-1.97} \times 10^{-6}$	0.64 $^{+0.03}_{-0.03}$	-0.73 $^{+0.02}_{-0.02}$	-7.11 $^{+1.93}_{-1.97}$	976 $^{+50}_{-50}$	22.52 $^{+2.61}_{-2.16} \times 10^{-6}$	2.0	3.0	3.2	
46.736~47.301	55.59	0.11 $^{+0.00}_{-0.00}$	-0.77 $^{+0.03}_{-0.03}$	469 $^{+40}_{-40}$	577 $^{+51}_{-51}$	10.64 $^{+1.46}_{-1.22} \times 10^{-6}$	0.64 $^{+0.04}_{-0.04}$	-0.77 $^{+0.03}_{-0.03}$	-6.93 $^{+2.16}_{-2.14}$	577 $^{+37}_{-37}$	10.70 $^{+1.31}_{-1.29} \times 10^{-6}$	1.9	2.9	3.1	
47.301~47.709	24.43	0.04 $^{+0.00}_{-0.00}$	-1.17 $^{+0.08}_{-0.08}$	518 $^{+160}_{-160}$	430 $^{+139}_{-139}$	2.84 $^{+1.16}_{-0.65} \times 10^{-6}$	0.65 $^{+0.06}_{-0.06}$	-1.16 $^{+0.08}_{-0.08}$	-5.57 $^{+2.95}_{-2.95}$	401 $^{+102}_{-102}$	3.06 $^{+0.78}_{-0.78} \times 10^{-6}$	2.4	1.2	1.7	
48.453~50.028	23.73	0.02 $^{+0.00}_{-0.00}$	-1.40 $^{+0.08}_{-0.08}$	723 $^{+364}_{-364}$	434 $^{+226}_{-213}$	1.08 $^{+0.51}_{-0.30} \times 10^{-6}$	0.36 $^{+0.04}_{-0.04}$	-1.18 $^{+0.15}_{-0.18}$	-4.57 $^{+0.89}_{-0.89}$	205 $^{+62}_{-66}$	0.98 $^{+0.66}_{-0.31} \times 10^{-6}$	-12.0	-0.6	-13.7	

Note—All columns are the same as Table A2 but for GRB 150118409.

Table A29. Time-resolved Spectral Fit Results of GRB 150201574

$t_{\text{start}} \sim t_{\text{stop}}$	S	Cutoff Power-Law Fitting				Band Fitting				Difference				
		K	α	E_c	E_p	F	K	α	β	E_p	F	ΔDIC	$p_{\text{DIC}}^{\text{CPL}}$	$p_{\text{DIC}}^{\text{Band}}$
(1)	(2)	(3)	(4)	(5)	(6)	(7)	(8)	(9)	(10)	(11)	(12)	(13)	(14)	(15)
Pulse 1														
-0.037~0.545	37.61	0.05 ^{+0.01} _{-0.01} -1.19 ^{+0.07} _{-0.07} 369 ⁺⁸⁰ ₋₇₁ 299 ⁺⁷⁰ ₋₆₆ 0.76 ^{+0.07} _{-0.07} -1.00 ^{+0.12} _{-0.12} -2.25 ^{+0.22} _{-0.22} 188 ⁺³⁶ ₋₃₉ 3.95 ^{+1.61} _{-1.39} 0.02 _{-0.01} $\times 10^{-6}$										-10.3	2.0	0.2
0.545~1.181	30.07	0.07 ^{+0.01} _{-0.01} -0.96 ^{+0.08} _{-0.09} 160 ⁺²⁴ ₋₂₅ 167 ⁺²⁸ ₋₂₉ 1.68 ^{+0.34} _{-0.32} $\times 10^{-6}$ 0.60 ^{+0.05} _{-0.05} -0.96 ^{+0.08} _{-0.08} -6.59 ^{+2.37} _{-2.36} 165 ⁺¹⁴ ₋₁₄ 1.66 ^{+0.32} _{-0.32} $\times 10^{-6}$										2.8	2.2	3.0
1.259~1.430	35.77	0.16 ^{+0.02} _{-0.02} -0.83 ^{+0.07} _{-0.07} 229 ⁺³³ ₋₃₃ 268 ⁺⁴² ₋₄₂ 5.93 ^{+1.34} _{-1.05} $\times 10^{-6}$ 1.06 ^{+0.10} _{-0.10} -0.83 ^{+0.08} _{-0.08} -6.16 ^{+2.47} _{-2.56} 263 ⁺²⁴ ₋₂₄ 6.03 ^{+1.55} _{-1.12} $\times 10^{-6}$										2.0	2.5	2.9
1.430~1.634	54.50	0.24 ^{+0.02} _{-0.02} -0.73 ^{+0.05} _{-0.05} 234 ⁺²³ ₋₂₃ 297 ⁺³¹ ₋₃₁ 10.18 ^{+1.64} _{-1.36} $\times 10^{-6}$ 1.08 ^{+0.11} _{-0.11} -0.48 ^{+0.11} _{-0.11} -2.29 ^{+0.15} _{-0.14} 205 ⁺²⁴ ₋₂₅ 13.87 ^{+4.93} _{-3.70} $\times 10^{-6}$										-14.7	2.8	3.1
1.634~1.747	52.44	0.34 ^{+0.02} _{-0.02} -0.71 ^{+0.05} _{-0.05} 238 ⁺²³ ₋₂₄ 307 ⁺³³ ₋₃₃ 14.98 ^{+2.34} _{-2.09} $\times 10^{-6}$ 1.73 ^{+0.15} _{-0.15} -0.68 ^{+0.07} _{-0.07} -5.12 ^{+2.40} _{-3.40} 292 ⁺²⁶ ₋₂₇ 15.74 ^{+3.55} _{-3.18} $\times 10^{-6}$										-1.1	2.8	1.5
1.747~2.013	92.54	0.40 ^{+0.02} _{-0.02} -0.82 ^{+0.03} _{-0.03} 244 ⁺¹⁶ ₋₁₆ 288 ⁺²⁰ ₋₂₀ 16.94 ^{+1.62} _{-1.37} $\times 10^{-6}$ 2.22 ^{+0.12} _{-0.12} -0.57 ^{+0.06} _{-0.06} -2.28 ^{+0.08} _{-0.07} 197 ⁺¹⁴ ₋₁₃ 22.95 ^{+4.29} _{-3.63} $\times 10^{-6}$										-44.6	3.0	3.8
2.013~2.168	57.07	0.32 ^{+0.02} _{-0.02} -0.87 ^{+0.05} _{-0.06} 192 ⁺¹⁹ ₋₂₀ 217 ⁺²⁴ ₋₂₅ 10.06 ^{+1.37} _{-1.35} $\times 10^{-6}$ 2.03 ^{+0.18} _{-0.19} -0.59 ^{+0.13} _{-0.12} -2.48 ^{+0.25} _{-0.05} 153 ⁺¹⁸ ₋₁₉ 12.89 ^{+5.21} _{-3.28} $\times 10^{-6}$										-11.6	2.7	2.1
2.168~3.772	147.58	0.30 ^{+0.01} _{-0.01} -0.84 ^{+0.02} _{-0.02} 143 ⁺⁵ ₋₅ 166 ⁺⁷ ₋₇ 6.75 ^{+0.39} _{-0.35} $\times 10^{-6}$ 1.87 ^{+0.05} _{-0.04} -0.63 ^{+0.04} _{-0.04} -2.47 ^{+0.4} _{-0.05} 130 ⁺⁴ ₋₄ 8.65 ^{+0.74} _{-0.66} $\times 10^{-6}$										-92.4	3.0	4.0
Pulse 2														
3.772~4.249	66.50	0.23 ^{+0.02} _{-0.02} -0.94 ^{+0.05} _{-0.05} 127 ⁺¹¹ ₋₁₁ 134 ⁺¹³ ₋₁₃ 4.47 ^{+0.64} _{-0.47} $\times 10^{-6}$ 1.86 ^{+0.10} _{-0.10} -0.77 ^{+0.08} _{-0.08} -2.57 ^{+0.13} _{-0.13} 111 ⁺⁷ ₋₇ 5.58 ^{+0.95} _{-0.72} $\times 10^{-6}$										-20.4	2.6	3.9
4.249~4.433	51.78	0.28 ^{+0.02} _{-0.02} -0.84 ^{+0.06} _{-0.06} 173 ⁺¹⁸ ₋₁₈ 201 ⁺²³ ₋₂₄ 7.88 ^{+1.17} _{-1.11} $\times 10^{-6}$ 1.84 ^{+0.14} _{-0.14} -0.75 ^{+0.09} _{-0.09} -3.09 ^{+0.69} _{-0.69} 176 ⁺¹⁹ ₋₁₉ 9.39 ^{+2.72} _{-2.14} $\times 10^{-6}$										-6.6	2.7	1.1
4.433~4.931	110.13	0.38 ^{+0.02} _{-0.02} -0.86 ^{+0.03} _{-0.03} 175 ⁺⁹ ₋₉ 199 ⁺¹² ₋₁₂ 10.86 ^{+0.77} _{-0.83} $\times 10^{-6}$ 2.52 ^{+0.11} _{-0.11} -0.70 ^{+0.06} _{-0.06} -2.58 ^{+0.13} _{-0.13} 161 ⁺¹⁰ ₋₁₀ 13.14 ^{+2.05} _{-1.74} $\times 10^{-6}$										-18.4	2.9	3.8
4.931~5.596	141.34	0.57 ^{+0.02} _{-0.02} -0.71 ^{+0.03} _{-0.03} 131 ⁺⁵ ₋₅ 169 ⁺⁷ ₋₇ 11.64 ^{+0.79} _{-0.66} $\times 10^{-6}$ 2.55 ^{+0.08} _{-0.08} -0.46 ^{+0.04} _{-0.04} -2.56 ^{+0.06} _{-0.06} 133 ⁺⁴ ₋₄ 14.39 ^{+4.35} _{-3.16} $\times 10^{-6}$										-76.4	2.9	4.0
5.596~5.710	48.53	0.49 ^{+0.06} _{-0.06} -0.73 ^{+0.08} _{-0.08} 110 ⁺¹² ₋₁₂ 140 ⁺¹⁷ ₋₁₇ 7.91 ^{+1.57} _{-1.32} $\times 10^{-6}$ 2.46 ^{+0.21} _{-0.21} -0.61 ^{+0.11} _{-0.11} -3.26 ^{+0.60} _{-0.15} 126 ⁺¹⁰ ₋₉ 8.87 ^{+1.99} _{-1.64} $\times 10^{-6}$										-6.0	2.4	2.3
5.710~6.157	79.29	0.38 ^{+0.03} _{-0.03} -0.81 ^{+0.05} _{-0.05} 105 ⁺⁷ ₋₇ 125 ⁺¹⁰ ₋₁₀ 5.96 ^{+0.71} _{-0.63} $\times 10^{-6}$ 2.32 ^{+0.11} _{-0.11} -0.66 ^{+0.06} _{-0.06} -2.81 ^{+0.13} _{-0.13} 109 ⁺⁴ ₋₄ 6.81 ^{+0.78} _{-0.68} $\times 10^{-6}$										-19.2	2.7	4.0
6.157~6.388	46.77	0.28 ^{+0.04} _{-0.04} -0.89 ^{+0.08} _{-0.08} 99 ⁺¹¹ ₋₁₁ 110 ⁺¹⁵ ₋₁₅ 4.08 ^{+0.88} _{-0.70} $\times 10^{-6}$ 1.99 ^{+0.16} _{-0.16} -0.71 ^{+0.14} _{-0.14} -3.31 ^{+0.74} _{-0.74} 95 ⁺¹⁰ ₋₁₀ 4.60 ^{+0.24} _{-0.24} $\times 10^{-6}$										-8.0	2.2	-1.1
6.388~8.017	89.50	0.18 ^{+0.01} _{-0.01} -0.96 ^{+0.04} _{-0.04} 95 ⁺⁵ ₋₅ 98 ⁺⁷ ₋₇ 2.64 ^{+0.24} _{-0.24} $\times 10^{-6}$ 1.60 ^{+0.05} _{-0.05} -0.88 ^{+0.05} _{-0.05} -3.09 ^{+0.08} _{-0.08} 91 ⁺³ ₋₃ 2.90 ^{+0.22} _{-0.22} $\times 10^{-6}$										-11.5	2.7	3.3
8.017~8.674	46.46	0.17 ^{+0.03} _{-0.03} -0.90 ^{+0.09} _{-0.09} 75 ⁺⁸ ₋₈ 82 ⁺¹¹ ₋₁₁ 1.87 ^{+0.41} _{-0.34} $\times 10^{-6}$ 1.30 ^{+0.08} _{-0.08} -0.73 ^{+0.15} _{-0.15} -3.26 ^{+0.62} _{-0.11} 73 ⁺⁶ ₋₆ 2.04 ^{+0.48} _{-0.34} $\times 10^{-6}$										-6.5	1.9	1.2
8.674~9.032	45.46	0.23 ^{+0.03} _{-0.03} -0.79 ^{+0.08} _{-0.08} 87 ⁺⁹ ₋₉ 106 ⁺¹³ ₋₁₃ 2.83 ^{+0.63} _{-0.63} $\times 10^{-6}$ 1.41 ^{+0.10} _{-0.10} -0.78 ^{+0.09} _{-0.09} -6.10 ^{+2.43} _{-2.55} 104 ⁺⁵ ₋₅ 2.85 ^{+0.40} _{-0.34} $\times 10^{-6}$										1.9	2.4	2.9
9.032~10.213	66.25	0.17 ^{+0.02} _{-0.02} -0.94 ^{+0.06} _{-0.06} 83 ⁺⁶ ₋₆ 88 ⁺⁸ ₋₈ 2.14 ^{+0.30} _{-0.28} $\times 10^{-6}$ 1.47 ^{+0.06} _{-0.06} -0.93 ^{+0.06} _{-0.06} -6.03 ^{+2.41} _{-2.57} 87 ⁺³ ₋₃ 2.14 ^{+0.19} _{-0.19} $\times 10^{-6}$										1.7	2.6	2.7
10.213~10.894	41.20	0.11 ^{+0.02} _{-0.02} -1.13 ^{+0.09} _{-0.09} 82 ⁺¹¹ ₋₁₁ 72 ⁺¹² ₋₁₂ 1.55 ^{+0.45} _{-0.33} $\times 10^{-6}$ 1.48 ^{+0.09} _{-0.09} -1.12 ^{+0.10} _{-0.10} -5.96 ^{+2.45} _{-2.66} 70 ⁺⁴ ₋₄ 1.58 ^{+0.15} _{-0.13} $\times 10^{-6}$										3.0	1.6	2.7
10.894~15.117	61.98	0.07 ^{+0.01} _{-0.01} -1.22 ^{+0.06} _{-0.06} 72 ⁺⁶ ₋₆ 56 ⁺⁶ ₋₆ 0.93 ^{+0.14} _{-0.12} $\times 10^{-6}$ 1.08 ^{+0.03} _{-0.03} -1.22 ^{+0.06} _{-0.06} -6.95 ^{+2.11} _{-2.13} 56 ⁺² ₋₂ 0.93 ^{+0.04} _{-0.04} $\times 10^{-6}$										3.3	2.4	3.1
15.117~17.374	64.99	0.09 ^{+0.01} _{-0.01} -1.20 ^{+0.05} _{-0.05} 92 ⁺⁸ ₋₈ 74 ⁺⁸ ₋₈ 1.43 ^{+0.20} _{-0.17} $\times 10^{-6}$ 1.35 ^{+0.05} _{-0.05} -1.18 ^{+0.06} _{-0.06} -5.57 ^{+2.32} _{-2.84} 72 ⁺³ ₋₃ 1.45 ^{+0.08} _{-0.08} $\times 10^{-6}$										1.2	2.6	2.1
17.374~18.252	26.83	0.05 ^{+0.02} _{-0.02} -1.35 ^{+0.16} _{-0.16} 75 ⁺¹⁸ ₋₁₉ 49 ⁺¹⁷ ₋₁₇ 0.83 ^{+0.49} _{-0.32} $\times 10^{-6}$ 1.09 ^{+0.08} _{-0.08} -1.10 ^{+0.33} _{-0.33} -4.70 ^{+2.05} _{-2.05} 42 ⁺⁵ ₋₅ 0.82 ^{+0.18} _{-0.18} $\times 10^{-6}$										5.3	-6.2	-1.8
18.252~20.000	21.26	0.04 ^{+0.01} _{-0.01} -1.32 ^{+0.21} _{-0.20} 62 ⁺¹⁷ ₋₁₇ 45 ⁺¹⁷ ₋₁₇ 0.45 ^{+0.40} _{-0.20} $\times 10^{-6}$ 0.04 ^{+0.02} _{-0.02} -1.27 ^{+0.20} _{-0.20} -6.32 ^{+2.44} _{-2.44} 39 ⁺⁴ ₋₃ 0.43 ^{+0.40} _{-0.21} $\times 10^{-6}$										14.0	-16.6	-2.5

Note—All columns are the same as Table A2 but for GRB 150201574.

Table A30. Time-resolved Spectral Fit Results of GRB 150330828

$t_{\text{start}} \sim t_{\text{stop}}$	S	Cutoff Power-Law Fitting						Band Fitting						Difference	
		K	α	E_c	E_p	F	K	α	β	E_p	F	ΔDIC	$p_{\text{DIC}}^{\text{CPL}}$	$p_{\text{DIC}}^{\text{Band}}$	
(1)	(2)	(3)	(4)	(5)	(6)	(7)	(8)	(9)	(10)	(11)	(12)	(13)	(14)	(15)	
Pulse 1															
1.389~3.158	36.78	$0.05^{+0.00}_{-0.00}$	$-0.24^{+0.07}_{-0.07}$	245^{+21}_{-21}	431^{+41}_{-40}	$3.24^{+0.63}_{-0.51} \times 10^{-6}$	$0.05^{+0.00}_{-0.00}$	$-0.24^{+0.07}_{-0.07}$	$-6.37^{+2.52}_{-2.07}$	$3.32^{+0.54}_{-0.39} \times 10^{-6}$	0.4	2.8	3.0		
3.158~4.433	20.37	$0.05^{+0.01}_{-0.01}$	$-0.27^{+0.12}_{-0.12}$	142^{+21}_{-20}	245^{+40}_{-39}	$1.22^{+0.43}_{-0.32} \times 10^{-6}$	$0.05^{+0.01}_{-0.01}$	$-0.20^{+0.16}_{-0.16}$	$-5.74^{+3.03}_{-2.83}$	$2.33^{+0.27}_{-0.28} \times 10^{-6}$	-1.7	1.9	0.1		
4.433~6.203	50.40	$0.08^{+0.01}_{-0.01}$	$-0.39^{+0.05}_{-0.05}$	173^{+13}_{-13}	279^{+23}_{-23}	$2.83^{+0.46}_{-0.35} \times 10^{-6}$	$0.12^{+0.02}_{-0.02}$	$-0.13^{+0.11}_{-0.11}$	$-2.17^{+0.11}_{-0.11}$	$2.08^{+0.18}_{-0.18} \times 10^{-6}$	4.67^{+1.30}_{-0.97} $\times 10^{-6}$	-21.4	2.8	1.6	
6.203~7.626	22.11	$0.07^{+0.01}_{-0.01}$	$-0.15^{+0.15}_{-0.15}$	84^{+12}_{-12}	156^{+25}_{-25}	$0.76^{+0.29}_{-0.21} \times 10^{-6}$	$0.08^{+0.02}_{-0.02}$	$-0.10^{+0.16}_{-0.17}$	$-6.24^{+2.61}_{-2.55}$	$1.52^{+11}_{-11} \times 10^{-6}$	0.77^{+0.31}_{-0.21} $\times 10^{-6}$	0.7	1.2	1.8	
Pulse 2															
97.913~116.283	20.80	$0.01^{+0.00}_{-0.00}$	$-0.98^{+0.09}_{-0.09}$	338^{+97}_{-93}	345^{+97}_{-100}	$0.32^{+0.12}_{-0.08} \times 10^{-6}$	$0.01^{+0.00}_{-0.00}$	$-0.97^{+0.10}_{-0.10}$	$-6.11^{+2.54}_{-2.57}$	$3.28^{+0.64}_{-0.67} \times 10^{-6}$	0.9	1.2	2.0		
116.283~124.506	23.38	$0.01^{+0.00}_{-0.00}$	$-0.92^{+0.10}_{-0.10}$	166^{+32}_{-32}	180^{+38}_{-39}	$0.34^{+0.11}_{-0.08} \times 10^{-6}$	$0.01^{+0.00}_{-0.00}$	$-0.89^{+0.11}_{-0.11}$	$-5.85^{+2.83}_{-2.85}$	$1.73^{+22}_{-22} \times 10^{-6}$	0.5	1.5	2.1		
125.368~127.186	42.29	$0.04^{+0.00}_{-0.00}$	$-0.84^{+0.05}_{-0.05}$	428^{+58}_{-58}	496^{+70}_{-70}	$3.19^{+0.64}_{-0.52} \times 10^{-6}$	$0.04^{+0.00}_{-0.00}$	$-0.77^{+0.07}_{-0.07}$	$-2.59^{+0.52}_{-0.50}$	$4.05^{+0.60}_{-0.59} \times 10^{-6}$	-11.6	2.7	-0.3		
127.186~128.900	73.12	$0.07^{+0.00}_{-0.00}$	$-0.91^{+0.03}_{-0.03}$	650^{+61}_{-61}	709^{+69}_{-69}	$7.80^{+0.98}_{-0.88} \times 10^{-6}$	$0.07^{+0.00}_{-0.00}$	$-0.85^{+0.03}_{-0.04}$	$-2.17^{+0.11}_{-0.11}$	$5.66^{+0.58}_{-0.60} \times 10^{-6}$	-21.9	2.9	3.4		
128.900~129.344	45.93	$0.09^{+0.01}_{-0.01}$	$-0.82^{+0.05}_{-0.05}$	455^{+64}_{-64}	537^{+79}_{-79}	$8.04^{+1.49}_{-1.37} \times 10^{-6}$	$0.11^{+0.01}_{-0.01}$	$-0.71^{+0.07}_{-0.07}$	$-2.16^{+0.13}_{-0.13}$	$3.99^{+0.54}_{-0.54} \times 10^{-6}$	-17.1	2.7	2.6		
129.344~130.080	69.90	$0.12^{+0.00}_{-0.00}$	$-0.84^{+0.03}_{-0.03}$	379^{+33}_{-33}	439^{+40}_{-40}	$8.17^{+0.96}_{-0.87} \times 10^{-6}$	$0.13^{+0.01}_{-0.01}$	$-0.79^{+0.05}_{-0.05}$	$-2.50^{+0.36}_{-0.36}$	$3.75^{+0.38}_{-0.38} \times 10^{-6}$	-11.3	2.9	2.0		
130.080~131.007	96.65	$0.15^{+0.00}_{-0.00}$	$-0.85^{+0.02}_{-0.02}$	474^{+32}_{-32}	545^{+38}_{-38}	$13.07^{+1.23}_{-1.03} \times 10^{-6}$	$0.17^{+0.01}_{-0.01}$	$-0.74^{+0.03}_{-0.03}$	$-2.09^{+0.06}_{-0.06}$	$3.86^{+0.27}_{-0.28} \times 10^{-6}$	-51.7	2.9	3.5		
131.007~131.517	102.21	$0.20^{+0.01}_{-0.01}$	$-0.93^{+0.03}_{-0.03}$	828^{+97}_{-97}	886^{+107}_{-106}	$28.79^{+4.30}_{-4.30} \times 10^{-6}$	$0.24^{+0.01}_{-0.01}$	$-0.80^{+0.03}_{-0.03}$	$-2.03^{+0.02}_{-0.02}$	$5.33^{+0.36}_{-0.36} \times 10^{-6}$	-136.3	2.7	3.1		
131.517~131.784	58.68	$0.19^{+0.01}_{-0.01}$	$-0.91^{+0.04}_{-0.04}$	372^{+46}_{-46}	405^{+52}_{-52}	$11.68^{+2.05}_{-2.05} \times 10^{-6}$	$0.23^{+0.02}_{-0.02}$	$-0.77^{+0.07}_{-0.07}$	$-2.18^{+0.12}_{-0.12}$	$2.87^{+0.32}_{-0.32} \times 10^{-6}$	-22.2	2.7	3.2		
131.784~132.534	81.67	$0.15^{+0.01}_{-0.01}$	$-0.92^{+0.03}_{-0.03}$	301^{+24}_{-24}	326^{+27}_{-27}	$7.82^{+0.80}_{-0.77} \times 10^{-6}$	$0.18^{+0.02}_{-0.02}$	$-0.83^{+0.06}_{-0.06}$	$-2.42^{+0.23}_{-0.23}$	$2.63^{+0.28}_{-0.29} \times 10^{-6}$	-10.9	2.9	3.0		
132.534~133.408	97.59	$0.18^{+0.01}_{-0.01}$	$-0.88^{+0.03}_{-0.03}$	278^{+18}_{-18}	311^{+22}_{-22}	$8.68^{+0.83}_{-0.83} \times 10^{-6}$	$0.23^{+0.02}_{-0.02}$	$-0.75^{+0.05}_{-0.05}$	$-2.23^{+0.11}_{-0.11}$	$2.36^{+0.20}_{-0.20} \times 10^{-6}$	-21.8	3.0	3.4		
133.408~133.886	97.39	$0.26^{+0.01}_{-0.01}$	$-0.85^{+0.03}_{-0.03}$	290^{+20}_{-20}	334^{+24}_{-24}	$13.12^{+1.17}_{-1.05} \times 10^{-6}$	$0.34^{+0.03}_{-0.03}$	$-0.69^{+0.05}_{-0.05}$	$-2.18^{+0.08}_{-0.08}$	$2.36^{+0.17}_{-0.17} \times 10^{-6}$	-41.1	2.9	3.7		
133.886~134.254	68.98	$0.19^{+0.01}_{-0.01}$	$-0.94^{+0.04}_{-0.04}$	296^{+29}_{-29}	314^{+33}_{-33}	$9.25^{+0.97}_{-0.97} \times 10^{-6}$	$0.28^{+0.04}_{-0.04}$	$-0.71^{+0.08}_{-0.08}$	$-2.10^{+0.08}_{-0.08}$	$2.00^{+0.20}_{-0.20} \times 10^{-6}$	-21.3	2.8	1.9		
134.254~134.883	66.71	$0.14^{+0.01}_{-0.01}$	$-0.98^{+0.04}_{-0.04}$	229^{+23}_{-23}	234^{+25}_{-25}	$5.06^{+0.57}_{-0.57} \times 10^{-6}$	$0.21^{+0.03}_{-0.03}$	$-0.75^{+0.08}_{-0.08}$	$-2.12^{+0.07}_{-0.07}$	$1.55^{+0.13}_{-0.13} \times 10^{-6}$	-24.0	2.8	2.6		
134.883~135.701	57.96	$0.10^{+0.01}_{-0.01}$	$-0.88^{+0.03}_{-0.03}$	278^{+18}_{-18}	311^{+22}_{-22}	$8.68^{+0.83}_{-0.83} \times 10^{-6}$	$0.23^{+0.02}_{-0.02}$	$-0.75^{+0.05}_{-0.05}$	$-2.23^{+0.11}_{-0.11}$	$1.24^{+0.20}_{-0.20} \times 10^{-6}$	-21.8	3.0	3.4		
135.701~136.550	74.48	$0.15^{+0.01}_{-0.01}$	$-0.91^{+0.04}_{-0.04}$	191^{+16}_{-16}	209^{+19}_{-19}	$4.66^{+0.52}_{-0.52} \times 10^{-6}$	$0.24^{+0.03}_{-0.03}$	$-0.66^{+0.07}_{-0.07}$	$-2.17^{+0.08}_{-0.08}$	$1.41^{+0.11}_{-0.11} \times 10^{-6}$	-27.1	2.8	2.7		
136.550~136.951	58.99	$0.18^{+0.01}_{-0.01}$	$-0.90^{+0.05}_{-0.05}$	195^{+20}_{-20}	215^{+25}_{-25}	$5.77^{+0.85}_{-0.85} \times 10^{-6}$	$0.26^{+0.04}_{-0.04}$	$-0.71^{+0.08}_{-0.08}$	$-2.32^{+0.15}_{-0.15}$	$1.61^{+0.15}_{-0.15} \times 10^{-6}$	-15.0	2.7	3.1		
136.951~137.564	87.39	$0.21^{+0.01}_{-0.01}$	$-0.89^{+0.03}_{-0.03}$	323^{+17}_{-17}	257^{+20}_{-20}	$7.94^{+0.89}_{-0.89} \times 10^{-6}$	$0.35^{+0.04}_{-0.04}$	$-0.60^{+0.06}_{-0.06}$	$-2.09^{+0.05}_{-0.05}$	$1.59^{+0.11}_{-0.11} \times 10^{-6}$	-47.3	2.9	3.1		
137.564~137.996	57.35	$0.14^{+0.01}_{-0.01}$	$-1.03^{+0.05}_{-0.05}$	243^{+28}_{-29}	236^{+30}_{-30}	$5.28^{+0.77}_{-0.66} \times 10^{-6}$	$0.14^{+0.01}_{-0.01}$	$-0.02^{+0.05}_{-0.05}$	$-5.98^{+0.26}_{-0.27}$	$2.31^{+0.20}_{-0.20} \times 10^{-6}$	0.1	2.7	2.8		
137.996~139.065	66.38	$0.11^{+0.01}_{-0.01}$	$-0.96^{+0.04}_{-0.04}$	176^{+16}_{-16}	183^{+18}_{-18}	$3.15^{+0.42}_{-0.33} \times 10^{-6}$	$0.15^{+0.02}_{-0.02}$	$-0.80^{+0.08}_{-0.08}$	$-2.32^{+0.17}_{-0.17}$	$1.42^{+0.14}_{-0.14} \times 10^{-6}$	-12.7	2.8	2.5		
139.065~140.985	64.68	$0.08^{+0.01}_{-0.01}$	$-0.97^{+0.05}_{-0.05}$	153^{+13}_{-13}	157^{+16}_{-16}	$1.99^{+0.22}_{-0.22} \times 10^{-6}$	$0.11^{+0.01}_{-0.01}$	$-0.84^{+0.08}_{-0.08}$	$-2.74^{+0.40}_{-0.40}$	$1.30^{+0.11}_{-0.11} \times 10^{-6}$	-14.6	2.8	-1.8		
140.985~144.925	62.09	$0.04^{+0.00}_{-0.00}$	$-1.15^{+0.04}_{-0.04}$	198^{+21}_{-21}	169^{+20}_{-20}	$1.33^{+0.17}_{-0.14} \times 10^{-6}$	$0.05^{+0.01}_{-0.01}$	$-1.04^{+0.09}_{-0.09}$	$-3.04^{+0.09}_{-0.09}$	$1.36^{+0.15}_{-0.15} \times 10^{-6}$	-16.8	2.7	-7.9		
Pulse 3															
144.925~145.559	34.18	$0.07^{+0.01}_{-0.01}$	$-0.99^{+0.08}_{-0.08}$	178^{+29}_{-29}	180^{+33}_{-34}	$1.90^{+0.46}_{-0.34} \times 10^{-6}$	$0.07^{+0.01}_{-0.01}$	$-0.96^{+0.09}_{-0.09}$	$-5.70^{+2.84}_{-2.92}$	$1.96^{+0.19}_{-0.19} \times 10^{-6}$	-0.3	2.2	2.2		
145.559~145.702	23.86	$0.07^{+0.01}_{-0.01}$	$-1.19^{+0.12}_{-0.12}$	454^{+201}_{-202}	368^{+172}_{-173}	$3.86^{+0.72}_{-0.72} \times 10^{-6}$	$0.08^{+0.02}_{-0.02}$	$-1.14^{+0.13}_{-0.13}$	$-5.16^{+2.84}_{-2.84}$	$2.98^{+0.12}_{-0.12} \times 10^{-6}$	0.5	-1.8	-0.3		
145.702~146.928	86.01	$0.13^{+0.01}_{-0.01}$	$-0.91^{+0.03}_{-0.03}$	230^{+17}_{-17}	251^{+19}_{-20}	$5.02^{+0.48}_{-0.48} \times 10^{-6}$	$0.18^{+0.02}_{-0.02}$	$-0.72^{+0.05}_{-0.05}$	$-2.21^{+0.08}_{-0.08}$	$1.81^{+0.13}_{-0.13} \times 10^{-6}$	-26.7	2.9	3.5		
146.928~148.171	70.48	$0.10^{+0.01}_{-0.01}$	$-1.02^{+0.04}_{-0.04}$	202^{+20}_{-20}	198^{+21}_{-21}	$3.12^{+0.41}_{-0.35} \times 10^{-6}$	$0.18^{+0.02}_{-0.02}$	$-0.70^{+0.07}_{-0.07}$	$-2.13^{+0.06}_{-0.06}$	$1.21^{+0.08}_{-0.08} \times 10^{-6}$	-34.6	2.7	3.1		
148.171~150.516	78.13	$0.08^{+0.01}_{-0.01}$	$-1.08^{+0.04}_{-0.04}$	172^{+14}_{-14}	158^{+15}_{-15}	$2.24^{+0.22}_{-0.20} \times 10^{-6}$	$0.12^{+0.01}_{-0.01}$	$-0.90^{+0.06}_{-0.06}$	$-2.25^{+0.08}_{-0.08}$	$1.19^{+0.08}_{-0.08} \times 10^{-6}$	-21.2	2.8	3.4		
150.516~151.314	34.03	$0.05^{+0.01}_{-0.01}$	$-1.18^{+0.09}_{-0.09}$	197^{+44}_{-44}	162^{+40}_{-40}	$1.48^{+0.15}_{-0.15} \times 10^{-6}$	$0.05^{+0.01}_{-0.01}$	$-1.12^{+0.11}_{-0.11}$	$-4.14^{+1.91}_{-1.91} \times 10^{-6}$	$1.70^{+0.11}_{-0.11} \times 10^{-6}$	-4.0	1.2	-0.2		
151.314~153.264	36.32	$0.04^{+0.01}_{-0.01}$	$-1.13^{+0.08}_{-0.08}$	160^{+27}_{-28}	139^{+28}_{-28}	$0.97^{+0.18}_{-0.18} \times 10^{-6}$	$0.04^{+0.01}_{-0.01}$	$-1.07^{+0.11}_{-0.11}$	$-4.15^{+1.86}_{-1.86} \times 10^{-6}$	$1.10^{+0.15}_{-0.15} \times 10^{-6}$	-5.4	1.8	-1.1		
153.264~158.201	34														

Table A31. Time-resolved Spectral Fit Results of GRB 151231443

$t_{\text{start}} \sim t_{\text{stop}}$	S	Cutoff Power-Law Fitting						Band Fitting						Difference		
		K	α	E_c	E_p	F	K	α	β	E_p	F	Δ_{DIC}	$p_{\text{DIC}}^{\text{CPL}}$	$p_{\text{DIC}}^{\text{Band}}$		
(1)	(2)	(3)	(4)	(5)	(6)	(7)	(8)	(9)	(10)	(11)	(12)	(13)	(14)	(15)		
Pulse 1																
1.675~4.148	30.43	0.09 ^{+0.01} _{-0.01}	-1.27 ^{+0.09} _{-0.08}	1.64 ⁺²³ ₋₂₄	11.9 ⁺²² ₋₂₂	2.54 ^{+0.49} _{-0.40}	$\times 10^{-6}$	0.10 ^{+0.01} _{-0.01}	-1.24 ^{+0.10} _{-0.10}	-6.00 ^{+2.76} _{-2.73}	114 ⁺⁸ ₋₈	2.61 ^{+0.59} _{-0.56}	$\times 10^{-6}$	-0.0	2.2	2.4
4.148~5.309	34.04	0.15 ^{+0.01} _{-0.01}	-0.81 ^{+0.07} _{-0.06}	2.54 ⁺²⁴ ₋₂₄	302 ⁺³⁴ ₋₃₃	6.45 ^{+0.76} _{-0.76}	$\times 10^{-6}$	0.83 ^{+0.15} _{-0.15}	-0.67 ^{+0.14} _{-0.15}	-3.67 ^{+3.41} _{-3.41}	7.15 ^{+3.36} _{-3.33}	260 ⁺³⁶ ₋₃₃	$\times 10^{-6}$	-11.4	2.8	-5.2
5.309~5.704	28.52	0.19 ^{+0.01} _{-0.01}	-0.81 ^{+0.08} _{-0.08}	324 ⁺³⁹ ₋₃₉	385 ⁺⁵³ ₋₅₃	11.47 ^{+2.08} _{-1.74}	$\times 10^{-6}$	1.22 ^{+0.20} _{-0.20}	-0.78 ^{+0.09} _{-0.09}	-5.43 ^{+2.46} _{-2.90}	370 ⁺³³ ₋₃₂	11.78 ^{+4.36} _{-3.00}	$\times 10^{-6}$	-0.2	2.7	1.7
5.704~7.705	48.87	0.14 ^{+0.00} _{-0.00}	-0.93 ^{+0.04} _{-0.04}	376 ⁺²⁸ ₋₂₈	402 ⁺³⁴ ₋₃₄	8.57 ^{+0.84} _{-0.84}	$\times 10^{-6}$	1.06 ^{+0.11} _{-0.12}	-0.86 ^{+0.07} _{-0.07}	-3.55 ^{+1.08} _{-1.08}	363 ⁺³⁵ ₋₃₆	9.43 ^{+2.79} _{-1.97}	$\times 10^{-6}$	-7.7	2.9	-1.5
7.705~8.760	23.44	0.10 ^{+0.01} _{-0.01}	-0.88 ^{+0.11} _{-0.11}	229 ⁺³⁵ ₋₃₆	256 ⁺⁴⁷ ₋₄₇	3.83 ^{+0.89} _{-0.89}	$\times 10^{-6}$	0.77 ^{+0.14} _{-0.14}	-0.85 ^{+0.12} _{-0.12}	-4.75 ^{+2.08} _{-2.08}	240 ⁺²⁴ ₋₂₅	4.04 ^{+1.48} _{-1.04}	$\times 10^{-6}$	-0.8	2.2	1.3
Pulse 2																
62.327~65.112	37.10	0.12 ^{+0.01} _{-0.01}	-0.85 ^{+0.07} _{-0.07}	174 ⁺¹⁷ ₋₁₇	200 ⁺²³ ₋₂₃	3.31 ^{+0.47} _{-0.42}	$\times 10^{-6}$	0.78 ^{+0.10} _{-0.10}	-0.75 ^{+0.11} _{-0.11}	-3.60 ^{+0.86} _{-0.68}	184 ⁺¹³ ₋₁₃	3.62 ^{+0.97} _{-0.74}	$\times 10^{-6}$	-6.0	2.6	0.2
65.112~66.217	30.58	0.14 ^{+0.01} _{-0.01}	-0.82 ^{+0.08} _{-0.08}	239 ⁺²⁶ ₋₂₆	282 ⁺³⁶ ₋₃₆	5.55 ^{+0.84} _{-0.71}	$\times 10^{-6}$	0.88 ^{+0.12} _{-0.12}	-0.80 ^{+0.08} _{-0.08}	-5.56 ^{+2.44} _{-2.79}	276 ⁺¹⁷ ₋₁₇	5.82 ^{+4.42} _{-1.30}	$\times 10^{-6}$	0.6	2.6	2.2
66.217~67.504	22.97	0.11 ^{+0.01} _{-0.01}	-0.85 ^{+0.11} _{-0.11}	168 ⁺²⁵ ₋₂₅	193 ⁺³⁴ ₋₃₄	2.83 ^{+0.75} _{-0.75}	$\times 10^{-6}$	0.76 ^{+0.13} _{-0.13}	-0.85 ^{+0.12} _{-0.12}	-6.17 ^{+2.47} _{-2.47}	188 ⁺¹⁴ ₋₁₄	2.87 ^{+0.85} _{-0.64}	$\times 10^{-6}$	2.3	2.2	2.7
68.505~71.641	43.49	0.20 ^{+0.02} _{-0.02}	-0.53 ^{+0.07} _{-0.07}	114 ⁺⁸ ₋₈	168 ⁺¹⁴ ₋₁₄	3.46 ^{+0.47} _{-0.38}	$\times 10^{-6}$	0.68 ^{+0.07} _{-0.07}	-0.52 ^{+0.07} _{-0.08}	-6.39 ^{+2.24} _{-2.36}	167 ⁺⁵ ₋₅	3.48 ^{+0.65} _{-0.50}	$\times 10^{-6}$	0.7	2.8	2.7

Note—All columns are the same as Table A2 but for GRB 151231443.

Table A32. Time-resolved Spectral Fit Results of GRB 160422499

$t_{\text{start}} \sim t_{\text{stop}}$	S	Cutoff Power-Law Fitting						Band Fitting						Difference		
		K	α	E_c	E_p	F	K	α	β	E_p	F	ΔDIC	$p_{\text{DIC}}^{\text{CPL}}$	$p_{\text{DIC}}^{\text{Band}}$		
(1)	(2)	(3)	(4)	(5)	(6)	(7)	(8)	(9)	(10)	(11)	(12)	(13)	(14)	(15)		
Pulse 1																
0.068~0.230	23.72	$0.27^{+0.10}_{-0.10}$	$-0.85^{+0.20}_{-0.20}$	62^{+15}_{-15}	72^{+21}_{-21}	$2.13^{+1.38}_{-0.86} \times 10^{-6}$	$1.68^{+0.17}_{-0.17}$	$-0.39^{+0.32}_{-0.32}$	$-2.62^{+0.23}_{-0.19}$	55^{+6}_{-6}	$2.54^{+0.99}_{-0.61} \times 10^{-6}$	1.8	-9.2	3.5		
0.230~0.614	50.66	$0.20^{+0.04}_{-0.03}$	$-1.16^{+0.09}_{-0.09}$	84^{+12}_{-12}	71^{+12}_{-12}	$3.05^{+0.70}_{-0.59} \times 10^{-6}$	$2.82^{+0.16}_{-0.17}$	$-0.09^{+0.07}_{-0.07}$	$-2.39^{+0.07}_{-0.07}$	43^{+4}_{-4}	$3.79^{+0.73}_{-0.73} \times 10^{-6}$	-54.8	1.0	2.5		
0.614~1.712	103.27	$0.12^{+0.00}_{-0.00}$	$-1.27^{+0.02}_{-0.02}$	829^{+72}_{-73}	605^{+55}_{-56}	$11.49^{+0.78}_{-0.76} \times 10^{-6}$	$2.32^{+0.05}_{-0.05}$	$-1.27^{+0.02}_{-0.02}$	$-6.04^{+2.52}_{-2.62}$	604^{+43}_{-43}	$11.60^{+0.89}_{-0.75} \times 10^{-6}$	2.2	3.0	2.8		
1.712~2.096	49.54	$0.14^{+0.01}_{-0.01}$	$-0.94^{+0.04}_{-0.04}$	317^{+32}_{-33}	336^{+37}_{-37}	$7.08^{+1.01}_{-0.81} \times 10^{-6}$	$1.17^{+0.06}_{-0.06}$	$-0.94^{+0.04}_{-0.04}$	$-6.66^{+2.30}_{-2.30}$	336^{+25}_{-25}	$7.14^{+1.06}_{-0.85} \times 10^{-6}$	2.3	2.9	3.1		
2.096~2.877	54.35	$0.13^{+0.01}_{-0.01}$	$-0.85^{+0.04}_{-0.04}$	188^{+16}_{-16}	217^{+20}_{-20}	$3.86^{+0.49}_{-0.42} \times 10^{-6}$	$0.88^{+0.04}_{-0.04}$	$-0.84^{+0.04}_{-0.04}$	$-6.33^{+2.58}_{-2.50}$	216^{+12}_{-11}	$3.94^{+0.52}_{-0.44} \times 10^{-6}$	1.7	2.9	3.0		
2.877~3.515	38.86	$0.20^{+0.03}_{-0.03}$	$-0.51^{+0.08}_{-0.08}$	81^{+7}_{-7}	121^{+13}_{-12}	$2.08^{+0.42}_{-0.33} \times 10^{-6}$	$0.65^{+0.05}_{-0.05}$	$-0.49^{+0.09}_{-0.09}$	$-5.30^{+2.20}_{-2.80}$	118^{+6}_{-6}	$2.19^{+0.44}_{-0.33} \times 10^{-6}$	-0.4	2.4	2.0		
Pulse 2																
3.515~4.610	60.02	$0.20^{+0.01}_{-0.01}$	$-0.63^{+0.05}_{-0.05}$	100^{+6}_{-10}	137^{+10}_{-10}	$2.76^{+0.35}_{-0.29} \times 10^{-6}$	$0.82^{+0.04}_{-0.04}$	$-0.59^{+0.07}_{-0.07}$	$-4.26^{+1.41}_{-2.37}$	131^{+7}_{-7}	$2.96^{+0.54}_{-0.39} \times 10^{-6}$	-5.1	2.8	-0.1		
4.610~5.435	77.51	$0.20^{+0.01}_{-0.01}$	$-0.75^{+0.03}_{-0.03}$	185^{+11}_{-11}	231^{+15}_{-15}	$6.26^{+0.53}_{-0.53} \times 10^{-6}$	$1.09^{+0.05}_{-0.05}$	$-0.70^{+0.04}_{-0.05}$	$-3.43^{+0.83}_{-0.83}$	215^{+13}_{-13}	$7.07^{+1.31}_{-1.06} \times 10^{-6}$	-6.8	2.9	0.5		
5.435~5.796	64.22	$0.21^{+0.01}_{-0.01}$	$-0.86^{+0.03}_{-0.03}$	296^{+23}_{-23}	337^{+28}_{-28}	$10.66^{+1.16}_{-1.02} \times 10^{-6}$	$1.43^{+0.09}_{-0.09}$	$-0.78^{+0.07}_{-0.07}$	$-2.81^{+0.66}_{-0.66}$	280^{+41}_{-39}	$14.22^{+4.53}_{-3.82} \times 10^{-6}$	-11.2	2.9	-2.9		
5.796~7.506	102.63	$0.15^{+0.00}_{-0.00}$	$-0.93^{+0.02}_{-0.02}$	272^{+14}_{-14}	291^{+16}_{-16}	$6.52^{+0.42}_{-0.41} \times 10^{-6}$	$1.16^{+0.04}_{-0.04}$	$-0.82^{+0.04}_{-0.04}$	$-2.33^{+0.12}_{-0.12}$	230^{+17}_{-17}	$8.76^{+1.33}_{-1.19} \times 10^{-6}$	-14.2	2.9	3.8		
Pulse 3																
7.506~7.633	36.57	$0.25^{+0.02}_{-0.02}$	$-0.76^{+0.07}_{-0.07}$	190^{+24}_{-24}	236^{+32}_{-32}	$7.87^{+1.76}_{-1.34} \times 10^{-6}$	$1.42^{+0.12}_{-0.12}$	$-0.76^{+0.07}_{-0.07}$	$-6.84^{+2.22}_{-2.19}$	235^{+19}_{-19}	$7.86^{+1.58}_{-1.23} \times 10^{-6}$	2.2	2.7	3.1		
7.633~8.036	81.64	$0.25^{+0.01}_{-0.01}$	$-0.89^{+0.03}_{-0.03}$	320^{+22}_{-22}	356^{+26}_{-26}	$13.65^{+1.23}_{-1.10} \times 10^{-6}$	$1.70^{+0.09}_{-0.09}$	$-0.71^{+0.06}_{-0.06}$	$-2.21^{+0.10}_{-0.09}$	243^{+23}_{-24}	$18.76^{+4.36}_{-3.36} \times 10^{-6}$	-15.8	2.9	3.5		
8.036~8.492	109.81	$0.32^{+0.01}_{-0.01}$	$-0.82^{+0.02}_{-0.02}$	458^{+22}_{-22}	540^{+28}_{-28}	$28.20^{+1.79}_{-1.86} \times 10^{-6}$	$2.10^{+0.07}_{-0.07}$	$-0.82^{+0.02}_{-0.02}$	$-6.12^{+2.41}_{-2.51}$	537^{+20}_{-20}	$28.50^{+2.17}_{-2.17} \times 10^{-6}$	1.2	3.0	2.8		
8.492~8.771	72.15	$0.29^{+0.01}_{-0.01}$	$-0.87^{+0.03}_{-0.03}$	305^{+23}_{-23}	345^{+27}_{-27}	$15.35^{+1.68}_{-1.37} \times 10^{-6}$	$2.02^{+0.10}_{-0.10}$	$-0.78^{+0.05}_{-0.05}$	$-2.41^{+0.17}_{-0.16}$	280^{+25}_{-25}	$19.91^{+3.76}_{-3.42} \times 10^{-6}$	-12.0	2.9	3.8		
8.771~9.434	125.68	$0.32^{+0.01}_{-0.01}$	$-0.94^{+0.02}_{-0.02}$	309^{+15}_{-15}	328^{+17}_{-17}	$16.31^{+1.03}_{-0.98} \times 10^{-6}$	$2.68^{+0.08}_{-0.08}$	$-0.88^{+0.03}_{-0.03}$	$-2.56^{+0.13}_{-0.13}$	282^{+15}_{-14}	$19.54^{+2.13}_{-1.84} \times 10^{-6}$	-17.2	3.0	4.0		
9.434~10.090	108.41	$0.28^{+0.01}_{-0.01}$	$-1.01^{+0.02}_{-0.02}$	227^{+13}_{-13}	225^{+13}_{-13}	$10.12^{+0.74}_{-0.61} \times 10^{-6}$	$2.69^{+0.11}_{-0.10}$	$-0.89^{+0.06}_{-0.06}$	$-2.66^{+0.39}_{-0.39}$	179^{+18}_{-18}	$12.85^{+2.74}_{-2.32} \times 10^{-6}$	-17.4	2.9	-3.3		
10.090~10.391	59.99	$0.24^{+0.02}_{-0.02}$	$-1.07^{+0.05}_{-0.05}$	164^{+17}_{-17}	153^{+18}_{-18}	$6.32^{+0.85}_{-0.77} \times 10^{-6}$	$2.69^{+0.13}_{-0.13}$	$-0.95^{+0.07}_{-0.07}$	$-2.55^{+0.21}_{-0.13}$	127^{+10}_{-10}	$7.89^{+1.33}_{-1.19} \times 10^{-6}$	-10.9	2.7	3.7		
10.391~10.693	47.99	$0.18^{+0.02}_{-0.02}$	$-1.09^{+0.06}_{-0.06}$	143^{+17}_{-17}	130^{+18}_{-18}	$4.12^{+0.80}_{-0.58} \times 10^{-6}$	$2.21^{+0.12}_{-0.12}$	$-1.07^{+0.08}_{-0.08}$	$-5.18^{+2.51}_{-3.08}$	123^{+11}_{-12}	$4.31^{+0.90}_{-0.61} \times 10^{-6}$	0.7	2.4	1.8		
10.693~11.309	54.03	$0.12^{+0.01}_{-0.01}$	$-1.22^{+0.05}_{-0.05}$	155^{+18}_{-18}	121^{+16}_{-16}	$3.15^{+0.48}_{-0.41} \times 10^{-6}$	$1.99^{+0.08}_{-0.09}$	$-1.20^{+0.06}_{-0.06}$	$-5.44^{+2.54}_{-2.96}$	117^{+8}_{-8}	$3.24^{+0.45}_{-0.29} \times 10^{-6}$	1.3	2.5	2.2		
11.309~12.156	44.36	$0.08^{+0.01}_{-0.01}$	$-1.27^{+0.06}_{-0.06}$	133^{+18}_{-18}	97^{+15}_{-16}	$1.89^{+0.34}_{-0.29} \times 10^{-6}$	$1.46^{+0.07}_{-0.07}$	$-1.26^{+0.07}_{-0.07}$	$-5.80^{+2.62}_{-2.76}$	95^{+7}_{-6}	$1.90^{+0.20}_{-0.16} \times 10^{-6}$	3.0	2.3	2.9		
12.156~13.244	33.22	$0.07^{+0.01}_{-0.01}$	$-1.23^{+0.10}_{-0.10}$	78^{+12}_{-12}	60^{+12}_{-12}	$1.02^{+0.24}_{-0.24} \times 10^{-6}$	$1.13^{+0.06}_{-0.06}$	$-1.24^{+0.10}_{-0.10}$	$-6.40^{+2.44}_{-2.42}$	59^{+3}_{-3}	$1.01^{+0.07}_{-0.07} \times 10^{-6}$	4.5	1.0	3.0		
13.244~15.000	25.82	$0.05^{+0.01}_{-0.01}$	$-1.12^{+0.12}_{-0.12}$	72^{+12}_{-13}	64^{+14}_{-14}	$0.60^{+0.21}_{-0.17} \times 10^{-6}$	$0.62^{+0.04}_{-0.04}$	$-1.10^{+0.13}_{-0.13}$	$-5.59^{+2.47}_{-2.80}$	61^{+4}_{-4}	$0.60^{+0.08}_{-0.06} \times 10^{-6}$	4.9	-0.4	2.7		

Note—All columns are the same as Table A2 but for GRB 160422499.

Table A33. Time-resolved Spectral Fit Results of GRB 160802259

$t_{\text{start}} \sim t_{\text{stop}}$	S	Cutoff Power-Law Fitting						Band Fitting						Difference	
		K	α	E_c	E_p	F	K	α	β	E_p	F	ΔDIC	p_{CPL}	p_{DIC}	
(1)	(2)	(3)	(4)	(5)	(6)	(7)	(8)	(9)	(10)	(11)	(12)	(13)	(14)	(15)	
Pulse 1															
0.125~0.238	27.49	0.09 $^{+0.01}_{-0.01}$	-0.59 $^{+0.09}_{-0.09}$	785 $^{+156}_{-154}$	1107 $^{+231}_{-228}$	23.44 $^{+10.43}_{-6.49}$	1.30×10^{-6}	0.37 $^{+0.07}_{-0.08}$	-0.59 $^{+0.09}_{-0.09}$	5.56 $^{+1.72}_{-1.70}$	1084 $^{+160}_{-159}$	23.85 $^{+11.93}_{-8.15} \times 10^{-6}$	-5.0	2.7	2.5
0.238~0.962	99.88	0.19 $^{+0.01}_{-0.01}$	-0.55 $^{+0.03}_{-0.03}$	406 $^{+26}_{-26}$	589 $^{+40}_{-39}$	20.77 $^{+2.79}_{-2.05}$	1.0×10^{-6}	0.68 $^{+0.04}_{-0.04}$	-0.54 $^{+0.03}_{-0.03}$	4.25 $^{+1.03}_{-1.22}$	21.79 $^{+2.69}_{-2.27}$	30.71 $^{+11.33}_{-7.89} \times 10^{-6}$	1.6	3.0	2.9
0.962~1.171	73.79	0.33 $^{+0.02}_{-0.02}$	-0.42 $^{+0.06}_{-0.06}$	291 $^{+26}_{-26}$	460 $^{+44}_{-45}$	25.03 $^{+5.01}_{-4.45}$	1.0×10^{-6}	0.77 $^{+0.08}_{-0.08}$	-0.29 $^{+0.08}_{-0.08}$	2.61 $^{+0.24}_{-0.20}$	30.71 $^{+3.36}_{-3.35}$	30.71 $^{+11.33}_{-7.89} \times 10^{-6}$	-7.9	2.9	3.5
1.171~1.695	103.17	0.34 $^{+0.01}_{-0.01}$	-0.39 $^{+0.04}_{-0.04}$	234 $^{+13}_{-13}$	376 $^{+23}_{-23}$	19.08 $^{+2.02}_{-1.88}$	1.0×10^{-6}	0.82 $^{+0.06}_{-0.06}$	-0.37 $^{+0.04}_{-0.04}$	4.28 $^{+1.04}_{-1.24}$	36.8 $^{+15}_{-15}$	19.46 $^{+3.23}_{-2.59} \times 10^{-6}$	-0.8	2.9	2.9
1.695~2.160	82.84	0.33 $^{+0.02}_{-0.02}$	-0.41 $^{+0.05}_{-0.06}$	176 $^{+13}_{-13}$	280 $^{+23}_{-23}$	11.34 $^{+1.84}_{-1.44}$	1.0×10^{-6}	0.71 $^{+0.08}_{-0.08}$	-0.20 $^{+0.11}_{-0.11}$	2.62 $^{+0.26}_{-0.21}$	226 $^{+21}_{-22}$	14.43 $^{+5.87}_{-3.98} \times 10^{-6}$	-10.5	2.8	3.1
2.160~2.504	61.11	0.32 $^{+0.03}_{-0.03}$	-0.38 $^{+0.08}_{-0.08}$	138 $^{+14}_{-14}$	224 $^{+25}_{-25}$	7.64 $^{+1.61}_{-1.31}$	1.0×10^{-6}	0.60 $^{+0.09}_{-0.09}$	0.00 $^{+0.17}_{-0.17}$	-2.38 $^{+0.18}_{-0.13}$	16.1 $^{+17}_{-17}$	10.81 $^{+6.29}_{-3.54} \times 10^{-6}$	-22.2	2.6	2.7
2.504~3.065	60.10	0.22 $^{+0.03}_{-0.03}$	-0.53 $^{+0.08}_{-0.08}$	136 $^{+15}_{-15}$	200 $^{+25}_{-25}$	4.92 $^{+1.10}_{-0.84}$	1.0×10^{-6}	0.64 $^{+0.07}_{-0.07}$	-0.24 $^{+0.14}_{-0.14}$	-2.43 $^{+0.17}_{-0.15}$	15.0 $^{+14}_{-14}$	6.78 $^{+2.51}_{-1.75} \times 10^{-6}$	-8.2	2.4	3.4
3.065~3.695	42.00	0.17 $^{+0.03}_{-0.03}$	-0.55 $^{+0.11}_{-0.11}$	107 $^{+14}_{-15}$	154 $^{+24}_{-24}$	2.59 $^{+0.73}_{-0.62}$	1.0×10^{-6}	0.56 $^{+0.08}_{-0.08}$	-0.43 $^{+0.19}_{-0.18}$	-3.83 $^{+1.40}_{-2.19}$	139 $^{+19}_{-20}$	2.91 $^{+1.43}_{-0.89} \times 10^{-6}$	7.1	1.9	0.2
Pulse 2															
3.655~4.001	47.09	0.18 $^{+0.02}_{-0.02}$	-0.72 $^{+0.09}_{-0.09}$	199 $^{+31}_{-31}$	255 $^{+44}_{-44}$	6.13 $^{+1.77}_{-1.30}$	1.0×10^{-6}	0.88 $^{+0.12}_{-0.12}$	-0.60 $^{+0.15}_{-0.15}$	-3.04 $^{+0.80}_{-1.06}$	21.7 $^{+3.36}_{-4.41}$	7.26 $^{+4.43}_{-2.58} \times 10^{-6}$	-0.6	2.2	1.5
4.001~4.406	40.82	0.21 $^{+0.04}_{-0.04}$	-0.51 $^{+0.13}_{-0.13}$	105 $^{+16}_{-16}$	157 $^{+27}_{-27}$	3.05 $^{+1.16}_{-0.74}$	1.0×10^{-6}	0.62 $^{+0.09}_{-0.09}$	-0.35 $^{+0.20}_{-0.20}$	-3.17 $^{+0.72}_{-0.72}$	13.7 $^{+18}_{-18}$	3.62 $^{+2.14}_{-2.14} \times 10^{-6}$	2.3	1.5	1.9
4.406~4.626	21.53	0.13 $^{+0.04}_{-0.04}$	-0.85 $^{+0.20}_{-0.20}$	110 $^{+30}_{-30}$	127 $^{+41}_{-43}$	1.87 $^{+1.34}_{-1.34}$	1.0×10^{-6}	0.84 $^{+0.15}_{-0.15}$	-0.76 $^{+0.29}_{-0.29}$	-3.61 $^{+1.12}_{-1.11}$	11.2 $^{+24}_{-24}$	1.93 $^{+1.43}_{-0.67} \times 10^{-6}$	7.3	-2.1	1.6
4.626~5.108	22.03	0.08 $^{+0.03}_{-0.03}$	-1.01 $^{+0.25}_{-0.25}$	104 $^{+39}_{-39}$	103 $^{+46}_{-48}$	1.12 $^{+0.66}_{-0.52}$	1.0×10^{-6}	0.74 $^{+0.12}_{-0.12}$	-0.90 $^{+0.29}_{-0.29}$	-3.33 $^{+0.92}_{-1.21}$	84 $^{+14}_{-15}$	1.19 $^{+0.71}_{-0.33} \times 10^{-6}$	20.6	-15.7	2.1
5.207~5.658	59.23	0.22 $^{+0.02}_{-0.02}$	-0.54 $^{+0.07}_{-0.07}$	167 $^{+18}_{-18}$	243 $^{+28}_{-28}$	6.48 $^{+1.37}_{-1.01}$	1.0×10^{-6}	0.74 $^{+0.07}_{-0.07}$	-0.52 $^{+0.08}_{-0.08}$	-4.56 $^{+1.26}_{-1.36}$	23.8 $^{+16}_{-16}$	6.69 $^{+1.47}_{-1.29} \times 10^{-6}$	-14.3	2.6	3.0
5.658~5.817	22.28	0.11 $^{+0.04}_{-0.04}$	-1.02 $^{+0.21}_{-0.20}$	161 $^{+56}_{-60}$	158 $^{+64}_{-67}$	2.46 $^{+1.63}_{-1.33}$	1.0×10^{-6}	1.07 $^{+0.19}_{-0.20}$	-0.98 $^{+0.22}_{-0.23}$	-3.90 $^{+1.19}_{-1.26}$	14.2 $^{+26}_{-31}$	2.50 $^{+1.41}_{-0.79} \times 10^{-6}$	5.2	-3.4	2.0
5.817~6.178	23.85	0.07 $^{+0.02}_{-0.02}$	-1.12 $^{+0.19}_{-0.20}$	145 $^{+50}_{-52}$	128 $^{+52}_{-54}$	1.59 $^{+1.00}_{-0.60}$	1.0×10^{-6}	0.09 $^{+0.03}_{-0.03}$	-1.04 $^{+0.21}_{-0.21}$	-5.88 $^{+2.61}_{-2.66}$	11.0 $^{+18}_{-18}$	1.48 $^{+1.00}_{-0.60} \times 10^{-6}$	3.6	-4.5	-1.0
Pulse 3															
15.519~15.668	24.18	0.07 $^{+0.01}_{-0.01}$	-0.83 $^{+0.11}_{-0.11}$	664 $^{+205}_{-215}$	777 $^{+251}_{-262}$	8.83 $^{+5.57}_{-2.82}$	1.0×10^{-6}	0.51 $^{+0.10}_{-0.10}$	-0.83 $^{+0.11}_{-0.11}$	-5.28 $^{+1.82}_{-1.83}$	73.8 $^{+182}_{-194}$	8.92 $^{+5.60}_{-3.29} \times 10^{-6}$	8.9	1.6	2.0
15.668~15.843	42.62	0.20 $^{+0.02}_{-0.02}$	-0.65 $^{+0.10}_{-0.09}$	252 $^{+43}_{-43}$	340 $^{+63}_{-63}$	9.58 $^{+3.27}_{-2.29}$	1.0×10^{-6}	0.82 $^{+0.13}_{-0.14}$	-0.52 $^{+0.16}_{-0.16}$	-2.90 $^{+0.72}_{-0.72}$	11.7 $^{+56}_{-58}$	4.81 $^{+4.81}_{-0.97} \times 10^{-6}$	1.4	2.3	0.6
15.843~16.183	76.31	0.43 $^{+0.05}_{-0.05}$	-0.57 $^{+0.07}_{-0.07}$	123 $^{+12}_{-12}$	175 $^{+19}_{-19}$	8.24 $^{+1.59}_{-1.40}$	1.0×10^{-6}	1.18 $^{+0.12}_{-0.12}$	0.04 $^{+0.14}_{-0.14}$	-2.27 $^{+0.07}_{-0.07}$	11.0 $^{+7}_{-7}$	12.26 $^{+3.59}_{-2.80} \times 10^{-6}$	-51.4	2.5	3.7
16.183~16.514	63.40	0.43 $^{+0.07}_{-0.07}$	-0.65 $^{+0.09}_{-0.09}$	88 $^{+10}_{-10}$	119 $^{+15}_{-16}$	5.05 $^{+1.28}_{-0.99}$	1.0×10^{-6}	1.63 $^{+0.15}_{-0.15}$	-0.23 $^{+0.17}_{-0.17}$	-2.60 $^{+0.15}_{-0.14}$	90 $^{+7}_{-7}$	6.28 $^{+1.97}_{-1.48} \times 10^{-6}$	-12.9	2.1	3.7
16.514~16.764	40.08	0.21 $^{+0.06}_{-0.05}$	-0.98 $^{+0.15}_{-0.14}$	101 $^{+21}_{-22}$	103 $^{+26}_{-27}$	3.18 $^{+1.38}_{-0.92}$	1.0×10^{-6}	1.93 $^{+0.20}_{-0.20}$	-0.82 $^{+0.20}_{-0.20}$	-2.81 $^{+0.45}_{-0.41}$	85 $^{+12}_{-12}$	3.93 $^{+1.57}_{-1.07} \times 10^{-6}$	4.8	-0.8	3.2
16.764~17.276	37.47	0.17 $^{+0.05}_{-0.05}$	-0.88 $^{+0.15}_{-0.15}$	71 $^{+14}_{-14}$	80 $^{+19}_{-19}$	1.68 $^{+0.78}_{-0.55}$	1.0×10^{-6}	1.26 $^{+0.12}_{-0.12}$	-0.83 $^{+0.17}_{-0.18}$	-3.71 $^{+0.93}_{-1.17}$	74 $^{+7}_{-7}$	1.78 $^{+0.43}_{-0.31} \times 10^{-6}$	7.1	-0.9	3.0
17.276~17.778	25.50	0.13 $^{+0.06}_{-0.06}$	-0.92 $^{+0.23}_{-0.23}$	62 $^{+16}_{-17}$	67 $^{+23}_{-23}$	1.06 $^{+0.80}_{-0.46}$	1.0×10^{-6}	1.01 $^{+0.12}_{-0.12}$	-0.89 $^{+0.25}_{-0.26}$	-4.24 $^{+1.27}_{-1.39}$	62 $^{+7}_{-7}$	1.05 $^{+0.28}_{-0.18} \times 10^{-6}$	13.7	-8.4	3.2

Note—All columns are the same as Table A2 but for GRB 160802259.

Table A34. Time-resolved Spectral Fit Results of GRB 170207906

$t_{\text{start}} \sim t_{\text{stop}}$	S	Cutoff Power-Law Fitting						Band Fitting						Difference									
		K			E_c			F			K			α	β	E_p	F	ΔDIC	$p_{\text{DIC}}^{\text{CPL}}$	$p_{\text{DIC}}^{\text{Band}}$			
		(1)	(2)	(3)	(4)	(5)	(6)	(7)	(8)	(9)	(10)	(11)	(12)	(13)	(14)	(15)							
Pulse 1																							
-0.282~0.754	20.22	0.21	+0.03	-0.41	+0.18	76	+14	120	+25	0.69	+0.47	-0.23	-0.22	-5.75	+2.81	112	-11	0.71	+0.38	0.6	1.2	2.1	
0.754~1.122	26.14	0.32	+0.05	-0.29	+0.15	88	+13	151	+26	1.84	+1.20	-0.32	+0.05	-0.32	-0.04	0.20	+0.04	-0.32	+0.22	-0.23	0.6	1.6	
1.122~1.791	23.16	0.51	+0.07	-0.76	+0.18	71	+15	88	+22	0.80	+0.47	-0.28	+0.16	-0.50	+0.06	-0.71	+0.19	-0.41	+2.57	147	-11	0.7	1.6
1.791~2.596	43.08	0.51	+0.04	-0.69	+0.08	142	+17	186	+25	2.30	+0.78	-0.20	-0.16	-0.46	+0.05	-0.52	+0.14	-2.66	+0.48	83	+8	0.81	+0.25
3.020~3.304	20.20	0.26	+0.05	-0.69	+0.14	335	+91	439	+128	3.14	+3.18	-1.33	+0.13	-0.25	+0.05	-0.67	+0.13	-6.17	+2.60	151	-19	3.29	+1.47
4.141~4.892	46.81	0.38	+0.03	-0.63	+0.06	270	+29	371	+42	4.91	+1.42	-1.01	+0.06	-0.38	+0.03	-0.62	+0.06	-6.17	+2.62	407	+69	3.29	+1.74
4.892~6.806	55.36	0.06	+0.00	-0.61	+0.04	375	+33	521	+49	4.96	+0.66	-0.68	+0.06	-0.23	+0.02	-0.61	+0.04	-6.40	+2.43	360	-30	5.17	+0.96
6.958~7.535	33.16	0.05	+0.00	-0.68	+0.07	574	+101	758	+140	6.72	+1.98	-1.58	+0.06	-0.23	+0.03	-0.68	+0.07	-5.96	+1.04	521	+33	5.03	+0.86
																				1.2	2.9	1.9	2.9
																				1.1	2.5	1.1	2.3
Pulse 2																							
17.086~17.799	56.50	0.08	+0.00	-0.65	+0.04	598	+61	807	+86	12.88	+2.18	-1.91	+0.10	-0.36	+0.03	-0.64	+0.04	-5.66	+2.49	799	+60	13.22	+2.73
18.082~18.581	49.04	0.10	+0.00	-0.55	+0.05	392	+40	569	+62	10.16	+1.88	-1.51	+0.05	-0.36	+0.03	-0.56	+0.05	-6.92	+2.23	567	+41	10.39	+2.38
18.581~19.216	46.28	0.07	+0.00	-0.76	+0.05	552	+71	685	+92	8.47	+1.78	-1.33	+0.06	-0.42	+0.02	-0.60	+0.07	-6.46	+2.38	556	+55	10.58	+3.26
																				6.35	+1.64	6.75	+2.37
Pulse 3																							
20.430~20.621	24.02	0.11	+0.01	-0.31	+0.12	234	+40	396	+73	6.22	+2.52	-1.62	+0.06	-0.22	+0.05	-0.31	+0.13	-6.23	+2.57	389	+43	6.46	+3.80
20.621~20.916	43.00	0.12	+0.01	-0.57	+0.06	356	+44	510	+67	10.36	+2.28	-1.97	+0.06	-0.44	+0.05	-0.55	+0.07	-5.09	+2.60	491	+48	11.26	+3.96
21.110~21.337	36.10	0.11	+0.01	-0.60	+0.07	399	+57	558	+84	10.29	+2.92	-1.51	+0.06	-0.43	+0.06	-0.60	+0.07	-6.46	+2.43	510	+58	10.58	+2.68
21.337~22.015	46.97	0.07	+0.00	-0.89	+0.05	469	+66	520	+77	6.07	+1.24	-0.98	+0.06	-0.57	+0.04	-0.89	+0.05	-5.70	+2.81	510	+58	6.35	+1.61
Pulse 4																							
38.763~40.046	21.25	0.03	+0.01	-1.08	+0.13	205	+57	188	+59	0.80	+0.35	-0.22	+0.04	-0.32	+0.04	-1.09	+0.13	-6.17	+2.48	180	+31	0.79	+0.25
40.046~40.428	35.54	0.09	+0.01	-0.82	+0.08	294	+51	347	+64	4.28	+1.24	-0.81	+0.06	-0.56	+0.06	-0.79	+0.09	-5.43	+2.95	327	+51	4.63	+2.47
																				0.5	2.3	0.5	1.7

Note—All columns are the same as Table A2 but for GRB 170207906.

Table A35. Time-resolved Spectral Fit Results of GRB 171120556

$t_{\text{start}} \sim t_{\text{stop}}$	S	Cutoff Power-Law Fitting						Band Fitting						Difference		
		K	α	E_c	E_p	F	K	α	β	E_p	F	ΔDIC	$p_{\text{DIC}}^{\text{CPL}}$	$p_{\text{DIC}}^{\text{Band}}$		
(1)	(2)	(3)	(4)	(5)	(6)	(7)	(8)	(9)	(10)	(11)	(12)	(13)	(14)	(15)		
Pulse 1																
0.064~0.173	22.64	0.85 ^{+0.12} _{-0.12}	-1.04 ^{+0.09} _{-0.09}	895 ⁺³²⁷ ₋₃₃₄	860 ⁺³²⁴ ₋₃₃₁	9.27 ^{+6.93} _{-3.62} $\times 10^{-6}$	0.83 ^{+0.12} _{-0.12}	-1.02 ^{+0.10} _{-0.10}	-5.80 ^{+2.83} _{-2.87}	733 ⁺²³⁸ ₋₂₄₇	9.55 ^{+5.32} _{-3.14} $\times 10^{-6}$	0.2	0.6	1.1		
0.173~0.330	46.72	0.97 ^{+0.09} _{-0.08}	-0.71 ^{+0.05} _{-0.05}	464 ⁺⁵⁰ ₋₅₁	598 ⁺⁶⁹ ₋₇₀	19.49 ^{+4.96} _{-4.00} $\times 10^{-6}$	0.97 ^{+0.08} _{-0.09}	-0.71 ^{+0.05} _{-0.05}	-6.66 ^{+1.22} _{-2.27}	592 ⁺⁴⁸ ₋₄₈	19.53 ^{+4.27} _{-3.44} $\times 10^{-6}$	0.7	2.7	3.1		
0.330~0.524	41.95	0.84 ^{+0.08} _{-0.08}	-0.60 ^{+0.07} _{-0.07}	209 ⁺²³ ₋₂₃	293 ⁺³⁶ ₋₃₆	8.29 ^{+2.37} _{-1.85} $\times 10^{-6}$	0.76 ^{+0.10} _{-0.10}	-0.48 ^{+0.15} _{-0.14}	+1.86 ^{+0.15} _{-0.14}	252 ⁺⁴² ₋₄₆	9.26 ^{+6.49} _{-3.25} $\times 10^{-6}$	-8.2	2.5	-2.8		
0.524~0.933	35.06	0.75 ^{+0.07} _{-0.07}	-0.79 ^{+0.09} _{-0.09}	145 ⁺²¹ ₋₂₁	175 ⁺²⁹ ₋₂₉	2.71 ^{+1.07} _{-0.65} $\times 10^{-6}$	0.56 ^{+0.07} _{-0.07}	-0.09 ^{+0.24} _{-0.23}	-2.14 ^{+0.09} _{-0.09}	4.47 ^{+2.19} _{-1.33} $\times 10^{-6}$	96 ⁺¹¹ ₋₁₂	-24.0	2.3	1.8		
0.933~1.129	44.48	0.27 ^{+0.03} _{-0.03}	-0.49 ^{+0.08} _{-0.08}	148 ⁺¹⁵ ₋₁₆	224 ⁺²⁶ ₋₂₆	6.68 ^{+1.47} _{-1.19} $\times 10^{-6}$	0.80 ^{+0.09} _{-0.09}	-0.44 ^{+0.11} _{-0.11}	-4.96 ^{+2.24} _{-3.08}	209 ⁺²⁰ ₋₂₁	7.16 ^{+2.77} _{-1.81} $\times 10^{-6}$	-2.1	2.6	0.9		
Pulse 2																
38.398~38.933	28.40	0.08 ^{+0.01} _{-0.01}	-0.80 ^{+0.10} _{-0.10}	154 ⁺²⁵ ₋₂₅	185 ⁺³⁴ ₋₃₄	2.00 ^{+0.57} _{-0.41} $\times 10^{-6}$	0.51 ^{+0.06} _{-0.06}	-0.74 ^{+0.13} _{-0.13}	-4.62 ^{+2.20} _{-3.18}	170 ⁺²³ ₋₂₅	2.21 ^{+1.04} _{-0.61} $\times 10^{-6}$	-0.7	1.8	1.1		
38.933~40.171	51.83	0.12 ^{+0.01} _{-0.01}	-0.85 ^{+0.06} _{-0.06}	112 ⁺¹⁰ ₋₁₀	128 ⁺¹³ ₋₁₃	2.04 ^{+0.30} _{-0.27} $\times 10^{-6}$	0.13 ^{+0.01} _{-0.01}	-0.81 ^{+0.04} _{-0.05}	-3.27 ^{+0.75} _{-0.53}	117 ⁺⁸ ₋₈	2.38 ^{+0.47} _{-0.41} $\times 10^{-6}$	-10.7	2.6	-1.2		
40.171~40.753	25.45	0.07 ^{+0.02} _{-0.02}	-1.08 ^{+0.12} _{-0.12}	118 ⁺²⁴ ₋₂₅	108 ⁺²⁶ ₋₂₇	1.35 ^{+0.47} _{-0.33} $\times 10^{-6}$	0.85 ^{+0.08} _{-0.08}	-1.02 ^{+0.14} _{-0.14}	-4.39 ^{+1.89} _{-1.89}	98 ⁺¹² ₋₁₂	1.45 ^{+0.42} _{-0.29} $\times 10^{-6}$	0.3	0.2	0.8		
40.753~41.988	22.46	0.05 ^{+0.01} _{-0.01}	-1.10 ^{+0.14} _{-0.14}	98 ⁺²² ₋₂₂	89 ⁺²⁴ ₋₂₄	0.76 ^{+0.34} _{-0.22} $\times 10^{-6}$	0.56 ^{+0.05} _{-0.05}	-0.95 ^{+0.21} _{-0.22}	-4.01 ^{+1.57} _{-2.77}	76 ⁺¹¹ ₋₁₁	0.83 ^{+0.29} _{-0.20} $\times 10^{-6}$	-0.0	-1.6	-0.5		

Note—All columns are the same as Table A2 but for GRB 171120556.

Table A36. Time-resolved Spectral Fit Results of GRB 17122700

$t_{\text{start}} \sim t_{\text{stop}}$	S	Cutoff Power-Law Fitting						Band Fitting						Difference		
		K	α	E_c	E_p	F	K	α	β	E_p	F	ΔDIC	$p_{\text{DIC}}^{\text{CPL}}$	$p_{\text{DIC}}^{\text{Band}}$		
Pulse 1																
-0.101~6.348	24.27	0.04 $^{+0.01}_{-0.01}$	-0.35 $^{+0.09}_{-0.09}$	398 $^{+558}_{-57}$	656 $^{+102}_{-101}$	2.21 $^{+1.51}_{-0.85}$ $\times 10^{-6}$	0.04 $^{+0.01}_{-0.01}$	-0.35 $^{+0.10}_{-0.09}$	-5.83 $^{+2.68}_{-2.79}$	648 $^{+64}_{-64}$	2.31 $^{+1.02}_{-0.70}\times 10^{-6}$	0.4	0.9	1.5		
6.348~14.390	50.11	0.12 $^{+0.01}_{-0.01}$	-0.59 $^{+0.05}_{-0.05}$	367 $^{+31}_{-31}$	517 $^{+48}_{-48}$	2.82 $^{+0.53}_{-0.53}$ $\times 10^{-6}$	0.12 $^{+0.01}_{-0.01}$	-0.58 $^{+0.05}_{-0.05}$	-6.72 $^{+2.18}_{-2.22}$	515 $^{+30}_{-30}$	2.86 $^{+0.53}_{-0.47}\times 10^{-6}$	0.5	2.6	3.0		
14.390~15.099	23.71	0.20 $^{+0.04}_{-0.04}$	-0.67 $^{+0.10}_{-0.10}$	702 $^{+166}_{-168}$	933 $^{+232}_{-234}$	7.23 $^{+6.20}_{-2.83}\times 10^{-6}$	0.20 $^{+0.04}_{-0.04}$	-0.67 $^{+0.09}_{-0.08}$	-5.75 $^{+2.59}_{-2.81}$	896 $^{+154}_{-152}$	7.59 $^{+3.84}_{-2.70}\times 10^{-6}$	0.2	0.8	1.4		
15.099~15.548	28.42	0.25 $^{+0.04}_{-0.05}$	-0.58 $^{+0.08}_{-0.08}$	614 $^{+100}_{-101}$	872 $^{+151}_{-152}$	11.95 $^{+6.39}_{-4.29}\times 10^{-6}$	0.25 $^{+0.04}_{-0.04}$	-0.57 $^{+0.08}_{-0.08}$	-6.32 $^{+2.44}_{-2.47}$	855 $^{+102}_{-102}$	12.00 $^{+4.95}_{-3.47}\times 10^{-6}$	0.4	2.0	2.4		
15.548~16.821	69.79	0.38 $^{+0.03}_{-0.03}$	-0.65 $^{+0.03}_{-0.03}$	1091 $^{+71}_{-71}$	1473 $^{+101}_{-101}$	30.46 $^{+5.60}_{-5.09}\times 10^{-6}$	0.36 $^{+0.03}_{-0.03}$	-0.63 $^{+0.03}_{-0.03}$	-3.50 $^{+0.48}_{-0.42}$	1386 $^{+79}_{-78}$	30.54 $^{+5.13}_{-4.22}\times 10^{-6}$	-9.1	2.9	3.4		
16.821~17.341	60.01	0.57 $^{+0.05}_{-0.04}$	-0.68 $^{+0.03}_{-0.03}$	1277 $^{+93}_{-94}$	1686 $^{+129}_{-130}$	47.86 $^{+9.99}_{-8.08}\times 10^{-6}$	0.55 $^{+0.05}_{-0.05}$	-0.66 $^{+0.04}_{-0.04}$	-3.53 $^{+0.63}_{-0.55}$	1570 $^{+117}_{-118}$	48.19 $^{+9.76}_{-9.74}\times 10^{-6}$	-7.9	2.9	2.8		
17.341~17.648	36.34	0.51 $^{+0.07}_{-0.07}$	-0.73 $^{+0.06}_{-0.06}$	997 $^{+159}_{-160}$	1267 $^{+210}_{-212}$	24.66 $^{+11.21}_{-7.04}\times 10^{-6}$	0.49 $^{+0.07}_{-0.07}$	-0.71 $^{+0.06}_{-0.06}$	-4.86 $^{+1.95}_{-2.85}$	1201 $^{+148}_{-146}$	25.62 $^{+8.81}_{-6.72}\times 10^{-6}$	-3.0	2.4	1.5		
17.648~17.820	44.67	0.73 $^{+0.09}_{-0.09}$	-0.67 $^{+0.05}_{-0.05}$	1336 $^{+147}_{-148}$	1778 $^{+267}_{-268}$	69.84 $^{+23.63}_{-16.81}\times 10^{-6}$	0.55 $^{+0.08}_{-0.08}$	-0.52 $^{+0.06}_{-0.06}$	-2.56 $^{+0.18}_{-0.18}$	1295 $^{+139}_{-137}$	66.51 $^{+25.10}_{-17.95}\times 10^{-6}$	-24.8	2.8	3.4		
17.820~18.185	47.21	0.54 $^{+0.06}_{-0.06}$	-0.62 $^{+0.05}_{-0.05}$	714 $^{+89}_{-90}$	985 $^{+127}_{-129}$	27.62 $^{+10.69}_{-7.10}\times 10^{-6}$	0.47 $^{+0.06}_{-0.06}$	-0.54 $^{+0.06}_{-0.06}$	-2.70 $^{+0.30}_{-0.16}$	83 $^{+87}_{-87}$	30.90 $^{+10.48}_{-7.99}\times 10^{-6}$	-12.3	2.4	3.2		
18.185~18.647	83.77	0.18 $^{+0.00}_{-0.00}$	-0.72 $^{+0.02}_{-0.02}$	1787 $^{+85}_{-85}$	2288 $^{+115}_{-115}$	104.30 $^{+9.30}_{-7.90}\times 10^{-6}$	0.79 $^{+0.06}_{-0.06}$	-0.63 $^{+0.03}_{-0.03}$	-2.59 $^{+0.12}_{-0.12}$	1741 $^{+113}_{-115}$	98.31 $^{+16.82}_{-14.16}\times 10^{-6}$	-49.5	3.0	3.9		
18.647~20.433	174.93	0.21 $^{+0.00}_{-0.00}$	-0.71 $^{+0.01}_{-0.01}$	1384 $^{+36}_{-36}$	1785 $^{+49}_{-49}$	88.97 $^{+3.94}_{-3.73}\times 10^{-6}$	0.91 $^{+0.03}_{-0.03}$	-0.63 $^{+0.01}_{-0.01}$	-2.74 $^{+0.06}_{-0.06}$	1457 $^{+40}_{-40}$	87.47 $^{+5.90}_{-6.29}\times 10^{-6}$	-170.9	3.0	4.0		
20.433~20.836	75.22	0.20 $^{+0.00}_{-0.00}$	-0.75 $^{+0.03}_{-0.03}$	995 $^{+81}_{-81}$	1244 $^{+105}_{-105}$	50.61 $^{+6.70}_{-5.50}\times 10^{-6}$	1.06 $^{+0.08}_{-0.08}$	-0.71 $^{+0.03}_{-0.03}$	-2.83 $^{+0.20}_{-0.20}$	1092 $^{+80}_{-78}$	52.92 $^{+10.50}_{-9.31}\times 10^{-6}$	-18.6	2.9	3.8		
20.836~21.554	73.95	0.14 $^{+0.00}_{-0.00}$	-0.71 $^{+0.03}_{-0.03}$	757 $^{+61}_{-61}$	977 $^{+182}_{-82}$	28.43 $^{+3.78}_{-3.30}\times 10^{-6}$	0.71 $^{+0.05}_{-0.05}$	-0.69 $^{+0.03}_{-0.03}$	-3.26 $^{+0.47}_{-0.23}$	932 $^{+60}_{-59}$	30.45 $^{+5.80}_{-4.67}\times 10^{-6}$	-6.7	3.0	3.2		
21.554~22.212	82.45	0.17 $^{+0.00}_{-0.00}$	-0.73 $^{+0.03}_{-0.03}$	876 $^{+65}_{-64}$	1113 $^{+86}_{-86}$	37.21 $^{+4.75}_{-3.45}\times 10^{-6}$	0.86 $^{+0.06}_{-0.06}$	-0.71 $^{+0.03}_{-0.03}$	-3.89 $^{+0.89}_{-0.62}$	1053 $^{+69}_{-68}$	38.63 $^{+6.14}_{-5.42}\times 10^{-6}$	-5.5	3.0	1.8		
22.212~22.728	65.49	0.15 $^{+0.00}_{-0.00}$	-0.79 $^{+0.04}_{-0.04}$	814 $^{+89}_{-89}$	985 $^{+113}_{-114}$	27.15 $^{+3.61}_{-3.61}\times 10^{-6}$	0.85 $^{+0.07}_{-0.07}$	-0.74 $^{+0.04}_{-0.04}$	-2.85 $^{+0.41}_{-0.18}$	852 $^{+90}_{-89}$	29.47 $^{+7.46}_{-5.86}\times 10^{-6}$	-8.2	2.9	2.9		
22.728~22.985	35.83	0.11 $^{+0.01}_{-0.01}$	-0.80 $^{+0.07}_{-0.07}$	586 $^{+101}_{-102}$	704 $^{+128}_{-129}$	13.56 $^{+3.77}_{-2.91}\times 10^{-6}$	0.72 $^{+0.10}_{-0.10}$	-0.80 $^{+0.07}_{-0.07}$	-6.63 $^{+2.82}_{-2.34}$	699 $^{+89}_{-89}$	13.70 $^{+4.37}_{-3.27}\times 10^{-6}$	1.9	2.7	2.8		
22.985~24.215	56.71	0.09 $^{+0.00}_{-0.00}$	-0.83 $^{+0.04}_{-0.04}$	555 $^{+60}_{-59}$	649 $^{+73}_{-73}$	9.43 $^{+1.53}_{-1.24}\times 10^{-6}$	0.57 $^{+0.04}_{-0.04}$	-0.82 $^{+0.04}_{-0.04}$	-5.25 $^{+2.89}_{-2.97}$	640 $^{+55}_{-56}$	9.71 $^{+2.24}_{-1.61}\times 10^{-6}$	-0.1	2.8	2.1		
Pulse 2																
24.215~25.597	43.05	0.06 $^{+0.00}_{-0.00}$	-0.80 $^{+0.06}_{-0.06}$	403 $^{+52}_{-52}$	484 $^{+67}_{-67}$	4.99 $^{+1.01}_{-0.79}\times 10^{-6}$	0.41 $^{+0.04}_{-0.04}$	-0.80 $^{+0.06}_{-0.06}$	-6.29 $^{+2.48}_{-2.49}$	485 $^{+44}_{-45}$	5.11 $^{+1.16}_{-0.96}\times 10^{-6}$	1.7	2.8	2.9		
25.597~25.942	31.20	0.08 $^{+0.00}_{-0.01}$	-0.81 $^{+0.07}_{-0.07}$	644 $^{+117}_{-119}$	767 $^{+147}_{-148}$	10.68 $^{+3.16}_{-2.19}\times 10^{-6}$	0.55 $^{+0.08}_{-0.08}$	-0.81 $^{+0.07}_{-0.07}$	-6.61 $^{+2.42}_{-2.39}$	756 $^{+103}_{-105}$	11.05 $^{+4.15}_{-2.64}\times 10^{-6}$	1.7	2.7	2.7		
25.942~26.489	27.80	0.05 $^{+0.00}_{-0.00}$	-1.06 $^{+0.08}_{-0.08}$	1096 $^{+405}_{-402}$	1030 $^{+405}_{-388}$	7.35 $^{+4.02}_{-2.05}\times 10^{-6}$	0.59 $^{+0.08}_{-0.08}$	-1.05 $^{+0.08}_{-0.08}$	-5.70 $^{+2.82}_{-2.91}$	937 $^{+287}_{-277}$	7.17 $^{+4.25}_{-2.13}\times 10^{-6}$	1.7	1.4	1.4		
26.489~26.738	40.67	0.13 $^{+0.01}_{-0.01}$	-0.82 $^{+0.05}_{-0.05}$	973 $^{+140}_{-141}$	1148 $^{+157}_{-157}$	26.68 $^{+6.12}_{-4.74}\times 10^{-6}$	0.85 $^{+0.10}_{-0.09}$	-0.82 $^{+0.05}_{-0.05}$	-5.98 $^{+2.50}_{-2.66}$	1138 $^{+129}_{-133}$	27.52 $^{+6.83}_{-5.70}\times 10^{-6}$	0.7	2.8	2.4		
26.738~27.252	40.34	0.09 $^{+0.00}_{-0.00}$	-0.85 $^{+0.06}_{-0.06}$	677 $^{+107}_{-108}$	779 $^{+130}_{-131}$	11.58 $^{+2.58}_{-2.36}\times 10^{-6}$	0.61 $^{+0.07}_{-0.07}$	-0.84 $^{+0.05}_{-0.05}$	-6.59 $^{+2.36}_{-2.36}$	770 $^{+91}_{-91}$	11.78 $^{+2.98}_{-2.42}\times 10^{-6}$	1.9	2.7	2.9		
27.252~27.403	31.82	0.14 $^{+0.01}_{-0.01}$	-0.76 $^{+0.08}_{-0.08}$	617 $^{+117}_{-118}$	764 $^{+154}_{-154}$	19.28 $^{+6.65}_{-4.39}\times 10^{-6}$	0.83 $^{+0.13}_{-0.13}$	-0.76 $^{+0.08}_{-0.08}$	-5.98 $^{+2.57}_{-2.69}$	755 $^{+106}_{-107}$	19.30 $^{+7.46}_{-4.99}\times 10^{-6}$	1.2	2.6	2.4		
27.403~27.557	52.66	0.21 $^{+0.01}_{-0.01}$	-0.81 $^{+0.03}_{-0.03}$	1527 $^{+157}_{-157}$	1817 $^{+153}_{-153}$	78.82 $^{+12.62}_{-11.79}\times 10^{-6}$	1.18 $^{+0.14}_{-0.14}$	-0.72 $^{+0.06}_{-0.06}$	-2.94 $^{+0.46}_{-0.46}$	1303 $^{+195}_{-192}$	72.79 $^{+25.00}_{-18.32}\times 10^{-6}$	-8.3	3.0	2.7		
27.557~28.019	59.57	0.15 $^{+0.01}_{-0.01}$	-0.83 $^{+0.04}_{-0.04}$	668 $^{+77}_{-77}$	781 $^{+94}_{-94}$	21.29 $^{+3.96}_{-3.08}\times 10^{-6}$	1.03 $^{+0.08}_{-0.08}$	-0.82 $^{+0.04}_{-0.04}$	-5.81 $^{+2.38}_{-2.69}$	676 $^{+64}_{-64}$	21.29 $^{+4.28}_{-3.45}\times 10^{-6}$	0.7	2.9	2.5		
28.019~28.712	63.96	0.13 $^{+0.00}_{-0.00}$	-0.89 $^{+0.04}_{-0.04}$	682 $^{+76}_{-76}$	757 $^{+89}_{-89}$	15.79 $^{+2.44}_{-1.98}\times 10^{-6}$	0.99 $^{+0.07}_{-0.07}$	-0.89 $^{+0.04}_{-0.04}$	-5.51 $^{+2.43}_{-2.43}$	746 $^{+65}_{-64}$	16.18 $^{+3.29}_{-2.59}\times 10^{-6}$	0.2	2.9	2.2		

Table A36 continued on next page

Table A36 (continued)

$t_{\text{start}} \sim t_{\text{stop}}$	S	Cutoff Power-Law Fitting						Band Fitting						Difference	
		K	α	E_c	E_p	F	K	α	β	E_p	F	ΔDIC	$p_{\text{DIC}}^{\text{CPL}}$	$p_{\text{DIC}}^{\text{Band}}$	
(1)	(2)	(3)	(4)	(5)	(6)	(7)	(8)	(9)	(10)	(11)	(12)	(13)	(14)	(15)	
28.712~29.102	37.20	$0.10^{+0.01}_{-0.01}$	$-0.88^{+0.06}_{-0.06}$	583^{+105}_{-107}	653^{+123}_{-125}	$10.52^{+2.73}_{-2.08} \times 10^{-6}$	$0.75^{+0.09}_{-0.09}$	$-0.88^{+0.06}_{-0.06}$	$-6.50^{+2.41}_{-2.41}$	645^{+87}_{-88}	$10.50^{+3.75}_{-2.26} \times 10^{-6}$	1.9	2.7	2.8	
29.102~29.373	45.58	$0.16^{+0.01}_{-0.01}$	$-0.80^{+0.06}_{-0.06}$	586^{+84}_{-85}	703^{+106}_{-108}	$18.91^{+3.91}_{-3.52} \times 10^{-6}$	$0.99^{+0.11}_{-0.11}$	$-0.80^{+0.06}_{-0.06}$	$-6.39^{+2.43}_{-2.44}$	688^{+78}_{-77}	$19.13^{+5.28}_{-4.92} \times 10^{-6}$	1.8	2.7	2.8	
29.373~29.910	44.06	$0.10^{+0.01}_{-0.01}$	$-1.01^{+0.05}_{-0.05}$	624^{+104}_{-105}	618^{+108}_{-108}	$9.40^{+2.14}_{-1.67} \times 10^{-6}$	$0.98^{+0.09}_{-0.09}$	$-1.01^{+0.05}_{-0.05}$	$-6.51^{+2.31}_{-2.34}$	614^{+77}_{-77}	$9.39^{+2.12}_{-1.65} \times 10^{-6}$	2.3	2.7	2.9	
Pulse 3															
29.910~31.369	41.28	$0.06^{+0.00}_{-0.00}$	$-0.98^{+0.07}_{-0.06}$	366^{+67}_{-67}	373^{+73}_{-72}	$3.47^{+0.79}_{-0.62} \times 10^{-6}$	$0.57^{+0.05}_{-0.05}$	$-0.97^{+0.07}_{-0.07}$	$-5.61^{+2.80}_{-2.97}$	362^{+51}_{-51}	$3.57^{+1.15}_{-0.72} \times 10^{-6}$	1.4	2.4	2.3	
31.369~31.757	28.28	$0.07^{+0.01}_{-0.01}$	$-1.04^{+0.08}_{-0.08}$	557^{+137}_{-141}	534^{+139}_{-142}	$5.55^{+1.89}_{-1.33} \times 10^{-6}$	$0.75^{+0.10}_{-0.10}$	$-1.04^{+0.08}_{-0.08}$	$-6.52^{+2.47}_{-2.41}$	529^{+99}_{-102}	$5.53^{+2.14}_{-1.26} \times 10^{-6}$	2.6	2.4	2.7	
31.757~32.395	22.39	$0.06^{+0.01}_{-0.01}$	$-0.83^{+0.15}_{-0.15}$	210^{+54}_{-57}	246^{+70}_{-74}	$2.09^{+1.63}_{-1.65} \times 10^{-6}$	$0.42^{+0.08}_{-0.08}$	$-0.81^{+0.15}_{-0.16}$	$-5.92^{+2.79}_{-2.76}$	230^{+41}_{-41}	$2.12^{+1.22}_{-0.66} \times 10^{-6}$	3.3	0.1	1.7	
32.395~38.267	45.60	$0.03^{+0.00}_{-0.00}$	$-1.14^{+0.07}_{-0.07}$	214^{+35}_{-35}	184^{+34}_{-34}	$1.13^{+0.24}_{-0.18} \times 10^{-6}$	$0.45^{+0.05}_{-0.05}$	$-1.00^{+0.19}_{-0.18}$	$-4.26^{+2.16}_{-2.16}$	1.52^{+36}_{-36}	$1.31^{+0.85}_{-0.45} \times 10^{-6}$	-8.3	2.1	-6.4	
38.511~39.062	36.92	$0.09^{+0.01}_{-0.01}$	$-1.00^{+0.08}_{-0.08}$	302^{+60}_{-60}	302^{+65}_{-65}	$4.29^{+1.11}_{-0.81} \times 10^{-6}$	$0.94^{+0.10}_{-0.10}$	$-1.01^{+0.08}_{-0.08}$	$-6.39^{+2.50}_{-2.51}$	298^{+40}_{-40}	$4.32^{+1.11}_{-0.87} \times 10^{-6}$	2.9	2.2	2.9	
39.062~40.274	44.83	$0.07^{+0.01}_{-0.01}$	$-1.15^{+0.07}_{-0.07}$	342^{+74}_{-74}	291^{+68}_{-67}	$3.21^{+0.62}_{-0.62} \times 10^{-6}$	$0.89^{+0.09}_{-0.09}$	$-1.08^{+0.11}_{-0.11}$	$-4.60^{+2.46}_{-2.33}$	253^{+55}_{-64}	$3.62^{+1.90}_{-1.09} \times 10^{-6}$	-2.1	2.0	-0.5	
40.274~42.928	40.68	$0.04^{+0.01}_{-0.01}$	$-1.25^{+0.09}_{-0.09}$	217^{+49}_{-55}	163^{+42}_{-45}	$1.38^{+0.43}_{-0.29} \times 10^{-6}$	$0.68^{+0.07}_{-0.07}$	$-1.00^{+0.18}_{-0.19}$	$-2.85^{+0.77}_{-0.77}$	110^{+23}_{-22}	$1.89^{+0.91}_{-0.58} \times 10^{-6}$	-11.7	0.1	-5.3	
42.928~45.357	27.42	$0.02^{+0.01}_{-0.01}$	$-1.44^{+0.13}_{-0.13}$	360^{+171}_{-170}	201^{+107}_{-106}	$1.06^{+0.53}_{-0.53} \times 10^{-6}$	$0.62^{+0.07}_{-0.07}$	$-1.36^{+0.17}_{-0.17}$	$-5.26^{+2.95}_{-3.14}$	156^{+49}_{-53}	$1.07^{+0.55}_{-0.28} \times 10^{-6}$	5.2	-5.1	-1.6	
45.357~46.238	27.43	$0.06^{+0.01}_{-0.01}$	$-1.13^{+0.14}_{-0.14}$	162^{+41}_{-44}	141^{+42}_{-45}	$1.46^{+0.67}_{-0.39} \times 10^{-6}$	$0.81^{+0.10}_{-0.10}$	$-1.13^{+0.14}_{-0.14}$	$-6.31^{+2.55}_{-2.55}$	132^{+18}_{-18}	$1.50^{+0.41}_{-0.30} \times 10^{-6}$	6.0	-0.8	2.9	
46.238~49.915	32.72	$0.04^{+0.01}_{-0.01}$	$-1.21^{+0.12}_{-0.11}$	128^{+26}_{-28}	101^{+26}_{-26}	$0.79^{+0.24}_{-0.18} \times 10^{-6}$	$0.58^{+0.05}_{-0.05}$	$-1.20^{+0.12}_{-0.12}$	$-6.28^{+2.53}_{-2.54}$	97^{+9}_{-9}	$0.78^{+0.14}_{-0.10} \times 10^{-6}$	4.7	0.8	3.1	
49.915~51.705	29.98	$0.06^{+0.02}_{-0.02}$	$-1.11^{+0.14}_{-0.15}$	96^{+19}_{-21}	85^{+22}_{-23}	$0.97^{+0.43}_{-0.28} \times 10^{-6}$	$0.77^{+0.08}_{-0.08}$	$-1.12^{+0.14}_{-0.14}$	$-6.43^{+2.46}_{-2.45}$	83^{+7}_{-7}	$0.95^{+0.15}_{-0.12} \times 10^{-6}$	5.9	-0.6	3.1	

Note—All columns are the same as Table A2 but for GRB 171227000.

Table A37. Time-resolved Spectral Fit Results of GRB 180113418

$t_{\text{start}} \sim t_{\text{stop}}$	S	Cutoff Power-Law Fitting						Band Fitting						Difference		
		K	α	E_c	E_p	F	K	α	β	E_p	F	ΔDIC	$p_{\text{DIC}}^{\text{CPL}}$	$p_{\text{DIC}}^{\text{Band}}$		
(1)	(2)	(3)	(4)	(5)	(6)	(7)	(8)	(9)	(10)	(11)	(12)	(13)	(14)	(15)		
Pulse 1																
3.730~6.055	25.23	0.02 $^{+0.00}_{-0.00}$	-0.74 $^{+0.05}_{-0.05}$	633 $^{+102}_{-102}$	797 $^{+132}_{-132}$	3.19 $^{+0.78}_{-0.60} \times 10^{-6}$	0.12 $^{+0.01}_{-0.01}$	-0.71 $^{+0.07}_{-0.07}$	-4.08 $^{+1.87}_{-1.14} \times 10^{-6}$	3.64 $^{+1.59}_{-1.24} \times 10^{-6}$	-3.9	2.6	0.1			
6.055~6.781	23.78	0.04 $^{+0.00}_{-0.00}$	-0.73 $^{+0.06}_{-0.06}$	849 $^{+161}_{-165}$	1078 $^{+211}_{-216}$	7.26 $^{+2.81}_{-1.63} \times 10^{-6}$	0.18 $^{+0.02}_{-0.02}$	-0.69 $^{+0.06}_{-0.07}$	-2.19 $^{+0.13}_{-0.13} \times 10^{-6}$	9.59 $^{+3.74}_{-2.46} \times 10^{-6}$	-18.5	2.5	3.1			
6.781~9.731	78.26	0.07 $^{+0.00}_{-0.00}$	-0.77 $^{+0.02}_{-0.02}$	630 $^{+137}_{-37}$	774 $^{+47}_{-48}$	9.83 $^{+0.89}_{-0.78} \times 10^{-6}$	0.38 $^{+0.02}_{-0.02}$	-0.70 $^{+0.03}_{-0.03}$	-2.24 $^{+0.07}_{-0.07} \times 10^{-6}$	12.62 $^{+1.54}_{-1.48} \times 10^{-6}$	-65.6	2.9	3.9			
9.731~9.849	26.26	0.11 $^{+0.01}_{-0.01}$	-0.78 $^{+0.07}_{-0.07}$	674 $^{+128}_{-130}$	823 $^{+165}_{-165}$	16.48 $^{+5.31}_{-3.82} \times 10^{-6}$	0.66 $^{+0.09}_{-0.09}$	-0.76 $^{+0.08}_{-0.07}$	-4.55 $^{+2.24}_{-3.26} \times 10^{-6}$	17.80 $^{+7.74}_{-5.48} \times 10^{-6}$	-2.4	2.6	0.8			
9.849~11.099	104.65	0.16 $^{+0.00}_{-0.00}$	-0.74 $^{+0.02}_{-0.02}$	565 $^{+28}_{-28}$	712 $^{+37}_{-37}$	20.87 $^{+1.61}_{-1.36} \times 10^{-6}$	0.82 $^{+0.03}_{-0.03}$	-0.67 $^{+0.02}_{-0.02}$	-2.23 $^{+0.06}_{-0.06} \times 10^{-6}$	27.23 $^{+2.78}_{-2.67} \times 10^{-6}$	-136.7	2.9	4.0			
11.099~12.818	103.62	0.15 $^{+0.00}_{-0.00}$	-0.77 $^{+0.02}_{-0.02}$	432 $^{+19}_{-19}$	531 $^{+25}_{-25}$	13.02 $^{+0.79}_{-0.75} \times 10^{-6}$	0.80 $^{+0.03}_{-0.03}$	-0.67 $^{+0.03}_{-0.03}$	-2.17 $^{+0.05}_{-0.05} \times 10^{-6}$	399 $^{+21}_{-21}$	18.23 $^{+1.86}_{-1.90} \times 10^{-6}$	-89.7	3.0	3.9		
12.818~13.855	69.20	0.12 $^{+0.00}_{-0.00}$	-0.82 $^{+0.03}_{-0.03}$	410 $^{+29}_{-29}$	484 $^{+37}_{-37}$	9.36 $^{+0.96}_{-0.78} \times 10^{-6}$	0.70 $^{+0.04}_{-0.04}$	-0.67 $^{+0.05}_{-0.05}$	-2.11 $^{+0.07}_{-0.07} \times 10^{-6}$	335 $^{+28}_{-28}$	13.54 $^{+2.55}_{-2.55} \times 10^{-6}$	-38.4	3.0	3.5		
13.855~15.242	89.06	0.15 $^{+0.00}_{-0.00}$	-0.71 $^{+0.02}_{-0.02}$	330 $^{+19}_{-19}$	425 $^{+21}_{-21}$	10.23 $^{+0.74}_{-0.67} \times 10^{-6}$	0.69 $^{+0.03}_{-0.03}$	-0.57 $^{+0.04}_{-0.04}$	-2.11 $^{+0.07}_{-0.06} \times 10^{-6}$	315 $^{+20}_{-20}$	14.74 $^{+2.21}_{-2.04} \times 10^{-6}$	-46.8	2.9	3.9		
15.242~18.387	103.70	0.14 $^{+0.00}_{-0.00}$	-0.79 $^{+0.02}_{-0.02}$	218 $^{+9}_{-9}$	264 $^{+12}_{-12}$	5.08 $^{+0.29}_{-0.28} \times 10^{-6}$	0.72 $^{+0.02}_{-0.02}$	-0.55 $^{+0.04}_{-0.04}$	-2.11 $^{+0.04}_{-0.04} \times 10^{-6}$	17.9 $^{+8}_{-7}$	8.17 $^{+0.91}_{-0.82} \times 10^{-6}$	-103.4	3.0	3.9		
18.387~18.936	40.20	0.11 $^{+0.01}_{-0.01}$	-0.88 $^{+0.06}_{-0.06}$	213 $^{+27}_{-26}$	238 $^{+32}_{-32}$	3.91 $^{+0.74}_{-0.55} \times 10^{-6}$	0.74 $^{+0.06}_{-0.06}$	-0.60 $^{+0.10}_{-0.10}$	-2.09 $^{+0.07}_{-0.07} \times 10^{-6}$	153 $^{+14}_{-14}$	6.37 $^{+1.76}_{-1.23} \times 10^{-6}$	-25.9	2.6	3.1		
Pulse 2																
18.936~20.502	46.94	0.08 $^{+0.01}_{-0.01}$	-0.91 $^{+0.05}_{-0.05}$	204 $^{+21}_{-21}$	222 $^{+25}_{-25}$	2.52 $^{+0.35}_{-0.30} \times 10^{-6}$	0.52 $^{+0.03}_{-0.03}$	-0.52 $^{+0.10}_{-0.10}$	-2.06 $^{+0.04}_{-0.04} \times 10^{-6}$	129 $^{+11}_{-11}$	4.20 $^{+0.96}_{-0.73} \times 10^{-6}$	-46.0	2.7	2.9		
20.502~21.483	52.56	0.08 $^{+0.00}_{-0.00}$	-1.02 $^{+0.04}_{-0.04}$	328 $^{+37}_{-37}$	433 $^{+38}_{-39}$	4.33 $^{+0.53}_{-0.53} \times 10^{-6}$	0.72 $^{+0.05}_{-0.04}$	-0.67 $^{+0.08}_{-0.04}$	-2.05 $^{+0.04}_{-0.04} \times 10^{-6}$	165 $^{+15}_{-15}$	6.39 $^{+1.32}_{-1.04} \times 10^{-6}$	-30.5	2.8	2.8		
21.483~22.177	60.39	0.11 $^{+0.00}_{-0.00}$	-0.99 $^{+0.03}_{-0.03}$	589 $^{+59}_{-59}$	595 $^{+62}_{-62}$	10.30 $^{+1.18}_{-1.18} \times 10^{-6}$	1.05 $^{+0.05}_{-0.05}$	-0.98 $^{+0.03}_{-0.03}$	-6.45 $^{+2.44}_{-2.44} \times 10^{-6}$	589 $^{+49}_{-49}$	10.42 $^{+1.34}_{-1.22} \times 10^{-6}$	2.2	2.9	3.0		
22.177~22.884	70.65	0.13 $^{+0.00}_{-0.00}$	-0.92 $^{+0.03}_{-0.03}$	606 $^{+52}_{-53}$	655 $^{+59}_{-60}$	13.80 $^{+1.62}_{-1.31} \times 10^{-6}$	0.98 $^{+0.05}_{-0.05}$	-0.83 $^{+0.05}_{-0.05}$	-2.23 $^{+0.13}_{-0.13} \times 10^{-6}$	485 $^{+61}_{-61}$	17.29 $^{+4.02}_{-3.08} \times 10^{-6}$	-20.1	2.9	3.4		
22.884~24.222	80.34	0.12 $^{+0.00}_{-0.00}$	-0.92 $^{+0.02}_{-0.02}$	438 $^{+28}_{-28}$	473 $^{+31}_{-32}$	8.78 $^{+0.73}_{-0.65} \times 10^{-6}$	0.95 $^{+0.03}_{-0.03}$	-0.91 $^{+0.02}_{-0.02}$	-6.57 $^{+2.39}_{-2.36} \times 10^{-6}$	472 $^{+23}_{-23}$	8.85 $^{+0.86}_{-0.70} \times 10^{-6}$	-2.1	3.0	3.1		
24.222~25.773	65.45	0.10 $^{+0.00}_{-0.00}$	-0.83 $^{+0.03}_{-0.03}$	282 $^{+19}_{-19}$	329 $^{+24}_{-24}$	4.83 $^{+0.45}_{-0.41} \times 10^{-6}$	0.65 $^{+0.03}_{-0.03}$	-0.82 $^{+0.03}_{-0.03}$	-6.36 $^{+2.39}_{-2.39} \times 10^{-6}$	329 $^{+16}_{-16}$	4.88 $^{+0.56}_{-0.48} \times 10^{-6}$	2.0	2.9	3.1		
25.773~26.971	47.68	0.10 $^{+0.01}_{-0.01}$	-0.63 $^{+0.04}_{-0.04}$	211 $^{+16}_{-16}$	288 $^{+24}_{-24}$	3.94 $^{+0.32}_{-0.44} \times 10^{-6}$	0.40 $^{+0.03}_{-0.03}$	-0.53 $^{+0.08}_{-0.09}$	-3.16 $^{+0.83}_{-1.30} \times 10^{-6}$	246 $^{+29}_{-25}$	5.03 $^{+1.58}_{-1.30} \times 10^{-6}$	-12.1	2.9	-3.7		
26.971~27.661	43.38	0.11 $^{+0.01}_{-0.01}$	-0.68 $^{+0.05}_{-0.05}$	239 $^{+22}_{-22}$	315 $^{+31}_{-31}$	4.84 $^{+0.78}_{-0.62} \times 10^{-6}$	0.51 $^{+0.04}_{-0.04}$	-0.66 $^{+0.06}_{-0.06}$	-4.23 $^{+1.69}_{-2.70} \times 10^{-6}$	302 $^{+23}_{-23}$	5.43 $^{+1.52}_{-1.08} \times 10^{-6}$	-3.2	2.9	1.0		
27.661~28.468	35.28	0.11 $^{+0.01}_{-0.01}$	-0.56 $^{+0.07}_{-0.07}$	138 $^{+14}_{-14}$	199 $^{+23}_{-23}$	2.51 $^{+0.51}_{-0.44} \times 10^{-6}$	0.35 $^{+0.04}_{-0.04}$	-0.30 $^{+0.13}_{-0.13}$	-2.30 $^{+0.15}_{-0.12} \times 10^{-6}$	151 $^{+14}_{-14}$	3.84 $^{+0.95}_{-0.75} \times 10^{-6}$	-12.6	2.5	3.5		
28.468~30.215	34.96	0.10 $^{+0.01}_{-0.01}$	-0.43 $^{+0.08}_{-0.08}$	98 $^{+9}_{-9}$	154 $^{+16}_{-16}$	1.37 $^{+0.36}_{-0.22} \times 10^{-6}$	0.23 $^{+0.02}_{-0.02}$	-0.10 $^{+0.15}_{-0.15}$	-2.37 $^{+0.15}_{-0.15} \times 10^{-6}$	119 $^{+10}_{-10}$	2.06 $^{+0.82}_{-0.54} \times 10^{-6}$	-14.3	2.5	3.2		
30.215~31.620	20.91	0.07 $^{+0.01}_{-0.01}$	-0.48 $^{+0.13}_{-0.13}$	91 $^{+14}_{-14}$	139 $^{+24}_{-24}$	0.81 $^{+0.31}_{-0.21} \times 10^{-6}$	0.19 $^{+0.03}_{-0.03}$	-0.37 $^{+0.18}_{-0.18} \times 10^{-6}$	125 $^{+14}_{-15}$	0.99 $^{+0.56}_{-0.32} \times 10^{-6}$	-3.7	1.1	0.3			
31.620~35.736	22.03	0.05 $^{+0.01}_{-0.01}$	-0.35 $^{+0.14}_{-0.14}$	76 $^{+11}_{-10}$	125 $^{+21}_{-20}$	0.44 $^{+0.16}_{-0.11} \times 10^{-6}$	0.10 $^{+0.02}_{-0.02}$	0.04 $^{+0.24}_{-0.24}$	-2.35 $^{+0.20}_{-0.16} \times 10^{-6}$	97 $^{+10}_{-11}$	0.73 $^{+0.41}_{-0.24} \times 10^{-6}$	-13.2	0.5	2.6		

Note—All columns are the same as Table A2 but for GRB 180113418.

Table A38. Time-resolved Spectral Fit Results of GRB 180120207

$t_{\text{start}} \sim t_{\text{stop}}$	S	Cutoff Power-Law Fitting						Band Fitting						Difference		
		K	α	E_c	E_p	F	K	α	β	E_p	F	ΔDIC	$p_{\text{DIC}}^{\text{GPI}}$	$p_{\text{DIC}}^{\text{Band}}$		
(1)	(2)	(3)	(4)	(5)	(6)	(7)	(8)	(9)	(10)	(11)	(12)	(13)	(14)	(15)		
Pulse 1																
0.208~0.741	24.77	$0.08^{+0.01}_{-0.01}$	$-0.48^{+0.10}_{-0.10}$	148^{+21}_{-22}	224^{+35}_{-36}	$2.00^{+0.63}_{-0.43} \times 10^{-6}$	$0.24^{+0.03}_{-0.03}$	$-0.48^{+0.11}_{-0.11}$	$-6.00^{+0.64}_{-0.67} \times 10^{-6}$	1.5	2.2	2.8				
0.741~1.314	36.99	$0.13^{+0.01}_{-0.01}$	$-0.57^{+0.07}_{-0.07}$	144^{+15}_{-15}	206^{+23}_{-23}	$3.13^{+0.50}_{-0.50} \times 10^{-6}$	$0.47^{+0.04}_{-0.04}$	$-0.53^{+0.08}_{-0.08}$	$-5.12^{+2.41}_{-3.06}$	198^{+16}_{-16}	$3.38^{+0.90}_{-0.73} \times 10^{-6}$	-1.2	2.6	1.6		
1.314~1.928	52.18	$0.17^{+0.01}_{-0.01}$	$-0.68^{+0.05}_{-0.05}$	151^{+12}_{-12}	199^{+18}_{-18}	$4.21^{+0.47}_{-0.47} \times 10^{-6}$	$0.82^{+0.05}_{-0.05}$	$-0.64^{+0.07}_{-0.07}$	$-4.79^{+2.10}_{-2.90}$	189^{+14}_{-16}	$4.56^{+1.13}_{-0.78} \times 10^{-6}$	-1.7	2.8	1.1		
1.928~3.676	97.84	$0.16^{+0.01}_{-0.01}$	$-0.87^{+0.03}_{-0.03}$	190^{+10}_{-10}	214^{+12}_{-12}	$4.84^{+0.31}_{-0.31} \times 10^{-6}$	$1.12^{+0.04}_{-0.04}$	$-0.82^{+0.04}_{-0.04}$	$-2.80^{+0.28}_{-0.28}$	195^{+10}_{-10}	$5.71^{+0.64}_{-0.64} \times 10^{-6}$	-8.6	2.9	3.5		
3.676~4.912	69.47	$0.13^{+0.01}_{-0.01}$	$-0.97^{+0.04}_{-0.04}$	157^{+11}_{-11}	162^{+13}_{-13}	$3.32^{+0.39}_{-0.39} \times 10^{-6}$	$1.21^{+0.05}_{-0.05}$	$-0.88^{+0.07}_{-0.07}$	$-2.94^{+0.58}_{-0.69}$	141^{+14}_{-13}	$4.12^{+0.88}_{-0.78} \times 10^{-6}$	-9.6	2.8	-1.1		
4.912~6.041	57.28	$0.09^{+0.01}_{-0.01}$	$-1.14^{+0.04}_{-0.04}$	204^{+20}_{-20}	175^{+19}_{-19}	$2.73^{+0.35}_{-0.35} \times 10^{-6}$	$1.19^{+0.05}_{-0.05}$	$-1.14^{+0.04}_{-0.04}$	$-6.77^{+2.16}_{-2.16}$	175^{+10}_{-10}	$2.77^{+0.26}_{-0.26} \times 10^{-6}$	3.0	2.8	3.2		
6.041~9.832	83.58	$0.08^{+0.00}_{-0.00}$	$-1.11^{+0.03}_{-0.03}$	150^{+9}_{-9}	134^{+9}_{-9}	$1.98^{+0.17}_{-0.17} \times 10^{-6}$	$1.04^{+0.03}_{-0.03}$	$-1.10^{+0.03}_{-0.03}$	$-5.25^{+2.10}_{-2.10}$	133^{+5}_{-5}	$2.03^{+0.15}_{-0.15} \times 10^{-6}$	0.2	2.9	2.1		
9.832~10.892	37.20	$0.08^{+0.01}_{-0.01}$	$-1.04^{+0.08}_{-0.08}$	106^{+14}_{-14}	102^{+16}_{-16}	$1.38^{+0.31}_{-0.24} \times 10^{-6}$	$0.99^{+0.01}_{-0.01}$	$-1.02^{+0.08}_{-0.08}$	$-6.22^{+2.73}_{-2.73}$	100^{+7}_{-7}	$1.40^{+0.36}_{-0.36} \times 10^{-6}$	0.2	2.1	2.4		
10.892~12.155	31.48	$0.08^{+0.02}_{-0.02}$	$-0.97^{+0.11}_{-0.11}$	73^{+11}_{-12}	75^{+14}_{-15}	$0.83^{+0.28}_{-0.22} \times 10^{-6}$	$0.66^{+0.05}_{-0.05}$	$-0.60^{+0.31}_{-0.34}$	$-3.37^{+0.98}_{-0.98}$	61^{+11}_{-10}	$0.95^{+0.44}_{-0.44} \times 10^{-6}$	-9.8	0.2	-6.3		
12.155~14.586	29.65	$0.08^{+0.02}_{-0.02}$	$-0.98^{+0.12}_{-0.12}$	51^{+7}_{-10}	52^{+9}_{-10}	$0.58^{+0.22}_{-0.15} \times 10^{-6}$	$0.70^{+0.03}_{-0.04}$	$-0.94^{+0.14}_{-0.14}$	$-5.76^{+2.53}_{-2.82}$	51^{+3}_{-3}	$0.58^{+0.06}_{-0.05} \times 10^{-6}$	5.1	-1.2	2.4		
Pulse 2																
14.586~15.500	33.74	$0.36^{+0.12}_{-0.12}$	$-0.62^{+0.16}_{-0.15}$	31^{+4}_{-5}	43^{+7}_{-7}	$0.96^{+0.54}_{-0.32} \times 10^{-6}$	$1.42^{+0.08}_{-0.08}$	$-0.61^{+0.16}_{-0.17}$	$-5.95^{+2.61}_{-2.61}$	42^{+2}_{-2}	$0.95^{+0.08}_{-0.08} \times 10^{-6}$	10.1	-6.9	2.6		
15.500~16.992	66.20	$0.07^{+0.01}_{-0.01}$	$-1.50^{+0.05}_{-0.05}$	137^{+18}_{-18}	69^{+11}_{-11}	$2.21^{+0.31}_{-0.29} \times 10^{-6}$	$2.44^{+0.13}_{-0.13}$	$-0.43^{+0.21}_{-0.22}$	$-2.27^{+0.04}_{-0.04}$	37^{+3}_{-3}	$2.62^{+0.40}_{-0.40} \times 10^{-6}$	-59.8	2.2	2.9		
16.992~17.787	59.25	$0.09^{+0.01}_{-0.01}$	$-1.28^{+0.04}_{-0.04}$	282^{+35}_{-35}	203^{+27}_{-28}	$3.72^{+0.46}_{-0.37} \times 10^{-6}$	$1.70^{+0.04}_{-0.06}$	$-1.28^{+0.04}_{-0.04}$	$-6.23^{+2.60}_{-2.59}$	199^{+15}_{-15}	$3.71^{+0.38}_{-0.38} \times 10^{-6}$	2.6	2.8	2.9		
17.787~18.292	58.65	$0.14^{+0.01}_{-0.01}$	$-1.07^{+0.04}_{-0.04}$	205^{+20}_{-20}	190^{+20}_{-20}	$4.69^{+0.58}_{-0.52} \times 10^{-6}$	$1.69^{+0.08}_{-0.08}$	$-1.07^{+0.04}_{-0.04}$	$-6.69^{+2.28}_{-2.28}$	190^{+11}_{-12}	$4.68^{+0.47}_{-0.38} \times 10^{-6}$	2.5	2.8	3.0		
18.292~19.997	90.02	$0.15^{+0.01}_{-0.01}$	$-0.93^{+0.03}_{-0.03}$	182^{+9}_{-10}	195^{+12}_{-12}	$4.24^{+0.32}_{-0.27} \times 10^{-6}$	$1.25^{+0.03}_{-0.03}$	$-0.93^{+0.03}_{-0.03}$	$-7.01^{+2.69}_{-2.69}$	194^{+6}_{-6}	$4.27^{+0.27}_{-0.23} \times 10^{-6}$	2.3	2.9	3.1		
19.998~23.713	117.64	$0.15^{+0.01}_{-0.01}$	$-0.91^{+0.02}_{-0.02}$	141^{+6}_{-6}	154^{+7}_{-7}	$3.28^{+0.19}_{-0.18} \times 10^{-6}$	$1.20^{+0.03}_{-0.03}$	$-0.91^{+0.02}_{-0.02}$	$-6.38^{+2.60}_{-2.51}$	153^{+4}_{-4}	$3.32^{+0.19}_{-0.17} \times 10^{-6}$	1.6	3.0	2.9		
23.713~24.293	37.89	$0.11^{+0.01}_{-0.01}$	$-1.07^{+0.08}_{-0.08}$	109^{+14}_{-14}	101^{+16}_{-15}	$1.89^{+0.39}_{-0.30} \times 10^{-6}$	$1.25^{+0.07}_{-0.07}$	$-1.07^{+0.08}_{-0.08}$	$-6.56^{+2.30}_{-2.34}$	100^{+6}_{-6}	$1.89^{+0.21}_{-0.19} \times 10^{-6}$	3.0	3.1			
24.293~25.259	33.04	$0.06^{+0.01}_{-0.01}$	$-1.24^{+0.09}_{-0.09}$	104^{+17}_{-16}	79^{+16}_{-16}	$1.22^{+0.30}_{-0.25} \times 10^{-6}$	$1.10^{+0.06}_{-0.06}$	$-1.24^{+0.08}_{-0.08}$	$-6.51^{+2.34}_{-2.36}$	78^{+5}_{-5}	$1.21^{+0.12}_{-0.09} \times 10^{-6}$	4.0	1.6	3.0		
25.259~26.222	22.81	$0.04^{+0.01}_{-0.01}$	$-1.34^{+0.17}_{-0.17}$	90^{+27}_{-28}	60^{+23}_{-24}	$0.78^{+0.42}_{-0.28} \times 10^{-6}$	$0.90^{+0.07}_{-0.07}$	$-1.12^{+0.34}_{-0.34}$	$-4.77^{+2.33}_{-2.33}$	50^{+8}_{-8}	$0.79^{+0.27}_{-0.27} \times 10^{-6}$	7.7	-8.5	-2.2		
26.222~36.400	40.47	$0.02^{+0.00}_{-0.00}$	$-1.46^{+0.08}_{-0.08}$	95^{+15}_{-15}	51^{+11}_{-11}	$0.47^{+0.10}_{-0.10} \times 10^{-6}$	$0.58^{+0.02}_{-0.02}$	$-1.39^{+0.10}_{-0.10}$	$-4.54^{+1.90}_{-3.04}$	48^{+3}_{-3}	$0.47^{+0.06}_{-0.04} \times 10^{-6}$	0.1	0.9	0.3		

Note—All columns are the same as Table A2 but for GRB 180120207.

Table A39. Time-resolved Spectral Fit Results of GRB 180722993

$t_{\text{start}} \sim t_{\text{stop}}$	S	Cutoff Power-Law Fitting				Band Fitting				Difference				
		K	α	E_{c}	E_{p}	F	K	α	β	E_{p}	F	ΔDIC	$p_{\text{DIC}}^{\text{CPL}}$	$p_{\text{DIC}}^{\text{Band}}$
(1)	(2)	(3)	(4)	(5)	(6)	(7)	(8)	(9)	(10)	(11)	(12)	(13)	(14)	(15)
Pulse 1														
2.398~5.905	20.66	$0.11^{+0.03}_{-0.03}$	$0.68^{+0.21}_{-0.21}$	5^{+6}_{-6}	147^{+21}_{-21}	$0.51^{+0.25}_{-0.21} \times 10^{-6}$	$0.02^{+0.01}_{-0.01}$	$0.72^{+0.21}_{-0.21}$	$-4.39^{+1.66}_{-1.66}$	140^{+9}_{-9}	$0.59^{+0.31}_{-0.22} \times 10^{-6}$	-4.6	-0.1	-0.0
5.905~6.967	20.15	$0.17^{+0.05}_{-0.05}$	$0.35^{+0.25}_{-0.24}$	58^{+8}_{-9}	135^{+25}_{-25}	$0.84^{+0.52}_{-0.31} \times 10^{-6}$	$0.08^{+0.02}_{-0.02}$	$0.31^{+0.27}_{-0.27}$	$-6.54^{+2.32}_{-2.37}$	133^{+9}_{-9}	$0.82^{+0.50}_{-0.29} \times 10^{-6}$	3.3	-1.8	1.8
6.967~10.468	46.30	$0.39^{+0.07}_{-0.06}$	$0.54^{+0.12}_{-0.12}$	42^{+3}_{-3}	106^{+8}_{-8}	$0.92^{+0.24}_{-0.19} \times 10^{-6}$	$0.11^{+0.01}_{-0.01}$	$0.63^{+0.15}_{-0.14}$	$-4.32^{+0.99}_{-0.86}$	103^{+3}_{-3}	$0.98^{+0.27}_{-0.21} \times 10^{-6}$	-5.6	1.8	2.0
10.468~13.314	30.97	$0.78^{+0.21}_{-0.20}$	$0.76^{+0.16}_{-0.16}$	27^{+2}_{-2}	74^{+7}_{-7}	$0.52^{+0.24}_{-0.14} \times 10^{-6}$	$0.13^{+0.02}_{-0.02}$	$0.76^{+0.16}_{-0.16}$	$-6.47^{+2.16}_{-2.34}$	74^{+2}_{-2}	$0.53^{+0.11}_{-0.10} \times 10^{-6}$	0.1	0.7	2.5
13.314~18.409	29.31	$1.05^{+0.51}_{-0.45}$	$0.56^{+0.24}_{-0.23}$	19^{+2}_{-2}	49^{+7}_{-7}	$0.30^{+0.25}_{-0.13} \times 10^{-6}$	$1.22^{+0.61}_{-0.57}$	$0.62^{+0.24}_{-0.25}$	$-5.72^{+1.87}_{-2.41}$	47^{+2}_{-2}	$0.31^{+0.28}_{-0.15} \times 10^{-6}$	2.5	-12.0	-8.5
Pulse 2														
35.587~37.363	24.83	$0.04^{+0.01}_{-0.01}$	$-0.61^{+0.14}_{-0.14}$	135^{+25}_{-26}	188^{+40}_{-41}	$0.90^{+0.40}_{-0.28} \times 10^{-6}$	$0.17^{+0.03}_{-0.03}$	$-0.58^{+0.15}_{-0.16}$	$-5.48^{+2.80}_{-3.06}$	178^{+22}_{-22}	$0.98^{+0.48}_{-0.30} \times 10^{-6}$	1.7	0.8	1.8
37.363~41.686	49.01	$0.07^{+0.01}_{-0.01}$	$-0.46^{+0.07}_{-0.07}$	109^{+9}_{-9}	167^{+16}_{-16}	$1.17^{+0.26}_{-0.16} \times 10^{-6}$	$0.21^{+0.02}_{-0.02}$	$-0.44^{+0.08}_{-0.08}$	$-5.83^{+2.61}_{-2.73}$	165^{+9}_{-8}	$1.20^{+0.27}_{-0.20} \times 10^{-6}$	0.9	2.6	2.8
41.686~45.793	55.14	$0.13^{+0.01}_{-0.01}$	$-0.37^{+0.08}_{-0.08}$	73^{+5}_{-5}	120^{+11}_{-10}	$1.09^{+0.19}_{-0.16} \times 10^{-6}$	$0.29^{+0.02}_{-0.02}$	$-0.34^{+0.09}_{-0.09}$	$-5.67^{+2.42}_{-2.80}$	117^{+5}_{-5}	$1.11^{+0.21}_{-0.16} \times 10^{-6}$	-0.2	2.4	2.1
45.793~50.716	44.91	$0.12^{+0.02}_{-0.02}$	$-0.36^{+0.10}_{-0.10}$	55^{+5}_{-5}	90^{+9}_{-10}	$0.65^{+0.17}_{-0.13} \times 10^{-6}$	$0.29^{+0.02}_{-0.02}$	$-0.36^{+0.11}_{-0.11}$	$-6.34^{+2.31}_{-2.42}$	88^{+3}_{-3}	$0.66^{+0.10}_{-0.08} \times 10^{-6}$	1.5	1.9	2.8
50.716~55.609	30.27	$0.08^{+0.02}_{-0.02}$	$-0.60^{+0.16}_{-0.16}$	48^{+7}_{-7}	67^{+12}_{-12}	$0.37^{+0.19}_{-0.11} \times 10^{-6}$	$0.31^{+0.03}_{-0.03}$	$-0.59^{+0.16}_{-0.17}$	$-6.25^{+2.45}_{-2.48}$	65^{+4}_{-4}	$0.38^{+0.07}_{-0.05} \times 10^{-6}$	5.7	-1.5	3.0

Note—All columns are the same as Table A2 but for GRB 180722993.

Table A40. Time-resolved Spectral Fit Results of GRB 190114873

$t_{\text{start}} \sim t_{\text{stop}}$	S	Cutoff Power-Law Fitting						Band Fitting						Difference	
		K	α	E_c	E_p	F	K	α	β	E_p	F	ΔDIC	$p_{\text{DIC}}^{\text{CPL}}$	$p_{\text{DIC}}^{\text{Band}}$	
(1)	(2)	(3)	(4)	(5)	(6)	(7)	(8)	(9)	(10)	(11)	(12)	(13)	(14)	(15)	
Pulse 1															
0.092~0.240	33.05	$0.10^{+0.01}_{-0.01}$	$-1.20^{+0.05}_{-0.05}$	1481^{+478}_{-484}	1185^{+390}_{-394}	$15.65^{+5.48}_{-3.48} \times 10^{-6}$	$0.12^{+0.00}_{-0.02}$	$-1.14^{+0.03}_{-0.09}$	$5.64^{+2.90}_{-2.93}$	895^{+283}_{-220}	$16.07^{+8.71}_{-4.30} \times 10^{-6}$	-10.2	2.4	-7.7	
0.240~0.429	60.49	$0.26^{+0.01}_{-0.01}$	$-0.91^{+0.04}_{-0.04}$	497^{+55}_{-55}	542^{+63}_{-63}	$22.62^{+3.10}_{-3.04} \times 10^{-6}$	$0.26^{+0.01}_{-0.01}$	$-0.91^{+0.04}_{-0.04}$	$-5.53^{+2.69}_{-2.47}$	$23.28^{+3.81}_{-3.81} \times 10^{-6}$	-0.9	2.9	2.5		
0.429~0.499	51.56	$0.43^{+0.02}_{-0.02}$	$-0.81^{+0.05}_{-0.05}$	429^{+52}_{-53}	511^{+66}_{-67}	$35.49^{+7.04}_{-5.13} \times 10^{-6}$	$0.44^{+0.02}_{-0.02}$	$-0.80^{+0.05}_{-0.05}$	$-6.41^{+2.50}_{-2.51}$	$36.25^{+5.50}_{-4.60} \times 10^{-6}$	0.1	2.9	3.0		
0.499~0.632	83.75	$0.60^{+0.02}_{-0.02}$	$-0.64^{+0.03}_{-0.03}$	335^{+21}_{-22}	456^{+31}_{-31}	$44.41^{+4.65}_{-4.13} \times 10^{-6}$	$0.60^{+0.02}_{-0.02}$	$-0.64^{+0.03}_{-0.03}$	$-6.43^{+2.39}_{-2.41}$	452^{+22}_{-21}	$44.78^{+3.67}_{-3.43} \times 10^{-6}$	0.3	2.9	3.1	
0.632~0.745	89.17	$0.75^{+0.03}_{-0.03}$	$-0.64^{+0.03}_{-0.03}$	332^{+21}_{-21}	452^{+30}_{-31}	$54.82^{+5.83}_{-4.89} \times 10^{-6}$	$0.78^{+0.03}_{-0.03}$	$-0.61^{+0.04}_{-0.04}$	$-3.58^{+0.55}_{-0.55}$	430^{+25}_{-24}	$60.28^{+8.17}_{-7.05} \times 10^{-6}$	-7.6	2.9	1.0	
0.745~1.598	261.45	$0.79^{+0.01}_{-0.01}$	$-0.67^{+0.01}_{-0.01}$	444^{+9}_{-9}	591^{+13}_{-13}	$81.93^{+2.69}_{-2.55} \times 10^{-6}$	$0.79^{+0.01}_{-0.01}$	$-0.67^{+0.01}_{-0.01}$	$-6.49^{+2.00}_{-2.07}$	592^{+9}_{-9}	$82.40^{+2.03}_{-1.87} \times 10^{-6}$	-0.8	3.0	2.6	
1.598~1.680	95.55	$0.83^{+0.02}_{-0.02}$	$-0.45^{+0.03}_{-0.03}$	558^{+28}_{-28}	864^{+47}_{-47}	$169.00^{+16.41}_{-14.74} \times 10^{-6}$	$0.83^{+0.02}_{-0.02}$	$-0.45^{+0.03}_{-0.03}$	$-6.50^{+2.04}_{-2.03}$	859^{+31}_{-32}	$169.50^{+12.54}_{-10.14} \times 10^{-6}$	-0.5	3.0	2.9	
1.680~1.800	102.04	$0.86^{+0.02}_{-0.02}$	$-0.53^{+0.03}_{-0.03}$	368^{+18}_{-18}	541^{+29}_{-29}	$83.04^{+7.59}_{-6.28} \times 10^{-6}$	$0.87^{+0.02}_{-0.02}$	$-0.53^{+0.03}_{-0.03}$	$-6.33^{+2.44}_{-2.51}$	537^{+20}_{-19}	$83.63^{+6.29}_{-4.72} \times 10^{-6}$	-0.3	3.0	2.9	
1.800~1.944	85.11	$0.63^{+0.03}_{-0.03}$	$-0.80^{+0.04}_{-0.04}$	252^{+19}_{-19}	302^{+25}_{-25}	$28.16^{+2.79}_{-2.39} \times 10^{-6}$	$0.98^{+0.14}_{-0.14}$	$-0.54^{+0.08}_{-0.08}$	$-2.14^{+0.08}_{-0.08}$	196^{+21}_{-20}	$42.14^{+10.36}_{-8.78} \times 10^{-6}$	-27.0	2.9	2.2	
1.944~2.154	71.60	$0.31^{+0.01}_{-0.01}$	$-1.01^{+0.03}_{-0.03}$	370^{+37}_{-37}	366^{+39}_{-38}	$18.19^{+2.29}_{-1.76} \times 10^{-6}$	$0.32^{+0.01}_{-0.01}$	$-1.01^{+0.03}_{-0.03}$	$-6.45^{+2.42}_{-2.45}$	363^{+27}_{-27}	$18.45^{+1.59}_{-1.59} \times 10^{-6}$	0.2	2.9	3.0	
2.154~2.415	62.49	$0.24^{+0.01}_{-0.01}$	$-1.03^{+0.04}_{-0.04}$	308^{+34}_{-34}	299^{+35}_{-35}	$11.69^{+1.57}_{-1.31} \times 10^{-6}$	$0.25^{+0.02}_{-0.02}$	$-1.02^{+0.04}_{-0.04}$	$-6.19^{+2.62}_{-2.60}$	294^{+26}_{-25}	$11.85^{+1.64}_{-1.31} \times 10^{-6}$	0.4	2.8	3.0	
Pulse 2															
2.415~2.450	33.45	$0.30^{+0.02}_{-0.02}$	$-0.97^{+0.06}_{-0.06}$	952^{+246}_{-252}	981^{+260}_{-266}	$44.56^{+18.22}_{-11.29} \times 10^{-6}$	$0.30^{+0.02}_{-0.02}$	$-0.96^{+0.06}_{-0.06}$	$-5.13^{+2.50}_{-2.58}$	927^{+201}_{-202}	$47.26^{+13.69}_{-9.93} \times 10^{-6}$	-1.2	2.3	2.1	
2.450~2.482	48.67	$0.60^{+0.03}_{-0.03}$	$-0.45^{+0.05}_{-0.05}$	534^{+55}_{-55}	827^{+89}_{-89}	$112.80^{+29}_{-25} \times 10^{-6}$	$0.60^{+0.03}_{-0.03}$	$-0.45^{+0.05}_{-0.05}$	$-6.81^{+2.20}_{-2.20}$	817^{+62}_{-63}	$114.00^{+11.53}_{-13.71} \times 10^{-6}$	0.5	2.9	3.1	
2.482~2.641	145.33	$0.99^{+0.01}_{-0.01}$	$-0.35^{+0.02}_{-0.02}$	468^{+15}_{-15}	772^{+27}_{-27}	$182.60^{+13.08}_{-11.31} \times 10^{-6}$	$1.00^{+0.01}_{-0.01}$	$-0.35^{+0.02}_{-0.02}$	$-6.93^{+2.03}_{-2.03}$	770^{+18}_{-18}	$183.60^{+7.40}_{-8.00} \times 10^{-6}$	-0.2	3.1	3.0	
2.641~2.863	132.23	$0.65^{+0.01}_{-0.01}$	$-0.50^{+0.02}_{-0.02}$	545^{+21}_{-20}	818^{+33}_{-32}	$116.40^{+8.80}_{-7.48} \times 10^{-6}$	$0.66^{+0.01}_{-0.01}$	$-0.50^{+0.02}_{-0.02}$	$-5.11^{+1.43}_{-1.43}$	811^{+22}_{-23}	$119.50^{+6.60}_{-6.27} \times 10^{-6}$	-3.4	3.0	2.3	
2.863~3.112	113.45	$0.45^{+0.01}_{-0.01}$	$-0.53^{+0.02}_{-0.02}$	698^{+29}_{-29}	1026^{+45}_{-45}	$110.60^{+8.35}_{-7.49} \times 10^{-6}$	$0.45^{+0.01}_{-0.01}$	$-0.53^{+0.02}_{-0.02}$	$-5.86^{+1.91}_{-2.44}$	1020^{+33}_{-34}	$112.20^{+6.47}_{-5.90} \times 10^{-6}$	-1.9	3.0	2.4	
3.112~3.213	87.15	$0.50^{+0.01}_{-0.01}$	$-0.47^{+0.03}_{-0.03}$	856^{+56}_{-55}	1309^{+89}_{-87}	$189.20^{+24.85}_{-19.46} \times 10^{-6}$	$0.52^{+0.01}_{-0.01}$	$-0.40^{+0.03}_{-0.03}$	$-2.78^{+0.13}_{-0.13}$	1107^{+53}_{-52}	$197.80^{+18.71}_{-16.94} \times 10^{-6}$	-55.6	3.0	4.0	
3.213~3.749	167.25	$0.45^{+0.00}_{-0.00}$	$-0.35^{+0.01}_{-0.01}$	622^{+17}_{-17}	1027^{+29}_{-28}	$129.90^{+7.64}_{-7.24} \times 10^{-6}$	$0.45^{+0.00}_{-0.00}$	$-0.34^{+0.01}_{-0.01}$	$-2.93^{+0.08}_{-0.08}$	982^{+20}_{-20}	$145.80^{+5.88}_{-6.21} \times 10^{-6}$	-110.3	3.0	3.9	
3.749~3.955	136.08	$0.64^{+0.01}_{-0.01}$	$-0.20^{+0.02}_{-0.02}$	532^{+18}_{-18}	958^{+34}_{-34}	$195.60^{+16.39}_{-13.48} \times 10^{-6}$	$0.66^{+0.01}_{-0.01}$	$-0.15^{+0.02}_{-0.02}$	$-2.70^{+0.07}_{-0.07}$	877^{+23}_{-23}	$228.90^{+13.21}_{-13.26} \times 10^{-6}$	-172.1	3.0	4.0	
3.955~4.010	89.93	$0.09^{+0.03}_{-0.03}$	$-0.18^{+0.04}_{-0.04}$	392^{+20}_{-20}	714^{+40}_{-39}	$195.20^{+23.23}_{-20.75} \times 10^{-6}$	$1.12^{+0.03}_{-0.03}$	$-0.15^{+0.04}_{-0.04}$	$-3.10^{+0.21}_{-0.20}$	674^{+27}_{-26}	$217.10^{+20.57}_{-17.98} \times 10^{-6}$	-18.1	2.9	4.0	
4.010~4.130	114.02	$0.88^{+0.02}_{-0.02}$	$-0.19^{+0.03}_{-0.03}$	392^{+14}_{-14}	709^{+28}_{-28}	$156.30^{+13.48}_{-11.63} \times 10^{-6}$	$0.88^{+0.02}_{-0.02}$	$-0.19^{+0.03}_{-0.03}$	$-5.22^{+1.59}_{-2.37}$	707^{+18}_{-18}	$161.00^{+9.01}_{-9.13} \times 10^{-6}$	-3.5	3.0	2.0	
4.130~4.438	160.69	$0.87^{+0.01}_{-0.01}$	$-0.45^{+0.02}_{-0.02}$	349^{+10}_{-10}	541^{+18}_{-18}	$85.66^{+4.52}_{-4.35} \times 10^{-6}$	$0.87^{+0.01}_{-0.01}$	$-0.45^{+0.02}_{-0.02}$	$-4.03^{+0.72}_{-0.43}$	534^{+12}_{-12}	$90.14^{+5.08}_{-4.44} \times 10^{-6}$	-6.5	3.0	2.4	
4.438~4.564	91.62	$0.67^{+0.02}_{-0.02}$	$-0.78^{+0.03}_{-0.03}$	413^{+26}_{-27}	504^{+35}_{-35}	$55.40^{+5.53}_{-5.11} \times 10^{-6}$	$0.67^{+0.02}_{-0.02}$	$-0.78^{+0.03}_{-0.02}$	$-6.02^{+2.57}_{-2.66}$	504^{+24}_{-24}	$56.64^{+4.89}_{-3.90} \times 10^{-6}$	-0.6	2.9	2.7	
4.564~4.760	126.24	$0.72^{+0.01}_{-0.01}$	$-0.62^{+0.02}_{-0.02}$	512^{+21}_{-21}	707^{+31}_{-32}	$97.41^{+7.03}_{-6.08} \times 10^{-6}$	$0.72^{+0.01}_{-0.01}$	$-0.62^{+0.02}_{-0.02}$	$-6.72^{+2.07}_{-2.07}$	708^{+22}_{-22}	$98.43^{+4.97}_{-4.41} \times 10^{-6}$	-0.1	3.0	3.1	
4.760~4.957	140.75	$0.98^{+0.02}_{-0.02}$	$-0.46^{+0.02}_{-0.02}$	345^{+12}_{-12}	532^{+20}_{-19}	$94.02^{+5.78}_{-5.22} \times 10^{-6}$	$0.99^{+0.02}_{-0.02}$	$-0.46^{+0.02}_{-0.02}$	$-7.42^{+1.83}_{-1.81}$	530^{+13}_{-12}	$93.92^{+4.08}_{-4.10} \times 10^{-6}$	0.5	3.0	3.2	
4.957~5.304	150.03	$0.65^{+0.01}_{-0.01}$	$-0.64^{+0.02}_{-0.02}$	460^{+16}_{-16}	626^{+23}_{-23}	$73.09^{+4.15}_{-3.80} \times 10^{-6}$	$0.65^{+0.01}_{-0.01}$	$-0.64^{+0.02}_{-0.02}$	$-7.24^{+1.86}_{-1.86}$	624^{+16}_{-16}	$73.42^{+3.07}_{-2.63} \times 10^{-6}$	0.4	2.9	3.1	

Table A40 *continued on next page*

Table A40 (continued)

$t_{\text{start}} \sim t_{\text{stop}}$	S	Cutoff Power-Law Fitting						Band Fitting						Difference
		K	α	E_c	E_p	F	K	α	β	E_p	F	ΔDIC	$p_{\text{DIC}}^{\text{CPL}}$	$p_{\text{DIC}}^{\text{Band}}$
(1)	(2)	(3)	(4)	(5)	(6)	(7)	(8)	(9)	(10)	(11)	(12)	(13)	(14)	(15)
5.304~5.617	158.91	$0.90^{+0.02}_{-0.02}$	$-0.52^{+0.02}_{-0.02}$	302^{+10}_{-10}	447^{+15}_{-15}	$65.34^{+3.69}_{-3.65} \times 10^{-6}$	$0.90^{+0.02}_{-0.02}$	$-0.52^{+0.02}_{-0.02}$	$-5.58^{+1.90}_{-2.53}$	444^{+10}_{-10}	$66.45^{+3.64}_{-2.92} \times 10^{-6}$	-2.0	3.0	2.2
5.617~5.711	72.87	$1.08^{+0.08}_{-0.08}$	$-0.60^{+0.05}_{-0.05}$	134^{+10}_{-10}	188^{+15}_{-15}	$22.87^{+3.07}_{-2.68} \times 10^{-6}$	$1.15^{+0.11}_{-0.11}$	$-0.56^{+0.06}_{-0.06}$	$-4.10^{+1.23}_{-1.69}$	180^{+10}_{-10}	$25.04^{+4.35}_{-3.65} \times 10^{-6}$	-4.9	2.8	1.4
5.711~5.833	66.58	$0.50^{+0.04}_{-0.04}$	$-1.02^{+0.05}_{-0.05}$	202^{+24}_{-24}	198^{+25}_{-25}	$15.90^{+2.28}_{-2.04} \times 10^{-6}$	$0.67^{+0.08}_{-0.08}$	$-0.87^{+0.07}_{-0.07}$	$-2.33^{+0.13}_{-0.12}$	152^{+14}_{-14}	$21.89^{+4.72}_{-4.10} \times 10^{-6}$	-16.9	2.7	3.5
5.833~5.996	53.72	$0.20^{+0.02}_{-0.02}$	$-1.46^{+0.07}_{-0.07}$	311^{+75}_{-75}	168^{+46}_{-48}	$8.88^{+1.82}_{-1.38} \times 10^{-6}$	$0.47^{+0.21}_{-0.18}$	$-1.08^{+0.21}_{-0.19}$	$-2.07^{+0.09}_{-0.09}$	82^{+19}_{-19}	$13.34^{+0.40}_{-0.33} \times 10^{-6}$	-54.3	1.4	-33.9
5.996~6.078	73.79	$0.10^{+0.01}_{-0.01}$	$-1.65^{+0.04}_{-0.04}$	363^{+73}_{-75}	127^{+29}_{-29}	$5.34^{+0.64}_{-0.53} \times 10^{-6}$	$0.15^{+0.03}_{-0.03}$	$-1.46^{+0.10}_{-0.10}$	$-2.17^{+0.08}_{-0.07}$	77^{+13}_{-13}	$6.98^{+2.43}_{-1.81} \times 10^{-6}$	-18.8	2.2	-2.9
6.678~7.463	57.16	$0.05^{+0.00}_{-0.00}$	$-1.72^{+0.02}_{-0.02}$	554^{+37}_{-39}	155^{+15}_{-16}	$3.72^{+0.15}_{-0.17} \times 10^{-6}$	$0.06^{+0.01}_{-0.01}$	$-1.75^{+0.02}_{-0.02}$	$-4.94^{+2.73}_{-2.71}$	229^{+57}_{-43}	$4.39^{+1.16}_{-0.70} \times 10^{-6}$	-48.8	2.1	-40.3
7.463~8.661	53.81	$0.04^{+0.00}_{-0.00}$	$-1.73^{+0.02}_{-0.02}$	531^{+54}_{-54}	143^{+18}_{-18}	$2.81^{+0.15}_{-0.14} \times 10^{-6}$	$0.04^{+0.00}_{-0.00}$	$-1.79^{+0.04}_{-0.04}$	$-4.48^{+2.41}_{-2.38}$	206^{+65}_{-65}	$3.45^{+0.71}_{-0.61} \times 10^{-6}$	-8.4	2.1	-0.6
8.661~11.337	60.73	$0.03^{+0.00}_{-0.00}$	$-1.80^{+0.02}_{-0.02}$	549^{+40}_{-40}	110^{+14}_{-14}	$2.02^{+0.08}_{-0.07} \times 10^{-6}$	$0.02^{+0.00}_{-0.00}$	$-1.87^{+0.03}_{-0.03}$	$-4.30^{+2.26}_{-2.12}$	210^{+68}_{-68}	$2.61^{+0.42}_{-0.36} \times 10^{-6}$	-15.9	2.2	-1.0
11.337~15.528	54.03	$0.02^{+0.00}_{-0.00}$	$-1.88^{+0.03}_{-0.03}$	467^{+93}_{-95}	56^{+18}_{-18}	$1.40^{+0.13}_{-0.10} \times 10^{-6}$	$0.02^{+0.00}_{-0.00}$	$-1.90^{+0.05}_{-0.06}$	$-4.88^{+2.55}_{-2.75}$	58^{+11}_{-17}	$1.56^{+0.47}_{-0.37} \times 10^{-6}$	-1.5	2.2	0.8
Pulse 3														
15.656~15.947	39.86	$0.09^{+0.01}_{-0.01}$	$-1.41^{+0.07}_{-0.07}$	409^{+113}_{-120}	241^{+73}_{-76}	$4.84^{+1.17}_{-0.87} \times 10^{-6}$	$0.10^{+0.02}_{-0.02}$	$-1.36^{+0.10}_{-0.10}$	$-4.64^{+2.42}_{-2.84}$	204^{+51}_{-57}	$5.17^{+2.19}_{-1.40} \times 10^{-6}$	-3.2	1.3	-0.8
15.947~16.155	43.00	$0.10^{+0.01}_{-0.01}$	$-1.54^{+0.05}_{-0.05}$	845^{+205}_{-319}	389^{+42}_{-153}	$7.36^{+1.77}_{-1.27} \times 10^{-6}$	$0.10^{+0.01}_{-0.01}$	$-1.53^{+0.05}_{-0.05}$	$-5.66^{+2.16}_{-2.20}$	356^{+98}_{-100}	$7.36^{+1.55}_{-0.99} \times 10^{-6}$	0.9	1.5	2.4
16.155~16.763	91.89	$0.21^{+0.01}_{-0.01}$	$-1.37^{+0.04}_{-0.04}$	197^{+20}_{-20}	124^{+15}_{-15}	$6.96^{+0.71}_{-0.62} \times 10^{-6}$	$0.28^{+0.03}_{-0.03}$	$-1.23^{+0.06}_{-0.06}$	$-2.40^{+0.10}_{-0.09}$	95^{+7}_{-7}	$8.47^{+1.61}_{-1.33} \times 10^{-6}$	-14.9	2.7	3.4
16.763~17.443	78.37	$0.12^{+0.01}_{-0.01}$	$-1.58^{+0.04}_{-0.04}$	254^{+39}_{-39}	107^{+19}_{-19}	$5.41^{+0.64}_{-0.60} \times 10^{-6}$	$0.15^{+0.02}_{-0.02}$	$-1.49^{+0.07}_{-0.07}$	$-3.09^{+0.65}_{-0.65}$	88^{+12}_{-11}	$6.12^{+1.51}_{-1.34} \times 10^{-6}$	-13.4	2.5	-5.1
17.443~17.839	47.46	$0.07^{+0.01}_{-0.01}$	$-1.76^{+0.07}_{-0.07}$	494^{+228}_{-218}	118^{+65}_{-63}	$4.41^{+1.05}_{-0.79} \times 10^{-6}$	$0.15^{+0.06}_{-0.06}$	$-1.45^{+0.18}_{-0.17}$	$-2.27^{+0.05}_{-0.05}$	55^{+16}_{-13}	$5.51^{+3.31}_{-2.42} \times 10^{-6}$	-24.2	-2.1	-17.6
17.839~20.564	95.39	$0.06^{+0.00}_{-0.00}$	$-1.72^{+0.03}_{-0.03}$	198^{+24}_{-24}	55^{+9}_{-9}	$2.94^{+0.30}_{-0.26} \times 10^{-6}$	$0.07^{+0.01}_{-0.01}$	$-1.65^{+0.05}_{-0.06}$	$-3.04^{+0.59}_{-0.59}$	51^{+3}_{-3}	$3.19^{+0.62}_{-0.59} \times 10^{-6}$	-11.2	2.5	-2.5
20.564~21.878	48.36	$0.03^{+0.00}_{-0.00}$	$-1.96^{+0.04}_{-0.04}$	196^{+34}_{-35}	8^{+8}_{-6}	$2.20^{+0.25}_{-0.23} \times 10^{-6}$	$0.07^{+0.02}_{-0.02}$	$-1.57^{+0.11}_{-0.11}$	$-2.76^{+0.25}_{-0.25}$	31^{+1}_{-1}	$1.97^{+1.02}_{-0.67} \times 10^{-6}$	7.8	1.8	-1.8
21.878~24.075	40.63	$0.02^{+0.00}_{-0.00}$	$-1.97^{+0.03}_{-0.03}$	282^{+61}_{-62}	8^{+9}_{-9}	$1.37^{+0.13}_{-0.11} \times 10^{-6}$	$0.03^{+0.00}_{-0.00}$	$-1.79^{+0.06}_{-0.06}$	$-4.75^{+2.23}_{-2.23}$	32^{+1}_{-1}	$1.27^{+0.33}_{-0.29} \times 10^{-6}$	10.1	1.7	0.0
24.075~28.056	38.77	$0.01^{+0.00}_{-0.00}$	$-1.90^{+0.06}_{-0.07}$	394^{+162}_{-162}	39^{+29}_{-32}	$0.95^{+0.19}_{-0.16} \times 10^{-6}$	$0.02^{+0.00}_{-0.00}$	$-1.83^{+0.08}_{-0.09}$	$-5.27^{+2.56}_{-2.56}$	34^{+8}_{-8}	$0.92^{+0.43}_{-0.33} \times 10^{-6}$	-0.0	-0.6	-0.3
28.056~36.886	38.79	$0.01^{+0.00}_{-0.00}$	$-1.96^{+0.03}_{-0.03}$	1548^{+1125}_{-930}	62^{+65}_{-59}	$0.80^{+0.10}_{-0.11} \times 10^{-6}$	$0.01^{+0.00}_{-0.00}$	$-1.94^{+0.05}_{-0.05}$	$-5.18^{+2.57}_{-2.59}$	72^{+41}_{-39}	$0.83^{+0.22}_{-0.22} \times 10^{-6}$	-1.3	-0.2	-2.2
36.886~44.922	27.62	$0.01^{+0.00}_{-0.00}$	$-1.93^{+0.03}_{-0.04}$	3738^{+2426}_{-2344}	262^{+204}_{-220}	$0.69^{+0.07}_{-0.10} \times 10^{-6}$	$0.01^{+0.00}_{-0.00}$	$-1.90^{+0.05}_{-0.07}$	$-5.32^{+2.59}_{-2.52}$	157^{+83}_{-75}	$0.65^{+0.17}_{-0.15} \times 10^{-6}$	-1.9	1.7	-0.3
44.922~64.083	28.28	$0.01^{+0.00}_{-0.00}$	$-1.85^{+0.08}_{-0.07}$	947^{+698}_{-618}	142^{+129}_{-114}	$0.42^{+0.10}_{-0.10} \times 10^{-6}$	$0.01^{+0.00}_{-0.00}$	$-1.72^{+0.15}_{-0.13}$	$-3.90^{+1.81}_{-2.92}$	65^{+20}_{-19}	$0.40^{+0.24}_{-0.15} \times 10^{-6}$	-9.1	-2.7	-9.4
64.083~90.519	20.55	$0.00^{+0.00}_{-0.00}$	$-1.83^{+0.05}_{-0.05}$	482^{+91}_{-96}	82^{+29}_{-29}	$0.24^{+0.33}_{-0.02} \times 10^{-6}$	$0.00^{+0.00}_{-0.00}$	$-1.91^{+0.07}_{-0.08}$	$-4.88^{+2.74}_{-2.80}$	72^{+22}_{-24}	$0.30^{+0.09}_{-0.09} \times 10^{-6}$	-10.0	2.2	-3.2

Note—All columns are the same as Table A2 but for GRB 190114873.